

University of Warwick institutional repository: <http://go.warwick.ac.uk/wrap>

A Thesis Submitted for the Degree of PhD at the University of Warwick

<http://go.warwick.ac.uk/wrap/64228>

This thesis is made available online and is protected by original copyright.

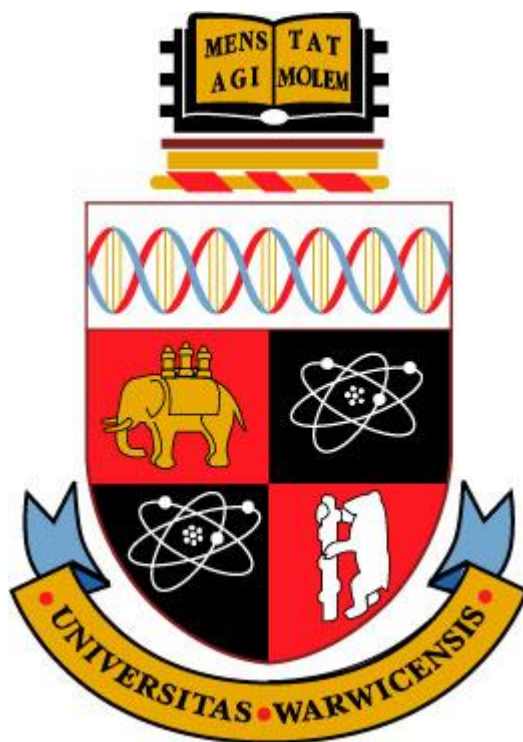
Please scroll down to view the document itself.

Please refer to the repository record for this item for information to help you to cite it. Our policy information is available from the repository home page.

**Mechanistic investigation of the RedG-catalysed
oxidative carbocyclisation of undecylprodigiosin to
streptorubin B**

David M. Withall

**Thesis submitted in partial fulfilment of the requirements for the degree of Doctor
of Philosophy in Life Science and Chemistry**



University of Warwick

Department of Chemistry

July 2014

<u>Content</u>	<u>Page</u>
Declaration	vi
Acknowledgements	vii
List of Figures	viii
List of Schemes	xix
List of Tables	xxvi
Abbreviations and definitions	xxviii
Chemical abbreviations and definitions	xxx
Abstract	xxxi
Chapter 1: Introduction	1
1.1 Introduction to prodiginines	2
1.2 <i>Streptomyces coelicolor</i> A3(2)	4
1.3 Early studies of prodiginine biosynthesis	6
1.4 The undecylprodigiosin and streptorubin B biosynthetic gene cluster	8
1.5 4-Methoxy-2,2'-bipyrrole-carboxaldehyde (MBC) biosynthesis	9
1.6 2-Undecylpyrrole (2-UP) biosynthesis	11
1.7 Condensation of MBC and 2-UP	12
1.8 Oxidative carbocyclisation	13
1.9 Proposed RedG catalytic mechanism	16
1.10 Relative and absolute stereochemistry of streptorubin B	17
1.10.1 Geometrical isomerism about the exocyclic double bond in prodiginine alkaloids	18
1.10.2 Atropisomerism of streptorubin B	18
1.10.3 Absolute stereochemistry of streptorubin B	20

1.11	Total synthesis of prodiginine antibiotics	22
1.11.1	Undecylprodigiosin total synthesis	22
1.11.2	Total synthesis of metacycloprodigiosin	23
1.11.3	Total synthesis of streptorubin B	25
1.12	Mutasynthesis of undecylprodigiosin and streptorubin B analogues	28
1.13	Aims and objectives	34
Chapter 2: Results and discussion: Synthesis of 4-methoxy-2,2'-bipyrrole-5-carboxaldehyde, 2-undecylpyrrole and analogues		35
2.1	Synthesis of 4-methoxy-2,2'-bipyrrole-5-carboxaldehyde (MBC)	36
2.2	Synthesis of 2-undecylpyrrole (2-UP)	38
2.3	Synthesis of ether containing 2-UP analogues	40
2.3.1	2-(5-Pentoxypentyl)-pyrrole	41
2.3.2	2-(7-Propoxyheptyl)-pyrrole	44
2.4	Synthesis of sulphur containing 2-UP analogues	45
2.4.1	2-(6-Butylsulphanylhexyl)-pyrrole	47
2.5	Synthesis of cyclopropane containing 2-UP analogues	48
2.6	Attempted synthesis of fluorine containing 2-UP analogues	55
2.6.1	2-(8-Fluoroundecyl)-pyrrole	62
2.6.2	2-(8, 8-Difluoroundecyl)-pyrrole	65
2.7	Synthesis of methyl-branched 2-UP analogues	66
2.7.1	2-(9-Methylundecyl)-pyrrole	67
2.7.2	2-(8-Methylundecyl)-pyrrole	71
2.8	Synthesis of 2-UP analogues with a methyl group on the pyrrole	71
2.9	Synthesis of stereoselectively deuterium-labelled 2-UP analogues	80

Chapter 3: Results and discussion: Feeding of 2-undecylpyrrole analogues to <i>Streptomyces coelicolor</i> mutants blocked in the biosynthesis of 2-undecylpyrrole	94
3.1 Feeding of 2-UP to <i>Streptomyces coelicolor redL</i> mutant	95
3.2 Feeding of sulphur containing 2-UP analogues to the <i>Streptomyces coelicolor redL</i> mutant	96
3.2.1 Feeding of sulphur containing 2-UP analogue 101	96
3.2.2 Feeding of sulphur containing 2-UP analogue 257	101
3.2.3 Feeding of sulphur containing 2-UP analogues 266 – 270	104
3.3 Feeding of ether containing 2-UP analogues to the <i>Streptomyces coelicolor redL</i> mutant	108
3.4 Problems with feeding to the <i>Streptomyces coelicolor redL</i> mutant	110
Chapter 4: Results and discussion: Feeding of 2-undecylpyrrole analogues to <i>Streptomyces albus</i> expressing <i>redHG</i>	112
4.1 <i>Streptomyces albus</i> as a heterologous host for expression of <i>redHG</i>	113
4.2 Feeding of sulphide containing 2-UP analogues to <i>Streptomyces albus</i> + <i>redHG</i>	117
4.2.1 Feeding of sulphur containing 2-UP analogue 101	118
4.2.2 Feeding of other sulphur containing 2-UP analogues	122
4.3 Feeding of ether containing 2-UP analogues to <i>Streptomyces albus</i> + <i>redHG</i>	129
4.3.1 Feeding of ether containing 2-UP analogue 85	129
4.3.2 Feeding of ether containing 2-UP analogue 86	133
4.4 Feeding of stereoselectively deuterated 2-UP to <i>Streptomyces albus</i> + <i>redHG</i>	134
4.5 Feeding of cyclopropyl containing 2-UP analogues to <i>Streptomyces albus</i> + <i>redHG</i>	140

4.6	Feeding of branched methyl 2-UP analogues to <i>Streptomyces albus</i>	
	+ <i>redHG</i>	143
4.6.1	Feeding of branched methyl 2-UP analogue 185	143
4.6.2	Feeding of branched methyl 2-UP analogue 180	144
4.7	Feeding of a methyl-substituted pyrrole analogue to <i>Streptomyces albus</i> + <i>redHG</i>	145
Chapter 5: Conclusions and future work		149
5.1	Sulphur containing 2-UP analogue	150
5.2	Ether containing 2-UP analogue	151
5.3	Cyclopropane containing 2-UP analogues	152
5.4	Branched methyl containing 2-UP analogues	152
5.5	Methyl substituted pyrrole containing 2-UP analogue	152
5.6	Stereoselectively deuterium-labelled 2-UP	152
5.7	Implications for RedH	153
5.8	Implications for the RedG mechanism	154
5.9	Future work	155
Chapter 6: Experimental		157
6.1	Chemistry experimental	158
6.1.1	Synthesis of sulphur containing 2-UP analogues	162
6.1.2	Synthesis of 2-UP 20	186
6.1.3	Synthesis of cyclopropane containing 2-UP analogues	187
6.1.4	Synthesis of branched methyl 2-UP analogue	198
6.1.5	Synthesis of methyl-substituted pyrrole containing 2-UP analogue	215
6.1.6	Synthesis of fluorine containing 2-UP analogues	223

6.1.7	Synthesis of ether containing 2-UP analogues	229
6.1.8	Stereoselectively deuterium-labelled 2-UP	243
6.2	Biology experimental	268
6.3	HPLC and LC-MS experimental	274
	References	280
	Appendix	296

Declaration

The experimental work reported in this thesis is original research carried out by the author, unless otherwise stated, in the Department of Chemistry, University of Warwick between September 2010 and April 2014. No material has been submitted for any other degree, or at any other institution.

Results from authors are referenced in the usual manner throughout the text.

Date: _____

David M. Withall

Acknowledgements

Firstly, I would like to thank my supervisor, Prof. Gregory L Challis, for allowing me to work on such an interesting project. His help, patience and sense of humour have made the past three years an enjoyable and rewarding experience.

Secondly, I would like to thank all the members of the Challis group, past and present, for their help and making those long hours in the lab more enjoyable; Orestis Lazos, Shanshan Zhou, Zdenek Kamenik, Gideon Idowu, Ruby Awodi, Joanna Bicz, Rebin Salih, Nicolas Malet, Sarah Barry, Daniel Griffiths and Yuki Inahashi. Special thanks go to Stuart Haynes for his previous work on the project, Paulina Sydor and Daniel Zabala for their help in all things biological and to Jeff, Bob, Bill, Pasta, Cider, Bendy and my 'favourite' minion (you know who you are!) for their friendship and providing me with hours of entertainment.

I would also like to thank all of my family (especially Archie) for their support over the past three years, and to the 'Cake Lady' for making me laugh after bad days and providing a never-ending supply of cake.

Finally, I would like to thank the support staff in the Chemistry Department at Warwick for their help. Thanks are also owed to the BBSRC and RSC for funding.

List of Figures

Figure 1.1 The 4-methoxypyrrolyldipyrromethane core common to all prodiginines (left) and a plate with *Streptomyces coelicolor* growing showing the intense red colour (right)

Figure 1.2 The structure of prodigiosin **1** and the initially proposed structures **2** and **3**

Figure 1.3 The structure of a selection of prodiginines including undecylprodigiosin **4**, metacycloprodigiosin **5**, streptorubin B **6**, nonylprodigiosin **7**, prodigiosin R1 **8** and the related compound roseophilin **9**

Figure 1.4 The structure of Obatoclax **10**

Figure 1.5 A selection of clinically utilised antibiotics produced by a variety of *Streptomyces* species

Figure 1.6 Undecylprodigiosin **4**, methylenomycin A **15**, actinorhodin **16**, streptorubin B **6** and coelimycin **17**, antibiotics produced by *S. coelicolor* A3(2)

Figure 1.7 The proposed biosynthetic route to prodigiosin **1** and undecylprodigiosin **4** with the results of feeding experiments using carbon-13 labelled precursors

Figure 1.8 The identical isotope labelling patterns for undecylprodigiosin **4** and metacycloprodigiosin **5** suggests metacycloprodigiosin **5** is derived from undecylprodigiosin **4** *via* an oxidative carbocyclisation reaction

Figure 1.9 The *red* gene cluster; green arrows represent genes involved in MBC **19** biosynthesis; blue arrows represent genes involved in 2-UP biosynthesis **20**; the black arrow represent a gene involved in the condensation of MBC **19** and 2-UP **20**; the orange arrow represents a gene involved in the oxidative cyclisation of **4** into **6**; white arrows represent genes of unknown function; grey arrows represent regulatory genes

Figure 1.10 The biosynthetic pathway to MBC **19**; PCP – peptidyl carrier protein, ACP – acyl carrier protein, KS – ketosynthase domain, OAS – α -oxoamine synthase domain

Figure 1.11 The biosynthetic pathway to 2-UP **20**; ACP – acyl carrier protein domain, A – adenylation domain, KS – ketosynthase domain, AT – acetyl transferase domain, OAS – α -oxoamine synthase domain

Figure 1.12 The condensation of MBC **19** and 2-UP **20** catalysed by RedH

Figure 1.13 The sequence comparison of RedG (*S. coelicolor*), McpG (*S. longispororuber*) and the Rieske non-haem iron dependent enzyme naphthalene dioxygenase (NDO); residues highlighted in yellow are proposed to ligate the [2Fe-2S] cluster and the non-haem iron atom; a mutation from aspartate in NDO to glutamate in RedG and McpG is highlighted in green

Figure 1.14 The proposed [2Fe-2S] Rieske cluster (blue), the non-haem iron catalytic site (red) and the bridging glutamate residue in RedG

Figure 1.15 The oxidative cyclisation reactions catalysed by non-haem iron-dependent enzymes in the biosynthesis of fosfomycin and the penicillins; the hydrogen atoms lost are highlighted in red while the new bonds formed are highlighted in green

Figure 1.16 The proposed catalytic mechanism of RedG based on the studied catalytic mechanism of NDO; A – substrate binds to the active site; B – an electron is transferred from the Rieske cluster to the non-haem iron centre, dioxygen binds and undergoes protonation; C – the resulting bridged iron(III) hydroperoxy species abstracts a hydrogen atom from the undecyl chain followed by cyclisation of the resulting radical; D – or the bridged iron(III) hydroperoxy species rearranges to a the iron(V) oxo-hydroxo species; E – and the iron (V) oxo-hydroxo species abstracts a hydrogen atom from the undecyl chain followed by cyclisation of the resulting radical; F – abstraction of a second hydrogen atom regenerates the aromatic pyrrole ring; G – regeneration of the resting enzyme by transfer of a second electron from the Rieske cluster

Figure 1.17 The equilibrium between *cis*- and *trans*-isomers of streptorubin B **6** indicating the unfavourable steric interaction between the *n*-butyl side chain and the methoxypyrrolidopyrromethene core

Figure 1.18 The atropisomeric *anti* and *syn* configurations of streptorubin B **6**

Figure 1.19 NOESY correlations observed for streptorubin B **6**

Figure 1.20 The mutasynthetic strategy utilised to biochemically confirm the stereochemistry of streptorubin B **6**

Figure 1.21 Undecylprodigiosin analogues produced *via* a mutasynthetic approach by Stuart Haynes

Figure 1.22 Streptorubin B and undecylprodigiosin analogues detected produced in mutasynthesis experiments utilising 2-UP analogues with altered hydrocarbon chain lengths

Figure 1.23 Streptorubin B analogues detected produced by mutasynthesis with 2-UP analogues bearing alterations to the hydrocarbon chain

Figure 1.24 The streptorubin B analogue **68** resulting from oxidative carbocyclisation of undecylprodigiosin analogue **70** (route A) and the mixture of desaturated undecylprodigiosin analogues **71** and **72** proposed to result from a competing desaturation reaction (route B)

Figure 1.25 The proposed mechanism for the RedG-catalysed desaturation reaction observed for the undecylprodigiosin analogue **70**

Figure 1.26 The proposed structure of the dealkylation product resulting from mutasynthesis with undecylprodigiosin analogue **74**. The streptorubin B **76** analogue was not observed

Figure 1.27 The proposed mechanism for the formation of dealkylated product **76**

Figure 1.28 A schematic representation of the mutasynthesis strategy envisaged for investigating the oxidative carbocyclisation reaction catalysed by RedG

Figure 2.1 The use of a metal-oxo species capable of enantioselective oxidation of sulphides to the corresponding sulfoxides

Figure 2.2 The reaction catalysed by the non-haem iron-dependent enzyme IPNS, resulting in the formation of the β -lactam and thiazolidine rings of the penicillins

Figure 2.3 A. The proposed mechanisms for β -lactam and thiazolidine formation catalysed by IPNS; B. The proposed mechanism for the formation of the β -lactam formed in the active site of IPNS upon incubation with a sulphide containing analogue of ACV

Figure 2.4 Products obtained from incubation of cyclopropane containing probes for radical intermediates with naphthalene dioxygenase

Figure 2.5 A comparison of the $^1\text{H-NMR}$ spectrum in CDCl_3 at 700 MHz of *E*- (top spectrum) and **Z-126** (bottom spectrum). The two singlets present in the bottom spectra at 0.92 ppm and 0.10 ppm are due to residual *t*-butyldimethyl silyl fluoride impurities

Figure 2.6 Stereochemical relationships of diastereotopic methylene protons (highlighted in green) with cyclopropane substituents, illustrating why the two sets of diastereotopic protons, give rise to significantly different $^1\text{H-NMR}$ signals

Figure 2.7 The proposed co-ordination of 1,8-octandiol to the silver(I) ion resulting in selective mono-benylation

Figure 2.8 The $^1\text{H-NMR}$ spectrum in CDCl_3 at 300 MHz of the byproduct resulting from the attempted fluorination of alcohol **151**

Figure 2.9 Alternative fluorinating agents investigated in attempts to overcome competing elimination in the conversion of secondary alcohol **151** to fluoride **156**

Figure 2.10 The ^1H -NMR spectrum in CDCl_3 at 400 MHz of monofluoro alcohol **172** showing the large coupling constant for the geminal proton H-13 and adjacent protons H-14

Figure 2.11 A comparison of the ^1H -NMR spectrum in CDCl_3 at 400 MHz of alkene **171** prepared from aldehyde **155** (top spectrum) and the ^1H -NMR spectrum in CDCl_3 at 250 MHz of the product resulting reaction of tosylate **173** with ethylmagnesium bromide and copper(I) iodide (bottom spectrum)

Figure 2.12 The ^1H -NMR spectrum in CDCl_3 at 400 MHz showing the ratio of brominated to chlorinated **175**

Figure 2.13 The ^1H -NMR spectrum in CDCl_3 at 400 MHz of *gem*-difluoro bromide **176**

Figure 2.14 Correlations between protons expected to be observed in the NOE spectra of 4-methyl-2-acyl pyrrole **205** and 3-methyl-2-acyl pyrrole **206**

Figure 2.15 NOE difference spectra for **206** in CDCl_3 at 600 MHz with no irradiation (top spectrum), irradiation at the frequency corresponding to the signal at 2.42 ppm (second spectrum), irradiation at the frequency corresponding to the signal at 6.10 ppm (third spectrum) and irradiation at the frequency corresponding to the signal at 6.89 ppm (bottom spectrum)

Figure 2.16 NOE difference spectra for **225** in CDCl_3 at 600 MHz with no irradiation (top spectrum), irradiation at the frequency corresponding to the signal at 2.02 ppm (second spectrum), irradiation at the frequency corresponding to the signal at 5.86 ppm (third spectrum) and irradiation at the frequency corresponding to the signal at 7.01 ppm (bottom spectrum)

Figure 2.17 Stereochemical course of the oxidative cyclisation reactions catalysed by HppE, IPNS and clavamate synthase. Only half of the curly arrows are shown for clarity

Figure 2.18 Use of stereoselectively deuterium-labelled substrates by Townsend *et al* to determine that the clavamate synthase-catalysed oxidative cyclisation occurs with retention of configuration

Figure 2.19 The ^1H -NMR spectrum in CDCl_3 at 400 MHz of the unknown side product resulting from the treatment of tosylate **243** with tetrabutylammonium fluoride and sodium bicarbonate

Figure 2.20 A comparison of the ^1H -NMR spectra in CDCl_3 at 700 MHz of (*S, R*)- (top spectrum), (*S, S*)- (second from top spectrum), (*R, R*)- (third from top spectrum) and (*R, S*)-**255** (bottom spectrum)

Figure 2.21 A comparison between 4.20 – 3.90 ppm and 1.80 – 0.70 ppm of the ^1H -NMR spectra in CDCl_3 at 700 MHz of (*S, R*)- (top spectrum), (*S, S*)- (second from top spectrum), (*R, R*)- (third from spectrum) and (*R, S*)-**255** (bottom spectrum)

Figure 2.22 A comparison of the ^1H -NMR spectra in CDCl_3 at 700 MHz of (*S, R*)- (top spectrum) and (*R, S*)- (third from top spectrum) at 25 °C and (*S, R*)- (second from top spectrum) and (*R, S*)-**255** (bottom spectrum) at 40 °C

Figure 2.23 A comparison between 4.20 – 3.90 ppm and 1.80 – 0.70 ppm of the ^1H -NMR spectrum in CDCl_3 at 700 MHz of (*S, R*)- (top spectrum) and (*R, S*)- (third from top spectrum) at 25 °C and (*S, R*)- (second from top spectrum) and (*R, S*)-**255** (bottom spectrum) at 40 °C

Figure 2.24 A comparison of the ^{13}C -NMR spectra in CDCl_3 at 400 MHz of undecanol (top spectrum), **S-249** (middle spectrum) and **R-249** (bottom spectrum)

Figure 3.1 A_{533} chromatograms from LC-MS analyses of mycelia extracts from *Streptomyces coelicolor* wild type (red), the *redL* mutant (blue) and the *redL* mutant supplemented with chemically synthesised 2-UP **20**

Figure 3.2 A_{533} chromatogram from LC-MS analysis of the mycelial extracts of the *redL* mutant fed with 2-UP analogue **101**

Figure 3.3 A_{533} chromatogram (black) and extracted ion chromatograms at $m/z = 412$ (red), $m/z = 428$ (yellow) and $m/z = 444$ (blue) from LC-MS analysis of the mycelial extracts of the *redL* mutant fed with 2-UP analogue **101**

Figure 3.4 Extracted ion chromatograms at $m/z = 412$ (red), $m/z = 428$ (yellow) and $m/z = 444$ (blue) from LC-MS analysis of the mycelial extracts of the *redL* mutant (solid lines) and *redLG* double mutant (dashed lines) fed with 2-UP analogue **101**

Figure 3.5 Extracted ion chromatograms at $m/z = 428$ (red) and $m/z = 430$ (blue) from LC-MS analysis of mycelial extract of the *redL* mutant fed with 2-UP analogue **101** under an atmosphere of $^{18}\text{O}_2$

Figure 3.6 Extracted ion chromatograms at $m/z = 444$ (red), $m/z = 446$ (blue) and $m/z = 448$ (yellow) from LC-MS analysis of mycelial extracts of the *redL* mutant fed with 2-UP analogue **101** under an atmosphere of $^{18}\text{O}_2$

Figure 3.7 A_{533} chromatogram resulting from LC-MS analysis of the mycelial extracts of the *redL* mutant fed with 2-UP analogue **257**

Figure 3.8 A_{533} chromatogram (black) and extracted ion chromatograms at $m/z = 412$ (red), $m/z = 428$ (blue), $m/z = 444$ (yellow), $m/z = 410$ (green) and $m/z = 342$ (brown) from LC-MS analysis of the mycelial extracts of the *redL* mutant fed with 2-UP analogue **257**

Figure 3.9 Extracted ion chromatograms at $m/z = 412$ (red), $m/z = 428$ (blue) and $m/z = 444$ (yellow) from LC-MS analysis of the mycelial extracts of the *redL* mutant (solid lines) and *redLG* double mutant (dashed lines) fed with 2-UP analogue **257**

Figure 3.10 A_{533} chromatogram from LC-MS analysis of the mycelia extracts of the *redL* mutant fed with 2-UP analogue **268** as a representative example

Figure 3.11 A_{533} chromatogram from LC-MS analysis of the mycelia extracts of the *redL* mutant fed with 2-UP analogue **85**

Figure 3.12 A_{533} chromatogram (black) and extracted ion chromatograms at $m/z = 396$ (red), $m/z = 326$ (blue) and $m/z = 394$ (yellow) from LC-MS analysis of the mycelia extracts of the *redL* mutant fed with 2-UP analogue **85**

Figure 4.1 A photograph of wild type *S. albus* (left), *S. albus* + *redH* (middle) and *S. albus* + *redHG* (right) after two days incubation at 30 °C fed with chemically synthesised 2-UP **20** and MBC **19**

Figure 4.2 A comparison of A_{533} chromatograms resulting from LC-MS analysis of the mycelial extracts of *S. albus* (red), *S. albus* + *redH* (blue) and *S. albus* + *redHG* (yellow) fed with chemically synthesised 2-UP **20** and MBC **19**

Figure 4.3 A comparison of *S. albus* + *redHG* (top plates) and *S. albus* + *redH* (bottom plates) immediately after feeding chemically synthesised 2-UP **20** and MBC **19** (left) and after two hours incubation at 30 °C (right)

Figure 4.4 A comparison of A_{533} chromatograms resulting from LC-MS analysis of the mycelial extracts of *S. albus* + *redHG* fed with chemically synthesised 2-UP **20** and MBC **19** immediately after conjugation (red) and after spores had been stored at -80 °C for one week (blue), three weeks (yellow) and five weeks (green)

Figure 4.5 Extracted ion chromatograms at $m/z = 412.24$ (red), $m/z = 428.23$ (blue) and $m/z = 444.23$ (yellow) from LC-MS analysis of the mycelial extracts of *S. albus* + *redHG* (solid lines) and *S. albus* + *redH* (dashed lines) fed with 2-UP analogue **101** and MBC **19**

Figure 4.6 Extracted ion chromatograms at $m/z = 412.24$ (red), $m/z = 428.23$ (blue) and $m/z = 444.23$ (yellow) from LC-MS analysis of the mycelial extracts of *S. albus* + *redHG* (solid

lines) fed with 2-UP analogue **101** and MBC **19** and solutions of the chemically synthesised authentic standards **102**, **103** and **256** (dashed lines)

Figure 4.7 A comparison of the MS/MS spectrum observed for the authentic standards (top spectra) and the mycelial extract of sulphide **102** (A), sulphoxide **103** (B) and sulphone **256** (C)

Figure 4.8 Extracted ion chromatograms at $m/z = 412.24$ (red), $m/z = 428.23$ (blue), $m/z = 444.23$ (yellow) and $m/z = 410.22$ (green) from LC-MS analysis of the mycelial extracts of *S. albus* + *redHG* fed with 2-UP analogue **270** and MBC **19**

Figure 4.9 A comparison of the HRMS for the compound eluting after 21.7 min in the LC-MS analysis of *S. albus* + *redHG* fed with 2-UP analogue **270** and MBC **19** (top spectrum) and the predicted mass spectrum for $C_{24}H_{32}N_3OS$ (bottom spectrum)

Figure 4.10 A_{533} chromatogram (black) and extracted ion chromatograms at $m/z = 412.24$ (red), $m/z = 428.23$ (blue), $m/z = 444.23$ (yellow) and $m/z = 410.21$ (green) from LC-MS analysis of the mycelial extracts of *S. albus* + *redHG* fed with 2-UP analogue **266** and MBC **19**

Figure 4.11 Extracted ion chromatograms at $m/z = 412.24$ (red), $m/z = 428.23$ (blue) and $m/z = 444.23$ (yellow) from LC-MS analysis of the mycelial extracts of *S. albus* + *redHG* fed with 2-UP analogue **266** and MBC **19**

Figure 4.12 A comparison of the HRMS for the compounds eluting after 19.0 min and 19.3 min in the LC-MS analysis (A and B, respectively, top spectrum) and the predicted mass spectrum for $C_{24}H_{32}N_3O_2S$ and $C_{24}H_{32}N_3O_3S$ (A and B, respectively, bottom spectrum)

Figure 4.13 Extracted ion chromatograms at $m/z = 396.26$ (red) and $m/z = 326.18$ (blue) from LC-MS analysis of the mycelial extract of *S. albus* + *redHG* (solid lines) and *S. albus* + *redH* (dashed lines) fed with 2-UP analogue **85** and MBC **19**

Figure 4.14 A comparison of the HRMS for the compound eluting after 18.5 min in the LC-MS analysis (top spectrum) and the predicted mass spectrum for $C_{19}H_{24}N_3O_2$ (bottom spectrum)

Figure 4.15 Extracted ion chromatograms for $m/z = 326.18$ from LC-MS analysis of the mycelial extracts of *S. albus* + *redHG* fed with 2-UP analogue **85** and MBC **19** (red) and the chemically synthesised authentic standard **76** (blue)

Figure 4.16 A comparison of the HRMS for the compound eluting after 18.5 min in LC-MS analysis of the mycelial extract of *S. albus* + *redHG* fed with 2-UP analogue **85** and MBC **19** (top spectrum), HRMS of the authentic standard **76** (middle spectrum) and the predicted mass spectrum for $C_{19}H_{24}N_3O_2$ (bottom spectrum)

Figure 4.17 A comparison of the MS/MS spectrum observed for the authentic standard of **76** (top spectrum) and **76** in the mycelial extract of *S. albus* + *redHG* fed with MBC **19** and 2-UP analogue **85** (bottom spectrum)

Figure 4.18 A_{533} chromatogram from LC-MS analysis of the mycelial extracts of *S. albus* + *redHG* fed with 2-UP analogue **86** and MBC **19** showing the single peak

Figure 4.19 A comparison of the A_{533} chromatograms from LC-MS analysis of the mycelial extracts of *S. albus* + *redHG* fed with *pro-S* labelled 2-UP **S-232** (red) and *pro-R* labelled 2-UP **R-232** (blue) with MBC **19**, respectively

Figure 4.20 A comparison of the HRMS for the compounds with a retention time of at 22.0 min in the LC-MS analyses of the mycelial extract of *S. albus* + *redHG* fed with MBC **19** and either 2-UP **20** (top), **S-232** (middle) or **R-232** (bottom)

Figure 4.21 An explanation for why most non-haem iron-dependent oxidative cyclases proceed with retention of configuration (route A), whereas the RedG-catalysed

carbocyclisation proceeds with inversion of configuration (route B). Only half of the curly arrows are shown for clarity

Figure 4.22 A_{533} chromatogram from LC-MS analysis of the mycelial extracts of *S. albus* + *redHG* fed with 2-UP analogue **Z-118** and MBC **19**

Figure 4.23 A_{533} chromatogram from LC-MS analysis of the mycelial extracts of *S. albus* + *redHG* fed with 2-UP analogue **E-118** and MBC **19**

Figure 4.24 A comparison of 'typical' *S. albus* + *redHG* fed with 2-UP **20** and MBC **19** (left) and the unusual effect resulting from feeding 2-UP analogue **Z-118** and MBC **19** (right)

Figure 4.25 A_{533} chromatogram from LC-MS analysis of the mycelial extracts of *S. albus* + *redHG* fed with 2-UP analogue **180** and MBC **19**

Figure 4.26 A comparison of the A_{533} chromatograms from the LC-MS analysis of the mycelial extracts of *S. albus* + *redHG* fed with MBC **19** and either 2-UP **20** (blue) or 2-UP analogue **207** (red)

Figure 4.27 A comparison of the extracted ion chromatograms at $m/z = 403.30$ from LC-MS analysis of the mycelial extracts of *S. albus* + *redHG* (red), *S. albus* + *redH* (blue) and *S. albus* wild type (yellow) fed with 2-UP analogue **207** and MBC **19**

Figure 5.1 A summary of the insight into the catalytic mechanism of RedG obtained through this work

List of Schemes

Scheme 1.1 The synthetic route utilised by Stuart Haynes for the stereoselective synthesis of deuterium labelled 2-UP analogues

Scheme 1.2 The synthetic route developed by D'Alessio *et al* for undecylprodigiosin **4**

Scheme 1.3 The synthetic route utilised by Wasserman for the total synthesis of racemic metacycloprodigiosin **5**

Scheme 1.4 The route utilised by Thomson and co-workers for the enantioselective total synthesis of metacycloprodigiosin **5**

Scheme 1.5 The route utilised by Furstner and coworkers for the total synthesis of racemic streptorubin B **6**

Scheme 1.6 The route utilised by Thomson for the enantioselective total synthesis of streptorubin B **6**

Scheme 2.1 The synthetic route to MBC **19** utilizing a palladium catalysed cross coupling to install the biaryl bond

Scheme 2.2 The synthesis of N-Boc-pyrrol-2-boronic acid **30** *via* a directed lithiation using lithium 2,2,6,6-tetramethylpiperidide

Scheme 2.3 The mechanism of the Vilsmeier-Haack reaction initially forming 2-bromo-4-methoxypyrrole **81** and subsequent formylation to yield the desired bromo-enamine **80**

Scheme 2.4 The synthetic route to 2-UP **20**

Scheme 2.5 The two competing pathways observed for final reduction of 2-ketopyrrole, illustrating the desired product and the undesired retro-aldol cleavage products and subsequent reduction

Scheme 2.6 Undecylprodigiosin analogue **88** predicted to result from RedG-catalysed C-7' hydroxylation 2-UP analogue **87**

Scheme 2.7 Stuart Haynes' synthetic route to 2-UP analogue **85**

Scheme 2.8 The alternative synthetic route to 2-UP analogue **85**

Scheme 2.9 The proposed mechanism for the oxidation of an aldehyde to the corresponding carboxylic acid using Oxone

Scheme 2.10 The synthetic route to 2-UP analogue **86**

Scheme 2.11 The expected undecylprodigiosin analogues **102** and **103** expected to result from the feeding of 2-UP analogue **101** to a mutant of *S. coelicolor* blocked in the biosynthesis of 2-UP **20**

Scheme 2.12 The synthetic route to 2-UP analogue **101**

Scheme 2.13 The synthetic route to dienophile **107** used by Danishefsky *et al.* The cyclopropane is highlighted in red. Only half of the curly arrows are shown for clarity

Scheme 2.14 The cobalt complex and cyclopropane substrate used by Golding *et al* to study the mechanism of α -methyleneglutarate mutase. The cyclopropane is highlighted in red

Scheme 2.15 The two potential homoallylic radicals **120** and **121** expected to result from the feeding of *E*- and/or *Z*-**118** to a mutant of *S. coelicolor* blocked in 2-UP biosynthesis

Scheme 2.16 The synthetic route to *Z*- and *E*-**118**

Scheme 2.17 The proposed mechanism of the 'alkyne zipper' reaction

Scheme 2.18 The proposed mechanism for the isomerisation of **132** to **135** catalysed by UDP-galp mutase and the two fluorinated substrate analogues used to probe the mechanism

Scheme 2.19 The undecylprodigiosin analogues **140** and **141** expected to result from feeding of 2-UP analogue **138** and **139** to a mutant of *S. coelicolor* blocked in the biosynthesis of 2-UP. Little or none of the corresponding streptorubin B analogues would be expected to be formed if the RedG-catalysed oxidative carbocyclisation reaction proceeds *via* a C-7' carbocation intermediate

Scheme 2.20 The generally-accepted mechanisms for the fluorination of alcohols and carbonyl compounds using DAST **144**

Scheme 2.21 The proposed synthetic route to mono-fluorinated and di-fluorinated 2-UP analogues **138** and **139**

Scheme 2.22 The mechanism for the nucleophilic displacement of activated alcohol **158** (pathway a, blue arrows) and the competing fluoride-promoted elimination reactions resulting in the formation of alkene side products (pathway b, red arrows)

Scheme 2.23 An alternative approach investigated for the synthesis of the corresponding triflate and subsequent treatment with a variety of fluoride sources

Scheme 2.24 Opening of epoxide **165** with fluoride used by Haufe *et al* to install a fluorine atom in the synthesis of lactone **167**

Scheme 2.25 Alternative route investigated for the synthesis of fluorinated 2-UP analogue **138**

Scheme 2.26 A possible mechanism for the conversion of fluoro tosylate **173** to alkene **171** involving single electron transfer (SET) reactions

Scheme 2.27 The new synthetic route to *gem*-difluorinated intermediate **179**

Scheme 2.28 The undecylprodigiosin analogue **181** and three potential oxidation products expected to result from the feeding of 2-UP analogue **180** to a mutant of *S. coelicolor* blocked in the biosynthesis of 2-UP

Scheme 2.29 The synthetic used by Stuart Haynes for the synthesis of 2-UP analogue **185**

Scheme 2.30 The alternative synthetic route to 2-UP analogue **185**

Scheme 2.31 The second generation synthetic route to 2-UP analogue **185**

Scheme 2.32 The synthetic route to 2-UP analogue **180**

Scheme 2.33 The expected undecylprodigiosin analogue **201** and a possible hydroxylation product **203** resulting from feeding 2-UP analogue **200** to a mutant of *S. coelicolor* blocked in the biosynthesis of 2-UP

Scheme 2.34 Initially investigated synthetic route to 2-UP analogue **200**

Scheme 2.35 Intermediates resulting from acylation of the Grignard reagent derived from 3-methylpyrrole at the 2- (black arrows) and 5- (red arrows) positions

Scheme 2.36 The expected undecylprodigiosin analogue **211** and streptorubin B analogue **212** from feeding 2-UP analogue **207** to a mutant of *S. coelicolor* blocked in the biosynthesis of 2-UP

Scheme 2.37 The alternative route to 2-UP analogue **200**

Scheme 2.38 Attempted conversion of 1,4-diketone **217** to pyrrole **218** reported by Trost *et al*

Scheme 2.39 A generalised scheme for the synthesis of N-sulphonyl-dialkyl pyrroles from a sulphonamide and a bromoalkyne

Scheme 2.40 The alternative synthetic route to 2-UP analogue **200**

Scheme 2.41 Different possible stereochemical courses for the RedG catalysed oxidative carbocyclisation, which could occur *via* primarily route A or route B, or *via* a mixture of routes A and B

Scheme 2.42 Possible products resulting from feeding of 2-UP **S-232** in which the *pro-S* hydrogen atom at C-7' has been stereospecifically labelled with deuterium to a mutant of *S. coelicolor* blocked in 2-UP biosynthesis

Scheme 2.43 The route used by Abad *et al* for the stereospecific incorporation of a deuterium label into hexadecanoic acid **236** by reduction of mesylate **235** with lithium aluminium deuteride

Scheme 2.44 The synthetic route to 2-UP stereoselectively deuterium-labelled at C-7'

Scheme 2.45 The assumed mechanism for the one-pot silyl ether deprotection and intramolecular cyclisation to convert tosylate **243** into epoxide **244**

Scheme 2.46 The proposed mechanism for formation of the unexpected cyclic carbonate byproduct **254**

Scheme 2.47 Synthesis of the Mosher esters of alcohols *R*- and *S*-**255**; Acid, DCC, DMAP, CHCl₃, 50 °C; **a.** (*R*)- α -methoxy- α -trifluorophenylacetic acid (*R, R*)- 50%, (*R, S*)-**255** 44%; **b.** (*S*)- α -methoxy- α -trifluorophenylacetic acid (*S, R*)- 50%, (*S, S*)-**255** 56%

Scheme 3.1 The expected undecylprodigiosin analogues **102** and **103** expected to result from the feeding of 2-UP analogue **101** to the *redL* mutant

Scheme 3.2 Products resulting from the feeding of 2-UP analogue **101** to the *redL* mutant

Scheme 3.3 The expected pattern of isotope labelling for sulphoxide ¹⁸O-**103** and sulphone ²¹⁸O-**256** resulting from the feeding of 2-UP analogue **101** to the *redL* mutant under an atmosphere of ¹⁸O₂

Scheme 3.4 The expected undecylprodigiosin analogues **258**, along with the dealkylated product **259** (pathway a) and carbocyclised product **260** (pathway b), expected to result from feeding 2-UP analogue **257** to the *redL* mutant

Scheme 3.5 The synthetic route to 2-UP analogue **257**

Scheme 3.6 The observed products resulting from feeding of 2-UP analogue **257** to the *redL* mutant

Scheme 3.7 The synthetic route to 2-UP analogues **266 – 271**

Scheme 3.8 The expected undecylprodigiosin analogue **272** and possible oxidation products that might result from feeding 2-UP analogue **269** to the *redL* mutant as a representative example

Scheme 3.9 The undecylprodigiosin analogue **74** and dealkylated product **76** expected to result from feeding 2-UP analogue **85** to the *redL* mutant

Scheme 4.1 The observed undecylprodigiosin analogue **102** and sulphur oxidation products **103** and **256** resulting from feeding 2-UP analogue **101** to the *S. coelicolor redL* mutant

Scheme 4.2 The synthetic route to the authentic standards of **102**, **103** and **256**

Scheme 4.3 The undecylprodigiosin analogue **288** and oxidised expected to result from feeding *S. albus + redHG* with 2-UP analogue **270** and MBC **19**, as a representative example

Scheme 4.4 The observed undecylprodigiosin analogue **276**, sulphur oxidation products **277** and **278** and streptorubin B analogues **279**, **293** and **294** resulting from LC-MS analysis of the mycelial extract of *S. albus + redHG* fed with 2-UP analogue **266** and MBC **19**

Scheme 4.5 The undecylprodigiosin analogue **74** and dealkylated product **76** expected to result from feeding 2-UP analogue **85** and MBC **19** to *S. albus + redHG*

- Scheme 4.6** The synthetic route to the authentic standard of dealkylated product **76**
- Scheme 4.7** The undecylprodigiosin analogue **87** and dealkylated aldehyde product **88** expected to result from feeding 2-UP analogue **86** and MBC **19** to *S. albus + redHG*
- Scheme 4.8** The undecylprodigiosin analogue **S-233** expected to result from feeding of stereoselectively deuterium-labelled 2-UP **232** with MBC **19** to *S. albus + redHG* and two possible outcomes for the conversion of **233** to streptorubin B **6**
- Scheme 4.9** The undecylprodigiosin analogues **E-** and **Z-119** and possible hydroxylated and desaturated products **297** and **298** expected to from feeding 2-UP analoges **Z-** and **E-118** to *S. albus + redHG*. Any streptorubin B analogues would have the same expected *m/z* and chemical formula as the desaturated product
- Scheme 4.10** The streptorubin B analogue **68** resulting from oxidative carbocyclisation (route A) and the mixture of desaturated undecylprodigiosin analogues **71** and **72** resulting from a competing desaturation reaction (route B) from feeding *S. albus + redHG* with 2-UP analogue **185** and MBC **19**
- Scheme 4.11** The undecylprodigiosin analogue **181** with the proposed desaturated products **182** and **183** in addition to the oxidative carbocyclised product **184** to result from feeding *S. albus + redHG* with 2-UP analogue **180** and MBC **19**
- Scheme 4.12** The undecylprodigiosin analogue **211** and proposed desaturated product **299**, hydroxylated product **300** in addition to the oxidative carbocyclised product **212** to result from feeding *S. albus + redHG* with 2-UP analogue **207** and MBC **19**
- Scheme 5.1** The analogous stereoselectively deuterium-labelled 2-UP experiment to investigate the stereochemical course of the McpG-catalysed oxidative carbocyclisation in metacycloprodigiosin **5** biosynthesis

List of Tables

- Table 2.1** Yields of products isolated from various fluorination reactions
- Table 2.2** The range of solvents, catalysts and additives screened in an attempt to improve the debenzylation of **190**
- Table 3.1** The yields for the synthesis of 2-UP analogues **266 – 271** as outlined in Scheme 3.7; step A for S-10' **266** resulted in 44% of the corresponding carboxylic acid
- Table 3.2** The observed products resulting from feeding of 2-UP analogues **101, 257** and **266 – 270** to the *redL* mutant; ✓ compound was observed; ? compound was barely detected; ✗ compound was not observed
- Table 4.1** The oxidant used for the sulphur oxidation; the yield of different sulphur oxidation products are shown in brackets
- Table 4.2** The observed products resulting from feeding of 2-UP analogues **101, 257** and **266 – 270** with MBC **19** to *S. albus + redHG*; ✓ compound was observed; ✗ compound was not observed; * other RedG-derived products were observed
- Table 6.1** Antibiotic stock solutions
- Table 6.2** HPLC conditions used for the purification of **76** and **102**
- Table 6.3** HPLC conditions used for the purification of **103** and **256**
- Table 6.4** Elution profile for low resolution LC-MS analysis
- Table 6.5** Alternative elution profile for low resolution LC-MS analysis
- Table 6.6** Elution profile for high resolution LC-MS
- Table 6.7** Elution profile for HPLC analysis of Mosher esters on a homochiral stationary phase

Table 6.8 HPLC conditions used for the purification of deuterium labelled streptorubin B analogues

Table 6.9 Elution profile for HPLC analysis of deuterium labelled streptorubin B analogues on a homochiral stationary phase

Abbreviations and definitions

Abbreviations	Definition
2-UP	2-Undecylpyrrole
A (domain)	Adenylation domain
ACP (domain)	Acyl carrier protien
ACV	δ -(L- α -aminoadipoyl)-L-cysteinyl-D-valine
ATP	Adenosine triphosphate
Bcl-2	B-Cell lymphoma 2
Bu	Butyl
°C	Degrees centigrade
C#	Carbon # of undecyl chain
CD	Circular dichorism
CLL	Chronic lymphocytic leukemia
COSY	Correlation spectroscopy
DFT	Density fuctional theory
EIC	Extracted ion chromatogram
eq	Equivalents
Et	Ethyl
FAD	Flavin adenine dinucleotide
His	Histidine residue
HPLC	High performance liquid chromatography
HRMS	High resolution mass spectrometry
IC ₅₀	Half maximal inhibitory concentration
IPNS	Isopenicillin N synthase
IR	Infared
KS (domain)	Ketosynthase domain
LC-MS	Liquid chromatography mass spectrometry
MBC	4-Methoxy-2,2'-bipyrrole-5-carboxaldehyde
Me	Methyl
mins	Minutes
NAD(P)H	Nicotinamide adenine dinucleotide phosphate
NDO	Naphthalene dioxygenase
NMR	Nuclear magnetic resonance
NOE	Nuclear Overhauser effect

NOESY	Nuclear Overhauser effect spectroscopy
MHz	Mega Hertz
<i>m/z</i>	Mass to charge ratio
OAS (domain)	α -Oxoamine synthase domain
OMe	Methoxy
PCP	Peptidyl carrier protein
PEPS	Phosphoenol pyruvate synthase
PLP	Pyridoxal-5'-phosphate
PPDK	Pyruvate-phosphate dikinase
PPTase	Phosphopantetheinyl transferase
rt	Room temperature
rpm	Revolutions per minute
SET	Single electron transfer
TLC	Thin layer chromatography
UV	Ultra-violet

Chemical abbreviations and definitions

Abbreviations	Definition
2M HCl	2M hydrochloric acid
Bn	Benzyl
BnBr	Benzyl bromide
BOC	<i>t</i> -Butyloxycarbonyl
CAN	Ceric ammonium nitrate
CDCl ₃	Deuterated chloroform
Cp ₂ TiCl ₂	Titanocene dichloride
DAST	Diethylaminosulphur trifluoride
d ₆ -DMSO	Deuterated dimethyl sulphoxide
DMPU	1,3-Dimethyl-3,4,5,6-tetrahydro-2(1H)-pyrimidinone
IBX	2-Iodoxybenzoic acid
IPA	Propan-2-ol
LDA	Lithium diisopropyl amide
LiAlD ₄	Lithium aluminium deuteride
<i>m</i> -CPBA	Meta-Chloroperbenzoic acid
MeB(OH) ₂	Methylboronic acid
NaBD ₄	Sodium borodeuteride
NBS	N-Bromosuccinimide
<i>n</i> -BuLi	<i>n</i> -Butyl lithium
Olah reagent	Pyridinium polyhydrofluoride
Oxone	Potassium peroxymonosulfate
Pd(OAc) ₂	Palladium(II) acetate
(PyS) ₂	2,2'-Dipyridyl disulphide
TBAF	Tetrabutyl ammonium fluoride
<i>t</i> -BDMSCl	<i>t</i> -Butyldimethylsilylchloride
THF	Tetrahydrofuran
Tf ₂ O	Triflic anhydride
TMS-CH ₂ N ₂	Trimethylsilyl diazomethane
TsCl	<i>p</i> -Toluene sulphonylchloride

Abstract

Prodiginines are a large family of red-pigmented antibiotics produced by a range of actinomycetes and other eubacteria that contain the highly-conjugated 4-methoxypyrrrolydipyrromethene core. It has recently been shown that the Rieske oxygenase-like non-haem iron-dependent enzyme RedG is responsible for catalysing the oxidative carbocyclisation of undecylprodigiosin to form the carbocyclic derivative streptorubin B, *via* functionalisation of an unactivated C-H bond.

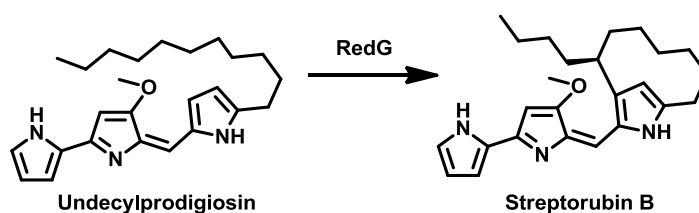


Figure 1: The oxidative carbocyclisation of undecylprodigiosin to streptorubin B catalysed by the Rieske oxygenase-like non-haem iron-dependent enzyme RedG

The mechanism of this chemically challenging reaction has been investigated using a mutasynthesis approach, employing analogues of key biosynthetic intermediates that bear specific functional groups, designed to probe different aspects of the proposed catalytic mechanism. Analogues of the biosynthetic intermediate 2-undecylpyrrole bearing sulphides, ethers, cyclopropanes, methyl substituents and deuterium labels in the undecyl chain have been synthesised and fed to *Streptomyces coelicolor* mutants blocked in the biosynthesis of 2-undecylpyrrole.

These 2-undecylpyrrole analogues have also been fed along with synthetic 4-methoxy-2,2'-bipyrrole carboxaldehyde to *Streptomyces albus* expressing *redH* and *redG*. The results of these feeding experiments have confirmed that RedG utilises molecular oxygen, is capable of catalysing dealkylation of an ether and revealed that the *pro-R* hydrogen atom from C-7' of the undecyl chain is specifically abstracted during the oxidative carbocyclisation. The results also showed that RedG is not able to tolerate substrate analogues with increase steric bulk close to the site of cyclisation.

1. Introduction

1.1 Introduction to prodiginines

Prodiginines are a large class of antibiotics produced by actinomycetes and other eubacteria. This family of compounds contains a common highly conjugated 4-methoxypyrrrolydipyrromethene that is responsible for their intense red colour, Figure 1.1. The different members of this family of compounds differ depending on the extent and position of the substitution pattern for R₁ to R₅.

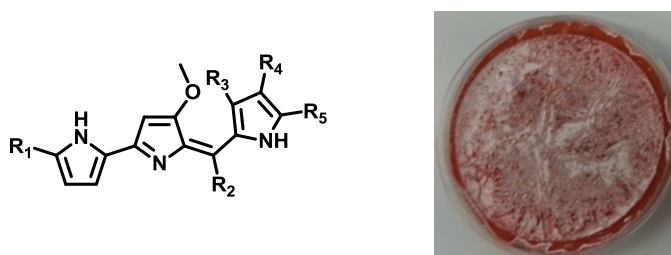


Figure 1.1: The 4-methoxypyrrrolydipyrromethene core common to all prodiginines (left) and a plate with *Streptomyces coelicolor* growing showing the intense red colour (right)

Prodigiosin **1**, the first member of the prodiginine family to be discovered, was isolated from the bacterium *Serratia marcescens* in 1902.¹ However, the structure of this unusual pigment was initially unclear, with a number of potential structures proposed, Figure 1.2. It was not until 1960 when the structure was confirmed as **1**.²

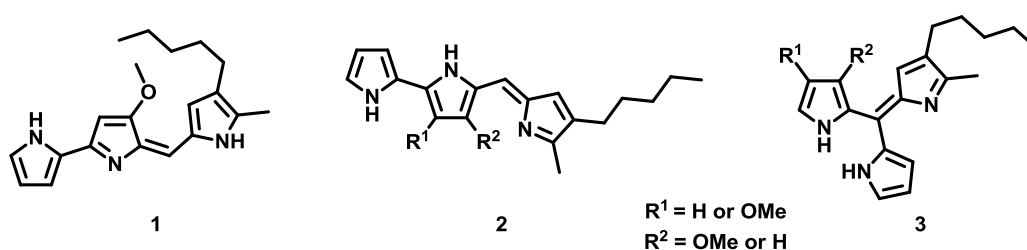


Figure 1.2: The structure of prodigiosin **1** and the initially proposed structures **2** and **3**

Since the discovery of prodigiosin **1**, a large number of other prodiginines have been isolated from a range of microorganisms, with the majority coming from actinomycetes. A selection of prodiginines are shown below in Figure 1.3, including the linear undecylprodigiosin **4** originally isolated from *Streptomyces* sp. Y-42 and several macrocyclic derivatives such as metacycloprodigiosin **5**, streptorubin B **6** and nonylprodigiosin **7**, isolated from *Actinomadura*

madurae.³ In addition to these cyclic derivatives, other prodiginine-like compounds have been observed including prodigiosin R1 **8** and roseophilin **9** isolated from *Streptomyces griseoviridis*.

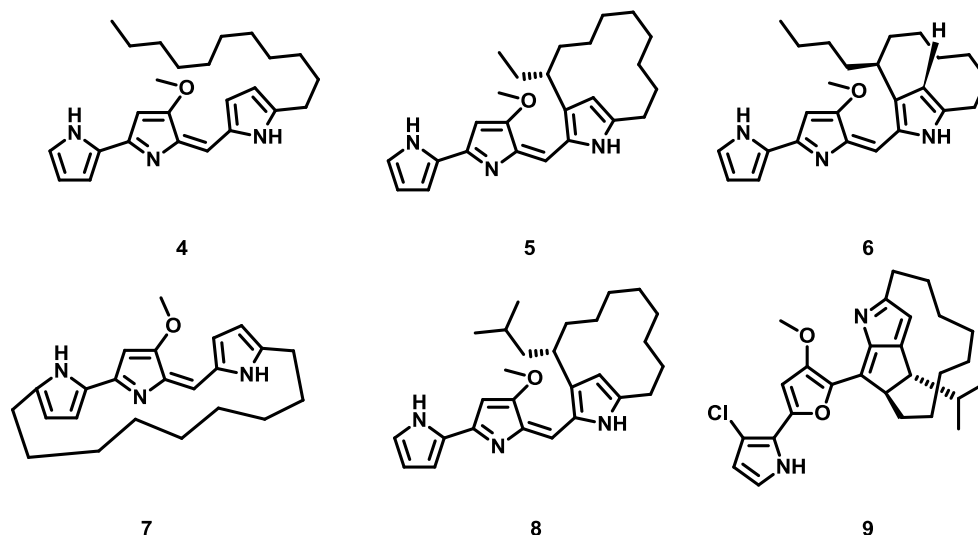


Figure 1.3: The structure of a selection of prodiginines including undecylprodigiosin **4**, metacycloprodigiosin **5**, streptorubin B **6**, nonylprodigiosin **7**, prodigiosin R1 **8** and the related compound roseophilin **9**

Prodiginines have received a lot of attention in recent years due to their wide range of biological activities. In addition to their antibacterial properties, prodiginines have also been shown to demonstrate immunosuppressant, anti-malarial and anti-cancer properties.^{4,5,6,7,8} Indeed, a synthetic analogue of streptorubin B **6**, Obatoclax **10**, has undergone Phase II clinical trials for the treatment of chronic lymphocytic leukemia (CLL), Figure 1.4.⁹ It has been shown that CLL cells, in addition to a number of other cancer cell lines, over-express the Bcl-2 family of anti-apoptotic proteins, thus preventing the normal cell death process from occurring.¹⁰ This family of proteins contain a conserved binding site that ordinarily binds pro-apoptotic proteins, such as Bax and Bak, preventing them from triggering the apoptotic pathway. It has been shown that Obatoclax **10** binds to this conserved binding site, resulting in the release of the pro-apoptotic proteins, restoring normal apoptotic processes.

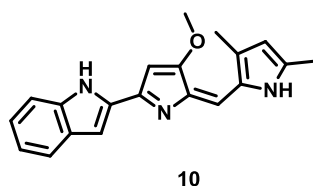


Figure 1.4: The structure of Obatoclox **10**

In addition to their anti-cancer properties, prodiginines have shown promise as anti-malarial agents. When screened against chloroquine-resistant *Plasmodium falciparum*, the parasite that causes malaria, undecylprodigiosin **4**, metacycloprodiginine **5** and streptorubin B **6** (IC₅₀ 7.7, 1.7 and 7.8 nM respectively) were found to be more potent than chloroquine (IC₅₀ 11 nM), although the mechanism of action is unknown.⁸ Furthermore, several synthetic analogues of these prodiginines demonstrated even greater potency and were even shown to cure malaria in several mice studies.¹¹

1.2 *Streptomyces coelicolor* A3(2)

Streptomyces are the largest genus of actinobacteria with over 500 different species currently known.¹² *Streptomyces* reside in soil and water and play a major role in the decomposition of organic matter in the environment. In addition, *Streptomyces* are known to produce a wide range of structurally diverse antibiotics, with 80% of the clinically used antibiotics originating from *Streptomyces* species including viomycin **11**, isolated from *Streptomyces puniceus*, chloramphenicol **12**, isolated from *Streptomyces venezuelae*, fosfomicin **13**, isolated from *Streptomyces fradiae* and streptomycin **14**, isolated from *Streptomyces griseus*, Figure 1.5.

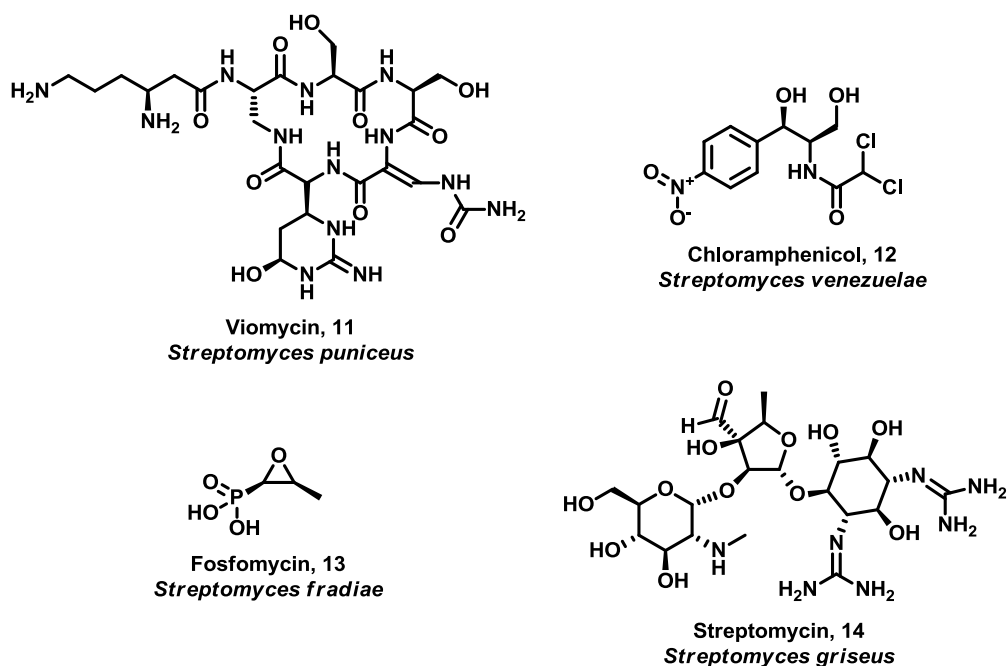


Figure 1.5: A selection of clinically utilised antibiotics produced by a variety of *Streptomyces* species

Streptomyces coelicolor A3(2) is a known producer of prodiginine antibiotics, specifically undecylprodigiosin **4** and streptorubin B **6**. In 2002, the complete genome sequence was reported making it an ideal model strain for the study of the biosynthesis of secondary metabolites such as the prodiginines.¹³ In addition to prodiginines, *S. coelicolor* A3(2) produces a range of other antibiotics including methylenomycin A **15**, actinorhodin **16**, an intensely blue coloured compound from which the species name of this strain derives, and coelimycin P1 **17**, Figure 1.6.

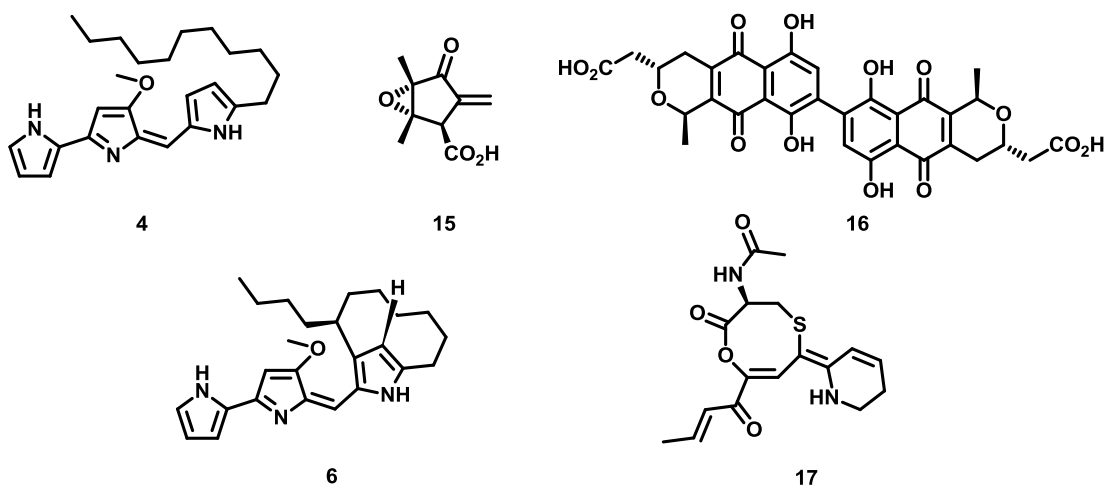


Figure 1.6: Undecylprodigiosin **4**, methylenomycin A **15**, actinorhodin **16**, streptorubin B **6** and coelimycin **17**, antibiotics produced by *S. coelicolor* A3(2)

1.3 Early studies of prodiginine biosynthesis

Early studies of the biosynthesis of prodiginines focused on prodigiosin **1** in *Serratia marcescens*, with later studies focusing on undecylprodigiosin **4** and metacycloprodigiosin **5** in *Streptomyces longispororuber*. A combination of feeding experiments utilising carbon-13 labelled precursors and isolation of putative biosynthetic intermediates lead to the hypothesis that the prodiginines are formed *via* the condensation of two late stage intermediates. Given the structural similarities between prodigiosin **1** and undecylprodigiosin **4**, it was expected that they would share a common biosynthetic intermediate, namely 4-methoxy-2,2'-bipyrrole-carboxaldehyde (MBC) **19**, Figure 1.7. Condensation of MBC **19** with either 2-methyl-3-pentylpyrrole **18** or 2-undecylpyrrole (2-UP) **20** would provide prodigiosin **1** and undecylprodigiosin **4**, respectively.^{14,15,16,17,18}

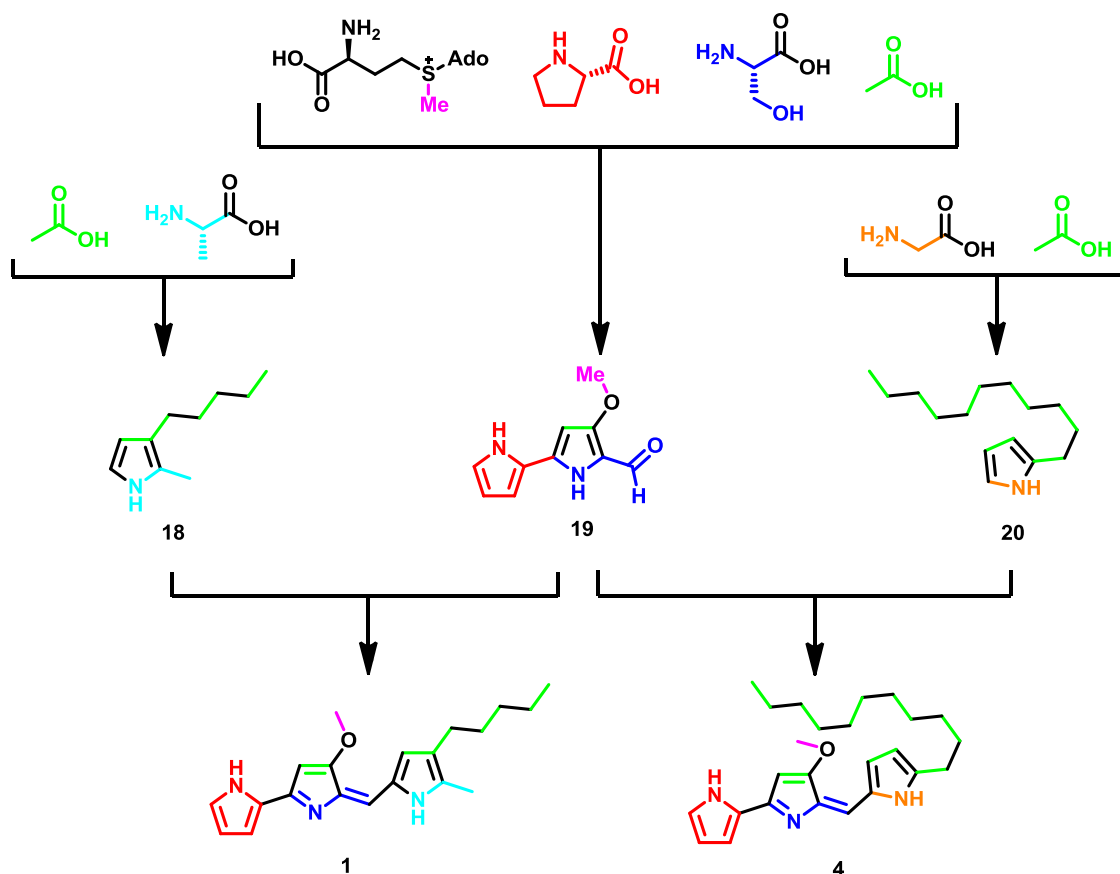


Figure 1.7: The proposed biosynthetic route to prodigiosin **1** and undecylprodigiosin **4** with the results of feeding experiments using carbon-13 labelled precursors

It was demonstrated from the feeding of isotopically labelled precursors that MBC **19**, in both systems, is biosynthesised from one unit of *L*-proline, carbons-2 and -3 of *L*-serine, the methyl group of *L*-methionine and one unit of acetate. In the case of prodigiosin **1**, 2-methyl-5-pentylpyrrole **18** is biosynthesised from carbons-2 and -3 of *L*-alanine and several units of acetate whereas 2-UP **20** is derived from glycine and several units of acetate.^{18,19,20,21}

In addition to the linear prodiginine undecylprodigiosin **4**, *S. longispororuber* is known to produce the carbocyclic derivative, metacycloprodigiosin **5**. The results of feeding experiments with isotopically labelled precursors revealed an identical incorporation pattern to that of undecylprodigiosin **4**. As a result, it was proposed that metacycloprodigiosin **5** is formed from undecylprodigiosin **4** *via* an oxidative carbocyclisation reaction, Figure 1.8. Since

metacycloprodigiosin **5** and streptorubin B **6** only differ by the size of their macrocycles, it was proposed by Challis *et al* that streptorubin B **6** was formed in an analogous manner.

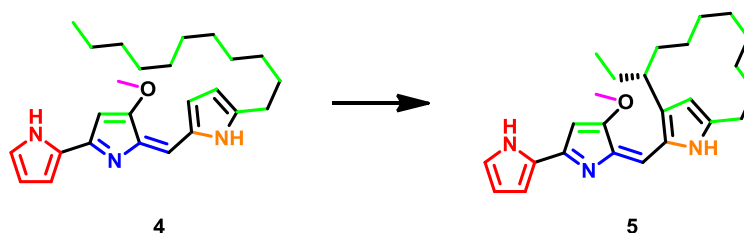


Figure 1.8: The identical isotope labelling patterns for undecylprodigiosin **4** and metacycloprodigiosin **5** (see Figure 1.7 for colour code) suggests metacycloprodigiosin **5** is derived from undecylprodigiosin **4** *via* an oxidative carbocyclisation reaction

1.4 The undecylprodigiosin **4** and streptorubin B **6** biosynthetic gene cluster

In 2002, the entire *S. coelicolor* A3(2) genome sequence was published and the gene cluster responsible for the biosynthesis of undecylprodigiosin **4** and streptorubin B **6** was identified, Figure 1.9.¹³ This gene cluster, known as the *red* cluster, contains twenty three genes arranged in four transcription units. Sequence comparisons of the encoded proteins with proteins of known function allowed a role for each gene within the cluster to be proposed. Since then, these enzymes have been studied extensively and the functions of the majority are now known.

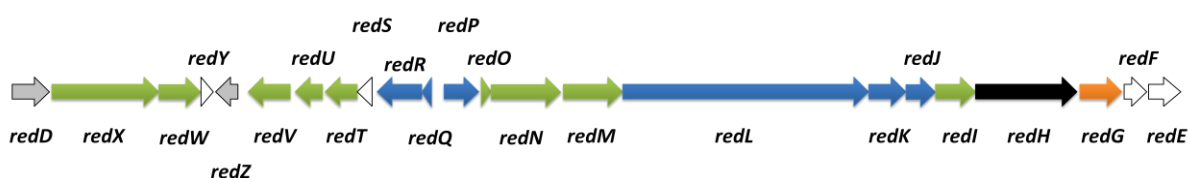


Figure 1.9: The *red* gene cluster; green arrows represent genes involved in MBC **19** biosynthesis; blue arrows represent genes involved in 2-UP **20** biosynthesis; the black arrow represents a gene involved in the condensation of MBC **19** and 2-UP **20**; the orange arrow represents a gene involved in the oxidative cyclisation of **4** into **6**; white arrows represent genes of unknown function; grey arrows represent regulatory genes

Of the twenty three genes in the *red* gene cluster, nine have been shown to be required for the biosynthesis of MBC **19** (*redI, M – N, T – W, Y*)^{22,23} while six are required for the biosynthesis of 2-UP **20** (*redJ – L, P – R*).^{24,25} Of the remaining genes, two are known to encode pathway specific regulators (*redD* and *redZ*),²⁶ one encodes the enzyme that catalyses the condensation of the two late stage intermediates MBC **19** and 2-UP **20**²⁷ (*redH*) and the other encodes the enzyme that catalyses the oxidative carbocyclisation which converts undecylprodigiosin **4** to streptorubin B **6** (*redG*). The remaining genes (*red S, F* and *E*) do not appear to be required for the biosynthesis of prodiginines.

1.5 4-Methoxy-2,2'-bipyrrole-carboxaldehyde (MBC, 19)

biosynthesis

As discussed in Section 1.3, MBC **19** is a common intermediate in the biosynthesis of prodigiosin **1** and undecylprodigiosin **4** in *Serratia* and *Streptomyces* species, respectively. In both cases, MBC **19** is biosynthesised from one unit of *L*-proline, *L*-serine, *L*-methionine and acetate. The mechanism for the biosynthesis of MBC **19** in *S. coelicolor* was initially proposed by Cerdeño *et al* and was later revised by Stanley *et al*.^{23 28}

The first step in the biosynthesis of MBC **19** involves the post-translational phosphopantetheinylation of the peptidyl carrier protein (PCP) RedO catalysed by RedU, a phosphopantetheinyl transferase (PPTase), Figure 1.10. Adenylation of the carboxyl group of *L*-proline, catalysed by RedM, activates it for loading onto the phosphopantethene thiol of RedO. Subsequent dehydrogenation, catalysed by the flavin adenine dinucleotide (FAD) dependent enzyme RedW, converts the pyrrolidine to a pyrrole ring.²⁹ Transfer of the resulting pyrrole-2-carboxyl intermediate to the C-terminal keto-synthase (KS) domain of RedX occurs directly and not *via* release and subsequent reloading of pyrrole-2-carboxylic acid. Subsequent decarboxylative condensation with a malonyl unit, attached to one of the acyl carrier protein (ACP) domains of RedN yields a β -keto-ACP-thioester. Condensation of

L-serine with this β -keto-ACP-thioester followed by loss of the serine carboxylate group as carbon dioxide, catalysed by the pyridoxal-5'-phosphate (PLP) dependent α -oxoamine synthase (OAS) domain, results in product release from the RedN enzyme. Subsequent cyclisation and dehydration provides the bipyrrole moiety. Oxidation of the primary alcohol to the corresponding aldehyde, catalysed by RedV,³⁰ and methylation of the pyrrole hydroxyl group, catalysed by RedI, completes the biosynthesis of MBC 19. The roles of RedT and RedY are currently unknown, however, mutant strains lacking these enzymes produce significantly less prodiginines which can be restored by feeding chemically synthesised MBC 19 to the mutants.

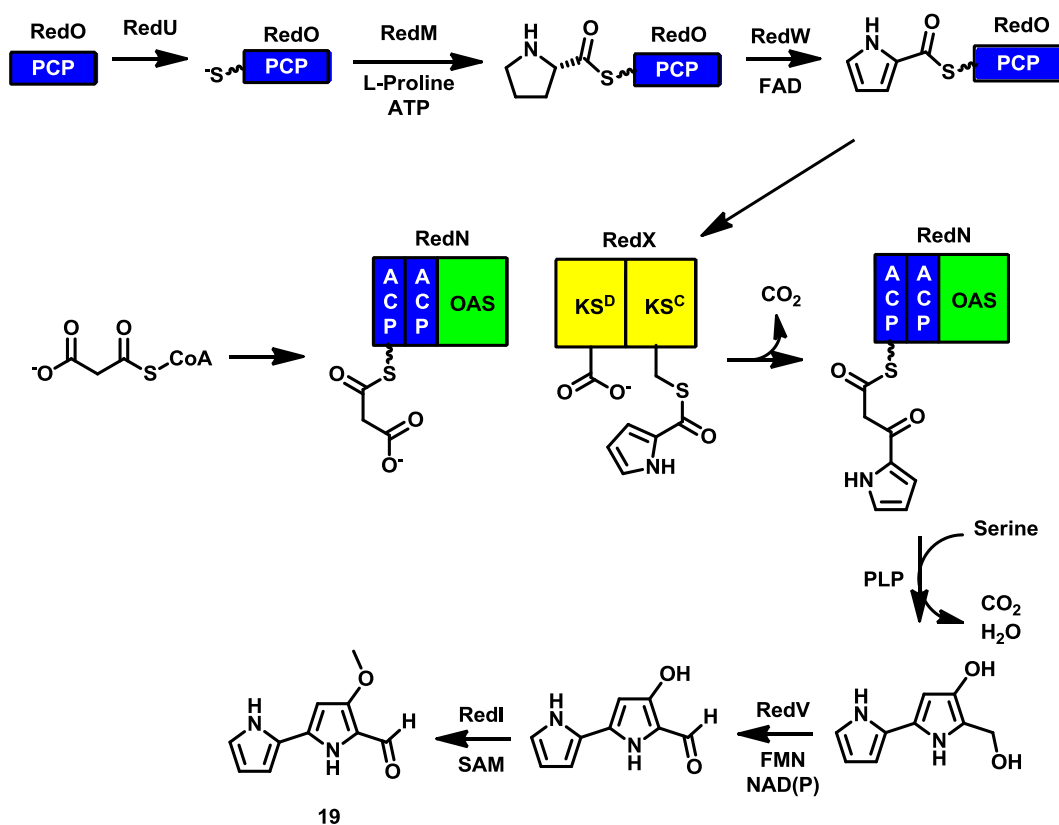


Figure 1.10: The biosynthetic pathway to MBC 19; PCP – peptidyl carrier protein, ACP – acyl carrier protein, KS – ketosynthase domain, OAS – α -oxoamine synthase domain

1.6 2-Undecylpyrrole (2-UP, 20) biosynthesis

As discussed in Section 1.3, it was demonstrated that 2-UP **20** is biosynthesised from one unit of glycine and several units of acetate. The initial steps in the biosynthesis of 2-UP **20** involve the formation of dodecanoic acid *via* the actions of RedP, RedQ, RedR and fatty acid biosynthetic enzymes in *S. coelicolor*, Figure 1.11.²⁴ RedP, a homologue of the fatty acid biosynthetic enzyme FabH, initiates the biosynthesis of dodecanoic acid by catalysing the decarboxylative condensation of acetyl-CoA with a malonyl extender unit bound to the ACP RedQ.²⁵ Subsequent keto-reduction, dehydration and enoyl-reduction catalysed by fatty acid biosynthetic enzymes yields a butylanoyl thioester attached to RedQ. This butylanoyl thioester then undergoes several rounds of chain elongation, dehydrations and reductions catalysed by RedR, a homologue of FabF, and fatty acid biosynthetic enzymes, ultimately resulting in the formation of a dodecanoyl thioester bound to RedQ.

Transfer of the dodecanoyl chain to N-terminal ACP domains of RedL has been shown to occur *via* hydrolysis of the thioester, catalysed by RedJ, to afford dodecanoic acid.³¹ This free carboxylic acid is then loaded onto the RedL N-terminal ACP domain, after activation by adenylation catalysed by the adenylation (A) domain of RedL. A final decarboxylative condensation with a malonyl group bound to the C-terminal ACP, catalysed by the KS domain, affords β -ketomyristoyl-ACP. In an analogous process to that in the biosynthesis of MBC **19**, condensation with glycine followed by decarboxylation catalysed by the OAS domain of RedL, releases the chain to yield 4-keto-2-undecylpyrroline after cyclisation and elimination of water. Finally, reduction of the resulting ketone by the NAD(P)H dependent enzyme RedK, followed by aromatisation *via* elimination of water provides 2-UP **20**.

phosphotransferase domains of phosphoenol pyruvate synthase (PEPS) and pyruvate-phosphate dikinase (PPDK).²⁴ The third domain of RedH does not show sequence similarity to any proteins of known function and was therefore proposed to be the MBC **19** and 2-UP **20** binding site.

It has been proposed that RedH activates the carbonyl group of MBC **19** by phosphorylation of the oxygen atom in an analogous manner to the phosphorylation of pyruvate by PEPS and PPDK, Figure 1.12. Subsequent nucleophilic attack of 2-UP **20**, followed by elimination of phosphate and rearomatisation yields undecylprodigiosin **4**.

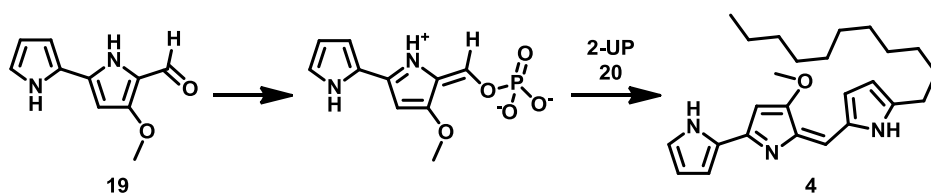


Figure 1.12: The condensation of MBC **19** and 2-UP **20** catalysed by RedH

1.8 Oxidative carbocyclisation

The final step in the biosynthesis of streptorubin B **6** is the oxidative carbocyclisation of undecylprodigiosin **4**, which yields the 10-membered *ansa*-bridged carbocycle. RedG was implicated in this chemically challenging reaction because a mutant of *S. coelicolor* lacking the *redG* gene produces undecylprodigiosin **4** but not streptorubin B **6**. Indeed, feeding of chemically synthesised MBC **19** and 2-UP **20** to the heterologous host *Streptomyces venezuelae* expressing both *redH* and *redG* results in the production of undecylprodigiosin **4** and streptorubin B **6**, indicating that RedG is responsible for catalysing the oxidative carbocyclisation of undecylprodigiosin **4** into streptorubin B **6**.³³

Sequence comparison of RedG with proteins of known function revealed a strong similarity to the Rieske non-haem iron-dependent enzyme, naphthalene dioxygenase (NDO), Figure 1.13. Indeed, McpG, a homologue of RedG from *Streptomyces longispororuber* that converts

undecylprodigiosin **4** to metacycloprodigiosin **5**, also exhibited a high sequence similarity to RedG and NDO.

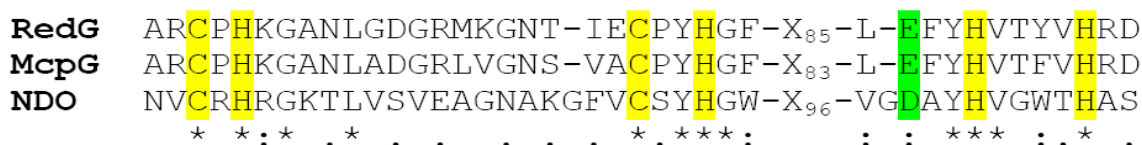


Figure 1.13: The sequence comparison of RedG (*S. coelicolor*), McpG (*S. longispororuber*) and the Rieske non-haem iron dependent enzyme naphthalene dioxygenase (NDO); residues highlighted in yellow are proposed to ligate the [2Fe-2S] cluster and the non-haem iron atom; a mutation from aspartate in NDO to glutamate in RedG and McpG is highlighted in green

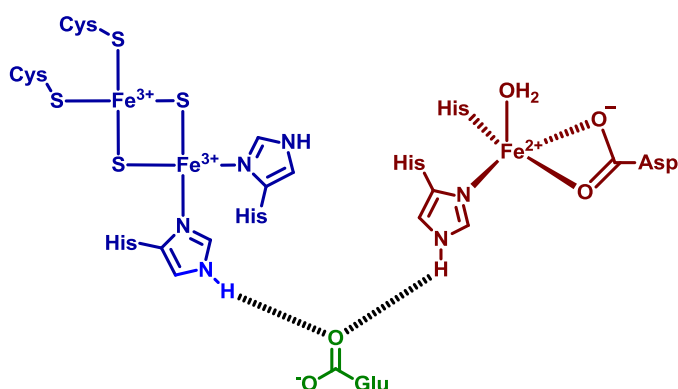


Figure 1.14: The proposed [2Fe-2S] Rieske cluster (blue), the non-haem iron catalytic site (red) and the bridging glutamate residue in RedG

As shown in Figure 1.13 and 1.14, the N-terminal domain of RedG contains the CXH and CX₂H motifs for [2Fe-2S] Rieske cluster binding in NDO. In the C-terminal domain, RedG contains an EX₂HX₄H motif that exhibits a strong similarity with the DX₂HX₄H motif in the substrate binding region of NDO. These two conserved histidine residues, in addition to an unidentified aspartate or glutamate residue, are proposed to bind the catalytic iron atom. The aspartate residue proposed to be involved in the transfer of electrons from the Rieske cluster to the non-haem iron centre during the catalytic cycle of NDO appears to be mutated to a glutamate residue in RedG. Since the side chains of aspartate and glutamate differ only in the length of the side chain, it is expected that this alteration has no impact on function.

Rieske enzymes, including NDO, are typically multicomponent enzymes with a dedicated reductase to accept electrons from NAD(P)H and a ferredoxin to transfer the electrons from the reductase to the oxygenase where substrate oxidation occurs. However, there are no genes within the *red* cluster that encode either a reductase or a ferredoxin protein. However, elsewhere in the *S. coelicolor* genome, there are six ferredoxin and three reductase encoding genes that could potentially be involved in mediating electron transfer to RedG.³⁴

While Rieske enzymes typically catalyse dihydroxylation reactions, other non-haem iron-dependent enzymes have previously been shown to catalyse oxidative cyclisation reactions in the biosynthesis of a variety of natural products. In the case of fosfomycin **13**, the epoxide ring essential for the observed antibacterial properties is installed by the non-haem iron-dependent enzyme HppE, Figure 1.15. Another example of a non-haem iron-dependent enzyme involved in the biosynthesis of a clinically important natural products is isopenicillin N synthase (IPNS). It has been demonstrated that IPNS is responsible for catalysing the formation of the β -lactam and thiazolidine rings of the penicillins.

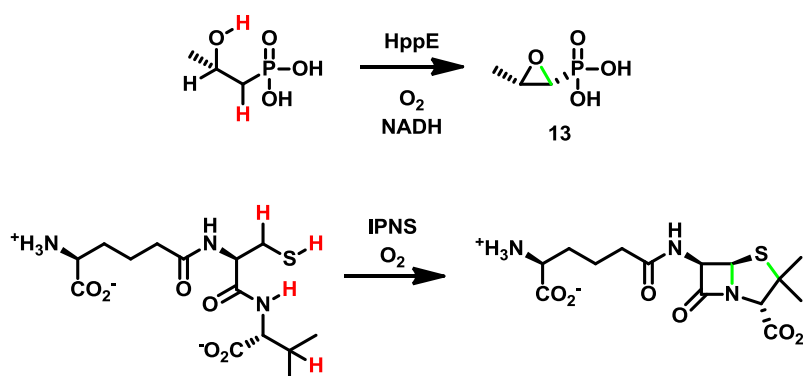


Figure 1.15: The oxidative cyclisation reactions catalysed by non-haem iron-dependent enzymes in the biosynthesis of fosfomycin and the penicillins; the hydrogen atoms lost are highlighted in red while the new bonds formed are highlighted in green

While a range of non-haem iron-dependent enzymes are known to catalyse oxidative cyclisation reactions at unactivated carbon centres, prior to the discovery of RedG, no such

enzyme was known that could catalyse the formation of a carbon-carbon bond. Moreover, no other Rieske oxygenase-like enzyme is known to catalyse an oxidative cyclisation reaction.

1.9 Proposed RedG catalytic mechanism

At present, there is no experimental evidence for the mechanism by which RedG catalyses the oxidative carbocyclisation of undecylprodigiosin **4** to streptorubin B **6**. However, the catalytic mechanisms of several other Rieske oxygenases, including NDO, have been studied.^{35,36,37} Thus, a plausible catalytic mechanism for RedG can be proposed based on what is known about these other enzymes, Figure 1.16.

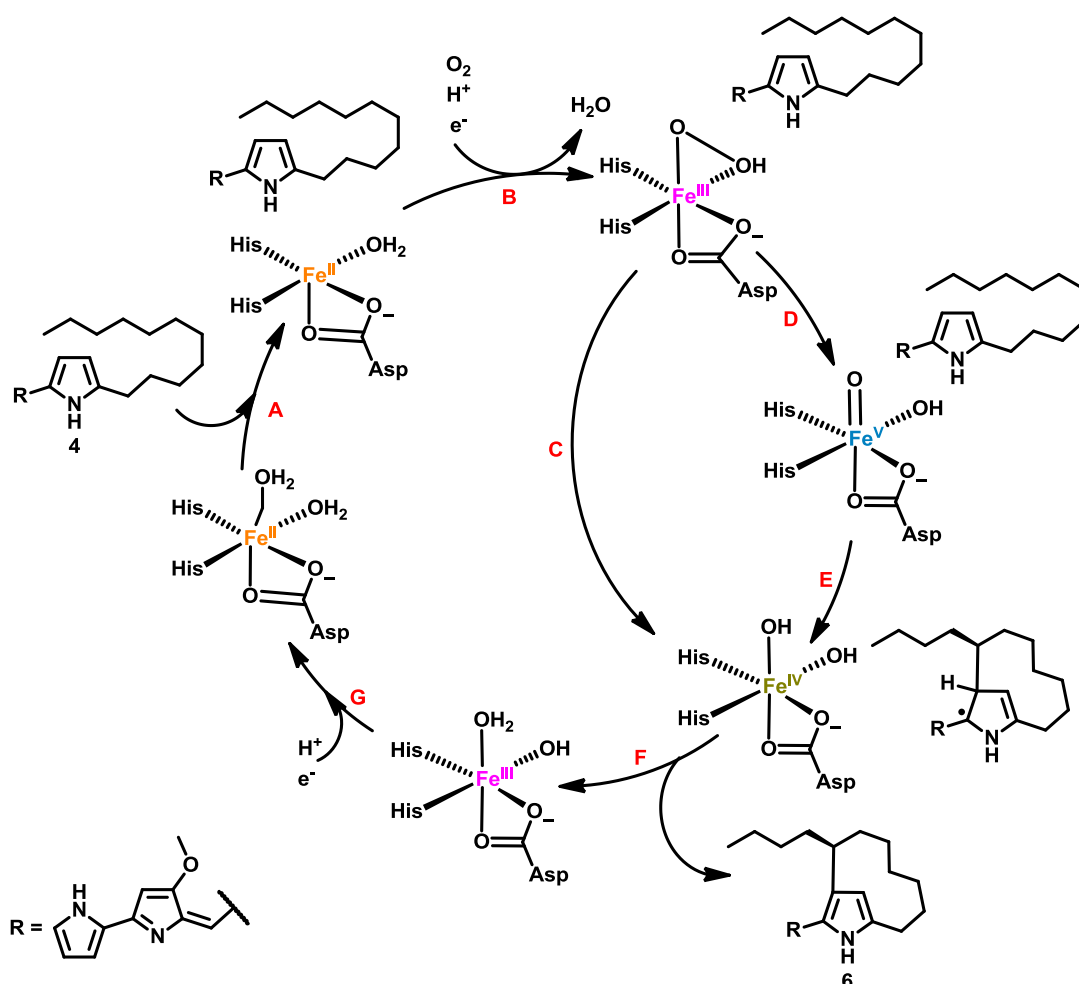


Figure 1.16: The proposed catalytic mechanism of RedG based on the studied catalytic mechanism of NDO; A – substrate binds to the active site; B – an electron is transferred from the Rieske cluster to the non-haem iron centre, dioxygen binds and undergoes protonation; C – the resulting bridged iron(III) hydroperoxy species abstracts a hydrogen atom from the

undecyl chain followed by cyclisation of the resulting radical; D – or the bridged iron(III) hydroperoxy species rearranges to a the iron(V) oxo-hydroxo species; E – and the iron(V) oxo-hydroxo species abstracts a hydrogen atom from the undecyl chain followed by cyclisation of the resulting radical; F – abstraction of a second hydrogen atom regenerates the aromatic pyrrole ring; G – regeneration of the resting enzyme by transfer of a second electron from the Rieske cluster

The catalytic cycle is initiated by undecylprodigiosin **4** binding to the active site, promoting loss of one of the water ligands, resulting in a vacant binding site on the non-haem iron atom, step A. A molecule of oxygen then binds to this vacant site and is subsequently reduced to the corresponding bridged hydroperoxy species utilising an electron from the non-haem iron atom and another electron from NAD(P)H transferred *via* the [2Fe-2S] Rieske cluster which is then protonated and displaces the second water ligand, step B. From here two pathways are possible. One involves abstraction of a hydrogen atom from C-7' of undecylprodigiosin **4** by the iron(III) bridged hydroperoxy species, generating a carbon-centred radical that subsequently cyclises onto the pyrrole ring, step C. The other involves heterolysis of the oxygen-oxygen bond of the bridged hydroperoxy complex to afford the corresponding iron(V) oxo-hydroxo species, step D. This iron(V) oxo-hydroxo species is then proposed to abstract a hydrogen atom from C-7' of undecylprodigiosin **4** to form a radical that adds to the pyrrole, step E. Abstraction of a second hydrogen atom regenerates the pyrrole, yielding the product streptorubin B **6**, step F. Transfer of a second electron from NAD(P)H *via* the Rieske cluster regenerates the resting state of RedG, step G.

1.10 Relative and absolute stereochemistry of streptorubin B **6**

The structure of streptorubin B **6** presents several interesting stereochemical features. In addition to the stereocentre at C-7' and the geometry of the exocyclic double bond, molecular

models indicate that free rotation of the methoxypyrrolidipyrromethene core through the *ansa*-bridged 10-membered carbocycle is likely to be highly restricted.

1.10.1 Geometrical isomerism about the exocyclic double bond in prodiginine alkaloids

D'Alessio and coworkers demonstrated that prodiginines generally exist as an equilibrium mixture of *cis*- and *trans*-isomers about the exocyclic double bond.³⁸ Such isomers are often observed during reverse-phase HPLC analysis. Broad peaks that exhibit extensive 'tailing' are typically observed, resulting from interconversion of isomers during passage through the column. The position of equilibrium is strongly dependent on the pH of the sample; at low pH, protonation of the central nitrogen atom occurs allowing an appropriate counter ion (e.g. chloride) to hydrogen bond with all three N-H groups, thus favouring the *cis*-isomer, Figure 1.17. At high pH, a greater proportion of the *trans*-isomer is present. In the case of streptorubin B **6**, steric interactions between the *n*-butyl group and the methoxypyrrolidipyrromethene core also favour the *cis*-isomer.

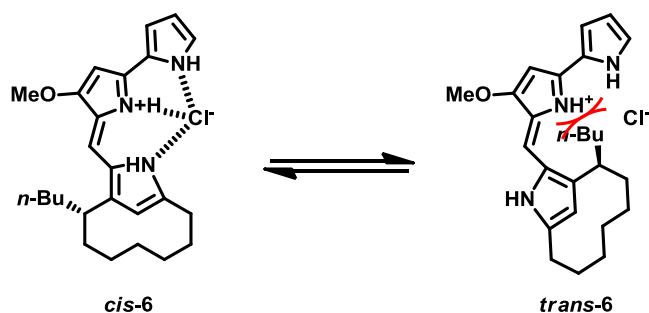


Figure 1.17: The equilibrium between *cis*- and *trans*-isomers of streptorubin B **6** indicating the unfavourable steric interaction between the *n*-butyl side chain and the methoxypyrrolidipyrromethene core

1.10.2 Atropisomerism of streptorubin B 6

Since rotation of the methoxypyrrolidipyrromethene core through the *ansa*-bridged 10-membered carbocycle is restricted, the *n*-butyl side chain and the methoxypyrrolidipyrromethene core are forced to adopt defined relative configurations,

namely *anti* and *syn*, Figure 1.18. Indeed, even at 120 °C, no signal broadening was observed in the $^1\text{H-NMR}$ spectrum of streptorubin B **6**, indicating it is conformationally stable at room temperature.

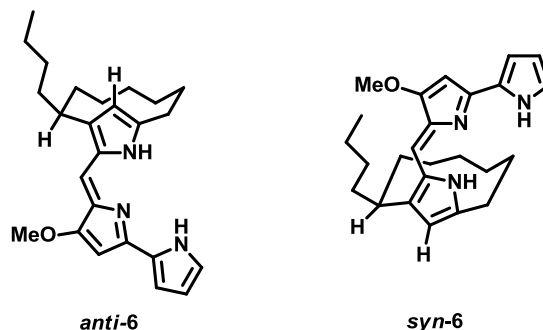


Figure 1.18: The atropisomeric *anti* and *syn* configurations of streptorubin B **6**

This conformational stability has a peculiar effect on the protons attached to C-4', Figure 1.19. One of the protons is held directly above the π -faces of a pyrrole resulting in a chemical shift of -1.54 ppm in the $^1\text{H-NMR}$ spectrum, while the other proton has a typical methylene chemical shift of 1.16 ppm. By measuring NOESY NMR spectra experiments of streptorubin B **6** isolated from *Streptomyces coelicolor* M511, Challis *et al* were able to demonstrate that the major atropisomer of streptorubin B **6** in solution is *anti*, Figure 1.19.³⁹ Correlation between H-7' and H-1'' in addition to a correlations between the protons attached to C-8' and H-3_C indicated that the *n*-butyl and C-1'' have an *anti* relationship as expected for the *anti* conformer. Correlations between H-7' and H-1'', H-1'' and H-1''', H-1''' and H-4_B and H-4_B and H-3_A also confirmed the *cis*-geometry of the exocyclic double bond. In addition to the peak at -1.54 ppm, a peak at -1.48 ppm with approximately 5% the intensity was observed, indicating a small amount of the *syn* conformer also present in solution.

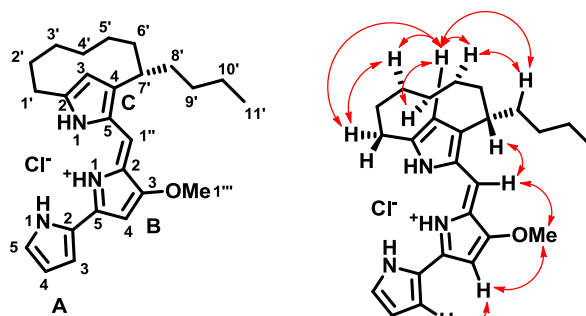


Figure 1.19: NOESY correlations observed for streptorubin B **6**

1.10.3 Absolute stereochemistry of streptorubin B **6**

Challis *et al* elucidated the absolute stereochemistry of streptorubin B **6** *via* a mutasynthesis approach, involving feeding of stereoselective deuterium-labelled 2-UP **25** to a mutant of *S. coelicolor* that is blocked in 2-UP **20** biosynthesis, to produce stereoselectively labelled streptorubin B **6**.³⁹ The large difference in chemical shift of the diastereotopic C-4' protons was exploited to assign the configuration of C-7'. Stuart Haynes, a previous PhD student in the Challis group, synthesised 2-UP analogues (**4'R**)-**25** and (**4'S**)-**25** with either the *pro-S* or *pro-R* hydrogen at C-4' replaced with a deuterium atom, Scheme 1.1 and Figure 1.20. Feeding of (**4'S**)-**25** resulted in streptorubin B **6** containing approximately 70% of the label in the position directly over the pyrrole π -face, whereas feeding of (**4'R**)-**25** resulted in approximately 30% labelling of the position directly over the pyrrole π -face as determined by ¹H-NMR spectroscopy. These data indicated that streptorubin B **6** has the 7'S configuration.

homochiral stationary phase. From this, they were able to deduce that partial racemisation during the synthesis of (4'R)- and (4'S)-**25** was the main reason for the scrambling of the label. However, a small amount of (7'R)-streptorubin B **6** was detected in the natural material, indicating that the RedG-catalysed oxidative carbocyclisation reaction proceeds without complete stereocontrol.

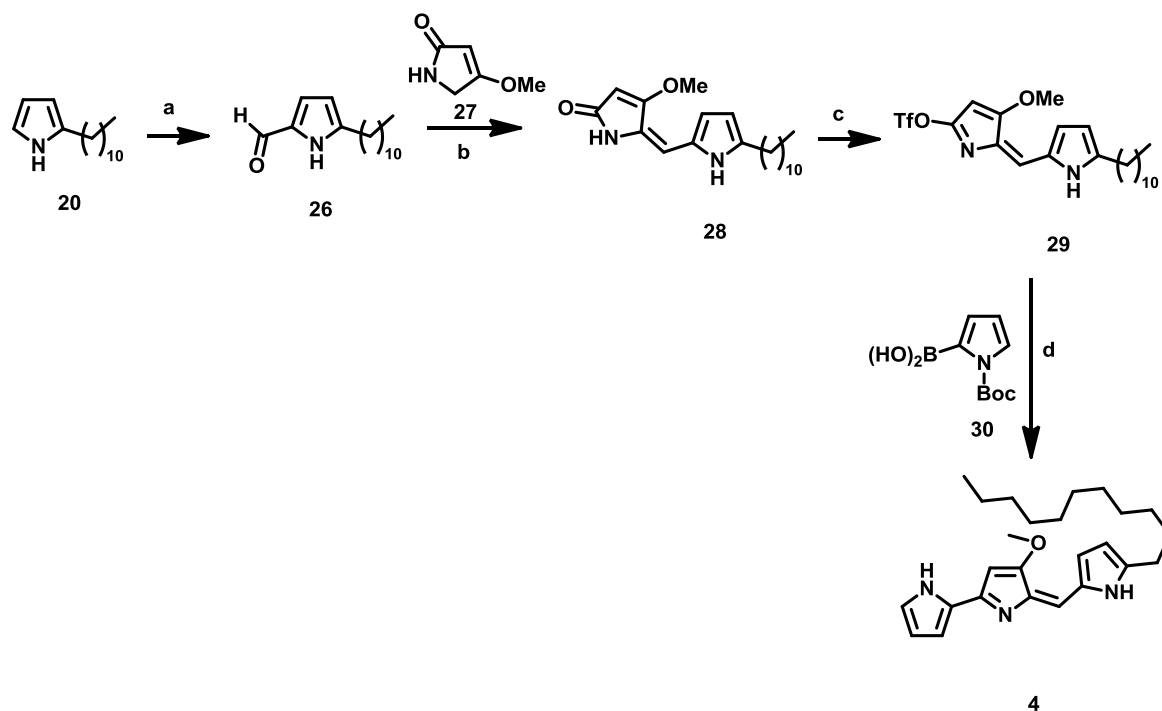
1.11 Total synthesis of prodiginine antibiotics

As a result of their interesting biological properties, the total synthesis of prodiginine antibiotics has been of particular interest. In addition, those prodiginines containing macrocycles have attracted considerable attention due to the synthetic challenge they present. Typically, the total synthesis of these compounds focuses on the synthesis of a macrocyclic monopyrrole moiety which is subsequently coupled with a bipyrrrole moiety.

1.11.1 Undecylprodigiosin **4** total synthesis

Undecylprodigiosin **4** has proved very amenable to total synthesis due to the simplicity of its structure. Indeed, Wasserman *et al* published a synthetic route to undecylprodigiosin **4** in 1966 that mimics the biosynthetic route in which MBC **19** is condensed with 2-UP **20** in an acidic ethanol solution.⁴⁰

An alternative synthetic route for the synthesis of undecylprodigiosin **4** that is more amenable to scale-up was reported in 1996 by D'Alessio *et al*.⁴¹ This is not dependent on the condensation of MBC **19** and 2-UP **20**, Scheme 1.2. Beginning from 2-UP **20**, D'Alessio utilised the Vilsmeier-Haack reaction to install an aldehyde group, yielding **26**, which was subsequently condensed with lactam **27** to provide **28**. Treatment of **28** with triflic anhydride afforded the corresponding triflate **29** which was subsequently cross-coupled with Boc-protected pyrroleboronic acid **30** using the Suzuki cross-coupling reaction to yield undecylprodigiosin **4**.

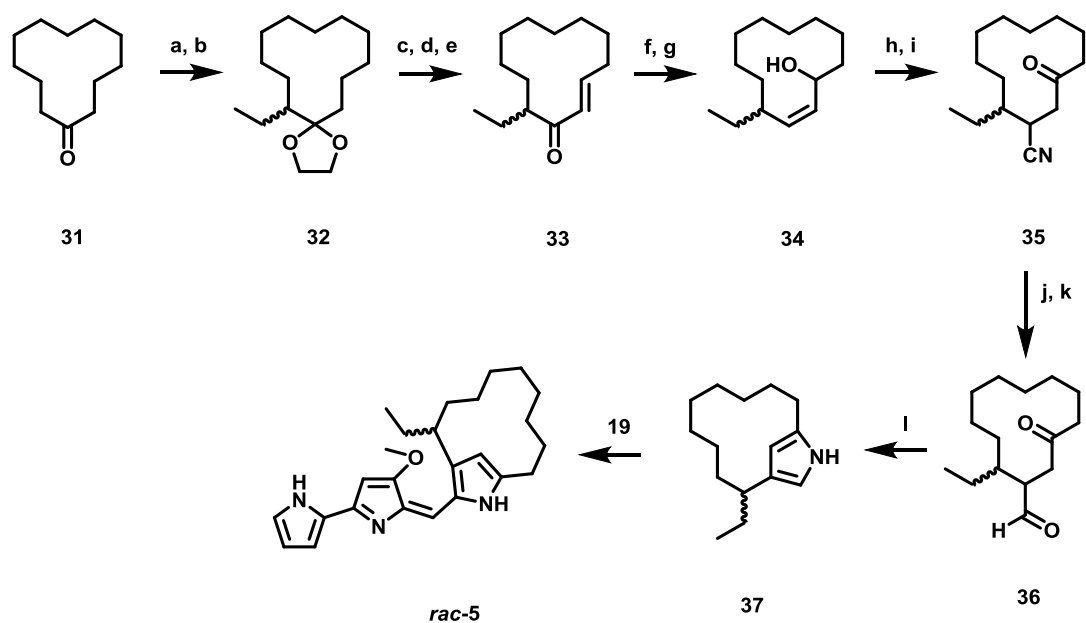


Scheme 1.2: The synthetic route developed by D'Alessio *et al* for undecylprodigiosin **4**;

a. POCl₃, DMF; b. NaOH, 60 °C; c. Tf₂O; d. Pd(PPh₃)₄, K₂CO₃, 90 °C

1.11.2 Total synthesis of metacycloprodigiosin **5**

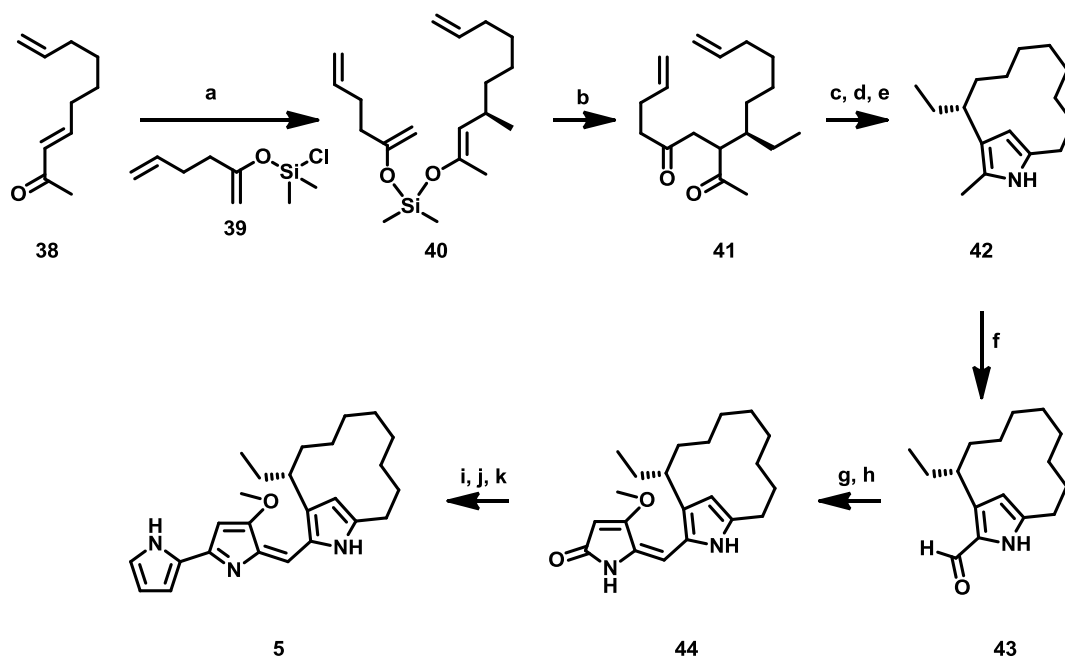
The first total synthesis of racemic metacycloprodigiosin *rac*-**5** was reported by Wasserman *et al* in 1969, Scheme 1.3.⁴² The enolate of cyclododecanone **31** was alkylated with ethyl bromide and subsequently protected as ketal **32**. Regioselective bromination of ketal **32**, followed by a high temperature elimination and ketal deprotection provided enone **33**. Epoxidation of this enone, followed by Wharton fragmentation of the resulting epoxide gave alcohol **34**. Oxidation and subsequent cyanation provided nitrile **35**, which was reduced, following ketone protection, and hydrolysed to give 1,4-dicarbonyl compound **36**. This was converted to the pyrrole **37** utilising the Paal-Knorr pyrrole synthesis. Coupling of the resulting pyrrole with MBC **19**, in an analogous manner to that used in the synthesis of undecylprodigiosin **4**, provided racemic metacycloprodigiosin *rac*-**5** in an overall yield of 0.02% over twelve linear steps.



Scheme 1.3: The synthetic route utilised by Wasserman for the total synthesis of racemic metacycloprodigiosin *rac-5*; **a.** NaNH_2 , EtBr; **b.** $\text{HO}(\text{CH}_2)_2\text{OH}$, *p*-TsOH; **c.** $\text{H}_5\text{C}_5\text{NH}^+\text{Br}_3^-$; **d.** DBN, 110°C ; **e.** *p*-TsOH; **f.** H_2O_2 , NaOH; **g.** N_2H_4 ; **h.** $\text{Na}_2\text{Cr}_2\text{O}_7$; **i.** KCN; **j.** *p*-TsOH, MeOH; **k.** DIBAL-H; **l.** $(\text{NH}_4)_2\text{CO}_3$

Since this pioneering work by Wasserman *et al* was published, several other synthetic routes have been developed for the synthesis of racemic metacycloprodigiosin *rac-5*, including two by Furstner *et al*.^{43,44} However, it was not until 2009 that the first enantioselective total synthesis of metacycloprodigiosin **5** was reported by Thomson *et al*, Scheme 1.4.⁴⁵ In their synthesis, the enantioselective 1,4-conjugate addition of ethyl cuprate to enone **38**, followed by trapping of the resulting enolate with a chlorosilyl enol ether **39** and oxidative C-C bond formation by treatment with cerium(IV) ammonium nitrate and 2,6-di-*t*-butylpyridine, afforded 1,4-diketone **41**. The stereochemistry of addition of the cuprate to the enone was controlled by addition of 6% (R, S)-JosiPhos and provided a 93:7 mixture of enantiomers. A ring-closing metathesis reaction utilising Grubbs second generation catalyst followed by hydrogenation afforded a macrocyclic 1,4-diketone, which was converted to the corresponding pyrrole **42** *via* the Paal-Knorr pyrrole synthesis. Oxidation of the methyl group in pyrrole **42** to an aldehyde **43** was achieved by treatment with DDQ. The synthesis was completed *via* a modification of the route developed by D'Alessio for the synthesis of

undecylprodigiosin **4**, Scheme 1.2. Comparison of the synthetic material with natural metacycloprodigiosin **5** confirmed the absolute stereochemistry as *R*.

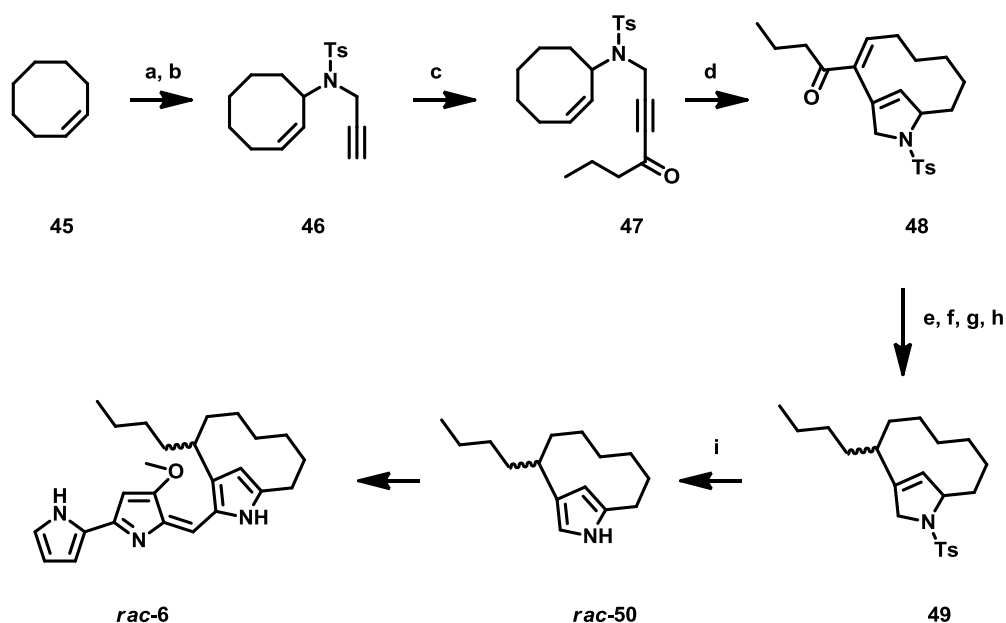


Scheme 1.4: The route utilised by Thomson and co-workers for the enantioselective total synthesis of metacycloprodigiosin **5**; **a.** EtMgBr, CuBr, (*R*, *S*)-JosiPhos; **b.** CAN, 2,6-di-*t*-Bu-Py; **c.** Grubbs II generation; **d.** Pd(OAc)₂, H₂; **e.** NH₄OAc; **f.** DDQ, H₂O; **g.** *i*-Pr₂Net, TMSOTf; **h.** HCl; **i.** Tf₂O; **j.** Pd(PPh₃)₄, **30**, Na₂CO₃; **k.** NaOMe

1.11.3 Total synthesis of streptorubin B **6**

The first total synthesis of racemic streptorubin B *rac-6* was not reported until 1998 by Furstner *et al*, Scheme 1.5.⁴⁶ This is presumably due to the fact that the 10-membered *ansa*-bridged carbocycle in streptorubin B **6** is much more strained than the corresponding 12-membered ring in metacycloprodigiosin **5**. In their synthetic route, Furstner and co-workers utilised an enyne metathesis reaction as a key step.

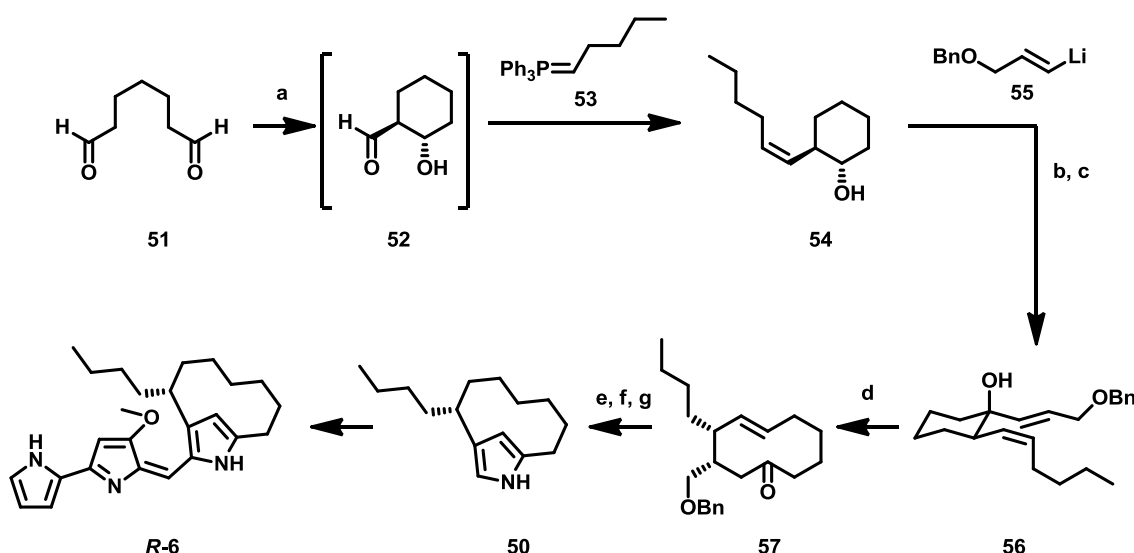
Treatment of cyclooctene **45** with elemental selenium and chloramine-T provided an amine which was alkylated with propargyl bromide to afford a tosylated alkyne **46** that was acylated to afford ketone **47**. An enyne metathesis skeletal rearrangement catalysed by palladium(II) chloride yielded the azabicyclododecane **48**. Reduction of the alkene and ketone followed by deoxygenation and removal of the N-tosyl protecting group gave pyrrole **rac-50**.



Scheme 1.5: The route utilised by Furstner and coworkers for the total synthesis of racemic streptorubin B **rac-6**; **a.** Se, Chloramine-T; **b.** NaH, Propargyl bromide; **c.** BuLi, ZnCl, MeCOCl; **d.** PtCl₂; **e.** Bu₃SnH, Pd(PPh₃)₄; **f.** LiAlH₄; **g.** PhOC(S)Cl; **h.** Bu₃SnH, AIBN; **i.** Potassium 1,3-diaminopropane

More recently, Thomson *et al* reported the first enantioselective total synthesis of streptorubin B **6**.⁴⁷ Their initial attempts to synthesise streptorubin B **6** focused on an analogous route to that already devised for the total synthesis of metacycloprodigiosin **5**, in which a ring-closing metathesis reaction was utilised to form the macrocycle. However, in the case of streptorubin B **6**, the corresponding ring-closing metathesis reaction was unsuccessful, presumably due to the increased transannular strain of the 10-membered ring relative to the 12-membered ring. Thus an anionic oxy-Cope rearrangement was used to form the macrocycle instead, Scheme 1.6. Thus, heptanedial **51** was treated with (*S*)-proline resulting in an

enantioselective *exo*-enol-6-*exo*-trig aldol reaction that gave aldehyde **52**, which was trapped *in situ* by exposure to the ylide **53**, yielding alkene **54**. Swern oxidation of the hydroxyl group in **54** to the corresponding ketone, followed by addition of organolithium **55** afforded dienol **56**. Treatment of the dienol with potassium hexamethyldisilazide resulted in the expected anionic oxy-Cope rearrangement. Subsequent simultaneous hydrogenation of the alkene and removal of the benzyl protecting group, followed by a Dess-Martin oxidation and Paal-Knorr pyrrole synthesis provided pyrrole **50**. An acid-catalysed coupling of pyrrole **50** with Boc-protect MBC provided streptorubin B **6**. This synthetic route yielded streptorubin B **6** in nine steps with an overall yield of 20%.



Scheme 1.6: The route utilised by Thomson for the enantioselective total synthesis of streptorubin B **6**; **a.** (*S*)-Proline; **b.** (COCl)₂, DMSO, *i*-Pr₂Et; **c.** **55**; **d.** KHMDs; **e.** H₂, Pd/C; **f.** Dess-Martin periodinane; **g.** NH₄OAc

Using this synthetic material, Thomson *et al* independently arrived at the same conclusion regarding the major atropisomer of streptorubin B **6** (see Section 1.10.2). Analysis of the product resulting from the condensation of dialkylpyrrole **50** and Boc-protected MBC revealed a 10:1 mixture of isomers, the major of which had different spectroscopic properties to natural streptorubin B **6**. However, after standing for ten days, reanalysis of the sample revealed that the mixture had completely converted to natural streptorubin B **6**. Thomson

et al were able to demonstrate that the initially formed product of the condensation reaction was actually the *syn* isomer of streptorubin B **6** which slowly isomerised to the more stable *anti* isomer over the course of ten days. Using the equilibrium ratio of 10:1 at room temperature, they were able to demonstrate that the *anti* isomer is approximately 1.4 kcal mol⁻¹ more stable than the *syn* isomer, presumably due to steric interactions between the *n*-butyl chain and the methoxypyrrolodipyrromethene core in the *syn* isomer.

Using CD spectroscopy, comparison of synthetic (7'*R*)-streptorubin B **6** prepared by Thomson *et al*, Scheme 1.6, with that isolated from *S. coelicolor* confirmed that natural streptorubin B **6** has 7'*S* absolute stereochemistry. This was further confirmed by X-ray crystallography.⁴⁷

1.12 Mutasynthesis of undecylprodigiosin and streptorubin B analogues

During his investigation of RedH, Stuart Haynes, a previous PhD student in the Challis group, employed a mutasynthesis approach in which MBC analogues were fed to a mutant blocked in the biosynthesis of MBC **19**.⁴⁸ He was able to demonstrate that RedH has a relatively relaxed substrate specificity with regard to the monosubstituted pyrrole with a number of other aromatic rings being tolerated, resulting in a range of novel undecylprodigiosin analogues, Figure 1.21. However, alterations to the central pyrromethene were not tolerated.

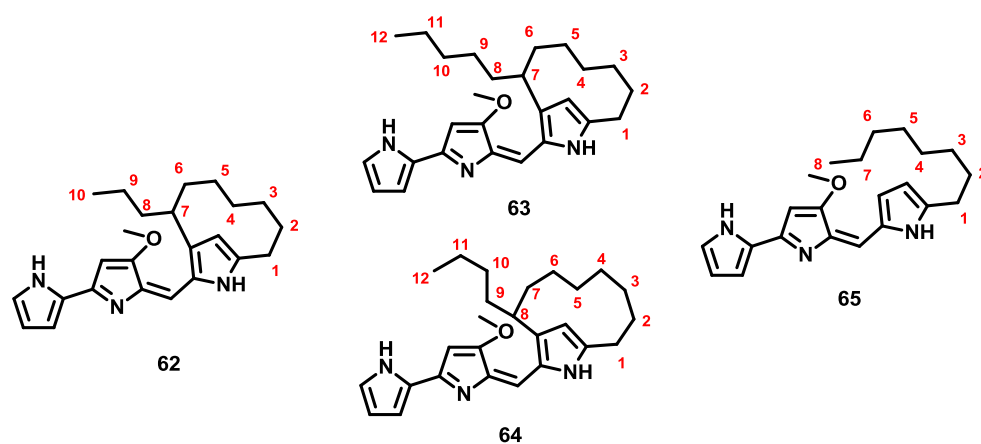


Figure 1.22: Streptorubin B and undecylprodigiosin analogues detected produced in mutasynthesis experiments utilising 2-UP analogues with altered hydrocarbon chain lengths

To further probe the substrate tolerance of RedG, Stuart Haynes synthesised a number of 2-UP analogues bearing additional functional groups within the undecyl chain. Analogues of 2-UP containing a methyl group at C-9' or C-10', an oxygen atom in place of C-3' and a double bond across C-10' / C-11' were all tolerated by RedG and yielded the corresponding streptorubin B analogues **66-69**, Figure 1.23.

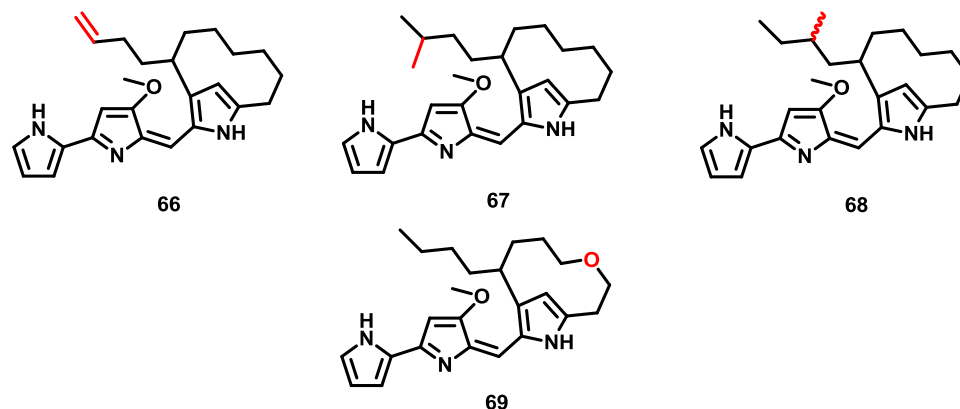


Figure 1.23: Streptorubin B analogues detected produced by mutasynthesis with 2-UP analogues bearing alterations to the hydrocarbon chain

In the case of the analogue with a methyl group at C-9', a second compound with the same *m/z* as streptorubin B analogue **68** was detected in LC-MS analyses of culture extracts. Isolation of this compound using reverse-phase HPLC and analysis by $^1\text{H-NMR}$ spectroscopy revealed proton signals at approximately 5.2 ppm, characteristic of alkene protons. It is proposed that this product results from a desaturation reaction that competes with oxidative

carbocyclisation; the regio- and stereochemistry of the alkene could not be determined unambiguously, Figure 1.24.

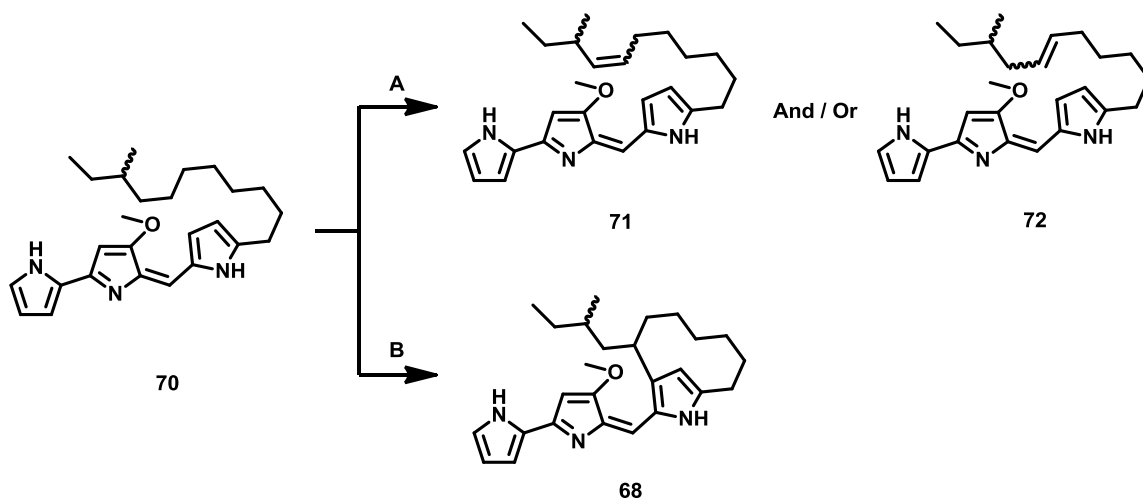


Figure 1.24: The streptorubin B analogue **68** resulting from oxidative carbocyclisation of undecylprodigiosin analogue **70** (route B) and the mixture of desaturated undecylprodigiosin analogues **71** and **72** proposed to result from a competing desaturation reaction (route A)

As discussed in Section 1.9, the iron(V) oxo-hydroxo species is proposed to abstract a hydrogen atom from C-7' resulting in a carbon-centred radical that subsequently attacks the pyrrole resulting in formation of the 10-membered *ansa*-bridged carbocycle. In the case of analogue **70**, it was hypothesised that the increased steric bulk at C-9' slows the rate of attack of the carbon-centred radical on the pyrrole. A second hydrogen abstraction from either C-6' or C-8' would result in the formation of the observed unsaturated undecylprodigiosin analogues **71** and/or **72**, Figure 1.25.

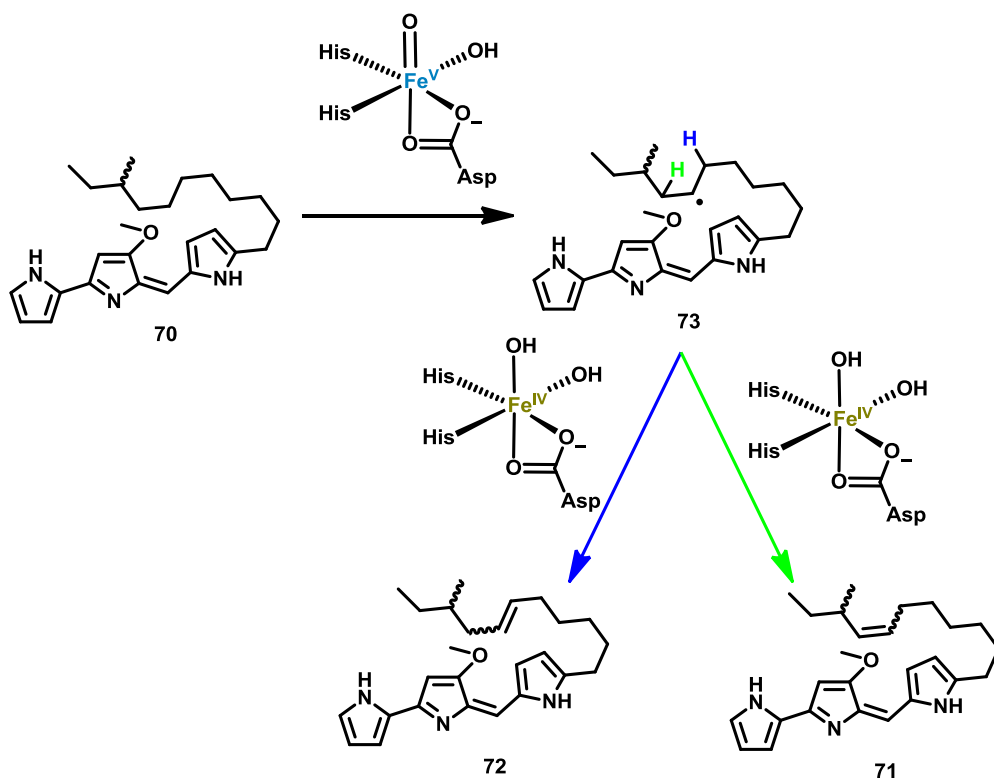


Figure 1.25: The proposed mechanism for the RedG-catalysed desaturation reaction observed for the undecylprodigiosin analogue **70**

Another interesting result was obtained when a 2-UP analogue containing an oxygen in place of C-6' was fed to mutants blocked in the biosynthesis of 2-UP **20**. In this case, no compound with the *m/z* corresponding to streptorubin B analogue **75** was detected. Instead, another prodiginine-like compound was detected by LC-MS that had a *m/z* corresponding to dealkylated undecylprodigiosin analogue **76**, Figure 1.26. However, due to the small quantity produced, it was not possible to purify and fully characterise this compound.

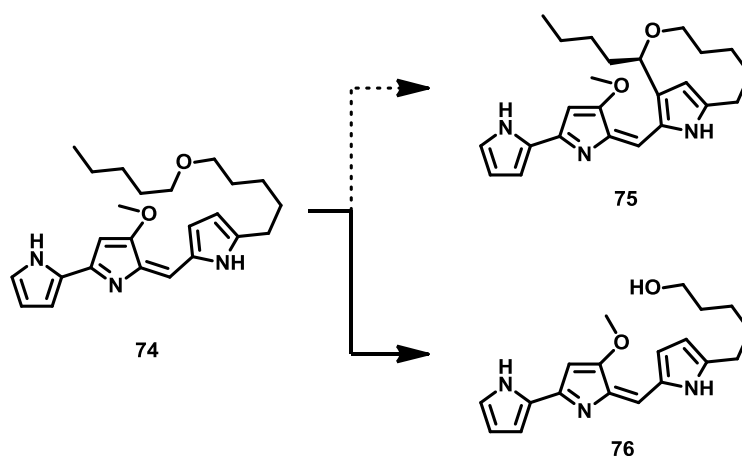


Figure 1.26: The proposed structure of the dealkylation product resulting from mutasynthesis with undecylprodigiosin analogue **74**. The streptorubin B **75** analogue was not observed

A plausible mechanism for the dealkylation process is shown in Figure 1.27. Initial abstraction of a hydrogen atom from C-7' would result in carbon-centred radical **77**. It was hypothesised that stabilisation of this radical by the adjacent oxygen atom lone pairs would slow down the addition of the radical to the pyrrole. Instead, hydroxylation occurs resulting in unstable hemiacetal **78**, which collapses to eliminate *n*-pentanal resulting in dealkylated product **76**. Attempts to detect *n*-pentanal as a by-product of this reaction failed, presumably due to its high volatility.

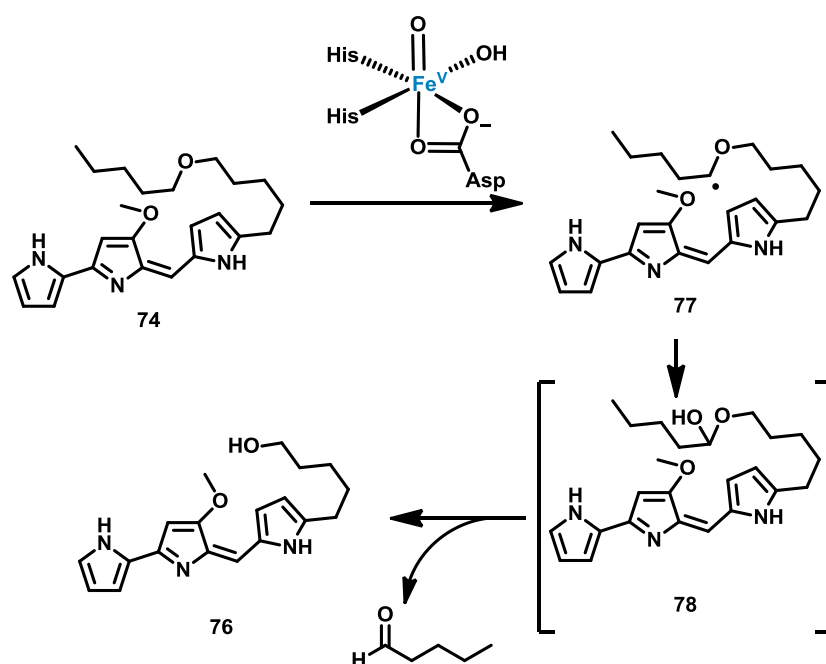


Figure 1.27: The proposed mechanism for the formation of dealkylated product **76**

1.13 Aims and objectives

The aim of this research project was to investigate the unusual oxidative carbocyclisation reaction catalysed by the non-haem iron-dependent Rieske oxygenase-like enzyme RedG. It was envisaged that a mutasynthesis approach could be employed involving feeding of chemically synthesised analogues of 2-UP **20**, bearing specific functional groups designed to probe various aspects of the proposed RedG catalytic cycle, to mutants of *S. coelicolor* blocked in the biosynthesis of 2-UP **20**, Figure 1.28.

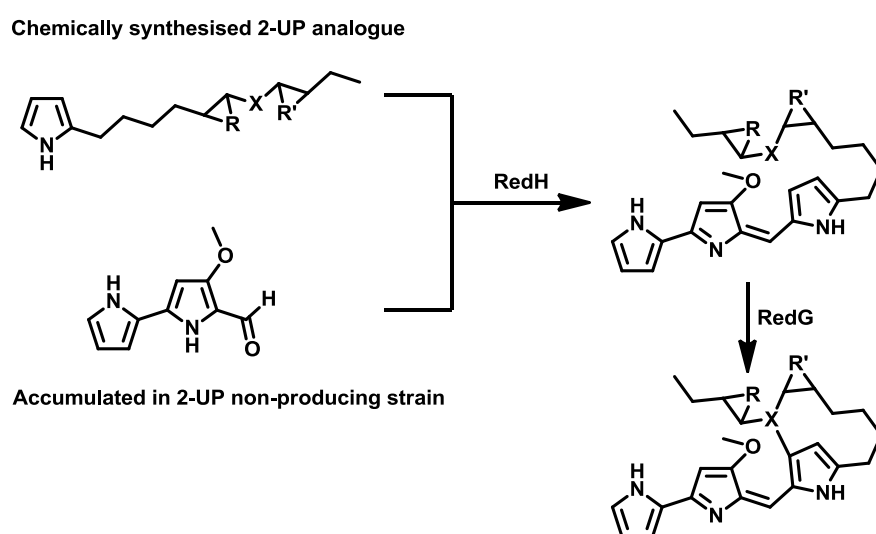


Figure 1.28: A schematic representation of the mutasynthesis strategy envisaged for investigating the oxidative carbocyclisation reaction catalysed by RedG

The resulting undecylprodigiosin and/or streptorubin B analogues would be extracted from the mutant strains and analysed using a variety of techniques including HR-LCMS and NMR spectroscopy.

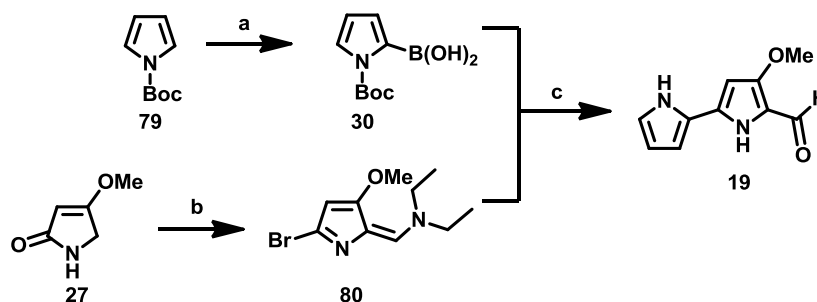
2. Results and discussion: Synthesis of 4-methoxy-2,2'-bipyrrole-5-carboxaldehyde, 2-undecylpyrrole and analogues

As discussed in Section 1.9, there are several interesting aspects of the proposed RedG catalytic cycle that could be probed using synthetic 2-UP analogues. These probes could be used to answer specific questions about the proposed catalytic cycle, e.g. does RedG utilise molecular oxygen, does RedG generate a carbon-centred radical or a carbocation, what is the stereochemical course of the RedG-catalysed reaction?

Before these analogues were synthesised, it was necessary to develop an efficient synthetic route to both late stage intermediates in the biosynthetic pathway, namely MBC **19** and 2-UP **20**. These synthetic intermediates would be required as positive controls in feeding experiments to ensure synthetic analogues can penetrate bacterial cells. In addition, it was desired that the synthetic route for 2-UP **20** was tolerant of a variety of functional groups to aid in the synthesis of the desired mechanistic probes.

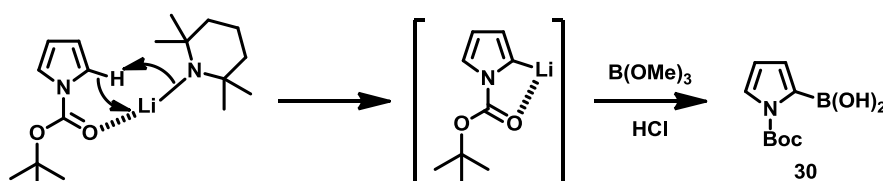
2.1 Synthesis of 4-methoxy-2,2'-bipyrrole-5-carboxaldehyde (MBC, 19)

Stuart Haynes, a previous PhD student in the Challis group, utilised a synthetic route originally reported in a patent relating to the synthesis of Obatoclox **10** for the synthesis of MBC **19**, Scheme 2.1.⁴⁹ More recently, this route has also been used in a number of papers detailing the total synthesis of several members of the prodiginine family.^{11,50,51}



Scheme 2.1: The synthetic route to MBC **19** utilizing a palladium catalysed cross coupling to install the biaryl bond; **a.** *n*-BuLi, 2,2,6,6-Tetramethylpiperidine, B(OMe)₃, THF, -78 °C, 54%; **b.** POBr₃, Et₂NCHO, CH₂Cl₂, 40 °C, 73%; **c.** i. Pd(OAc)₂, PPh₃, Na₂CO₃ ii. NaOMe, iii. HCl, 76%

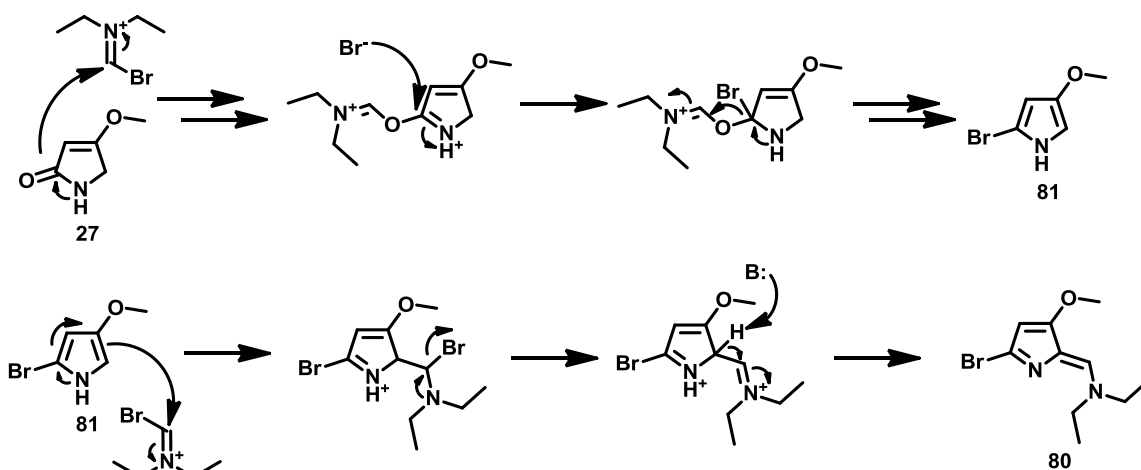
The first step in the synthesis of MBC **19** involved the conversion of N-Boc-pyrrole **79** to N-Boc-pyrrole-2-boronic acid **30** via regioselective lithiation at the 2-position using lithium 2,2,6,6-tetramethylpiperidide, Scheme 2.2.⁵² The presence of the *t*-butyloxycarbonyl group is essential to achieve regioselectivity for a number of reasons. Firstly, the electron-withdrawing properties of the *t*-butyloxycarbonyl group increases the acidity of the hydrogen atoms α to the pyrrole nitrogen atom, allowing efficient deprotonation. Secondly, the *t*-butyloxycarbonyl group ensures the regioselective lithiation by co-ordination of the carbonyl oxygen atom with the lithium ion.⁵³ This directing effect has been observed in a variety of aromatic systems containing a variety of different directing groups.



Scheme 2.2: The synthesis of N-Boc-pyrrol-2-boronic acid **30** via a directed lithiation using lithium 2,2,6,6-tetramethylpiperidide

Haloformylation of commercially available 4-methoxy-3-pyrrolin-2-one **27** with two equivalents of the Vilsmeier-Haack salt, generated *in situ* from diethylformamide and phosphorus(V) oxybromide, yielded the desired bromo-enamine in 73% yield. This reaction involves several separate steps, Scheme 2.3. After initial formation of the Vilsmeier-Haack salt, nucleophilic attack by the electron rich oxygen atom of the amide occurs, followed by

several addition-elimination and tautomerisation steps to provide 2-bromo-4-methoxypyrrole **81**. This electron rich aromatic ring can then react with another equivalent of Vilsmeier-Haack salt to provide the desired bromo-enamine **80**. It is important to ensure that the product is not exposed to aqueous acidic conditions because this would lead to rapid hydrolysis of the enamine, resulting in formation of the corresponding aldehyde.



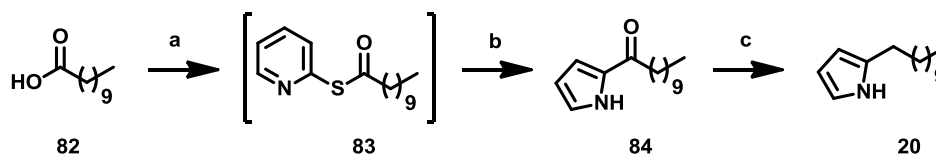
Scheme 2.3: The mechanism of the Vilsmeier-Haack reaction initially forming 2-bromo-4-methoxypyrrole **81** and subsequent formylation to yield the desired bromo-enamine **80**

The final step in the synthesis of MBC **19** was the palladium-catalysed Suzuki coupling between the boronic acid **30** and bromo-enamine **80**. Reduction of palladium(II) acetate *in situ* by heating with triphenylphosphine under anaerobic conditions provided the active palladium(0) species required for the coupling reaction. Methanolysis of the *t*-butyloxycarbonyl group and hydrolysis of the enamine was achieved during the work up to give MBC **19** as a precipitate. Washing of this insoluble product with cold acetone removed residual palladium and triphenylphosphine impurities.

2.2 Synthesis of 2-undecylpyrrole (2-UP, **20**)

A route devised by Stuart Haynes in which undecanoic acid **82** is activated as the pyridylthioester **83** and is subsequently treated with pyrrolmagnesium bromide to provide the

2-ketopyrrole **84** was utilised for the synthesis of 2-UP **20**.^{54,55,56} Reduction of the resulting ketone to the corresponding methylene would then yield 2-UP **20**, Scheme 2.4.



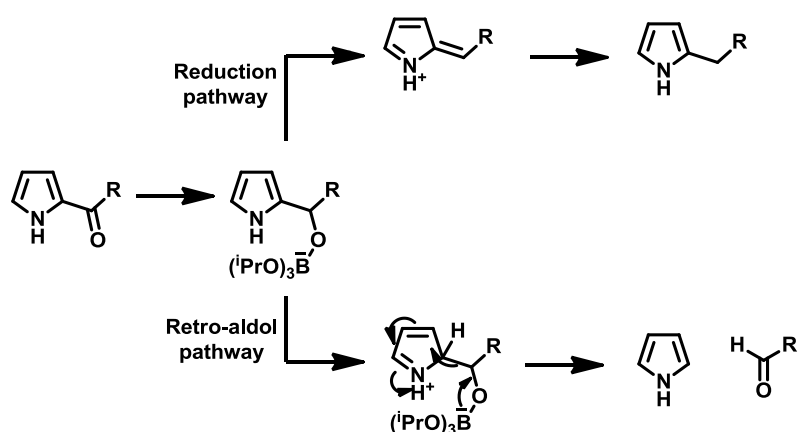
Scheme 2.4: The synthetic route to 2-UP **20**; a. $(\text{PyS})_2$, PPh_3 , toluene, $25\text{ }^\circ\text{C}$; b. EtMgBr , pyrrole, toluene, $-78\text{ }^\circ\text{C}$, 83%; c. NaBH_4 , IPA, $85\text{ }^\circ\text{C}$, 83%

Thus, undecanoic acid **82** was activated as the pyridylthioester **83** by treatment with 2,2'-dipyridyldisulphide and triphenylphosphine. This pyridylthioester **83** was then converted to the 2-ketopyrrole **84** by reaction with pyrrolylmagnesium bromide, generated *in situ* from freshly distilled pyrrole and ethylmagnesium bromide. It was necessary to distil the pyrrole immediately prior to use to remove polymeric pyrrole-derived impurities, in addition to removing any water present, which would quench the ethylmagnesium bromide during the reaction. Subsequent reduction of the ketone using excess sodium borohydride in refluxing reagent grade isopropanol provided 2-UP **20** in excellent yield of 83%.

This relatively simple method 2-UP **20** synthesis was shown by Stuart Haynes to be useful for the synthesis of a range of 2-UP analogues. It was therefore envisaged that this chemistry could be utilised to synthesise the desired mechanistic probes.

It should be noted that alkyl pyrroles are unstable, especially under acidic conditions and often degrade when allowed to stand for protracted periods of time. Typically, after purification, 2-UP **20** was a white waxy solid. However, after a week stored at $4\text{ }^\circ\text{C}$, the white solid began to turn brown and additional signals appeared in the $^1\text{H-NMR}$ spectrum. As a result, compounds were stored as the 2-ketopyrrole until required because the carbonyl group withdraws electron density from the pyrrole and thus prevents polymerisation. Indeed, 2-ketopyrrole **84** can be stored at $4\text{ }^\circ\text{C}$ for several months without apparent degradation.

In order for the final reduction of the ketone to proceed efficiently, it was essential that the sodium borohydride was refluxed in reagent grade isopropanol prior to the addition of the 2-ketopyrrole. If the reduction was performed in dry isopropanol, or below reflux temperature, substantial amounts of pyrrole and 1-undecanol by products were generated. These presumably arise *via* a retro-aldol type reaction, involving the elimination of pyrrole to give undecanal which in the presence of excess sodium borohydride, is further reduced to the corresponding alcohol, Scheme 2.5.



Scheme 2.5: The two competing pathways observed for final reduction of 2-ketopyrrole, illustrating the desired product and the undesired retro-aldol cleavage products and subsequent reduction

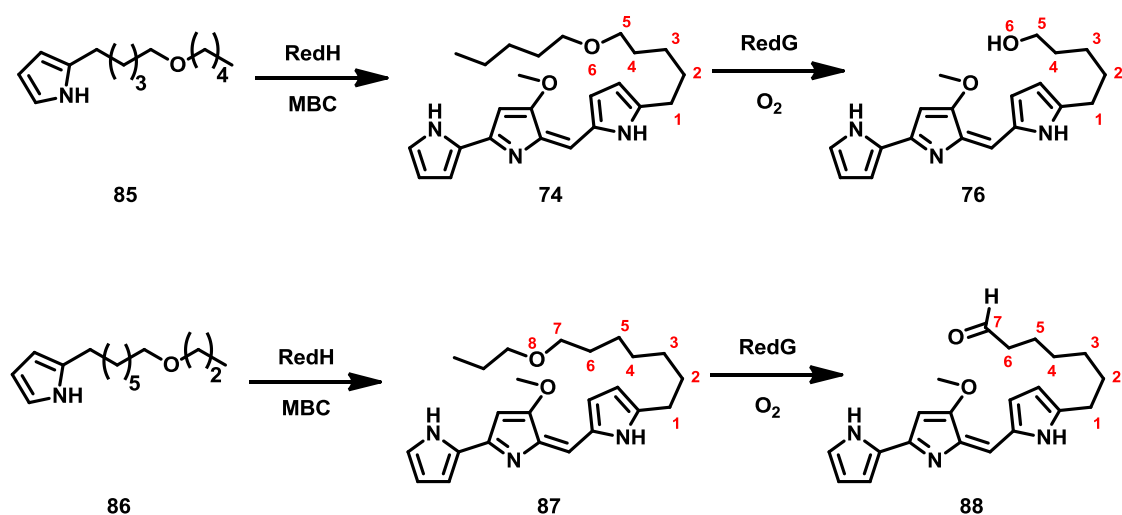
Protonation of the pyrrole appears to be required for the retro-aldol side reaction to occur. However, trace amounts of water present in the reagent grade isopropanol, would react with the sodium borohydride to produce sodium hydroxide in addition to sodium isopropoxide resulting from the reaction between the isopropanol and sodium borohydride. This increase in basicity would prevent the initial protonation required for the undesired retro-aldol side reaction to occur.

2.3 Synthesis of ether containing 2-UP analogues

Previous work by Stuart Haynes, as discussed in Section 1.12, indicated that RedG is not only capable of catalysing an oxidative carbocyclisation, but also a dealkylation reaction. However,

due to the small quantity produced, it was not possible to purify and fully characterise this compound. In order to further investigate this process, the 2-UP analogue **85** was resynthesised, in addition to an authentic standard of the putative dealkylation product **76**, Scheme 2.6.

This dealkylation process is proposed to occur *via* the formation of an unstable hemiacetal which, under acidic conditions, collapses with loss of *n*-pentanal, which is not detected due to its high volatility Scheme 1.27. It was therefore decided to synthesise an additional ether analogue with an oxygen atom replacing C-8' **86**. In this case, collapse of the hemiacetal formed by hydroxylation at C-7' would yield propanol and the corresponding aldehyde undecylprodigiosin analogue **88**, Scheme 2.6.

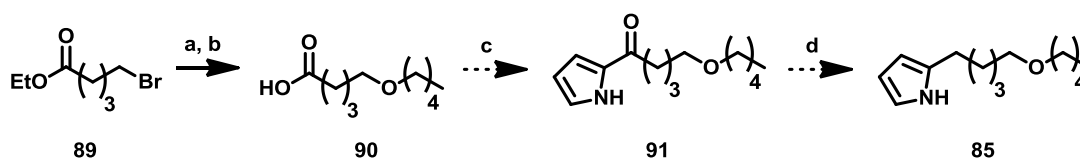


Scheme 2.6: The undecylprodigiosin analogue **74** and dealkylated product **76** expected to result from feeding 2-UP analogue **85** to the *redL* mutant and the undecylprodigiosin analogue **87** and dealkylated product **88** predicted to result from feeding 2-UP analogue **86** to the *redL* mutant

2.3.1 2-(5-Pentoxypentyl)-pyrrole **85**

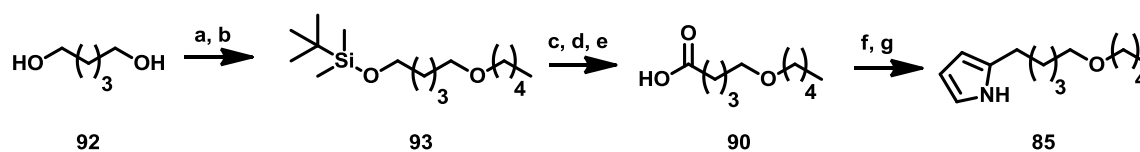
Initial attempts to resynthesise 2-UP analogue **85** followed the route developed by Stuart Haynes, Scheme 2.7. This route utilised the Williamson ether synthesis in which sodium *n*-pentoxide is generated *in situ* and alkylated with ethyl 5-bromopentanoate **89**.

Hydrolysis of the ethyl ester would generate the desired carboxylic acid **90**, which could then be converted to 2-UP analogue **85** via the route already outlined for the synthesis of 2-UP **20**.



Scheme 2.7: Stuart Haynes' synthetic route to 2-UP analogue **85**; **a.** $\text{CH}_3(\text{CH}_2)_4\text{OH}$, NaH, THF, <10% desired product; **b.** NaOH, THF:Water, 75 °C; **c.** $(\text{PyS})_2$, PPh_3 , toluene, 25 °C then EtMgBr, pyrrole, toluene, -78 °C; **d.** NaBH_4 , IPA, 85 °C

In practice, the yield of the initial alkylation reaction was very poor and resulted in a complex mixture of products. The undesired side products arose from a competing transesterification process, in which the sodium *n*-pentoxide attacks the carbonyl group of the ester resulting in the displacement of ethoxide. As a result, a mixture of ethoxide and pentoxide alkylation products was formed. Consequently, an alternative route was devised that avoids this problematic alkylation reaction, Scheme 2.8.



Scheme 2.8: The alternative synthetic route to 2-UP analogue **85**; **a.** NaH, *t*-BDMSCl, THF, 70%; **b.** NaH, 1-bromopentane, DMF, 80%; **c.** TBAF, THF, 0 °C, 97%; **d.** IBX, DMSO, 25 °C, 80%; **e.** Oxone, DMF, 25 °C, 88%; **f.** $(\text{PyS})_2$, PPh_3 , toluene, 25 °C then EtMgBr, pyrrole, toluene, -78 °C, 40%; **g.** NaBH_4 , IPA, 85 °C, 85%

The first step in this new synthetic route to **85** was the monosilylation of 1,5-pentanediol **92** with *t*-butyldimethylsilyl chloride. Typically, monoprotection of symmetrical diols is very difficult and usually results in a statistical distribution of the unprotected, mono- and diprotected products. However, work by McDougal *et al* showed that the yield of the desired monoprotected product could be improved if the monosodium salt is initially formed using one equivalent of sodium hydride, prior to the addition of the silylating reagent.⁵⁷ Since the

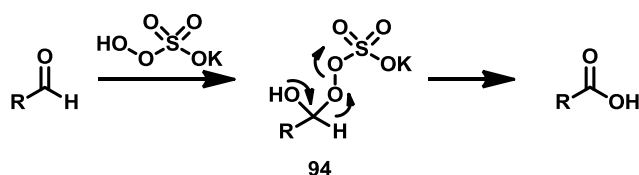
monosodium salt of the diol is insoluble in THF and precipitates out of solution, it is proposed that this prevents deprotonation of the alkoxide, which would lead to the diprotected species, from occurring. Upon addition of the silylating reagent, the small amount of monosodium salt in solution reacts, thus drawing some of the precipitate into solution. Using this procedure, a 70% yield of the monoprotected diol was obtained.

Alkylation of the alkoxide derived from the monoprotected alcohol with 1-bromopentane provided the protected ether **93**. Removal of the silyl protecting group with tetrabutylammonium fluoride afforded the corresponding alcohol.

Oxidation of this alcohol would provide the desired carboxylic acid **90** that could be used to complete the synthesis of 2-UP analogue **85**. Methods for oxidation of alcohols directly to carboxylic acids, for example the Jones oxidation, typically require the use of harsh reaction conditions, in addition to extensive purification procedures to isolate the pure carboxylic acid. While it is possible to purify carboxylic acids using a variety of techniques, including recrystallisation, flash column chromatography and HPLC, these can often prove problematic. Due to the length of the chain in carboxylic acid **90**, it was expected that it would be an oil and that recrystallisation would therefore not be applicable. While it is possible to purify carboxylic acids using silica flash chromatography, the procedure is often complicated by the fact that the acid 'streaks', becoming very diffuse and difficult to detect in the fractions leading to a reduced yield. While reverse-phase HPLC could be used to purify the carboxylic acid **90**, this is often a laborious and time consuming procedure and was thus avoided.

To circumvent such potential problems, an alternative method for oxidising the alcohol to the carboxylic acid was required. A search of the literature revealed a method for oxidising aldehydes to the corresponding carboxylic acids using Oxone (potassium peroxymonosulphate).⁵⁸ One advantage of this method is that a simple aqueous workup provides the pure carboxylic acid. It is proposed that this reaction proceeds *via* a Baeyer-

Villiger type mechanism in which a peroxyacetal **94** is formed, which undergoes rearrangement resulting in the elimination of sulphate, Scheme 2.9.⁵⁹

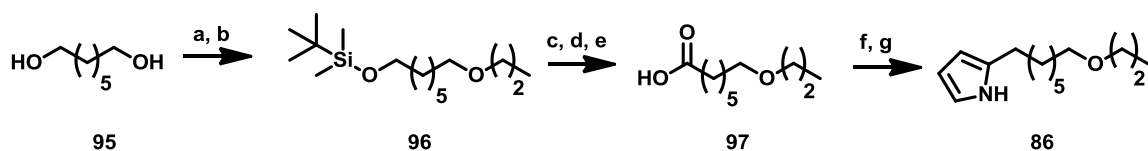


Scheme 2.9: The proposed mechanism for the oxidation of an aldehyde to the corresponding carboxylic acid using Oxone

Thus, a suitable method for oxidising the alcohol to the corresponding aldehyde was required. Several methods are available, including the Swern oxidation and the use of hypervalent iodine reagents such as 2-iodoxybenzoic acid (IBX).^{60,61,62} Treatment of the alcohol with IBX followed by oxidation of the aldehyde with Oxone provided the desired carboxylic acid **90** in a yield of 71% over two steps. Through subsequent work it was discovered that, provided the starting aldehyde was clean, the Oxone oxidation yielded the pure carboxylic acid. The synthesis of 2-UP analogue **85** was completed by coupling of carboxylic acid **90** with pyrrole and reduction of the resulting 2-ketopyrrole as described previously.

2.3.2 2-(7-Propoxyheptyl)-pyrrole **86**

The synthetic route to 2-UP analogue **86** is shown in Scheme 2.10. It is analogous to the route used for the synthesis of 2-UP analogue **85**.



Scheme 2.10: The synthetic route to 2-UP analogue **86**; **a.** NaH, *t*-BDMSCl, THF, 45%; **b.** NaH, 1-bromopropane, DMF, 84%; **c.** TBAF, THF, 0 °C, 93%; **d.** IBX, DMSO, 25 °C, 67%; **e.** Oxone, DMF, 25 °C, 94%; **f.** (PyS)₂, PPh₃, toluene, 25 °C then EtMgBr, pyrrole, toluene, -78 °C, 40%; **g.** NaBH₄, IPA, 85 °C, 85%

An interesting point to note is the difference in yields for the initial monosilylation reaction. In the case of 1,5-pentandiol **92** a yield of 70% was achieved. However, when 1,7-heptandiol **95** was used, the yield was only 45%. This is proposed to be due to the decreased polarity of the monosodium salt of 1,7-heptandiol, resulting from the increased alkyl chain length. As a result, a greater proportion remains in solution than the monosodium salt of 1,4-pentandiol. This allows more double deprotonation to occur, leading to more of the diprotected product.

Alkylation of the resulting primary alcohol with bromopropane provided the desired silyl protected ether **96** in 84% yield. Subsequent deprotection, oxidation to carboxylic acid **97**, coupling with pyrrole and reduction provided the desired 2-UP analogue **86**.

2.4 Synthesis of sulphur containing 2-UP analogues

It is proposed that RedG belongs to the non-haem iron-dependent oxygenase family of enzymes, more specifically the Rieske subfamily, which utilize molecular oxygen as the oxidant. To probe whether RedG utilises molecular oxygen as an oxidant, it was decided to synthesise a 2-UP analogue with a sulphur atom at C-7'. A sulphur atom placed at the site of C-H functionalisation would be expected to intercept the proposed iron(V)-oxo-hydroxy. This would be expected to result in formation of the corresponding sulphoxide. Indeed, it is known that sulphides react with metal-oxo species because such complexes have been utilized in the asymmetric oxidation of sulphides. For example, Fujita *et al* demonstrated that methyl phenyl sulphide **98** can be enantioselectively oxidised to a sulphoxide using oxovanadium(IV) complex **99** in the presence of hydrogen peroxide, Figure 2.1.⁶³

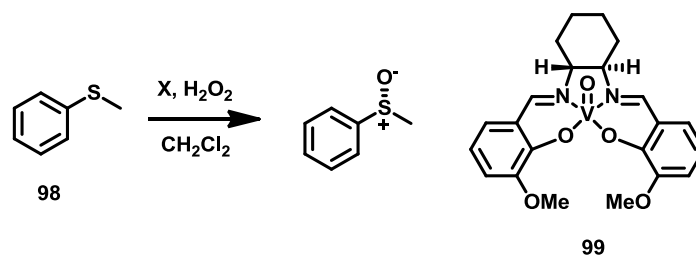


Figure 2.1: The use of a metal-oxo species capable of enantioselective oxidation of sulphides to the corresponding sulfoxides

The use of sulphides to trap reactive oxidants has been used to probe other non-haem iron-dependent enzymes. For example, Burzlaff *et al* utilised a sulphide analogue of δ -(L- α -aminoadipoyl)-L-cysteinyl-D-valine (ACV, **100**) to probe the mechanism of isopenicillin N synthase (IPNS), which is responsible for the formation of the β -lactam and thiazolidine rings of the penicillins, Figure 2.2.⁶⁴

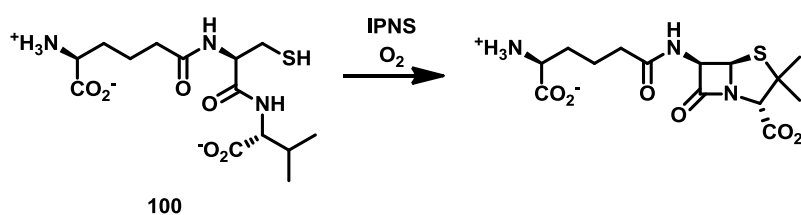


Figure 2.2: The reaction catalysed by the non-haem iron-dependent enzyme IPNS, resulting in the formation of the β -lactam and thiazolidine rings of the penicillins

To resolve the question of which of the two rings was formed first, they utilized X-ray crystallography and an analogue of ACV in which the D-valine residue is replaced with D-S-methyl-cysteine, B in Figure 2.3. They were able to demonstrate that the reaction proceeds with initial formation of the β -lactam, which gives rise to an iron-(IV)-oxo species that was trapped by reaction with the sulphide in the ACV analogue for form the corresponding sulfoxide, B in Figure 2.3. While they were unable to observe the iron(IV)-oxo species directly, but they were able to observe the sulfoxide product bound to the enzyme's active site using X-ray crystallography.

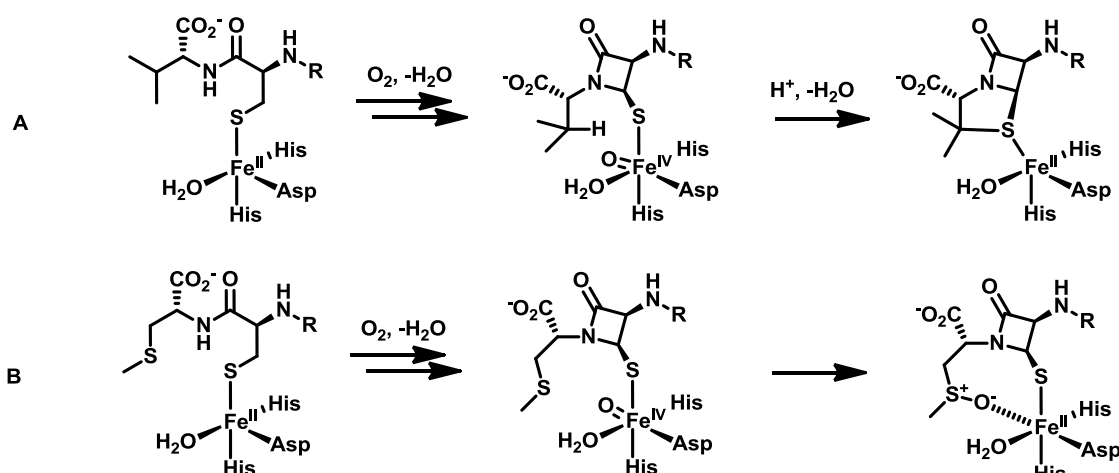
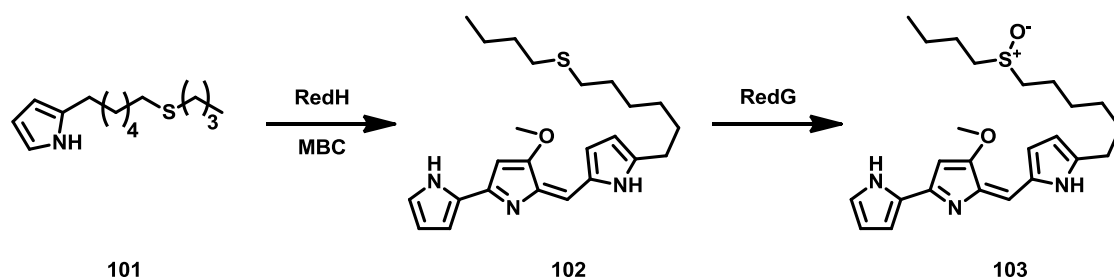


Figure 2.3: A. The proposed mechanisms for β -lactam and thiazolidine formation catalysed by IPNS; B. The proposed mechanism for the formation of the β -lactam formed in the active site of IPNS upon incubation with a sulphide containing analogue of ACV

It was therefore hypothesised that feeding a sulphide containing 2-UP analogue **101** to a mutant of *S. coelicolor* blocked in 2-UP biosynthesis would result in the formation of the corresponding undecylprodigiosin analogue **102**, which could trap the reactive oxidant formed by RedG to produce the corresponding sulfoxide **103**, Scheme 2.11.

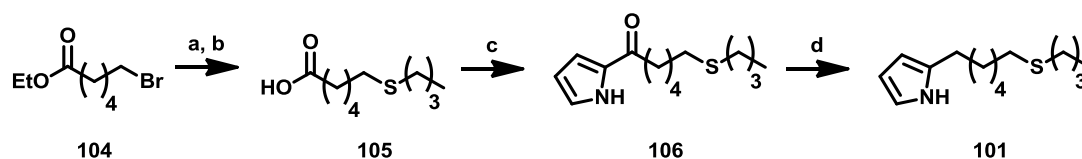


Scheme 2.11: The expected undecylprodigiosin analogues **102** and **103** expected to result from the feeding of 2-UP analogue **101** to a mutant of *S. coelicolor* blocked in the biosynthesis of 2-UP **20**

2.4.1 2-(6-Butylsulphanylhexyl)-pyrrole **101**

Sulphides are typically synthesised *via* the displacement of halides by thiolates.¹¹ Alkylation of lithium *n*-butylthiolate, generated *in situ* by treatment of *n*-butanthiol with *n*-butyllithium, with ethyl 6-bromohexanoate **104** followed by ester hydrolysis, generated carboxylic acid **105**

in high yields, Scheme 2.12. Carboxylic acid **105** was converted to 2-UP analogue **101** using the methodology described for the synthesis of 2-UP **20**.



Scheme 2.12: The synthetic route to 2-UP analogue **101**; **a.** $\text{CH}_3(\text{CH}_2)_3\text{SH}$, $n\text{-BuLi}$, THF, 0 °C, 98%; **b.** NaOH , THF:Water, 75 °C, 96%; **c.** i. $(\text{PyS})_2$, PPh_3 , toluene, 25 °C ii. EtMgBr , pyrrole, toluene, -78 °C, 81%; **d.** NaBH_4 , IPA, 85 °C, 71%

During the synthesis of **101**, it was noticed that storage of the sulphide-containing intermediates in air resulted in partial oxidation to the corresponding sulphoxides. To prevent this unwanted oxidation process, all intermediates were stored under an inert atmosphere of argon. However, even with these measures in place, small amounts of the corresponding sulphoxide could be detected in the mass spectrum of the final 2-UP analogue **101**. As a result, purification by column chromatography was performed immediately before the feeding experiments to remove the sulphoxide.

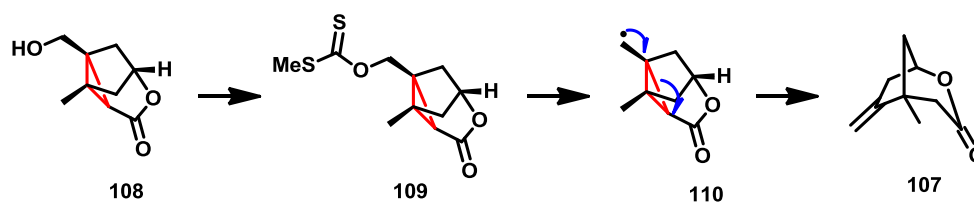
2.5 Synthesis of cyclopropane containing 2-UP analogues

As discussed in Section 1.9, it is proposed that the RedG-catalysed reaction involves abstraction of a hydrogen atom from C-7' of undecylprodigiosin **4** to generate a carbon-centred radical. This radical is then proposed to attack the pyrrole resulting in the formation of the 10-membered carbocycle present in streptorubin B **6**, after rearomatisation *via* abstraction of a second hydrogen atom.

Probes that undergo a characteristic skeletal rearrangement upon formation of a radical have been widely used to investigate the involvement of radical intermediates in a range of enzymatic and non-enzymatic reactions. One such species that undergoes such a skeletal rearrangement is the cyclopropylcarbinyl radical. Thus, cyclopropane-containing mechanistic

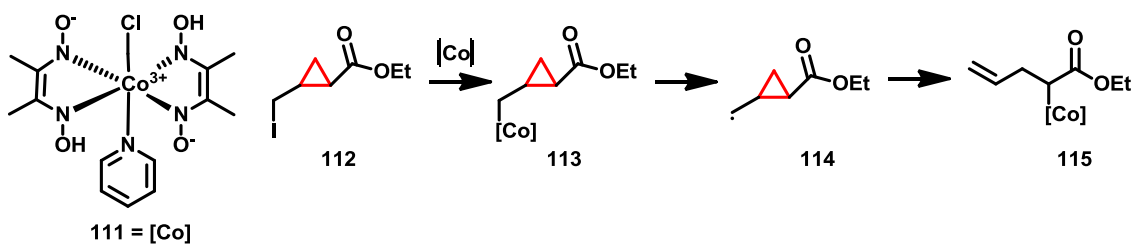
probes are commonly used to detect radical intermediates. Depending on the ratio of unrearranged to rearranged products obtained using such probes, an estimate of the radical lifetime can be obtained.⁶⁵

The rearrangement of cyclopropylcarbinyl radicals has been used extensively in organic synthesis. One example, reported recently by Danishefsky *et al* in the total synthesis of the natural product spirotenuipesines A and B, is the synthesis of dienophile **107**, Scheme 2.13.⁶⁶ Cyclopropane **108** was converted to the [3.2.1]bicyclolactone **107** by a skeletal rearrangement of radical **110** generated from the corresponding xanthate **109**.



Scheme 2.13: The synthetic route to dienophile **107** used by Danishefsky *et al*. The cyclopropane is highlighted in red. Only half of the curly arrows are shown for clarity

In addition to their use in organic synthesis, cyclopropanes have been used in a number of enzyme mechanism studies. While studying the enzyme α -methylene-glutarate mutase, a coenzyme-B₁₂ dependent enzyme, Golding *et al* investigated a model cobalt complex chloro(pyridine)cobaloxime **111** as an enzyme mimic. Using **111** and the cyclopropane containing substrate **112**, they aimed to investigate whether the cobalt atom remained attached to the substrate throughout the rearrangement, or whether a discrete carbon-centred radical was formed, Scheme 2.14.⁶⁷ They were able to demonstrate that the only observable product was **115** that resulting from rearrangement of cyclopropylcarbinyl radical **114**.



Scheme 2.14: The cobalt complex and cyclopropane substrate used by Golding *et al* to study the mechanism of α -methylene-glutarate mutase. The cyclopropane is highlighted in red

More recently, work conducted by Lipscomb *et al* on naphthalene dioxygenase (NDO), a Rieske oxygenase showing sequence similarity to RedG, used norcarane **116** and bicyclohexane **117** as mechanistic probes.⁶⁸ In each case, substantial amounts of products resulting from rearrangement of a cyclopropylcarbinyl radical were observed, Figure 2.4.

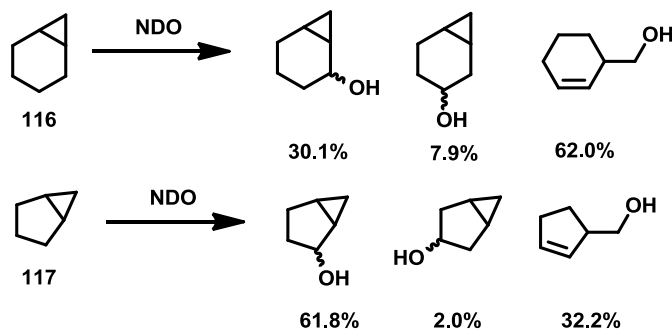
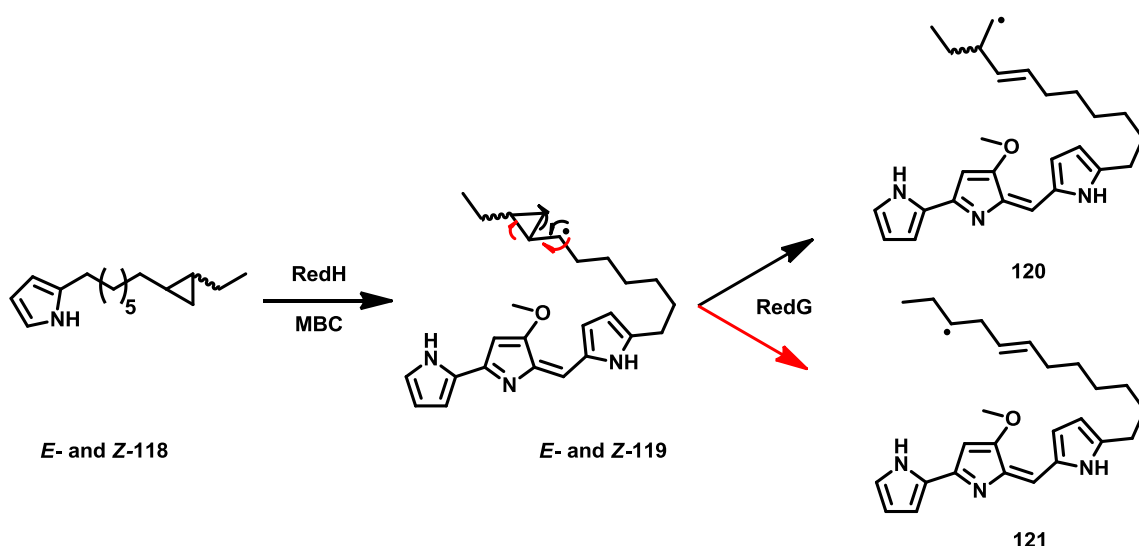


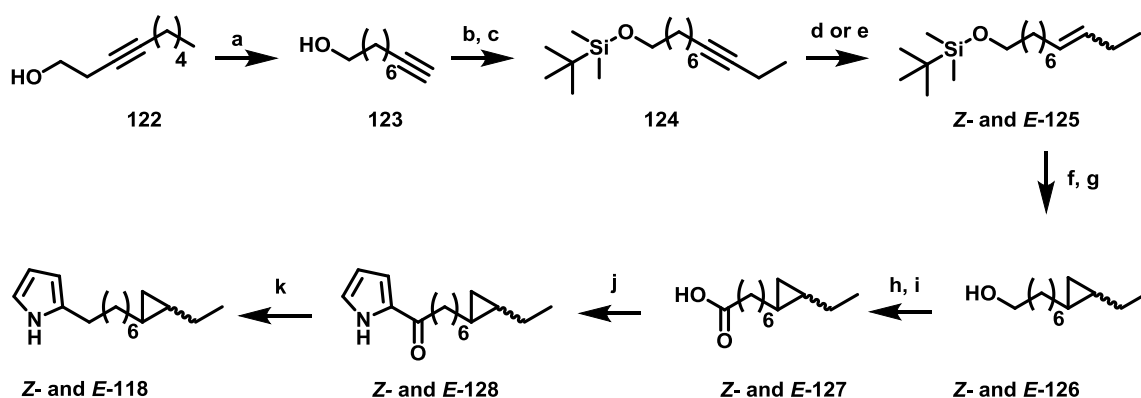
Figure 2.4: Products obtained from incubation of cyclopropane containing probes for radical intermediates with naphthalene dioxygenase

Thus, we decided to investigate feeding of cyclopropane containing 2-UP analogues **E**- and **Z**-**118** to a mutant of *S. coelicolor* blocked in the biosynthesis of 2-UP **20**. These would be expected to be converted to the corresponding undecylprodigiosin analogues **E**- and **Z**-**119** via the action of RedH, Scheme 2.15. Subsequent hydrogen atom abstraction at C-7' by RedG should trigger a skeletal rearrangement of the resulting cyclopropylcarbinyl radicals to one of the homoallylic radicals **120** or **121**. The fate of these homoallylic radicals is difficult to predict but in principal, they could undergo hydroxylation, desaturation or carbocyclisation.



Scheme 2.15: The two potential homoallylic radicals **120** and **121** expected to result from the feeding of **E- and/or Z-118** to a mutant of *S. coelicolor* blocked in 2-UP biosynthesis

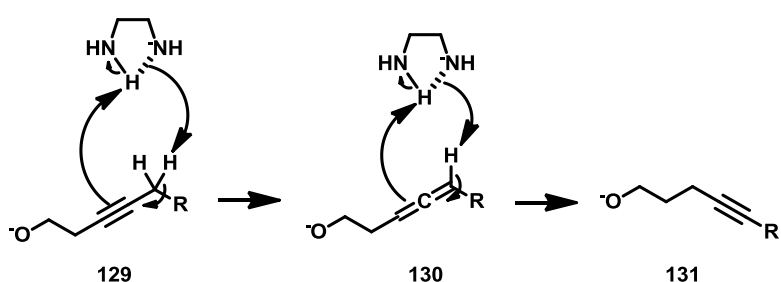
Cyclopropanes are commonly prepared from the corresponding alkene using the Simmons-Smith reaction.⁶⁹ This involves the treatment of an alkene with an organozinc carbenoid generated *in situ* from diethylzinc and diiodomethane. Since the carbenoid is delivered to both carbon atoms of the alkene simultaneously, the stereochemistry of the starting alkene is preserved.⁷⁰ Thus, the *cis*- and *trans*-cyclopropane-containing 2-UP analogues **E- and Z-118** can be obtained from the corresponding *cis*- and *trans*-alkenes. A synthetic route to both alkene isomers was therefore devised, Scheme 2.16.



Scheme 2.16: The synthetic route to **Z- and E-118**; **a**. Ethylene diamine, NaH, 60 °C, 67%; **b**. TBDMSCl, Imadazole, CH₂Cl₂, 94%; **c**. *n*-BuLi, EtI, DMPU, -40 °C to RT, 88%; **d**. H₂, Lindlar's catalyst, quinoline, THF, 98%; **e**. Na, NH₃ (l), -78 °C, 89%; **f**. ZnEt₂, CH₂l₂, CH₂Cl₂, used in next

step without purification; **g.** TBAF, THF, 0 °C to RT, *Z* 89%, *E* 58%; **h.** IBX, DMSO, 25 °C, *Z* 87%, *E* 70%; **i.** Oxone, DMF, 25 °C, *Z* 91%, *E* 95%; **j.** i. (PyS)₂, PPh₃, toluene, 25°C ii. EtMgBr, pyrrole, toluene, -78 °C, *Z* 69%, *E* 44%; **k.** NaBH₄, IPA, 85 °C, *Z* 60%, *E* 65%

The first step in the synthesis of the two cyclopropanes analogues **Z-** and **E-118** involves the isomerisation of commercially available 3-nonyn-1-ol **122** to the terminal alkyne isomer **123** in a 67% yield, utilising the 'alkyne zipper' reaction.⁷¹ The proposed mechanism for this isomerisation reaction is shown in Scheme 2.17.



Scheme 2.17: The proposed mechanism of the 'alkyne zipper' reaction

The monoanion of ethylene diamine deprotonates the methylene adjacent to the alkyne, with protonation of the alkyne itself, resulting in the formation of allene **130**. Deprotonation of the allene **130** concomitant with protonation regenerates an alkyne **131** that has migrated one carbon along the chain. This reaction is unusual because it converts the more stable internal alkyne to the less stable terminal alkyne. Presumably, reversible alkyne migration occurs continuously until the terminal alkyne is formed, at which point, under the highly basic conditions, it is deprotonated, trapping it as the acetylide anion. It should be noted that no intermediate allene or internal alkyne products were observed. Protection of the hydroxyl group in **123** with a *t*-butyldimethylsilyl group followed by alkylation of the terminal alkyne with iodoethane generated the desired alkyne **124** in excellent yield.

With silyl protected alkyne **124** in hand, a divergent synthetic route to the *cis*- and *trans*-**125** was envisaged. Stereoselective reduction of alkyne **124** would provide the required *cis*- and *trans*-alkenes required for the Simmons-Smith cyclopropanation. It is well known in organic

chemistry that treatment of an alkyne with sodium dissolved in liquid ammonia will provide the corresponding *trans*-alkene, whereas hydrogenation of an alkyne over Lindlar's catalyst affords the corresponding *cis*-alkene.⁷² Thus, alkyne **124** was converted to **Z**- and **E-125** in excellent yields of 98% and 89% respectively.

During the formation of *cis*-**125**, it was discovered that commercial Lindlar's catalyst was too active and substantial over-reduction to the corresponding alkane was observed. In order to prevent this, the catalyst was further deactivated by addition of quinoline. López *et al* have, on the basis of DFT calculations, hypothesised that quinoline adsorbs to the surface of the catalyst blocking some hydrogen and alkyne binding sites.⁷³ This, in addition to the effect of the lead poisoning, which disfavours alkene binding, improves the product selectivity of the catalyst. Indeed, when quinoline was added to the reaction, no over-reduction to the corresponding alkane was observed. It was not possible to unambiguously confirm the stereochemistry of the products of the reduction reactions employing Lindlar's catalyst and sodium in liquid ammonia due to signal overlap in the ¹H-NMR spectra, even at 700 MHz. However, GC-MS analysis indicated they are stereoisomers due to a small difference in their retention times.

Cyclopropanation of the alkenes was achieved by reaction with the organozinc carbenoid generated *in situ* from diethylzinc and diiodomethane. The product of these reactions were difficult to visualise on TLC plates and so the reactions were monitored using GC-MS. Thus, once the reaction had gone to completion, sodium hydroxide was cautiously added to quench them and precipitate the zinc-containing by-products, which could be easily removed *via* filtration. The *t*-butyldimethylsilyl groups were removed directly from the crude products using tetrabutylammonium fluoride, yielding **E**- and **Z-126** in yields of 58% and 89%, respectively, over the two steps.

Comparison of the $^1\text{H-NMR}$ of *E*- and *Z*-**126** revealed some subtle differences, Figure 2.5. In the case of *E*-**126** (top spectra in Figure 2.5) the multiplet at 0.08 ppm corresponds to H-9, the two diastereotopic methylene protons of the cyclopropane. However, in the case of *Z*-**126** (bottom spectra in Figure 2.5) the two multiplets at 0.52 ppm and -0.38 ppm correspond to the two diastereotopic methylene protons of the cyclopropane. In addition, singals for the two terminal methyl groups have substantially different chemical shifts; 0.87 ppm in the case of *E*-**126** and 0.98 ppm in *Z*-**126**.

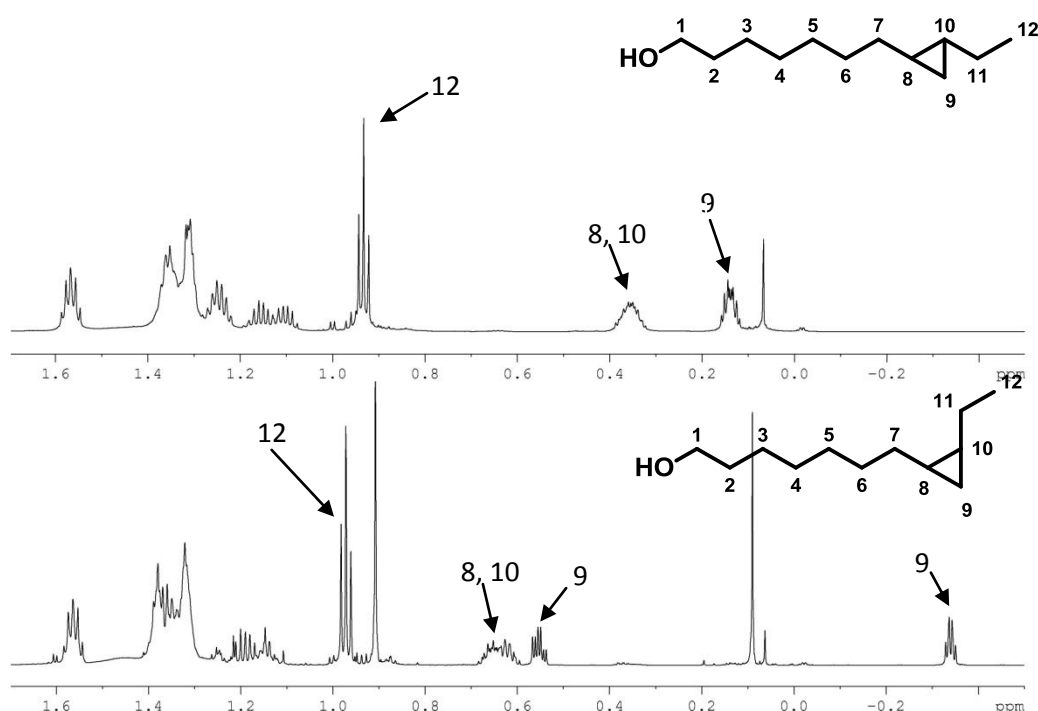


Figure 2.5: A comparison of the $^1\text{H-NMR}$ spectrum in CDCl_3 at 700 MHz of *E*-**126** (top spectrum) and *Z*-**126** (bottom spectrum). The two singlets present in the bottom spectra at 0.92 ppm and 0.10 ppm are due to residual *t*-butyldimethyl silyl fluoride impurities

This significant difference in the $^1\text{H-NMR}$ spectrum can be explained by the stereochemistry of the cyclopropane, Figure 2.6. In the case of *E*-**126**, the diastereotopic methylene protons (highlighted in green) are each *syn* to one alkyl chain and one proton, as highlighted by the red and blue arrows. Thus, they occupy similar chemical environments and their resonances therefore have similar chemical shifts in the $^1\text{H-NMR}$ spectrum. However, in the case of *Z*-**126**, the diastereotopic methylene protons of the cyclopropyl (highlighted in green) occupy very different chemical environments. One of these protons is *syn* to two alkyl groups,

indicated by the red arrows, whereas the other proton is *syn* to two protons, indicated by the blue arrows. As a result, the resonances due to these two diastereotopic protons have significantly different chemical shifts. These significant differences in the $^1\text{H-NMR}$ spectrum of *E*- and *Z*-**126** are consistent with the expected stereochemical outcomes of the alkyne reduction reactions.

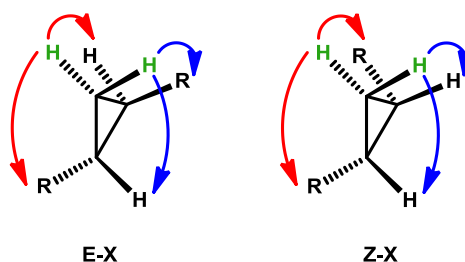


Figure 2.6: Stereochemical relationships of diastereotopic methylene protons (highlighted in green) with cyclopropane substituents, illustrating why the two sets of diastereotopic protons, give rise to significantly different $^1\text{H-NMR}$ signals

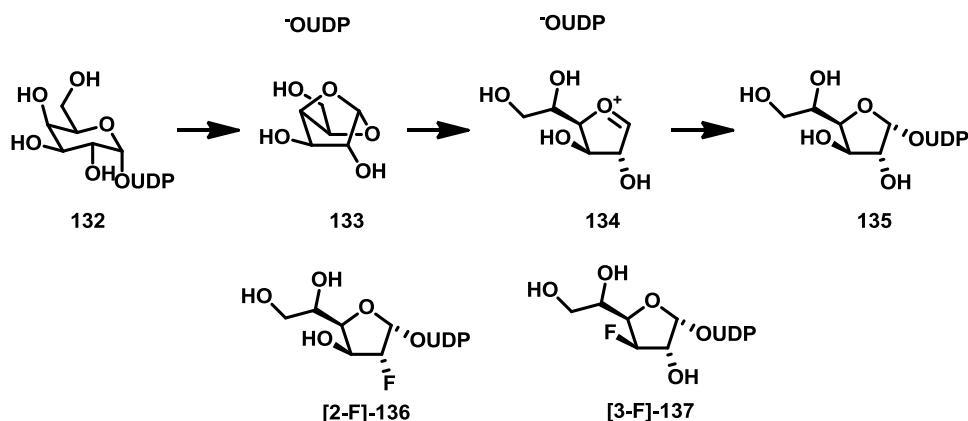
With primary alcohols *E*- and *Z*-**126** in hand, the synthesis of the 2-UP analogues *E*- and *Z*-**118** could be completed. Oxidation of the primary alcohols to the corresponding carboxylic acids, *via* the aldehydes, using the chemistry previously outlined for the synthesis of 2-UP analogue **85** provided *E*- and *Z*-**127** in good yields. Coupling of the carboxylic acids *E*- and *Z*-**127** with pyrrole and reduction of the resulting 2-ketopyrroles using the methodology described for the synthesis of 2-UP **20**, afforded 2-UP analogues *E*- and *Z*-**118**.

2.6 Attempted synthesis of fluorine containing 2-UP analogues

As discussed in Section 1.9, the proposed RedG catalytic mechanism involves the formation of a carbon-centred radical at C-7' which attacks the pyrrole to form the carbocycle. However, an alternative mechanism involves formation of a carbocation at C-7' which the pyrrole ring then nucleophilically attacks resulting in the macrocycle. To probe this, it was decided to synthesise 2-UP analogues with one or two fluorine atoms adjacent to C-7'. Due to its high

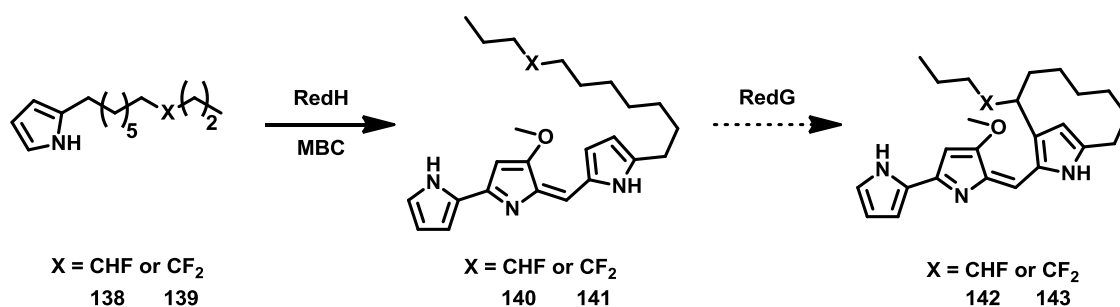
electronegativity, fluorine should destabilise formation of a carbocation and slow its rate of formation.

A similar approach has been used previously by Liu *et al* when studying the mechanism of UDP-galactopyranose mutase (UDP-Galp mutase), an enzyme present in several bacteria responsible for the isomerisation of UDP-galactopyranose **132** to UDP-galactofuranose **135**. One proposed mechanism for this isomerisation involves the formation of oxocarbenium intermediate **134**, Scheme 2.18. To probe this possibility, the kinetics of the reactions using **132** and two fluorinated analogues, [2-F]-**136** and [3-F]-**137**, as substrates was compared, demonstrating that the rate constant for both fluorinated analogues was significantly smaller than for the natural substrate (k_{cat} for natural substrate **132** = 27s^{-1} , k_{cat} for [2-F]-**136** = 0.033s^{-1} and k_{cat} for [3-F]-**137** = 5.7s^{-1}). This dramatic rate reduction was attributed to the electron withdrawing properties of the fluoro substituents, which destabilise the proposed oxocarbenium intermediate **134**.



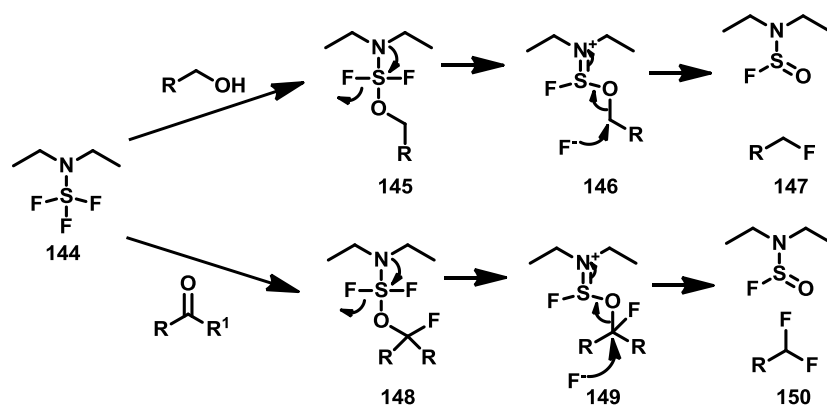
Scheme 2.18: The proposed mechanism for the isomerisation of **132** to **135** catalysed by UDP-galp mutase and the two fluorinated substrate analogues used to probe the mechanism

It was therefore hypothesised that feeding of 2-UP analogues **138** and **139** with one or two fluorine atoms at C-8' to a mutant of *S. coelicolor* blocked in the biosynthesis of 2-UP **20** would result in the formation of the corresponding undecylprodigiosin analogues **140** and **141** via the action of RedH, but that little or none of the corresponding streptorubin B analogues **142** or **143** would be formed, Scheme 2.19.



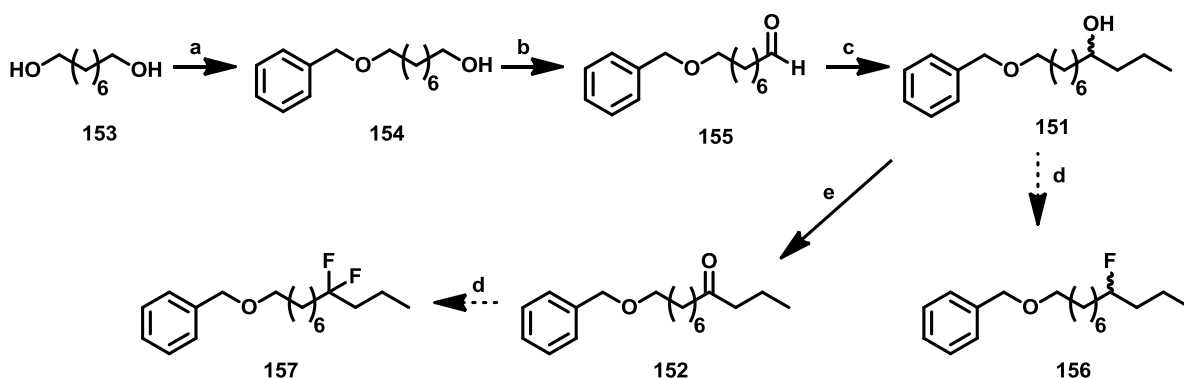
Scheme 2.19: The undecylprodigiosin analogues **140** and **141** expected to result from feeding of 2-UP analogue **138** and **139** to a mutant of *S. coelicolor* blocked in the biosynthesis of 2-UP. Little or none of the corresponding streptorubin B analogues would be expected to be formed if the RedG-catalysed oxidative carbocyclisation reaction proceeds *via* a C-7' carbocation intermediate

Deoxy-fluorination is commonly employed for the incorporation of fluorine atoms into organic molecules. Such reactions typically activate an alcohol or carbonyl compound towards nucleophilic attack by fluoride, resulting in the replacement of the hydroxyl group / oxygen atom with one or two fluorine atoms, generating mono-fluoro or *gem*-difluoro products, respectively. One commercially-available deoxy-fluorination reagent is diethylaminosulphur tetrafluoride (DAST) **144**. The generally-accepted mechanism for the fluorination of alcohols and carbonyl compounds by DAST **144** is shown in Scheme 2.20.⁷⁴ In the case of an alcohol, the initial nucleophilic displacement of a fluoride ion from DAST **144** by the hydroxyl group results in the alkyloxylaminosulphur difluoride intermediate **145**. Elimination of a second fluoride ion from this intermediate, followed by nucleophilic attack of fluoride on the activated carbon atom generates the monofluorinated product **147**. The mechanism for *gem*-difluorination of a carbonyl group is similar, Scheme 2.20.



Scheme 2.20: The generally-accepted mechanisms for the fluorination of alcohols and carbonyl compounds using DAST **144**

A synthetic route to 1-benzyloxy-8-undecanol **151** was designed that could to provide access to mono-fluorinated 2-UP analogue **138** and 1-benzyloxy-2-undecanone **152** to provide access to the *gem*-difluorinated 2-UP analogue **139**, Scheme 2.21.



Scheme 2.21: The proposed synthetic route to mono-fluorinated and di-fluorinated 2-UP analogues **138** and **139**; **a.** Ag₂O, BnBr, CH₂Cl₂, 74%; **b.** (COCl)₂, DMSO, Et₃N, CH₂Cl₂, -78 °C, 81%; **c.** *n*-PrMgBr, THF, -78 °C, 91%; **d.** DAST, CH₂Cl₂; **e.** (COCl)₂, DMSO, Et₃N, CH₂Cl₂, -78 °C, 82%

The first step in the synthesis was the mono-protection of 1,8-octandiol **153**. As shown in Scheme 2.20, the use of DAST **144** as a fluorination agent results in the formation of fluoride ions *in situ*. Thus, a silyl protecting group was not suitable. Monobenzylation was attempted using a similar approach to that described in Section 2.3.1 for the selective monosilylation of diols. However, the yield of the monobenzylated product **154** was only 50%; a significant amount of the unprotected and dibenzylated products were also formed. Examination of the

literature revealed an alternative method for the monobenylation of symmetrical diols utilising silver(I) oxide.⁷⁵ Thus, treatment of 1,8-octandiol **153** with benzyl bromide in the presence of silver(I) oxide provided the desired monobenzylated alcohol **154** in 74% yield.

Sauvé *et al* have proposed that the selectivity of this reaction arises from the co-ordination of the diol to the silver(I) ion, which acts as a Lewis acid, Figure 2.7. As a result, the acidity of the diol proton not involved in hydrogen bonding is increased, resulting in selective deprotonation, leading to benzylation.

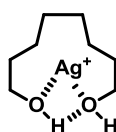


Figure 2.7: The proposed co-ordination of 1,8-octandiol to the silver(I) ion resulting in selective mono-benylation

Swern oxidation of the primary alcohol **154** to the corresponding aldehyde **155** followed by addition of propylmagnesium bromide afforded secondary alcohol **151** in 74% yield over two steps. It was anticipated that this secondary alcohol could be converted to the corresponding mono-fluorinated compound **156** by treatment with DAST **144**. Oxidation of the secondary alcohol **151** would yield the corresponding ketone **152**, which could then also be converted to the corresponding *gem*-difluoro compound **157** by treatment with DAST **144**.

Initial attempts to convert secondary alcohol **151** and ketone **152** to mono-**156** and *gem*-difluorinated **157**, respectively, using DAST **144** were unsuccessful. Only 3% of the desired monofluorinated product **156** was isolated along with 15% of a byproduct when secondary alcohol **151** was used (75% of the unreacted starting material was recovered). Moreover, it proved difficult to separate the monofluorinated product from the byproduct; several rounds of flash column chromatography were required. The ¹H-NMR spectrum of the byproduct is shown in Figure 2.8.

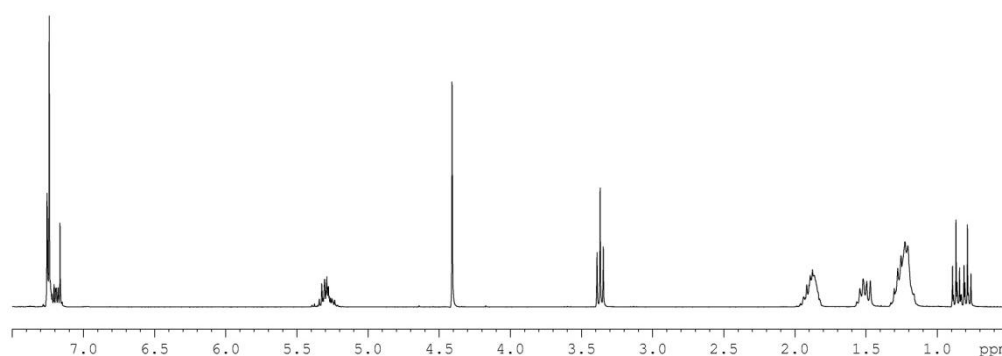
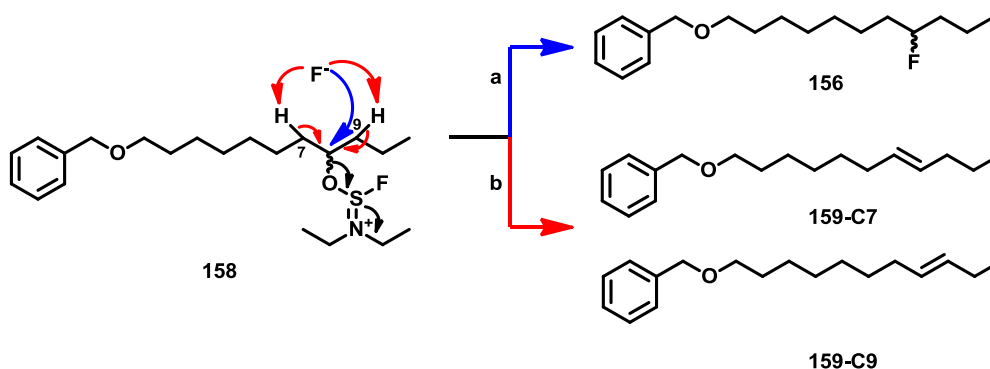


Figure 2.8: The $^1\text{H-NMR}$ spectrum in CDCl_3 at 300 MHz of the byproduct resulting from the attempted fluorination of alcohol **151**

Examination of the $^1\text{H-NMR}$ spectrum of this unknown byproduct revealed a signal typical of alkene protons at 5.30 ppm. Thus, it was hypothesised that the byproduct results from a competing elimination reaction, in which fluoride ions act as a base, resulting in the formation of an alkene **159**, Scheme 2.22. Since the starting material is a secondary alcohol, fluoride ions could deprotonate at either C-7 or C-9. This would give rise to two regioisomeric alkene byproducts **159-C7** and **159-C9**, respectively, Scheme 2.22. The observation of two triplets at 0.87 ppm and 0.79 ppm in the two products is consistent with this hypothesis.



Scheme 2.22: The mechanism for the nucleophilic displacement of activated alcohol **158** (pathway a, blue arrows) and the competing fluoride-promoted elimination reactions resulting in the formation of alkene side products **159-C7** and **159-C9** (pathway b, red arrows)

Elimination reactions are a known problem when attempting to use fluoride ion as a nucleophile. Indeed, fluoride can be utilised as a mild base in organic synthesis.^{76,77} In an effort to overcome the problem of the competing elimination reaction, a range of other

fluorinating agents were investigated, Figure 2.9. These included the other commercially available aminosulphur trifluorides Morpho-DAST **160** and Deoxo-Fluor **161** in addition to XtalFluor-E **162** and XtalFluor-M **163**, which were prepared from the corresponding aminosulphur trifluorides by treatment with boron trifluoride.⁷⁸ The results of these investigations are summarised in Table 2.1.

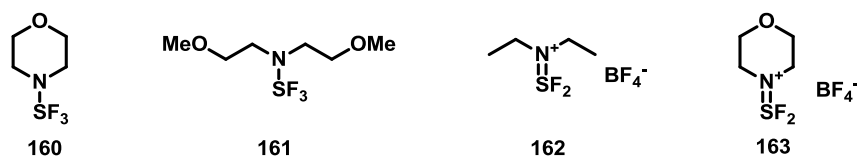
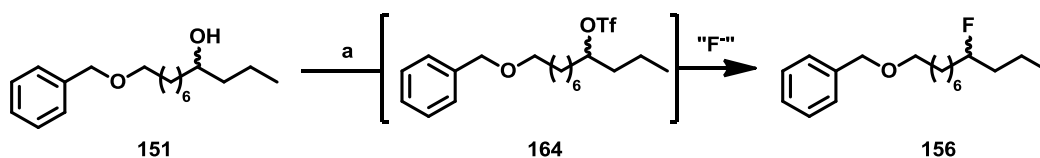


Figure 2.9: Alternative fluorinating agents investigated in attempts to overcome competing elimination in the conversion of secondary alcohol **151** to fluoride **156**

Reagent	Starting material		Fluorinated product		Elimination product	
	151	152	156	157		
144	75%	89%	3%	0%	15%	3%
160	95%	94%	1%	0%	4%	0%
161	83%	90%	5%	0%	10%	0%
162	50%	-	2%	-	38%	-
163	70%	-	6%	-	20%	-

Table 2.1: Yields of products isolated from various fluorination reactions

As can be seen from Table 2.1, none of the alternative methods investigated provided the mono- or *gem*-difluorinated products in acceptable yields. Thus, an alternative strategy for synthesis of the target compounds was investigated. Kim *et al* recently reported activation of a hydroxyl group as the corresponding triflate followed by displacement of the triflate with tetrabutylammonium bifluoride. Tetrabutylammonium fluoride and tetrabutylammonium dihydrogentrifluoride were also screened investigated as fluorinating agents using the triflate derivative of alcohol **164**, Scheme 2.23.



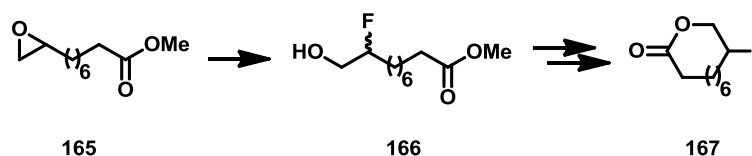
Scheme 2.23: An alternative approach investigated for the synthesis of the corresponding triflate and subsequent treatment with a variety of fluoride sources

The major products in each case resulted from elimination. Only trace amounts of desired fluorinated product was formed. As a consequence, a new strategy for the synthesis of fluorinated 2-UP analogues **138** and **139** was devised.

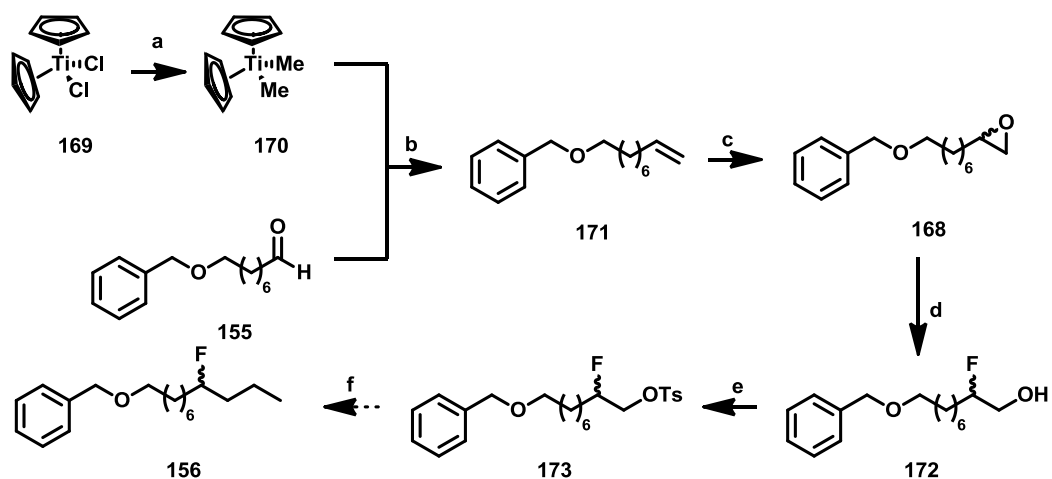
2.6.1 2-(8-Floroundecyl)-pyrrole **138**

Examination of the literature indicated that opening of an epoxide with fluoride could be used to install the fluorine atom. For example, Haufe *et al* used the regioselective ring opening of epoxide **165** with Olah's reagent⁷⁹ in their synthesis of fluorinated lactone **167**, Scheme 2.24.⁸⁰

Thus, a synthetic route to epoxide **168** was devised, Scheme 2.25.



Scheme 2.24: Opening of epoxide **165** with fluoride used by Haufe *et al* to install a fluorine atom in the synthesis of lactone **167**



Scheme 2.25: Alternative route investigated for the synthesis of fluorinated 2-UP analogue **138**; **a.** MeLi, Toluene, 0 °C, 98%; **b.** THF, 85 °C, 57%; **c.** *m*-CPBA, CH₂Cl₂, 0 °C, 84%; **d.** Py.xHF, CH₂Cl₂, 0 °C, 48%; **e.** TsCl, DMAP, Et₃N, CH₂Cl₂, 59%; **f.** EtMgBr, CuI, THF, 0 °C,

Aldehyde **155**, as described in Scheme 2.21, was converted to epoxide **168** via alkene **171** by treatment with dimethyltitanocene **170**^{81,82} followed by *m*-chloroperbenzoic acid. Regioselective opening of epoxide **168** using Olah's reagent afforded fluorinated product **172** in 40% yield. Large coupling constants for the H-13 and H-14 signals in the ¹H-NMR spectrum confirmed the presence of a fluorine atom, Figure 2.10.

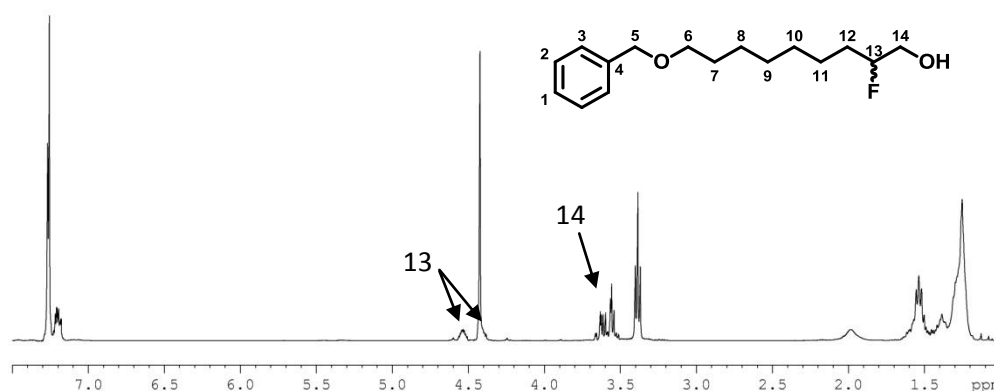


Figure 2.10: The ¹H-NMR spectrum in CDCl₃ at 400 MHz of monofluoro alcohol **172** showing the large coupling constant for the geminal proton H-13 and adjacent protons H-14

The displacement of tosylates by alkyl cuprates is well-precedented.⁸³ Thus, fluorinated alcohol **172** was converted to the corresponding tosylate **173** and subsequently reacted with the cuprate generated *in situ* from ethylmagnesium bromide and copper(I) iodide.

Surprisingly, the sole product of this reaction was alkene **171** resulting from loss of both the tosyl and fluoro groups, Figure 2.11. A possible mechanism for this unexpected reaction is shown in Scheme 2.26 involving single electron transfers from the cuprate.

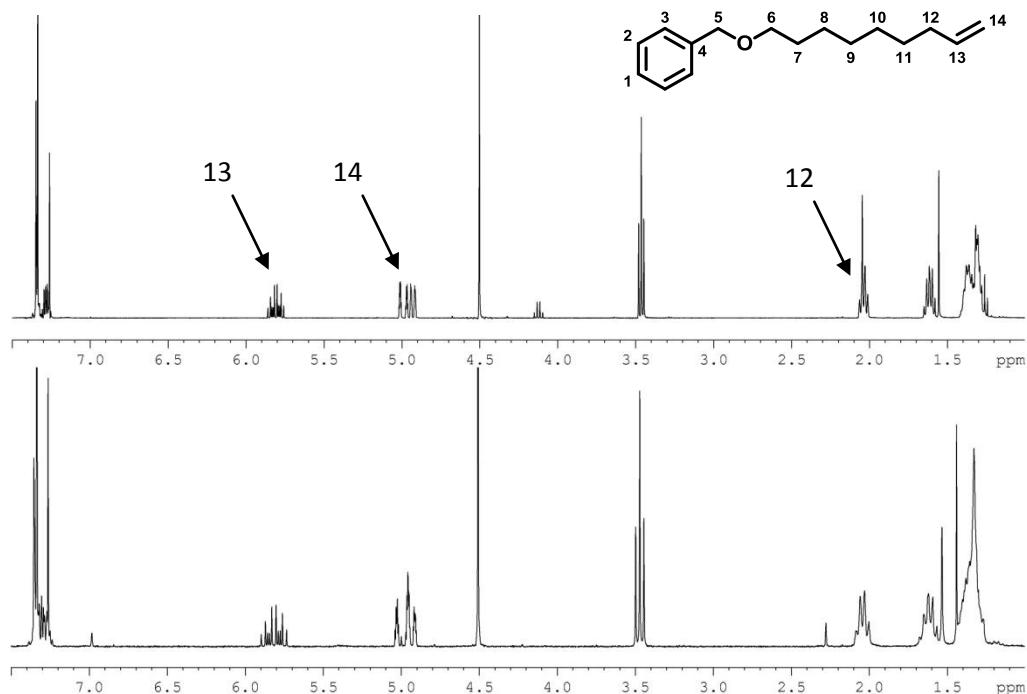
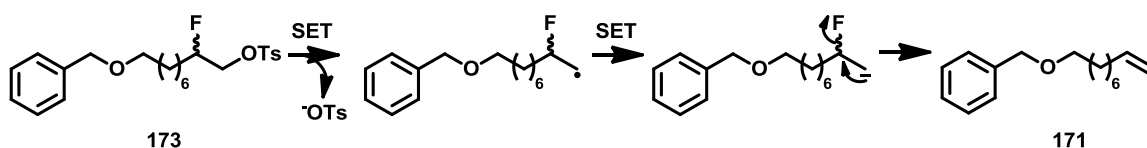


Figure 2.11: A comparison of the ¹H-NMR spectrum in CDCl₃ at 400 MHz of alkene **171** prepared from aldehyde **155** (top spectrum) and the ¹H-NMR spectrum in CDCl₃ at 250 MHz of the product resulting reaction of tosylate **173** with ethylmagnesium bromide and copper(I) iodide (bottom spectrum)

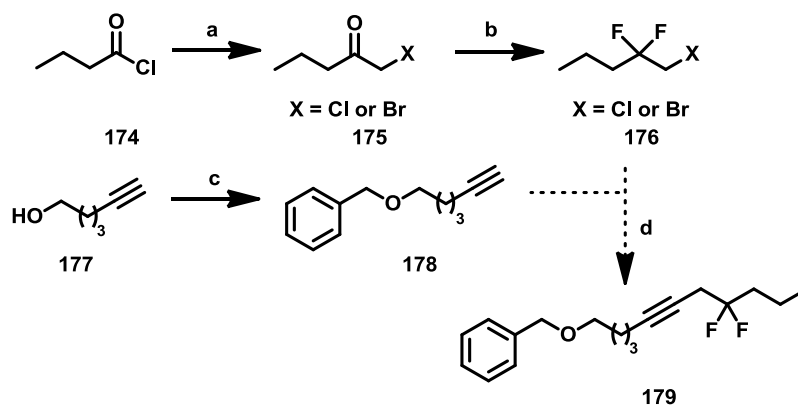


Scheme 2.26: A possible mechanism for the conversion of tosylate **173** to alkene **171** involving single electron transfer (SET) reactions

Due to the lack of success encountered with the synthetic approaches described above, as well as several other approaches that are not discussed here, it was decided to abandon the synthesis of monofluorinated 2-UP analogue **138** and focus our efforts on the *gem*-difluorinated 2-UP analogue **139** instead.

2.6.2 2-(8, 8-Difluoroundecyl)-pyrrole 139

Due to the failure of DAST to convert ketone **152** to its *gem*-difluoro derivative, an alternative route was devised for the synthesis of *gem*-difluorinated 2-UP analogue **139**, Scheme 2.27.⁸⁴



Scheme 2.27: The new synthetic route to *gem*-difluorinated intermediate **179**; **a.** TMS-CH₂N₂, 20% HBr in acetic acid, CH₃CN, 94%; **b.** DAST, CH₂Cl₂, 0 °C, 42%; **c.** BnBr, NaH, DMF, 65 °C, 85%; **d.** *n*-BuLi, THF, 65 °C

Thus, butanoylchloride **174** was converted to the corresponding bromoketone **175** by treatment with TMS-diazomethane and hydrobromic acid.⁸⁵ While it was anticipated that the bromide would be the exclusive product, a 3:1 ratio of bromide:chloride was isolated, as estimated from the ¹H-NMR spectrum, Figure 2.12.

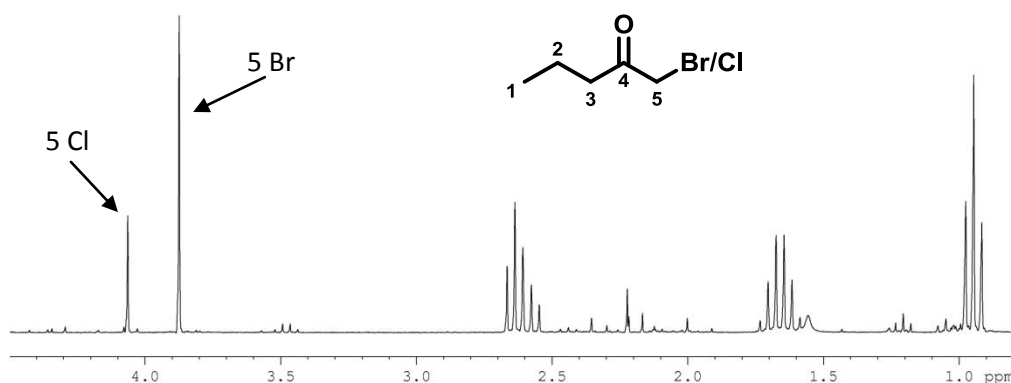


Figure 2.12: The ¹H-NMR spectrum in CDCl₃ at 400 MHz showing the ratio of brominated to chlorinated **175**

Treatment of the mixture of bromo- and chloro-**175** with DAST **144** yielded *gem*-difluoro bromide **176** as the sole product in 42% yield. Presumably *gem*-difluoro chloride **176** was lost

during the workup due to its greater volatility. Examination of the $^1\text{H-NMR}$ spectrum of **176** revealed a triplet at 3.44 ppm with a large coupling constant ($J = 13\text{Hz}$), consistent with a methylene group adjacent to a difluoromethylene group, Figure 2.13.

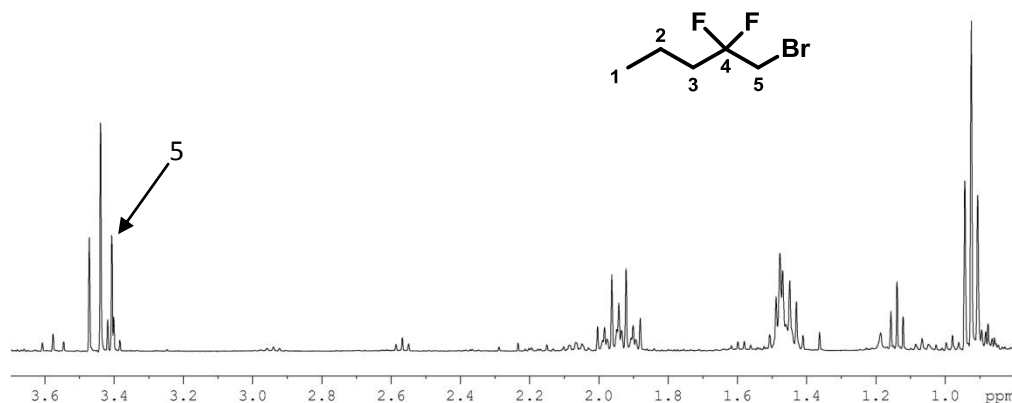


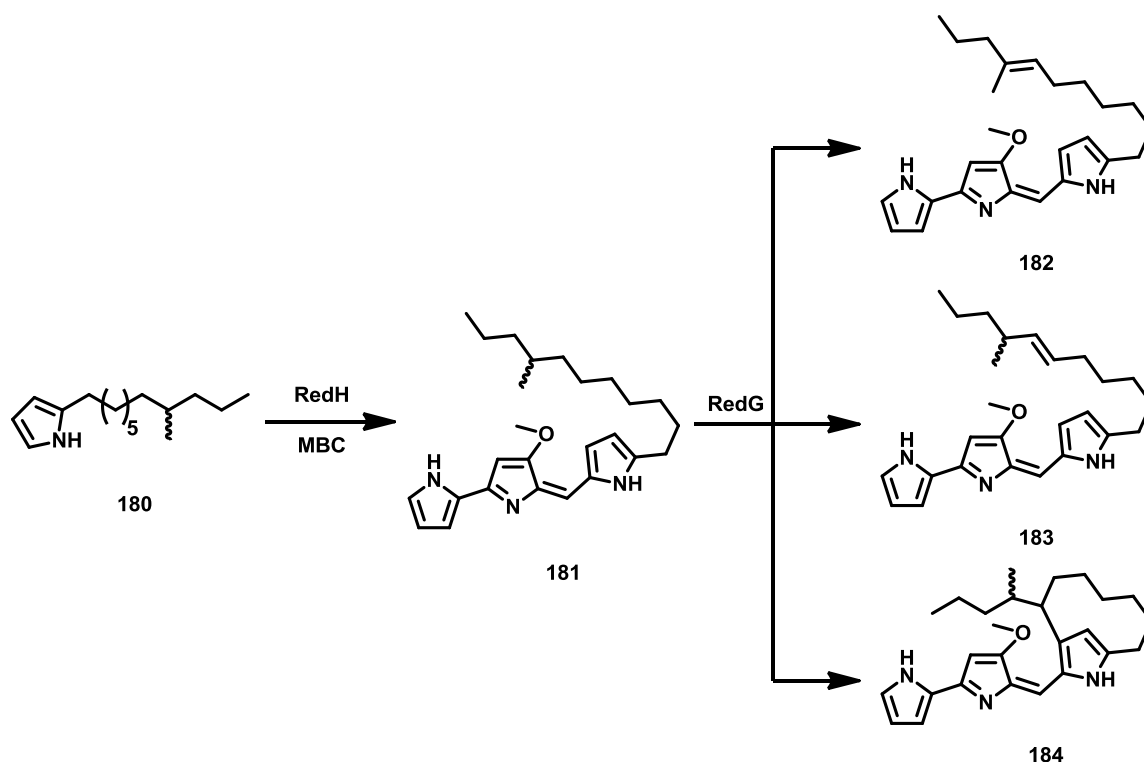
Figure 2.13: The $^1\text{H-NMR}$ spectrum in CDCl_3 at 400 MHz of *gem*-difluoro bromide **176**

With *gem*-difluoro bromide **176** in hand, alkylation of the acetylide resulting from deprotonation of alkyne **178** was investigated. Analysis of the reaction mixture by TLC and mass spectrometry after 16 hours stirring at room temperature revealed that no reaction had occurred. The reaction was repeated at $65\text{ }^\circ\text{C}$ overnight. Analysis of the reaction mixture by TLC and mass spectrometry indicated that it contained a complex, inseparable mixture of compounds. Due to time constraints, the synthesis of the *gem*-difluoro 2-UP analogue **139** was not investigated further.

2.7 Synthesis of methyl-branched 2-UP analogues

Previous work by Stuart Haynes, as discussed in Section 1.12, indicated that RedG catalyses the desaturation of a 2-UP analogue bearing a methyl substituent at C-9'. This desaturation reaction was proposed to result from increased steric bulk at C-9', due to the methyl group, which slows down the rate of cyclisation. To probe the generability of this desaturation reaction, a 2-UP analogue bearing a methyl substituent at C-8' **180** was synthesised. It was hypothesised that a greater proportion of desaturation to carbocyclisation would occur with

the C-8' methylated analogue than the C-9' methylated analogue due to the increased steric bulk in the vicinity of C-7', Scheme 2.28.

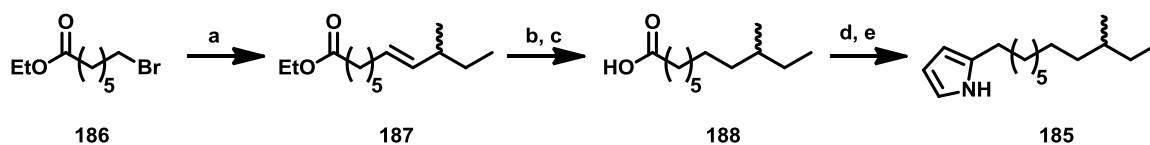


Scheme 2.28: The undecylprodigiosin analogue **181** and three potential oxidation products expected to result from the feeding of 2-UP analogue **180** to a mutant of *S. coelicolor* blocked in the biosynthesis of 2-UP

It proved necessary to resynthesize 2-UP analogue **185** bearing a methyl substituent at C-9' since the material provided by Stuart Haynes had degraded.

2.7.1 2-(9-Methylundecyl)-pyrrole **185**

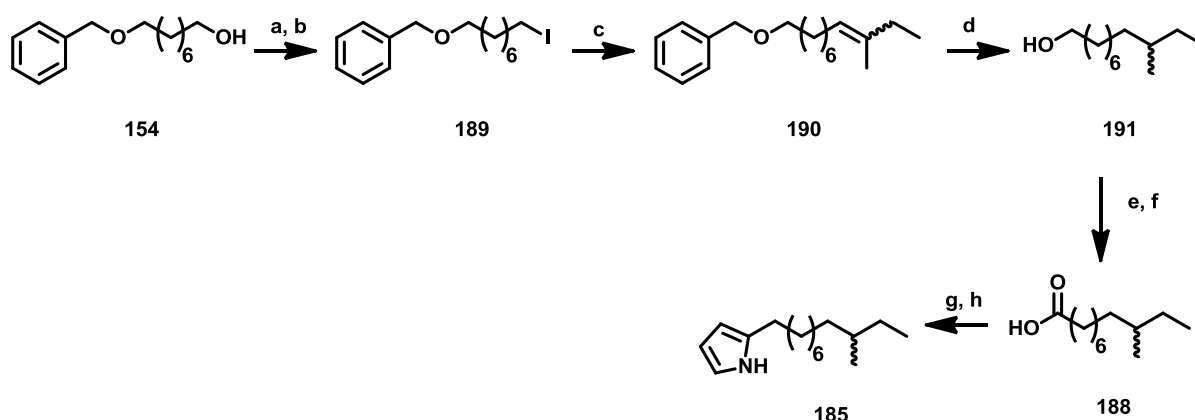
The synthetic route employed by Stuart Haynes for the synthesis of 2-UP analogue **185** is shown in Scheme 2.29. Ethyl 7-bromoheptanoate **186** was converted to the corresponding phosphonium salt and used in a Wittig reaction with isovaleraldehyde to yield alkene **187**. However, he observed a side reaction in which *n*-BuLi acted as a nucleophile, adding to the ester carbonyl group, rather than acting as a base. This resulted in a mixture of products.



Scheme 2.29: The synthetic used by Stuart Haynes for the synthesis of 2-UP analogue **185**;

a. i. PPh_3 , Toluene, $120\text{ }^\circ\text{C}$ ii. $n\text{-BuLi}$, Isovaleraldehyde, THF, $-78\text{ }^\circ\text{C}$; **b.** H_2 , Pd/C, THF; **c.** NaOH, THF; **d.** $(\text{PyS})_2$, PPh_3 , toluene, $25\text{ }^\circ\text{C}$ then EtMgBr, pyrrole, toluene, $-78\text{ }^\circ\text{C}$; **e.** NaBH_4 , IPA, $85\text{ }^\circ\text{C}$

In an attempt to eliminate the side reaction observed by Stuart Haynes, the more sterically hindered base LDA was used to generate the ylide. Unfortunately, this resulted in a complex mixture of inseparable products. Lithium bis(trimethylsilyl)amide was also used, but this also resulted in a complex mixture of products. Thus, an alternative synthetic route was devised, Scheme 2.30.



Scheme 2.30: The alternative synthetic route to 2-UP analogue **185**; **a.** TsCl, DMAP, Et_3N , CH_2Cl_2 , 85%; **b.** KI, Acetone, $65\text{ }^\circ\text{C}$, 100%; **c.** i. PPh_3 , Toluene, $120\text{ }^\circ\text{C}$ ii. $n\text{-BuLi}$, Butanone, THF, $-78\text{ }^\circ\text{C}$, 85%; **d.** i. Li, naphthalene, THF, $50\text{ }^\circ\text{C}$, ii. H_2 , Pd/C, THF, 96%; **e.** IBX, DMSO, 73%; **f.** Oxone, DMF, 99%; **g.** i. $(\text{PyS})_2$, PPh_3 , toluene, $25\text{ }^\circ\text{C}$ ii. EtMgBr, pyrrole, toluene, $-78\text{ }^\circ\text{C}$, 83%; **h.** NaBH_4 , IPA, $85\text{ }^\circ\text{C}$, 66%

Monobenzyl protected alcohol **154**, Scheme 2.21, was converted to the corresponding iodide **189**, via the tosylate, in 85% overall yield. Conversion of iodide **189** to phosphonium salt and subsequent Wittig reaction with butanone yielded alkene **190** as an inseparable mixture of stereoisomers. The ratio of stereoisomers was $\sim 2:3$, as estimated by $^1\text{H-NMR}$ spectroscopy. Alkene **190** proved difficult to purify due to co-purification of the triphenylphosphine oxide

byproduct, which was eventually removed by repeated silica gel column chromatography and precipitation/filtration.

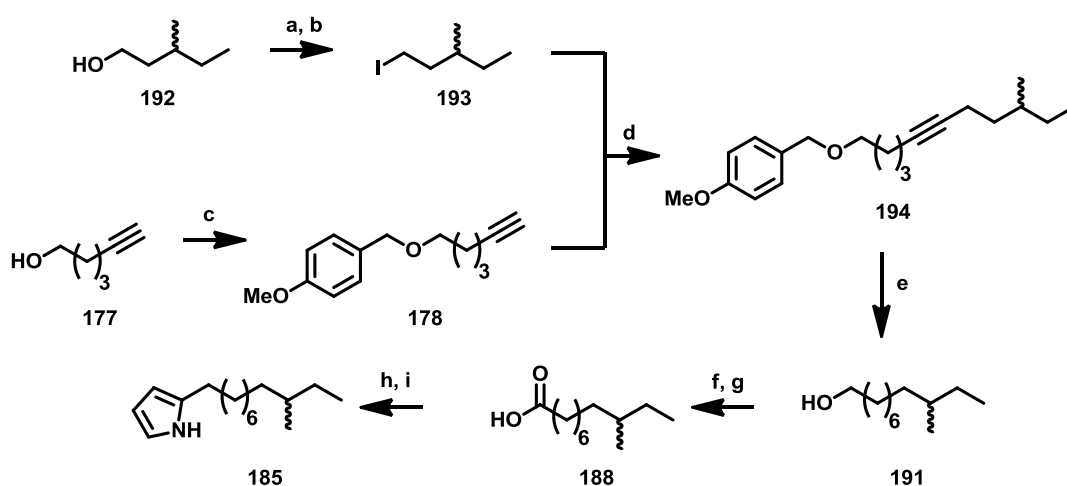
Subsequent hydrogenolysis of the benzyl protecting group with concurrent reduction of the alkene should have provided alcohol **191**. However, even after 14 days, only 15% debenzilation was observed, although complete reduction of the alkene had occurred. In an attempt to improve the hydrogenolysis rate, a range of solvents, palladium catalysts and additives were screened, Table 2.2. Addition of Amberlyst-15 as an acid catalyst improved the conversion rate to 35% after 7 days. However, this was still not practical and alternative methods for debenzilation were sought.

Solvent	Catalysts	Additives
THF	10% Pd/C	Silica gel
Methanol	45% Pd/C	Trifluoroacetic acid
Ethyl acetate	Pd(OAc) ₂	Amberlyst-15
Hexane	-	-

Table 2.2: The range of solvents, catalysts and additives screened in an attempt to improve the debenzilation of **190**

Examination of the literature revealed several alternative reagents for the deprotection of benzyl ethers, including concentrated hydrobromic acid⁸⁶, triphenylphosphine hydrobromide⁸⁷, chlorosulfonyl isocyanate-sodium hydroxide⁸⁸ and lithium naphthalenide.⁸⁹ Lithium naphthalenide was selected because it appeared to be the mildest and simplest method to implement. Thus, benzyl protected **190** was treated with lithium naphthalenide and subsequent hydrogenation of the alkene provided alcohol **191** in 96% overall yield. Oxidation of alcohol **191** to the corresponding carboxylic acid **188**, followed by coupling with pyrrole and reduction of the resulting 2-ketopyrrole, using the methodology described for the synthesis of 2-UP **20**, yielded 2-UP analogue **185**.

While this synthetic route provided the desired 2-UP analogue **185**, there were significant issues associated with several steps that required substantial amounts of time and effort to resolve. In addition, the synthesis of monobenzyl protected alcohol **154** requires stoichiometric amounts of expensive silver(I) oxide. Thus, an alternative synthetic route was developed in parallel that avoided the problematic steps and required less expensive reagents, Scheme 2.31.



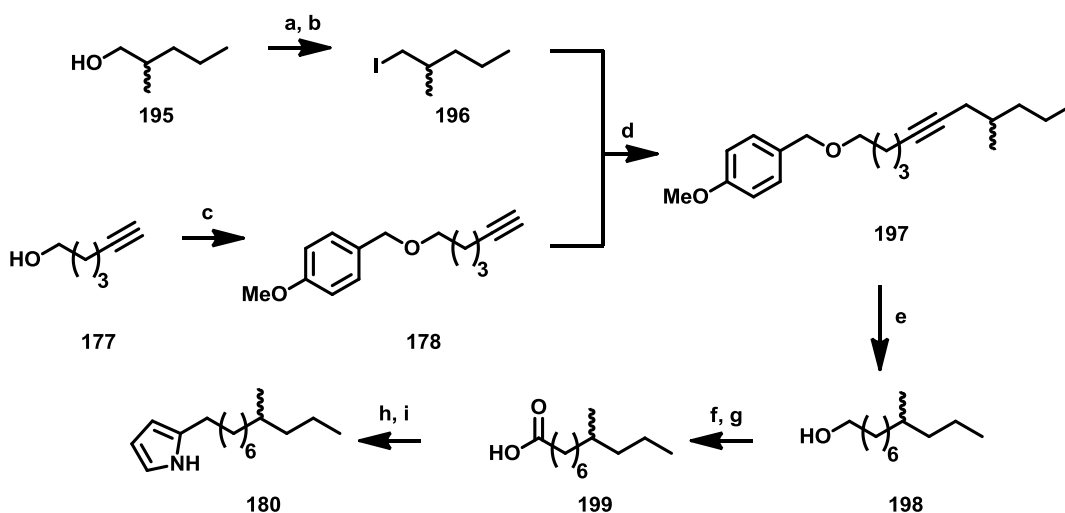
Scheme 2.31: The second generation synthetic route to 2-UP analogue **185**; **a.** TsCl, DMAP, Et₃N, CH₂Cl₂, 90%; **b.** KI, Acetone, 60 °C, 100%; **c.** NaH, PMBCl, THF, 95%; **d.** *n*-BuLi, THF, -78 °C up to 75 °C, 75%; **e.** H₂, Pd/C, THF, 71%; **f.** IBX, DMSO, 73%; **g.** Oxone, DMF, 99%; **h.** 2,2'-dipyridyl disulphide, PPh₃, toluene, 25 °C then EtMgBr, pyrrole, toluene, -78 °C, 83%; **i.** NaBH₄, IPA, 85 °C, 66%

In this alternative synthetic route, 3-methylpentan-1-ol **192** was converted to 1-iodo-3-methylpentane **193** via the corresponding tosylate in 90% yield of over the two steps. Protection of 5-hexyn-1-ol **177** with 4-methoxybenzyl chloride provided protected alkyne **178** in 85% yield. The 4-methoxybenzyl group was selected because of its greater reactivity under hydrogenation conditions and is thus easier to remove. Alkylation of alkyne **178** with iodide **193** followed by hydrogenation provided alcohol **191**. Oxidation of alcohol **191** to the corresponding carboxylic acid **188** followed by coupling with pyrrole and reduction of the

resulting 2-ketopyrrole using the methodology described for the synthesis of 2-UP **20** provided 2-UP analogue **188**.

2.7.2 2-(8-Methylundecyl)-pyrrole **180**

The route employed for the synthesis of the 2-UP analogue **180** with a methyl group at C-8' is shown in Scheme 2.32. It is analogous to the second generation synthesis of the 2-UP analogue **185** with a methyl group at C-9', see Section 2.7.1.

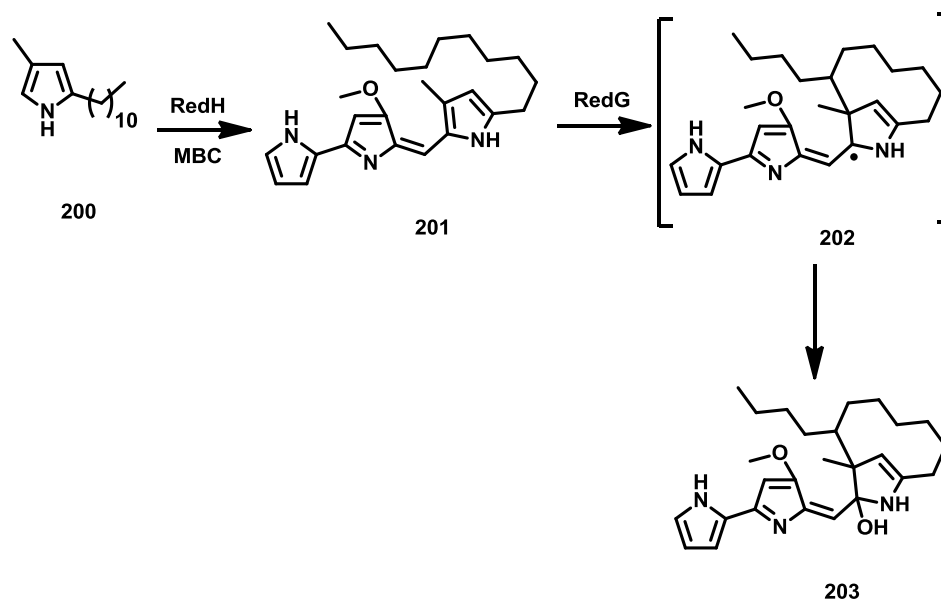


Scheme 2.32: The synthetic route to 2-UP analogue **180**; **a.** TsCl, DMAP, Et₃N, CH₂Cl₂, 98%; **b.** KI, Acetone, 60 °C, 80%; **c.** NaH, THF, 85%; **d.** *n*-BuLi, THF, -78 °C upto 75 °C, 65%; **e.** H₂, Pd/C, THF, 79%; **f.** IBX, DMSO, 68%; **g.** Oxone, DMF, 95%; **h.** (PyS)₂, PPh₃, toluene, 25 °C then EtMgBr, pyrrole, toluene, -78 °C, 71%; **i.** NaBH₄, IPA, 85 °C, 59%

2.8 Synthesis of 2-UP analogues with a methyl group on the pyrrole

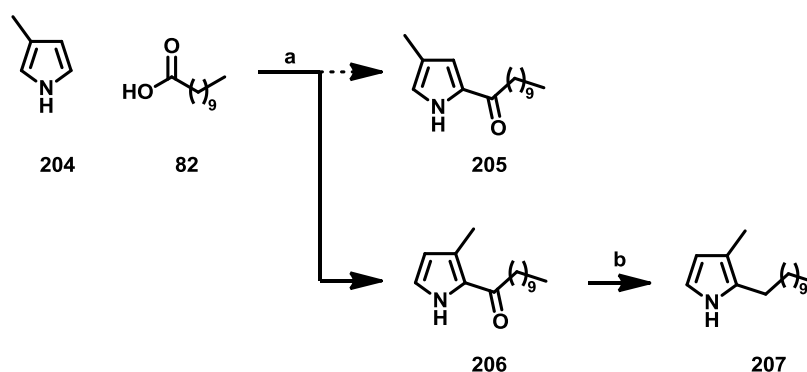
As discussed in Section 1.9, the proposed RedG catalytic mechanism involves the formation of a carbon-centred radical at C-7', which attacks the pyrrole. Subsequent abstraction of the hydrogen atom at the 4-position of the resulting intermediate regenerates the aromatic system. Thus, it was decided to replace the hydrogen atom at the 4-position of the pyrrole with a methyl group **200**, to investigate whether the intermediate radical **202** can be trapped,

Scheme 2.33. While it is difficult to predict the fate of the trapped radical, one possibility would be reaction with the Fe(IV)=O(OH) intermediate to form a hydroxylated product **203**.



Scheme 2.33: The expected undecylprodigiosin analogue **201** and a possible hydroxylation product **203** resulting from feeding 2-UP analogue **200** to a mutant of *S. coelicolor* blocked in the biosynthesis of 2-UP

It was expected that 2-UP analogue **200** could be synthesised in an analogous manner to that utilised for 2-UP **20** using 3-methylpyrrole **204** instead of pyrrole, Scheme 2.34. It was anticipated that steric interaction between the methyl group and the acylating agent would facilitate selective acylation of 3-methylpyrrole **204** at the 5-position.



Scheme 2.34: Initially investigated synthetic route to 2-UP analogue **200**; **a.** i. (PyS)₂, PPh₃, toluene, 25 °C ii. EtMgBr, pyrrole, toluene, -78 °C, 53%; **b.** NaBH₄, IPA, 85 °C, 68%

The aromatic region of the $^1\text{H-NMR}$ spectrum of the product resulting from acylation of 3-methylpyrrole with the thioester derived from reaction of undecanoic acid with (2,2')-dipyridyldisulphide and triphenylphosphine, revealed two multiplets, in contrast to the two singlets expected for **205**. In addition, a correlation between the two aromatic protons was observed in the COSY spectrum, indicating that they are adjacent to each other. This implied that acylation had occurred at the 2-position, yielding the regioisomer **206** of the desired product, Figure 2.14. To confirm the regiochemistry of the product of the acylation reaction, a series of NOE experiments was performed. For the desired regioisomer **205**, it was expected that correlations would be observed between each of the aromatic protons and the methyl group, but not between the aromatic protons themselves. Conversely, for regioisomer **206**, it was expected that correlations between the two aromatic protons and one of the aromatic protons and the methyl group would be observed, Figure 2.15.

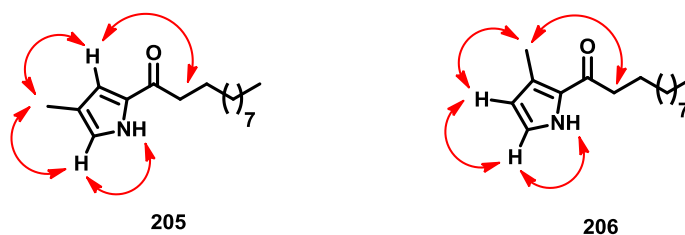


Figure 2.14: Correlations between protons expected to be observed in the NOE spectra of 4-methyl-2-acyl pyrrole **205** and 3-methyl-2-acyl pyrrole **206**

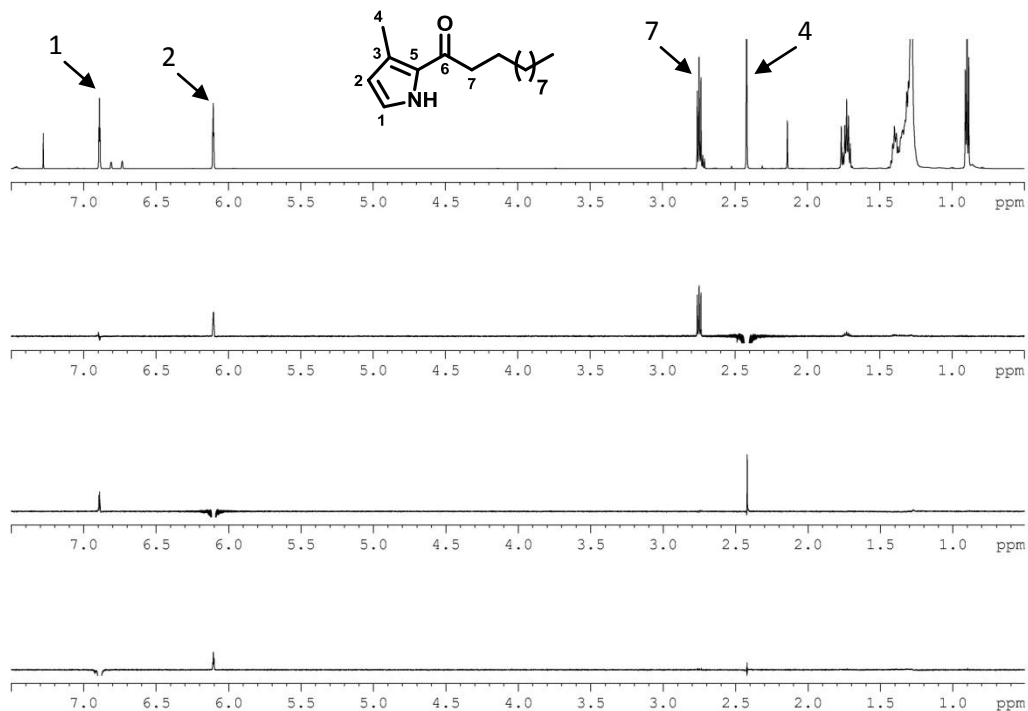
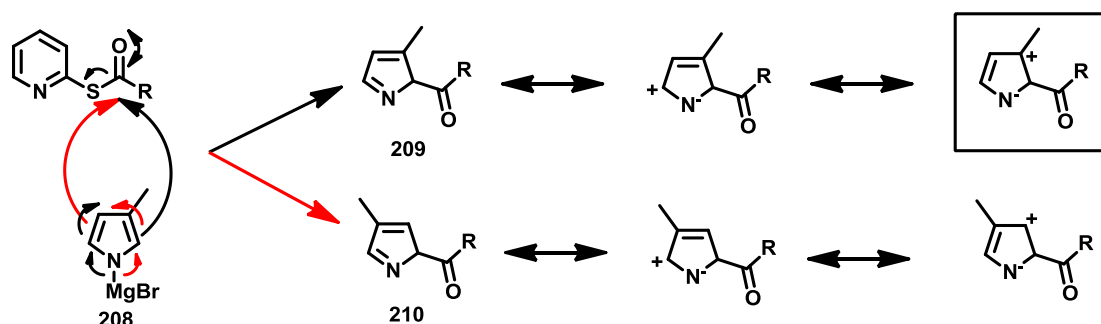


Figure 2.15: NOE difference spectra for **206** in CDCl_3 at 600 MHz with no irradiation (top spectrum), irradiation at the frequency corresponding to the signal at 2.42 ppm (second spectrum), irradiation at the frequency corresponding to the signal at 6.10 ppm (third spectrum) and irradiation at the frequency corresponding to the signal at 6.89 ppm (bottom spectrum)

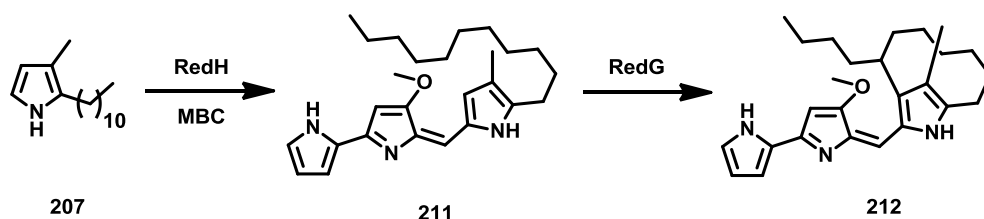
Irradiation at the frequency corresponding to the signal at 2.42 ppm, resulting from the pyrrole methyl group, resulted in enhancement of the signals due to one of the aromatic protons and protons α to the keto group. Conversely, irradiation at the frequency corresponding to the signal at 6.10 ppm resulted in enhancement of the signal at 6.89 ppm and *vice versa*. Thus, the product of the acylation reaction was confirmed as the 3-methyl-2-acyl pyrrole **206**. This unexpected result can be explained by considering the electronic properties of the two intermediates resulting from acylation of the Grignard reagent **208** derived from 3-methylpyrrole at the 2- and 5-position, Scheme 2.35.



Scheme 2.35: Intermediates resulting from acylation of the Grignard reagent **208** derived from 3-methylpyrrole at the 2- (black arrows) and 5- (red arrows) positions

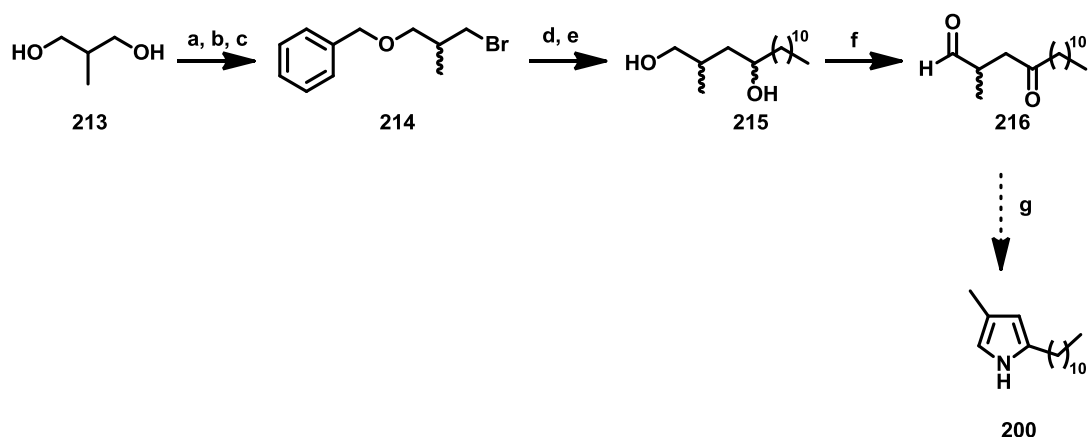
The presence of the electronegative nitrogen atom polarises the π -system of intermediates **209** and **210**. Acylation at the 2-position allows the partial positive charge to be stabilised by hyperconjugation from the methyl group, whereas acylation at the 5-position does not. Thus, the energy of the transition state for 2-acylation is lower and regioisomer **206** is formed.

It was decided to reduce the keto group of **206** to provide the 2-UP analogue **207**. This analogue could be used to probe the steric ability of RedG to tolerate additional substituent's on the pyrrole involved in the oxidative carbocyclisation reaction, Scheme 2.36.



Scheme 2.36: The expected undecylprodigiosin analogue **211** and streptorubin B analogue **212** from feeding 2-UP analogue **207** to a mutant of *S. coelicolor* blocked in the biosynthesis of 2-UP

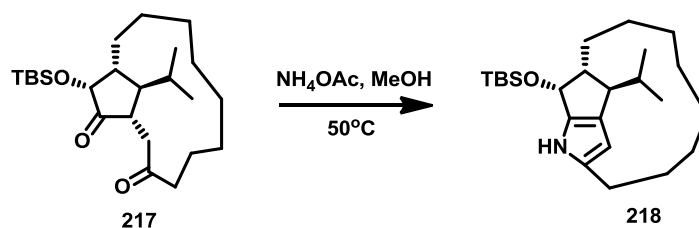
An alternative synthetic route was devised for the synthesis of 2-UP analogue **200**, Scheme 2.37. This route involves the Paal-Knorr pyrrole synthesis, a reaction that converts 1,4-dicarbonyl compounds upon heating with an amine to the corresponding pyrrole.^{90,91}



Scheme 2.37: The alternative route to 2-UP analogue **200**; **a.** Ag₂O, BnBr, CH₂Cl₂, 90%; **b.** TsCl, DMAP, Et₃N, CH₂Cl₂, 95%; **c.** LiBr, acetone, 65 °C, 87%; **d.** i. Mg (s), THF, 50 °C ii. Dodecanal, THF, 60%; **e.** H₂ (g), Pd/C, THF, 89%; **f.** (COCl)₂, DMSO, Et₃N, CH₂Cl₂, -78 °C, 75%; **g.** Nitrogen source, THF, 70 °C

Monobenylation of 2-methyl-1,3-propanediol **213** in the presence of silver(I) oxide, as discussed previously, and conversion of the resulting monoprotected alcohol to the corresponding bromide **214** via the tosylate was achieved in 74% overall yield. Treatment of bromide **214** with magnesium turnings afforded the corresponding Grignard reagent *in situ* which was reacted with dodecanal to yield diol **215**, after hydrogenolytic debenylation. The diastereoisomeric mixture of diols was not separated because both stereocentres are absent from the final product. Swern oxidation of diol **215** yielded 1,4-dicarbonyl **216** in 75% yield.

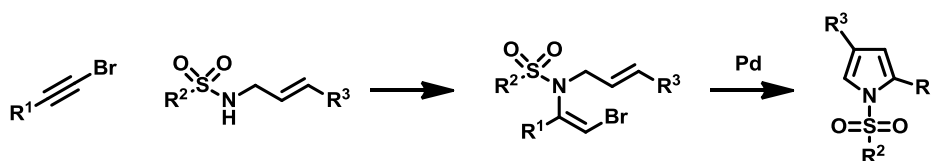
Attempts to convert 1,4-dicarbonyl **216** to the desired 2-UP analogue **200** using Paal-Knorr chemistry proved unsuccessful. Heating with a range of nitrogen sources including ammonium acetate, ammonium hydroxide and ammonium chloride resulted in the consumption of starting material but yielded complex mixtures of inseparable products. These complex mixtures of products presumably arise due to the instability of the initially-formed dialkylpyrrole. Indeed, during the total synthesis of the roseophillin macrocycle, Trost *et al* reported that the trialkylated pyrrole **218** was unstable and prone to degradation during its formation under Paal-Knorr conditions, Scheme 2.38.⁹²



Scheme 2.38: Attempted conversion of 1,4-diketone **217** to pyrrole **218** reported by Trost *et al*

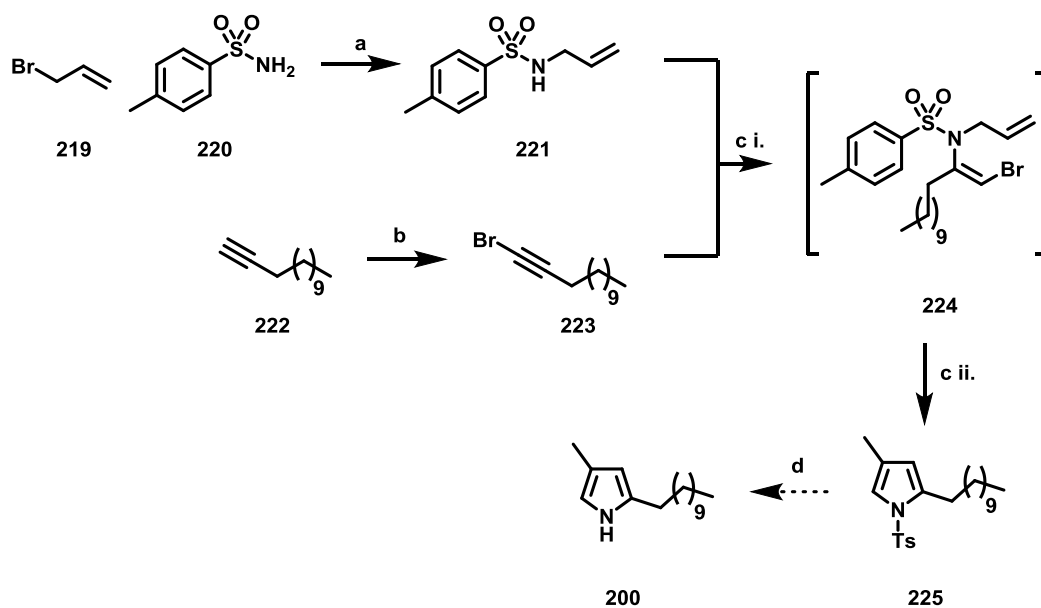
The instability of the dialkylpyrrole is most likely due to its electron-rich nature resulting from the electron-donating effects of the additional methyl group. Addition of an electron-withdrawing group to the pyrrole nitrogen would therefore be expected to stabilise the dialkylpyrrole product. Unfortunately, placing an electron withdrawing substituent on the nitrogen source in the Paal-Knorr reaction would also reduce its nucleophilicity, thus it would be expected not to react. An alternative synthetic route was therefore sought.

Urabe *et al* have recently reported the use of sulphonamides and bromoacetylenes as building blocks for pyrrole rings.⁹³ They demonstrated that sulphonamides were able to act as nucleophiles towards electron-deficient halo-alkynes, resulting in functionalised alkenes that can be converted to *N*-sulphonyl-dialkyl pyrroles using a palladium catalyst, Scheme 2.39.



Scheme 2.39: A generalised scheme for the synthesis of *N*-sulphonyl-dialkyl pyrroles from a sulphonamide and a bromoalkyne

Thus, an alternative synthetic route to the desired 2-UP analogue **200** could be envisaged that utilises this chemistry, Scheme 2.40.



Scheme 2.40: The alternative synthetic route to 2-UP analogue **200**; **a.** K₂CO₃, NaI, Acetone, 60 °C, 32%; **b.** AgNO₃, NBS, Acetone, 82%; **c. i.** K₃PO₄, DMF, 120 °C **ii.** Bu₄NBr, Pd(OAc)₂, 120 °C, 30%; **d.** KOH, MeOH, 60 °C

Sulphonamide **200** was alkylated with potassium carbonate and allyl bromide **219** to give a 1:1:1 mixture of unalkylated, monoalkylated and dialkylated products, from which the monoalkylated product **221** was isolated by flash column chromatography in 32% yield. Reaction of alkyne **222** with *N*-bromosuccinimide and silver nitrate yielded bromoalkyne **223** in 82% yield. Treatment of sulphonamide **221** and bromoalkyne **223** with K₃PO₄ resulted in the formation of bromoalkene **224**, which was converted to pyrrole **225** *via* a Heck reaction.

To confirm the regiochemistry of the methyl group in **225**, NOE experiments were performed. It was expected that correlations between each of the pyrrole protons and the methyl group, but not the pyrrole protons themselves would be observed, Figure 2.16.

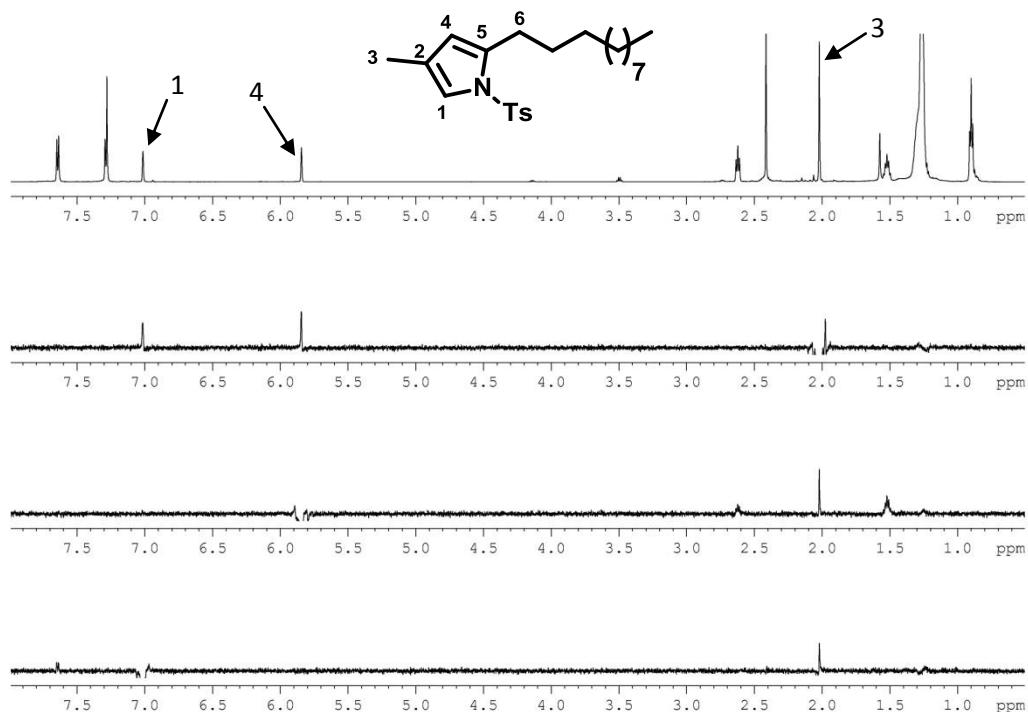


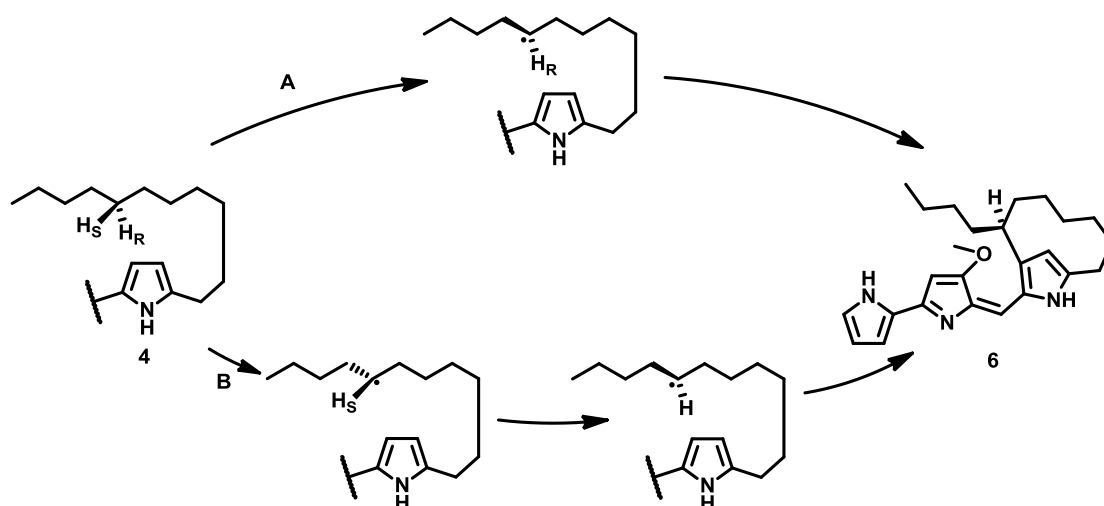
Figure 2.16: NOE difference spectra for **225** in CDCl₃ at 600 MHz with no irradiation (top spectrum), irradiation at the frequency corresponding to the signal at 2.02 ppm (second spectrum), irradiation at the frequency corresponding to the signal at 5.86 ppm (third spectrum) and irradiation at the frequency corresponding to the signal at 7.01 ppm (bottom spectrum)

Irradiation at the frequency corresponding to the signal at 2.02 ppm due to the methyl group of the pyrrole, resulted in enhancement of the signals for the two aromatic protons. In addition, no correlation between the pyrrole protons is observed. It was anticipated that removal of the tosyl group using potassium hydroxide would provide 2-UP analogue **200**. However, prolonged elevated temperatures were required which resulted in substantial degradation of the product. Due to time constraints, alternative methods for the deprotection were not investigated.

2.9 Synthesis of stereoselectively deuterium-labelled 2-UP analogues

analogues

As discussed in Section 1.10.3, RedG catalyses the stereoselective oxidative carbocyclisation of undecylprodigiosin **4** to streptorubin B **6**, to give an 9:1 mixture of *S*:*R* stereoisomers. There are several possible stereochemical courses for this reaction. Firstly, RedG could stereoselectively abstract the *pro-S* hydrogen atom from C-7', followed by attack of the resulting carbon-centred radical on the pyrrole with retention of stereochemistry (i.e. abstraction of the *pro-S* hydrogen atom leads to the *S* stereochemistry), route A Scheme 2.41. Alternatively, RedG could stereoselectively abstract the *pro-R* hydrogen atom from C-7' followed by attack of the resulting carbon-centred radical on the pyrrole with inversion of stereochemistry (i.e. abstraction of *pro-R* hydrogen atom leads to *S* stereochemistry), route B Scheme 2.41. A third possibility is non-stereoselective abstraction of either *pro-S* or *pro-R* hydrogen atoms from C-7' resulting in carbocyclisation *via* a mixture of routes A and B, Scheme 2.41. Presumably, restricted rotation of the undecyl chain, when bound to the RedG active site, prevents a mixture of *pro-R* and *pro-S* hydrogen atom abstraction.



Scheme 2.41: Different possible stereochemical courses for the RedG catalysed oxidative carbocyclisation, which could occur *via* primarily route A or route B, or *via* a mixture of routes A and B

The stereochemical course of several other reactions catalysed by non-haem iron-dependent oxidative cyclases has been studied in detail. These include: the conversion of **226** to **13**, catalysed by HppE, in fosfomicin biosynthesis^{94,95}; the conversion of *L, L, D*-ACV **100** to isopenicillin, catalysed by IPNS^{96,97}; and the conversion of **227** to **228** catalysed by clavamate synthase in clavulanic acid biosynthesis.^{98,99} In the HppE catalysed reaction, the *pro-R* hydrogen atom is removed from C-1 of the substrate resulting in inversion of configuration at the newly-formed stereocentre, Figure 2.17 A. However, this proposed inversion of stereochemistry is based on an X-ray crystal structure and no stereoselectively labelled substrate investigations has been undertaken. In contrast, it has been shown that both the IPNS and clavamate synthase-catalysed reactions proceed with retention of configuration at the carbon atom undergoing functionalisation *via* the use of stereoselectively labelled substrates, B and C respectively in Figure 2.17.

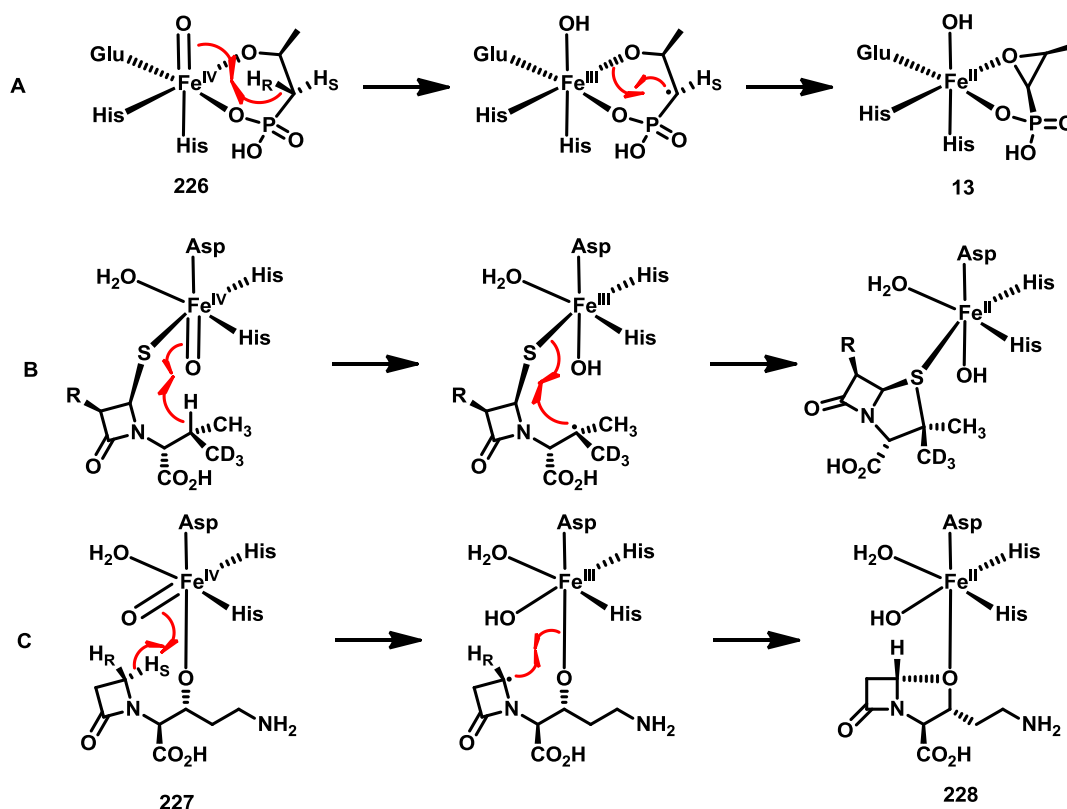


Figure 2.17: Stereochemical course of the oxidative cyclisation reactions catalysed by HppE, IPNS and clavamate synthase. Only half of the curly arrows are shown for clarity

To investigate the stereochemical course of the clavamate synthase-catalysed oxidative cyclisation, Townsend *et al* synthesised two stereoselectively deuterium-labelled substrates **pro-R 229** and **pro-S 229**, Figure 2.18. Incubation of the substrate in which the *pro-R* hydrogen atom attached to C-3 was labelled with clavamate synthase resulted in 94% retention of the label. However, incubation of the substrate in which the *pro-S* hydrogen atom attached to C-3 has been labelled with clavamate synthase resulted in only 12% retention of the label. Thus, Townsend *et al* concluded that clavamate synthase stereoselectively abstracts the *pro-S* hydrogen atom and that oxidative cyclisation proceeds with retention of configuration.

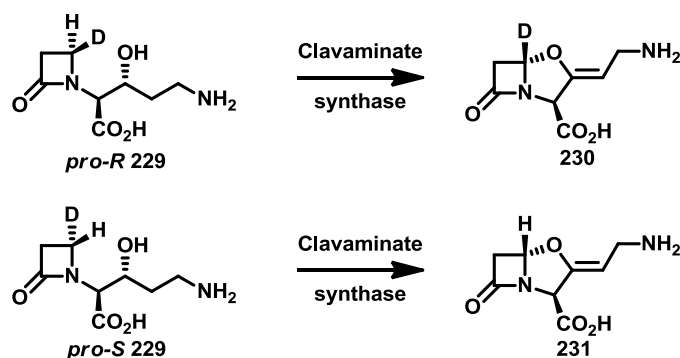
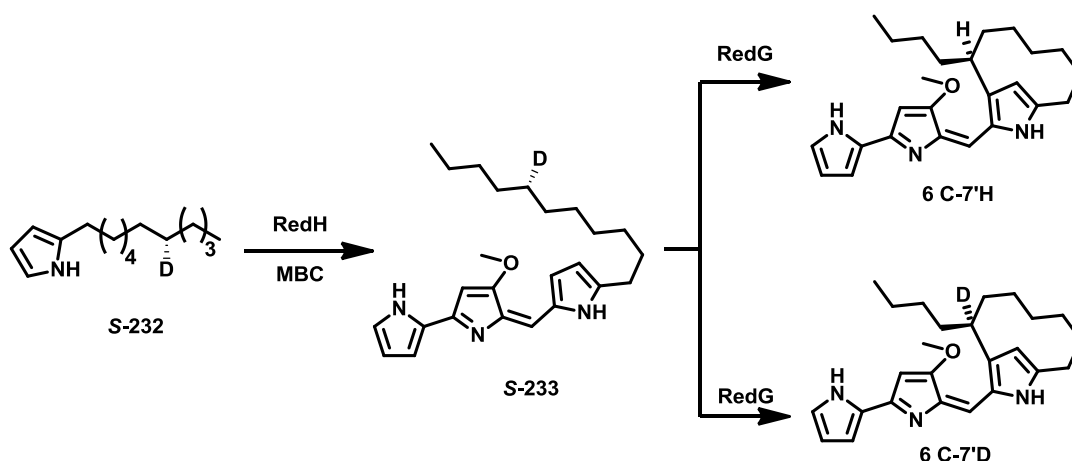


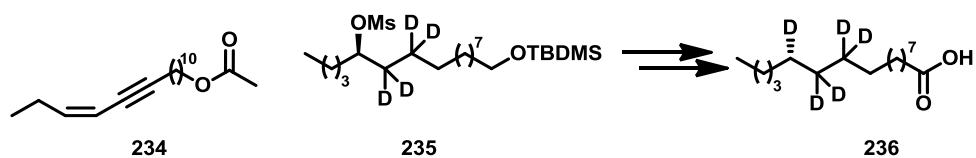
Figure 2.18: Use of stereoselectively deuterium-labelled substrates by Townsend *et al* to determine that the clavamate synthase-catalysed oxidative cyclisation occurs with retention of configuration

It was envisaged that a similar approach could be employed to investigate the stereochemical course of the RedG-catalysed oxidative carbocyclisation. By synthesising 2-UP analogues stereoselectively deuterium-labelled at C-7', **R-232** and **S-232**, it would be possible to distinguish between the three possible scenarios outlined in Scheme 2.41. If RedG stereoselectively abstracts the *pro-S* hydrogen atom from C-7', feeding of 2-UP analogue **S-232** would result in predominant loss of the deuterium label, **6 C-7'H**. Alternatively, if RedG stereoselectively abstracts the *pro-R* hydrogen atom from C-7', then feeding of 2-UP analogue **S-232** should result in predominant retention of the deuterium label, **6 C-7'D**. In the third scenario outlined in Scheme 2.41, about 50% of the deuterium label would be retained, Scheme 2.42.



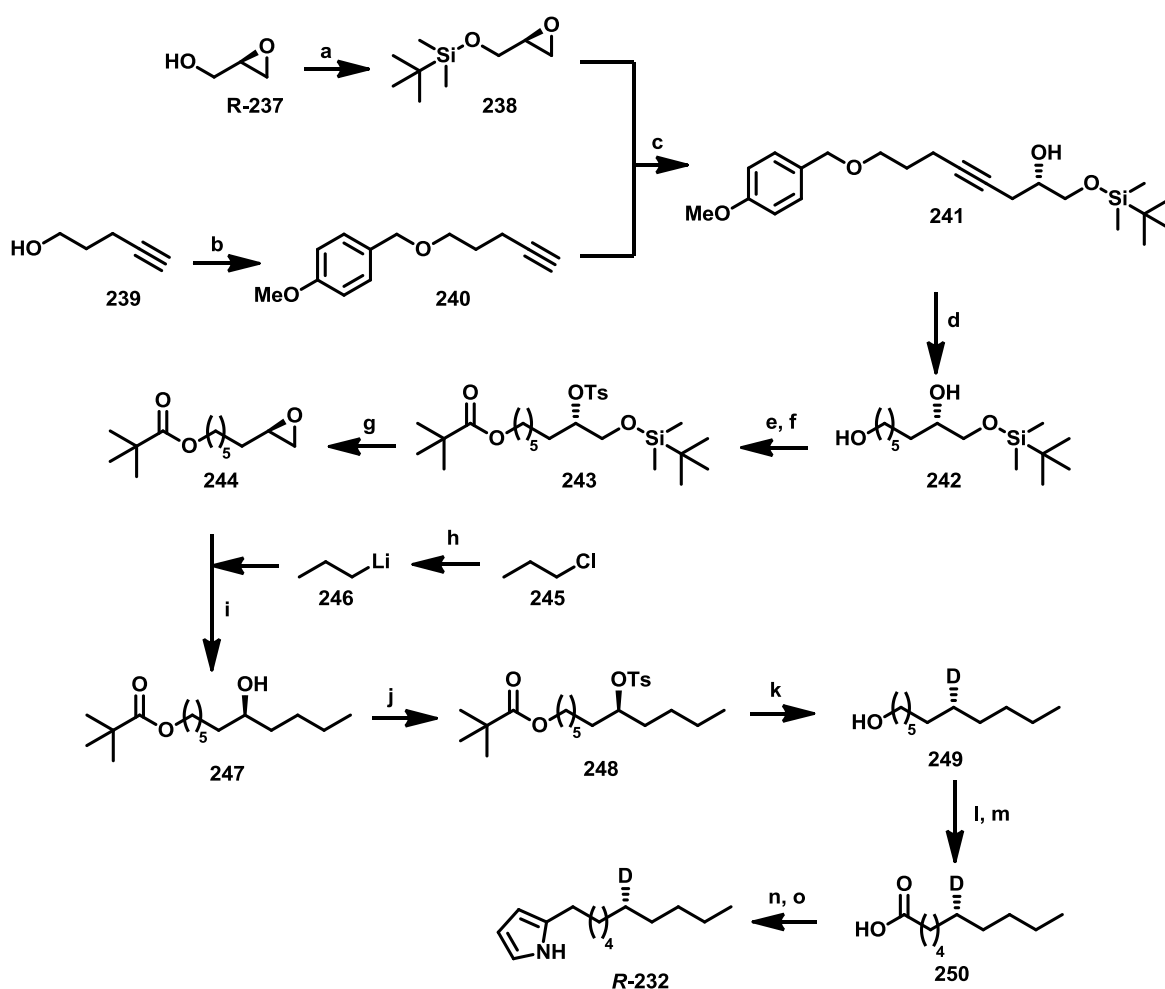
Scheme 2.42: Possible products resulting from feeding of 2-UP **S-232** in which the *pro-S* hydrogen atom at C-7' has been stereospecifically labelled with deuterium to a mutant of *S. coelicolor* blocked in 2-UP biosynthesis

Thus, a synthetic method for the stereoselective incorporation of deuterium into C-7' of 2-UP was required. Examination of the literature revealed surprisingly few methods for the stereoselective incorporation of deuterium into hydrocarbons. One method that has been demonstrated to be stereoselective is reductive displacement of certain leaving groups with lithium aluminium deuteride. One of the first uses of this method was reported by Chickos *et al.*¹⁰⁰ More recently, Ashby *et al* undertook a rigorous investigation of the mechanism for the reduction of organic halides with lithium aluminium hydride.¹⁰¹ Using a variety of techniques and mechanistic probes, they demonstrated that the lithium aluminium hydride reduction of alkyl chlorides and tosylates occurs exclusively *via* an S_N2 process with concomitant inversion of configuration. This chemistry has been utilised by Abad *et al* for the synthesis of several stereoselectively deuterium-labelled fatty acids.^{102,103} For example, during their study of the biosynthesis of (*Z*)-13-hexadecene-11-ynyl acetate **234**, stereoselective deuterium labelled (*Z*)-11-hexadecanoic acid **236** was required, Scheme 2.43. This was synthesised *via* lithium aluminium deuteride reduction of enantioenriched mesylate **235**.



Scheme 2.43: The route used by Abad *et al* for the stereospecific incorporation of a deuterium label into hexadecanoic acid **236** by reduction of mesylate **235** with lithium aluminium deuteride

Thus, we designed a stereoselective synthetic route to tosylates **R-** and **S-248**, Scheme 2.44. Commercially available enantiomerically enriched **R-(+)**- and **S-(-)**-glycidol **R-** and **S-237** (98% ee) were used as starting materials for the synthesis.

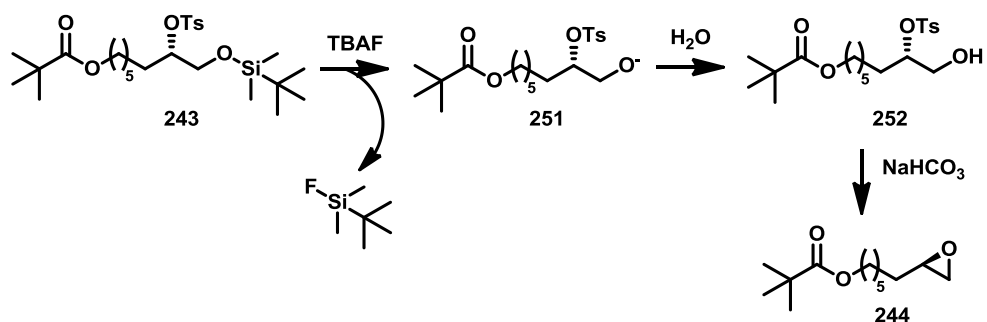


Scheme 2.44: The synthetic route to 2-UP stereoselectively deuterium-labelled at C-7';
a. TBDMSCl, DMAP, Et₃N, CH₂Cl₂, R 91%, S 86%; **b.** NaH, PMBCl, DMF, 70 °C, 83%; **c.** *n*-BuLi, BF₃·Et₂O, THF, -78 °C, R 63%, S 89%; **d.** H₂, Pd/C, THF, R 67%, S 52%; **e.** PivCl, Pyridine, CH₂Cl₂, -20 °C, R 80%, S 77%; **f.** TsCl, DMAP, Et₃N, CHCl₃, 70 °C, R 79%, S 81%; **g.** TBAF, THF, R 86%,

S 72%; **h.** Li, Hexane, 0 °C; **i.** CuCN, BF₃·Et₂O, Et₂O, -78 °C, R 75%, S 50%; **j.** TsCl, DMAP, Et₃N, CHCl₃, 70 °C, R 25%, S 24% **k.** LiAlD₄, THF, R 56%, S 24%; **l.** (COCl)₂, DMSO, Et₃N, CH₂Cl₂, -78 °C, R 67%, S 59%; **m.** Oxone, DMF, R 75%, S 74%; **n.** 2,2'-dipyridyl disulphide, PPh₃, toluene, 25 °C then EtMgBr, pyrrole, toluene, -78 °C, R 63%, S 87%; **o.** NaBH₄, IPA, 85 °C, R 99%, S 54%

t-Butyldimethyl silyl ether protection of glycidol **237** and 4-methoxybenzyl ether protection of alkyne **239** proceeded in excellent yields. Boron trifluoride promoted regioselective ring opening at the least hindered end of epoxide **238** with lithium acetylide **240** yielded alcohol **241**. Simultaneous hydrogenation of the alkyne and hydrogenolysis of the 4-methoxybenzyl protecting group was achieved with hydrogen and a palladium on carbon catalyst yielding diol **242**. Selective protection of the primary alcohol as the pivaloyl ester was achieved by treatment with pivaloyl chloride, giving 88% and 77% yields for the *R* and *S* enantiomers, respectively. Tosylation of this secondary alcohol required prolonged reaction times and elevated temperatures for complete conversion of the starting material.

Initial attempts at the one-pot silyl ether deprotection and intramolecular displacement of the tosylate to provide epoxide **244** were performed in the presence of sodium bicarbonate because commercially available tetrabutylammonium fluoride is sold as a trihydrate. Thus, it was assumed that protonation of the intermediate alkoxide **251** would occur and that a base would be required to deprotonate alcohol **252** prior to displacement of the tosylate to form epoxide **244**, Scheme 2.45. However, a substantial amount of an unknown byproduct was isolated from the reaction mixture. The ¹H-NMR spectrum of this unknown byproduct is shown in Figure 2.19.



Scheme 2.45: The assumed mechanism for the one-pot silyl ether deprotection and intramolecular cyclisation to convert tosylate **243** into epoxide **244**

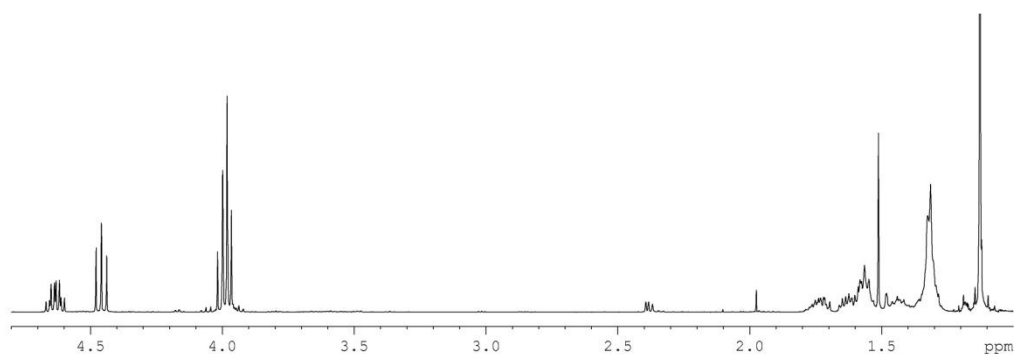
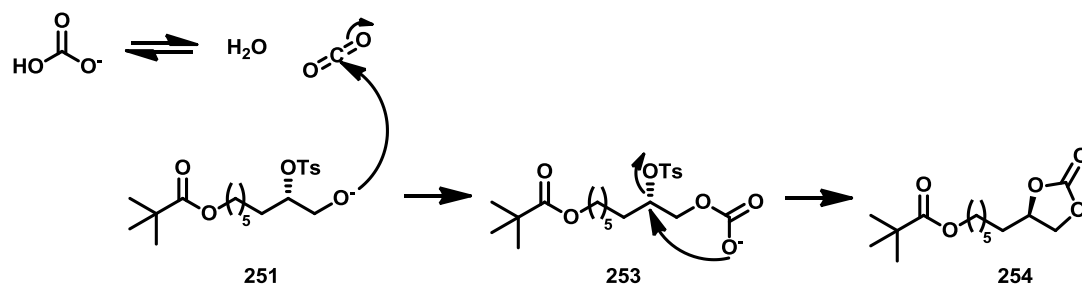


Figure 2.19: The $^1\text{H-NMR}$ spectrum in CDCl_3 at 400 MHz of the unknown side product resulting from the treatment of tosylate **243** with tetrabutylammonium fluoride and sodium bicarbonate

Examination of the $^1\text{H-NMR}$, $^{13}\text{C-NMR}$, mass and IR spectra of this byproduct lead to structural assignment as the cyclic carbonate **254**, Scheme 2.46. While the carbonyl carbon signals were not visible in the $^{13}\text{C-NMR}$ spectrum, correlations were observed in the HMBC spectrum consistent with two separate carbonyl groups. The IR spectrum also supported the cyclic carbonate **254**, due to the presence of two absorbances at 1794cm^{-1} and 1720cm^{-1} , indicative of two carbonyl groups. HRMS of the byproduct provided a molecular formula of $\text{C}_{14}\text{H}_{24}\text{O}_5$, which is also consistent with the cyclic carbonate structure **254**.

With hindsight, the use of sodium bicarbonate as a base was ill-judged, due to the equilibrium that exists between the bicarbonate anion and carbon dioxide in solution, Scheme 2.46. It was hypothesised that the cyclic carbonate byproduct results from nucleophilic attack of the

intermediate alkoxide **253** onto carbon dioxide. Subsequent intramolecular displacement of the tosylate by the carbonate anion would generate the cyclic carbonate **254**.



Scheme 2.46: The proposed mechanism for formation of the unexpected cyclic carbonate byproduct **254**

The one-pot silyl deprotection and intramolecular elimination reaction was repeated without addition of bicarbonate to provide epoxide **244** in 82% and 72% yields for the *R* and *S* enantiomers, respectively. In neither case was any trace of the deprotected alcohol observed, presumably because protonation by water is a reversible process.

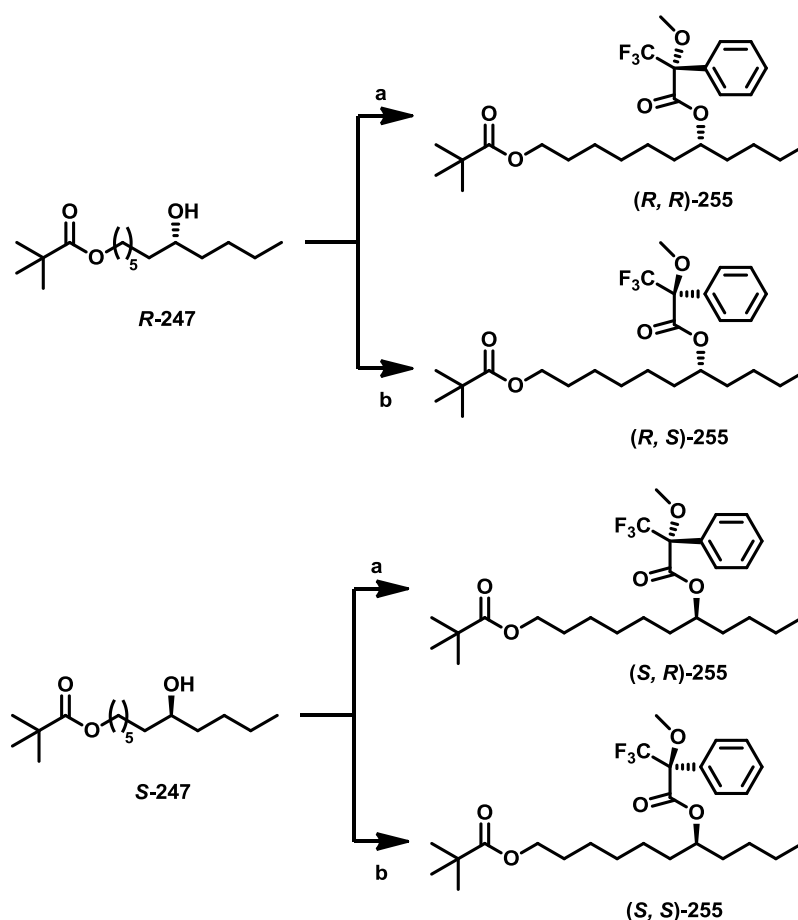
To complete the synthesis of the undecyl chain, regioselective ring opening of epoxide **244** with a propyl anion was required. This ring opening reaction was complicated by the presence of the pivaloyl ester protecting group. Examination of the literature revealed that higher order mixed metal organocuprates, $\text{R}_2\text{Cu}(\text{CN})\text{Li}_2$, selectively react with epoxides in the presence of esters and can be readily prepared from copper(I) cyanide and two equivalents of the desired alkyl lithium.^{104,105}

Unfortunately, *n*-propyllithium **246** is not commercially available and therefore it needed to be synthesised.¹⁰⁶ Thus, *n*-propyl chloride **245** was treated with two equivalents of lithium dust to yield a solution of *n*-propyllithium **245** in hexane. The concentration of *n*-propyllithium **246** was determined using the titration method described in the Experimental section for *n*-butyllithium.

With *n*-propyllithium in hand, epoxide **244** was treated with the higher order organocuprate prepared *in situ*. Initially, poor conversion of the starting epoxide **244** was observed, but

addition of boron trifluoride vastly increased the rate of the reaction yielding alcohol **247** in 75% and 50% yields for the *R* and *S* enantiomers, respectively.

To determine their enantiopurity, both of the secondary alcohols **247** were derivatised with both enantiomers of α -methoxy- α -trifluoromethylphenyl acetic acid to yield (*R, R*)-, (*R, S*)-, (*S, R*)- and (*S, S*)-**255** were synthesised, Scheme 2.47.^{107,108} A comparison of the ¹H-NMR spectrum of the four diastereoisomers is shown in Figures 2.20 and 2.21.



Scheme 2.47: Synthesis of the Mosher esters of alcohols *R*- and *S*-**255**; Acid, DCC, DMAP, CHCl₃, 50 °C; **a.** (*R*)- α -methoxy- α -trifluorophenylacetic acid (*R, R*)- 50%, (*R, S*)-**255** 44%; **b.** (*S*)- α -methoxy- α -trifluorophenylacetic acid(*S, R*)-**255** 50%, (*S, S*)-**255** 56%

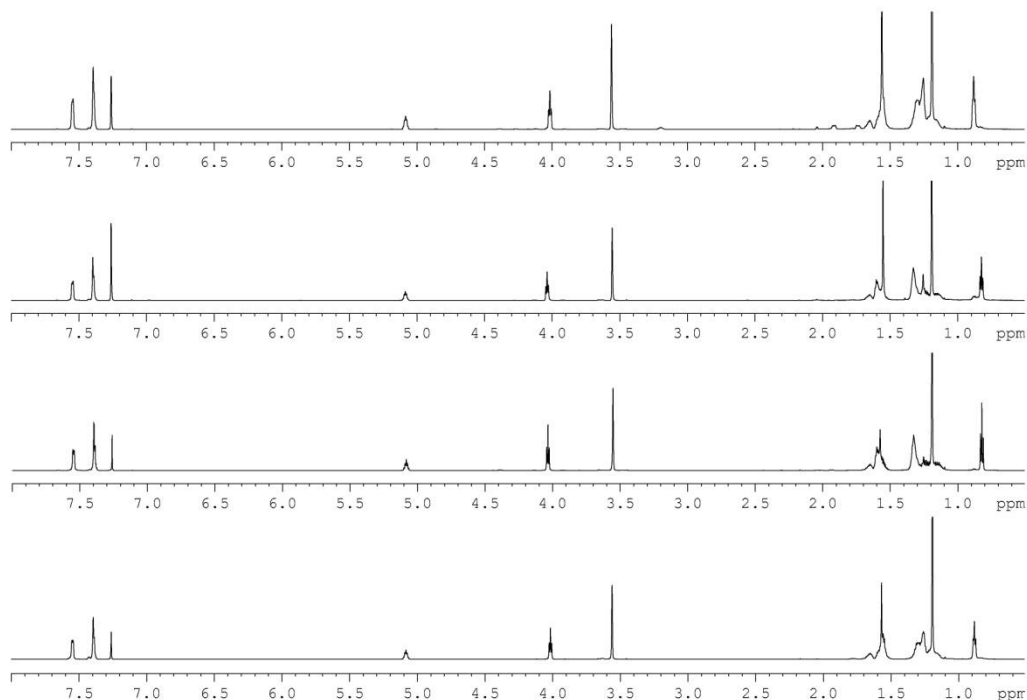


Figure 2.20: A comparison of the ^1H -NMR spectra in CDCl_3 at 700 MHz of (*S*, *R*)-**255** (top spectrum), (*S*, *S*)-**255** (second from top spectrum), (*R*, *R*)-**255** (third from top spectrum) and (*R*, *S*)-**255** (bottom spectrum)

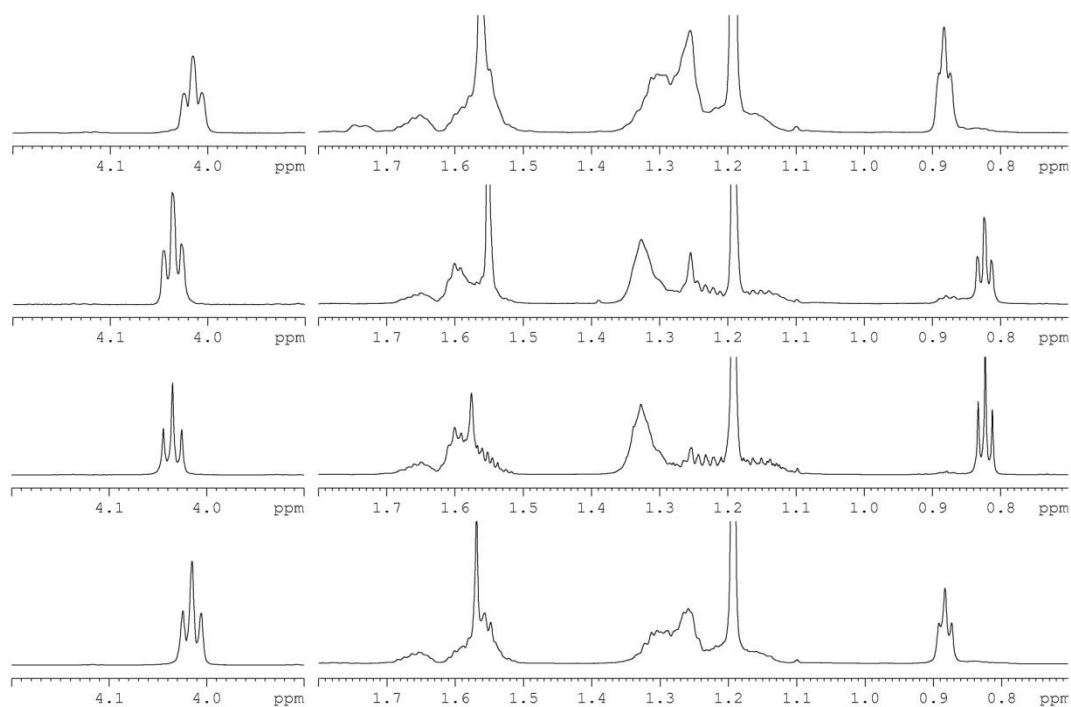


Figure 2.21: A comparison between 4.20 – 3.90 ppm and 1.80 – 0.70 ppm of the ^1H -NMR spectra in CDCl_3 at 700 MHz of (*S*, *R*)-**255** (top spectrum), (*S*, *S*)-**255** (second from top spectrum), (*R*, *R*)-**255** (third from spectrum) and (*R*, *S*)-**255** (bottom spectrum)

As expected, the pairs of enantiomers (***R, R***)- and (***S, S***)- and (***R, S***)- and (***S, R***)-**255** have identical ¹H-NMR spectra but the spectra of diastereoisomers exhibit subtle differences. These differences are most profound for the two triplets observed between 4.10 – 4.00 ppm and 0.90 – 0.85 ppm, corresponding to the protons adjacent to the pivalyl ester and of the terminal methyl group respectively, Figure 2.21. In the case of the (***R, R***)- and (***S, S***)-**255** pair, the triplets resonate at 4.04 ppm and 0.82 ppm, whereas for the (***R, S***)- and (***S, R***)-**255** pair, these signals are at 4.02 ppm and 0.88 ppm. Thus, utilising these chemical shift differences between the diastereoisomers, the expected absolute stereochemistry of the major components was confirmed.

For (***R, R***)- and (***S, S***)-**255**, there appears to be significant signal broadening, most notably for the terminal methyl group triplet at 0.88 ppm. This indicated presence of rotamers that are interchanging conformation on the timescale of the NMR experiment. To investigate this hypothesis, the ¹H-NMR experiments for these two samples were repeated at 40 °C, Figure 2.22 and 2.23. At 40 °C, the signal broadening was significantly reduced, confirming the presence of rotamers.

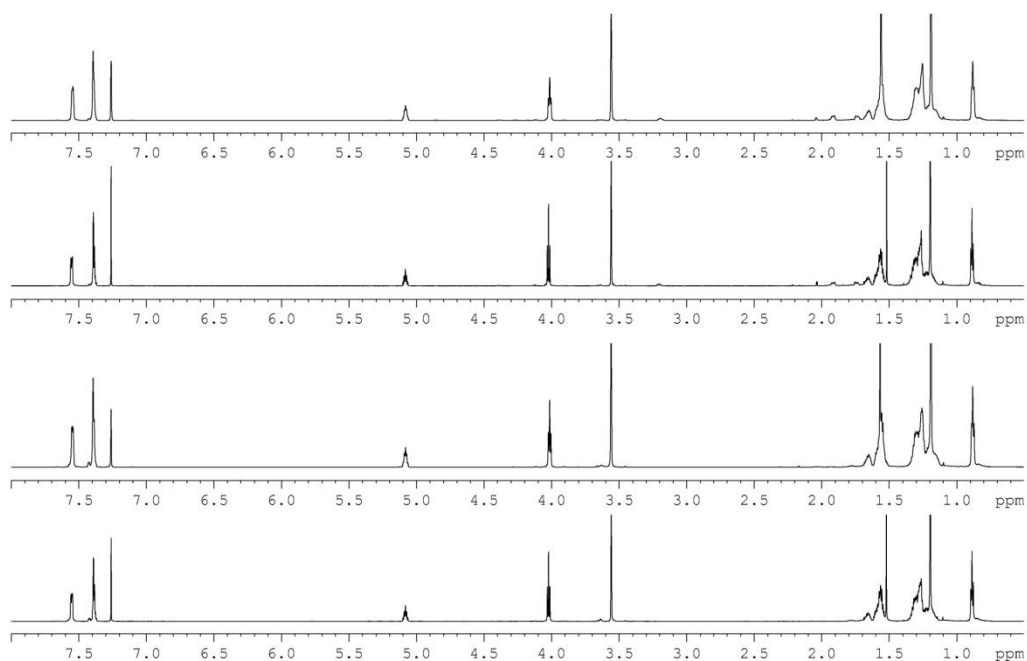


Figure 2.22: A comparison of the ^1H -NMR spectra in CDCl_3 at 700 MHz of (*S, R*)-**255** (top spectrum) and (*R, S*)-**255** (third from top spectrum) at 25 °C and (*S, R*)-**255** (second from top spectrum) and (*R, S*)-**255** (bottom spectrum) at 40 °C

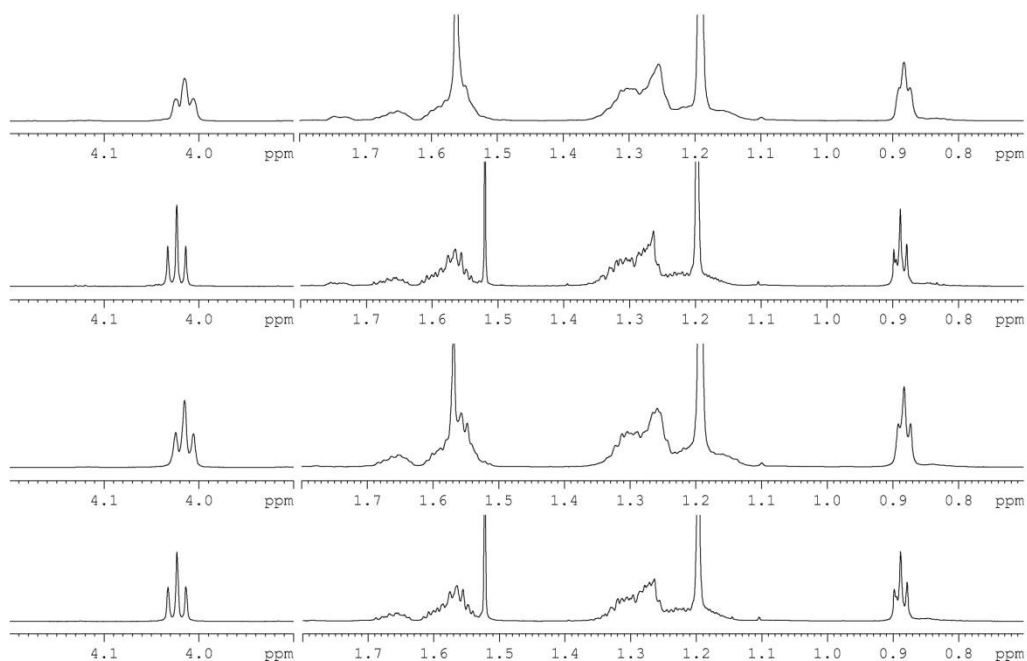


Figure 2.23: A comparison between 4.20 – 3.90 ppm and 1.80 – 0.70 ppm of the ^1H -NMR spectrum in CDCl_3 at 700 MHz of (*S, R*)-**255** (top spectrum) and (*R, S*)-**255** (third from top spectrum) at 25 °C and (*S, R*)-**255** (second from top spectrum) and (*R, S*)-**255** (bottom spectrum) at 40 °C

While the absolute stereochemistry of the major component of *R*- and *S*-**247** was confirmed, it was not possible to determine the exact ratio of enantiomers because, even at 700 MHz, the triplets at 0.88 ppm and 0.82 ppm are not completely resolved. Thus, the four diastereoisomers were analysed *via* HPLC using a variety of achiral and homochiral stationary phases. Unfortunately, it was not possible to resolve the minor diastereoisomer for any of the Mosher esters. It was therefore assumed that *R*- and *S*-**247** had an optical purity of no greater than 97% ee.

With the absolute stereochemistry of **247** confirmed, secondary alcohol **247** was converted to the corresponding tosylate **248**. Treatment with lithium aluminium deuteride simultaneously stereospecifically substituted the tosyl group and cleaved the pivalyl ester protecting group to yield alcohol **249**. Attempts to obtain a molecular formula to confirm the presence of a deuterium atom using high-resolution mass spectrometry proved unsuccessful, presumably due to low ionisation of **249**. As such, the ¹³C-NMR spectra of *R*- and *S*-**249** were compared to undecanol, Figure 2.24.

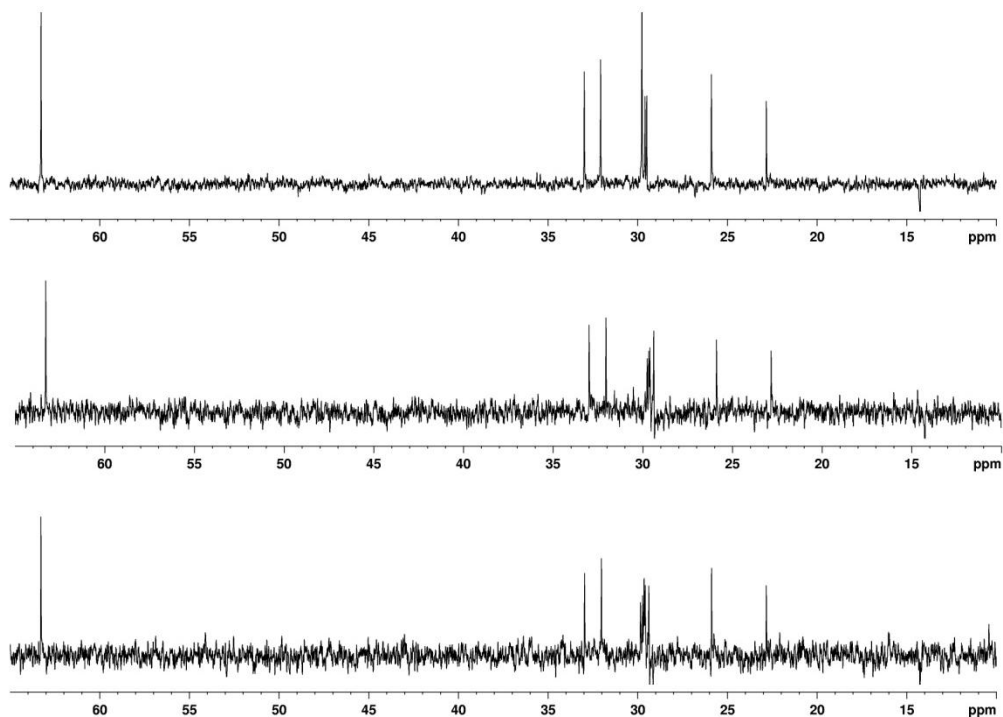


Figure 2.24: A comparison of the ^{13}C -NMR spectrum in CDCl_3 at 400 MHz of undecanol (top spectrum), **S-249** (middle spectrum) and **R-249** (bottom spectrum)

Comparison of the ^{13}C -NMR spectrum of **S-** and **R-249** with undecanol revealed the presence of additional signals at approximately 30 ppm, as a result of signal splitting caused by the deuterium atom.

Oxidation of alcohols **S-** and **R-249** to the corresponding carboxylic acids **S-** and **R-250** was achieved using the methodology previously described. Ionisation of both **S-** and **R-250** in the electrospray mass spectrometer was more efficient and molecular formulae were obtained that confirmed the presence of a deuterium atom. The synthesis of 2-UP analogues **S-** and **R-232** was completed by coupling with pyrrole followed by reduction of the 2-ketopyrrole using the methodology previously described for the synthesis of 2-UP **20**.

3. Results and discussion: Feeding of 2-undecylpyrrole analogues to *Streptomyces coelicolor* mutants blocked in the biosynthesis of 2-undecylpyrrole

With the synthesis of a selection of 2-UP analogues bearing specific functional groups complete, the mutasynthetic approach to probe the oxidative carbocyclisation catalysed by RedG was investigated. A typical feeding experiment involved inoculating an agar plate containing R5 medium with 10 µl of the *redL* mutant spore stock and incubating for three days at 30 °C. 3 mg of a 2-UP analogue was then added to the plate as a suspension in 200 µl of methanol and 2 ml of water and the culture was incubated for a further three days at 30 °C.

3.1 Feeding 2-UP 20 to *Streptomyces coelicolor redL* mutant

During Stuart Haynes preliminary investigations of RedG, he used a mutant constructed by Anna Stanley, a previous member of the Challis group, in which the *redL* gene was replaced with an apramycin resistance cassette.¹⁰⁹ Since RedL is involved in the biosynthesis of 2-UP 20, Section 1.6, this mutant does not produce either undecylprodigiosin 4 or streptorubin B 6. However, feeding this mutant with chemically synthesised 2-UP 20 restores the production of both undecylprodigiosin 4 and streptorubin B 6.

When feeding 2-UP 20 to this mutant, Stuart Haynes observed that the ratio of streptorubin B 6 to undecylprodigiosin 4 was much lower than in the wild type and in many cases, streptorubin B 6 was barely detectable. In an effort to increase the amount of streptorubin B 6 produced, Paulina Sydor, a previous member of the Challis group, introduced a plasmid containing an additional copy of both *redH* and *redG* into the *redL* mutant.¹¹⁰ For clarity, this strain will henceforth be referred to as the *redL* mutant.

As shown in Figure 3.1, the *redL* mutant expressing additional copies of both *redH* and *redG* does not produce either undecylprodigiosin 4 or streptorubin B 6 (blue chromatogram). Supplementing this mutant with chemically synthesised 2-UP 20 restored the production of both undecylprodigiosin 4 and streptorubin B 6 (yellow chromatogram) to levels approaching the wild type (red chromatogram).

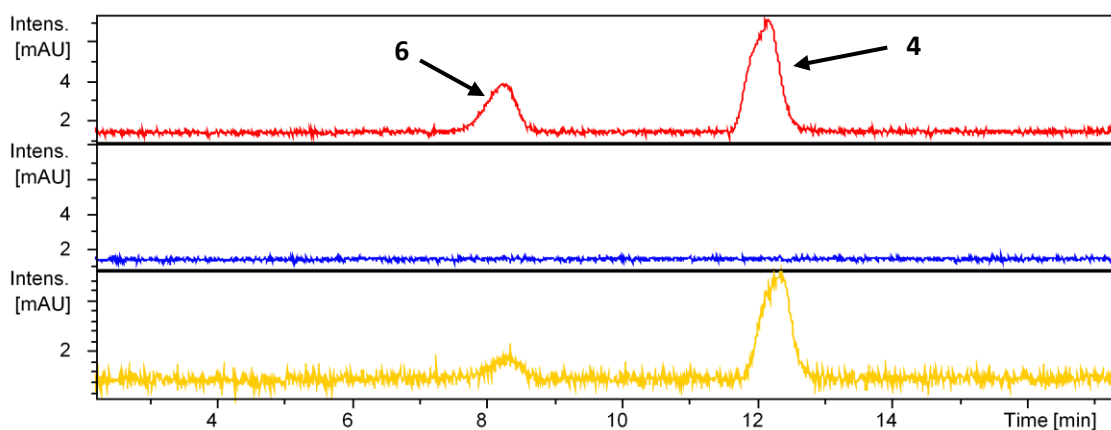
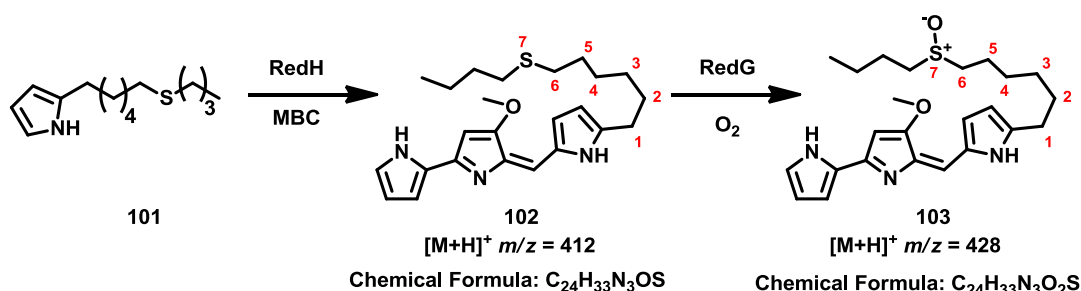


Figure 3.1: A_{533} chromatograms from LC-MS analyses of mycelial extracts from *Streptomyces coelicolor* wild type (red), the *redL* mutant (blue) and the *redL* mutant supplemented with chemically synthesised 2-UP **20**

3.2 Feeding of sulphur containing 2-UP analogues to the *Streptomyces coelicolor redL* mutant

3.2.1 Feeding of sulphur containing 2-UP analogue **101**

As discussed in Section 2.4, feeding of a 2-UP analogue bearing a sulphur atom at the site of cyclisation was expected to trap the reactive oxygen species generated by RedG as the corresponding sulphoxide, Scheme 3.1.



Scheme 3.1: The expected undecylprodigiosin analogues **102** and **103** expected to result from the feeding of 2-UP analogue **101** to the *redL* mutant

LC-MS analysis of the mycelial extract resulting from feeding the *redL* mutant with 2-UP analogue **101** gave a surprising result. As shown in Figure 3.2, three distinct peaks were

observed in the A_{533} chromatogram, the characteristic λ_{\max} of prodiginine hydrochloride salts.¹¹¹

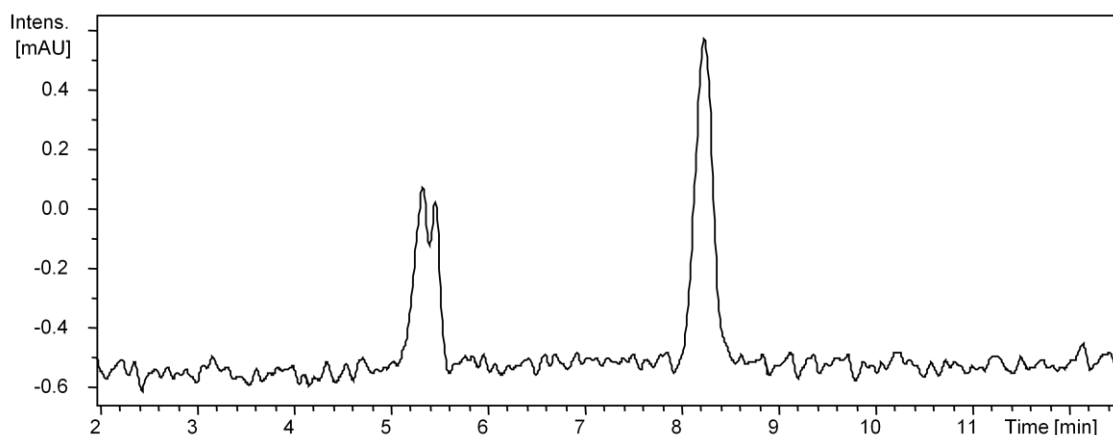
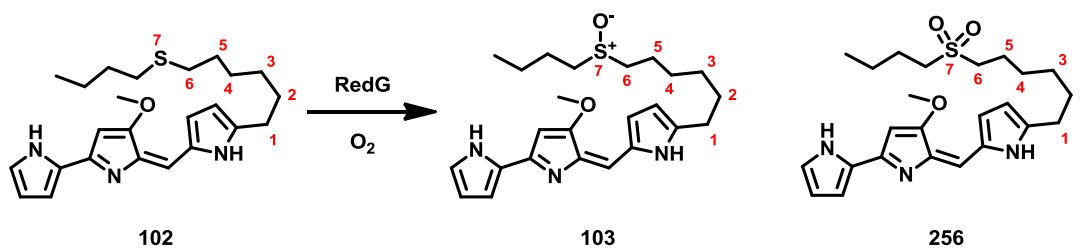


Figure 3.2: A_{533} chromatogram from LC-MS analysis of the mycelial extracts of the *redL* mutant fed with 2-UP analogue **101**

Examination of the mass spectrum for the peak with a retention time of 8.3 min revealed the expected $m/z = 412$, corresponding to the undecylprodiginin sulphide analogue **102**. Likewise, examination of the mass spectrum for the peak with a retention time of 5.5 min revealed the expected $m/z = 428$, corresponding to the undecylprodiginin sulphoxide analogue **103**. High-resolution mass spectrometry confirmed the molecular formulae of these compounds as $C_{24}H_{34}N_3OS$ and $C_{24}H_{34}N_3O_2S$, respectively.

Examination of the mass spectrum for the remaining unexpected peak with a retention time of 5.2 min revealed an $m/z = 444$, 32 mass units higher than the corresponding sulphide **102** and 16 mass units higher than the corresponding sulphoxide **103**. It was therefore proposed that RedG not only catalyses the oxidation of sulphide **102** to sulphoxide **103** as anticipated, but further converts sulphide **102** to sulphone **256**, Scheme 3.2 and Figure 3.3. The molecular formula obtained from high-resolution mass spectrometry, $C_{24}H_{34}N_3O_3S$, was consistent with sulphone **256**.



Scheme 3.2: Products resulting from the feeding of 2-UP analogue **101** to the *redL* mutant

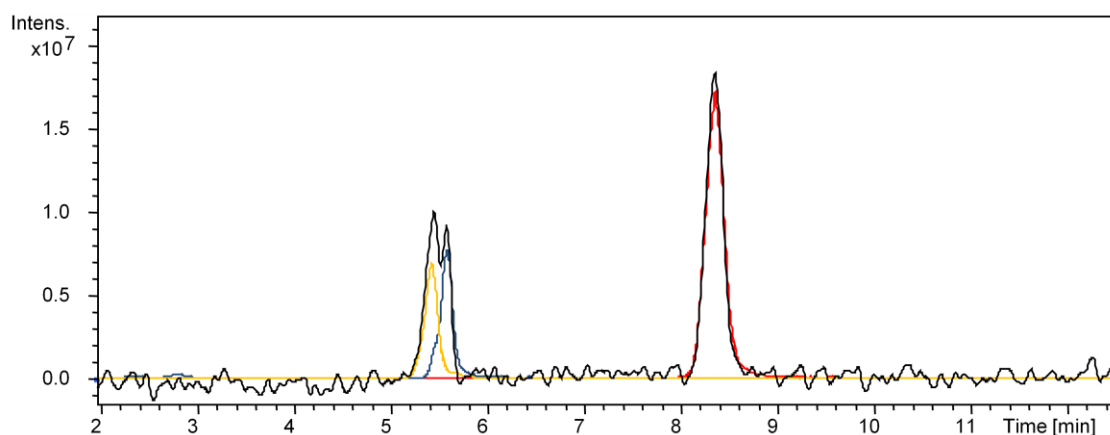


Figure 3.3: A_{533} chromatogram (black) and extracted ion chromatograms at $m/z = 412$ (red), $m/z = 428$ (blue) and $m/z = 444$ (yellow) from LC-MS analysis of the mycelial extracts of the *redL* mutant fed with 2-UP analogue **101**

During the synthesis of 2-UP analogue **101**, it was noticed that exposure of the sulphide to air resulted in partial oxidation to the corresponding sulphoxide (see Section 2.4.1). Since these feeding experiments were performed under aerobic conditions, it was possible that the observed sulphoxide **103** was produced as a result of non-enzymatic oxidation by air. To confirm that RedG was responsible for the oxidation of the sulphide, the feeding experiment was repeated with a mutant lacking the *redG* gene in addition to the *redL* gene, Figure 3.4.

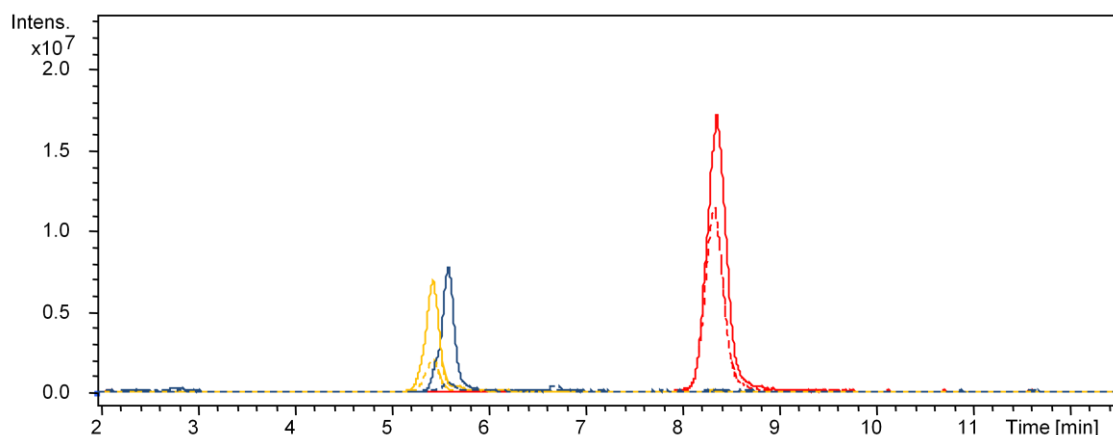
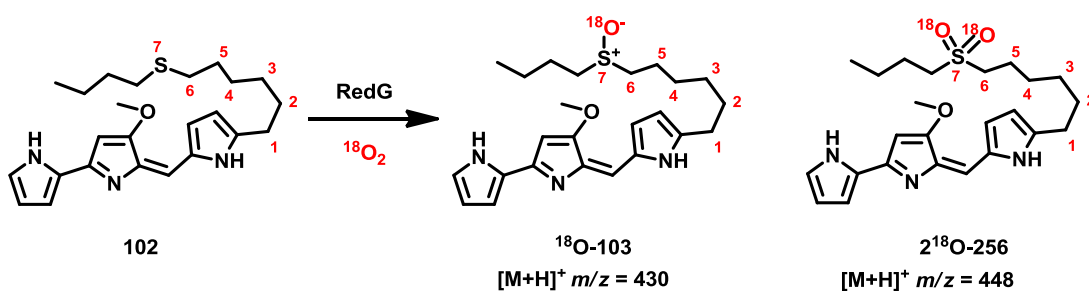


Figure 3.4: Extracted ion chromatograms at $m/z = 412$ (red), $m/z = 428$ (blue) and $m/z = 444$ (yellow) from LC-MS analysis of the mycelial extracts of the *redL* mutant (solid lines) and *redLG* double mutant (dashed lines) fed with 2-UP analogue **101**

As shown in Figure 3.4, the amount of both oxidised products is substantially reduced in the *redLG* double mutant (dashed line chromatograms), indicating that RedG was indeed responsible for the majority of the oxidation observed. As shown by the yellow dashed extracted ion chromatogram ($m/z = 444$), a reasonable amount of sulphone **256** was still observed in the *redLG* double mutant. While no oxidation to the sulphone was observed during the synthesis of 2-UP analogue **101**, the reduced levels observed in the feeding experiment with the *redLG* double mutant may result from the action of a non-specific oxidative enzyme in *Streptomyces coelicolor*.

As expected, feeding of 2-UP analogue **101** bearing a sulphur atom at the site of cyclisation resulted in the formation of the corresponding sulphoxide **103** in addition to the unexpected sulphone **256**. To confirm that the oxygen atoms incorporated into these oxidised products originate from molecular oxygen, the feeding experiments were repeated under an $^{18}\text{O}_2$ atmosphere. If the oxygen atoms present in the oxidised products originate from molecular oxygen, a shift of two mass units for the sulphoxide ^{18}O -**103** and four mass units for the sulphone ^{18}O -**256** would be observed, Scheme 3.3 and Figure 3.5 and 3.6.



Scheme 3.3: The expected pattern of isotope labelling for sulphoxide **¹⁸O-103** and sulphone **²¹⁸O-256** resulting from the feeding of 2-UP analogue **101** to the *redL* mutant under an atmosphere of ¹⁸O₂

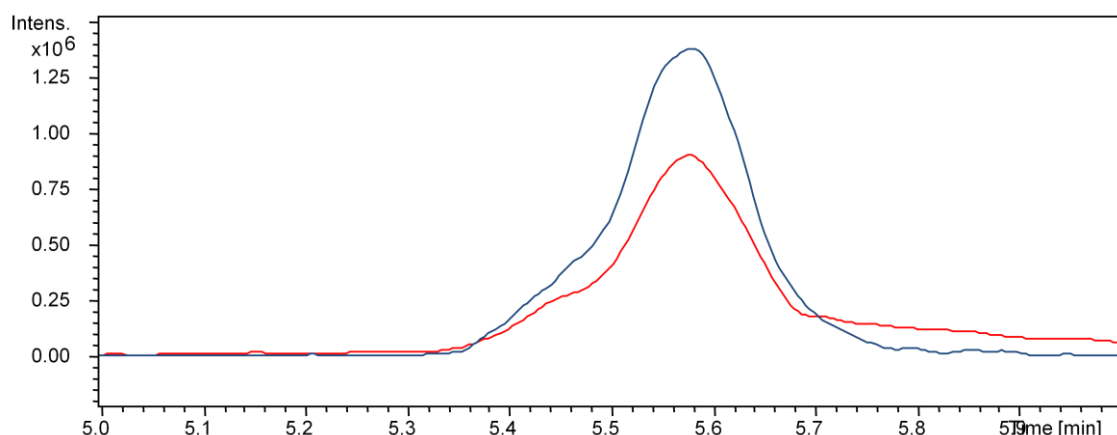


Figure 3.5: Extracted ion chromatograms at $m/z = 428$ (red) and $m/z = 430$ (blue) from LC-MS analysis of mycelial extracts of the *redL* mutant fed with 2-UP analogue **101** under an atmosphere of ¹⁸O₂

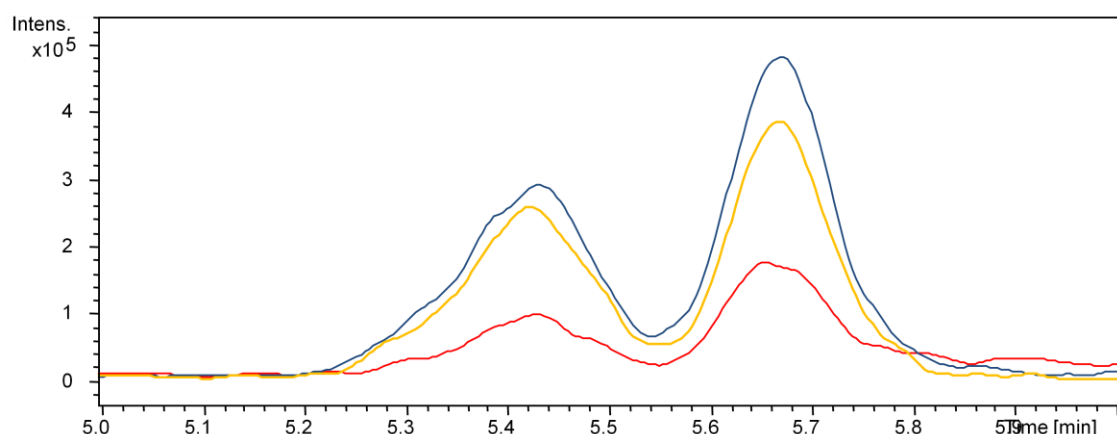
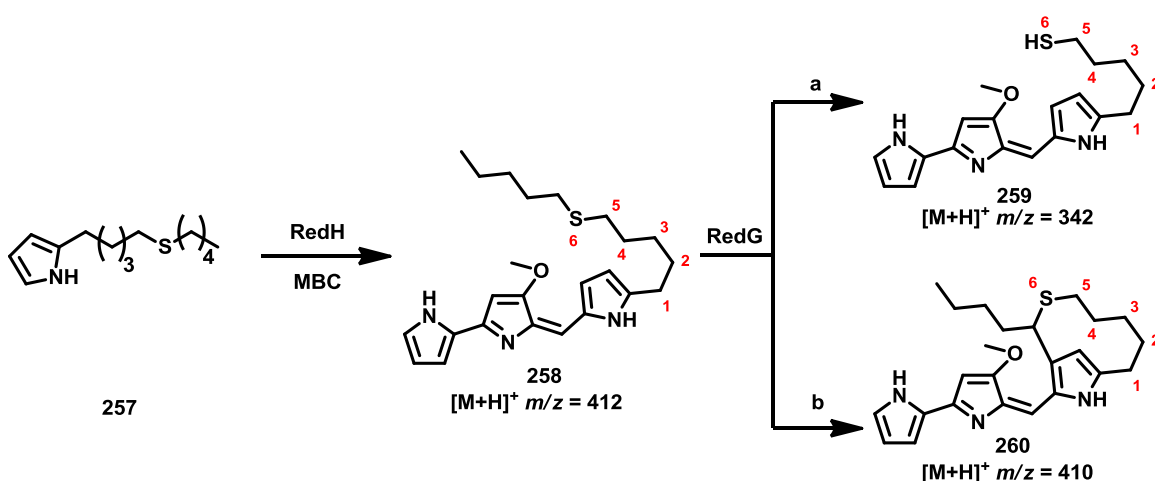


Figure 3.6: Extracted ion chromatograms at $m/z = 444$ (red), $m/z = 446$ (blue) and $m/z = 448$ (yellow) from LC-MS analysis of mycelial extracts of the *redL* mutant fed with 2-UP analogue **101** under an atmosphere of ¹⁸O₂

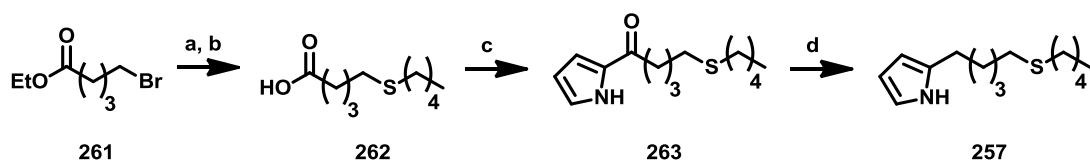
As shown in both Figure 3.5 and 3.6, a significant amount of ^{18}O was incorporated into both oxidised products, in addition to ^{16}O , presumably resulting from atmospheric oxygen. Interestingly, significant amounts of sulphone **256** were observed that contain one ^{16}O atom and one ^{18}O atom, as highlighted by the blue chromatogram in Figure 3.6. This result implies that the oxidation of sulphide **102** to sulphone **256** occurs in two distinct steps.

3.2.2 Feeding of sulphur containing 2-UP analogue **257**

With the successful trapping of the reactive oxygen species generated by RedG using 2-UP analogue **101**, it was decided to investigate another sulphur containing 2-UP analogue, this time with the sulphur atom replacing C-6' **257**. As discussed in Section 1.12, feeding of 2-UP analogue **85** bearing an ether linkage resulted in a RedG catalysed dealkylation process. Since sulphur is much larger than oxygen, it was hypothesised that there would be less efficient overlap between the sulphur lone pairs and the carbon-centred radical resulting in less of the dealkylation product **259** and more carbocyclised product **260**, Scheme 3.4. 2-UP analogue **257** was synthesised *via* an analogue route to that described in Section 2.4.1 for 2-UP analogue **101**, Scheme 3.5.



Scheme 3.4: The expected undecylprodigiosin analogues **258**, along with the dealkylated product **259** (pathway a) and carbocyclised product **260** (pathway b), expected to result from feeding 2-UP analogue **257** to the *redL* mutant



Scheme 3.5: The synthetic route to 2-UP analogue **257**; **a.** $\text{CH}_3(\text{CH}_2)_4\text{SH}$, *n*-BuLi, THF, 0 °C, 96%; **b.** NaOH, THF:Water, 75 °C, 91%; **c.** i. $(\text{PyS})_2$, PPh_3 , toluene, 25 °C ii. EtMgBr, pyrrole, toluene, -78 °C, 81%; **d.** NaBH_4 , IPA, 85 °C, 81%

LC-MS analysis of the mycelial extract resulting from feeding the *redL* mutant with 2-UP analogue **257** revealed a surprising result. As shown in Figure 3.7, the A_{533} chromatogram bears a striking similarity with that resulting from feeding the *redL* mutant with 2-UP analogue **101**.

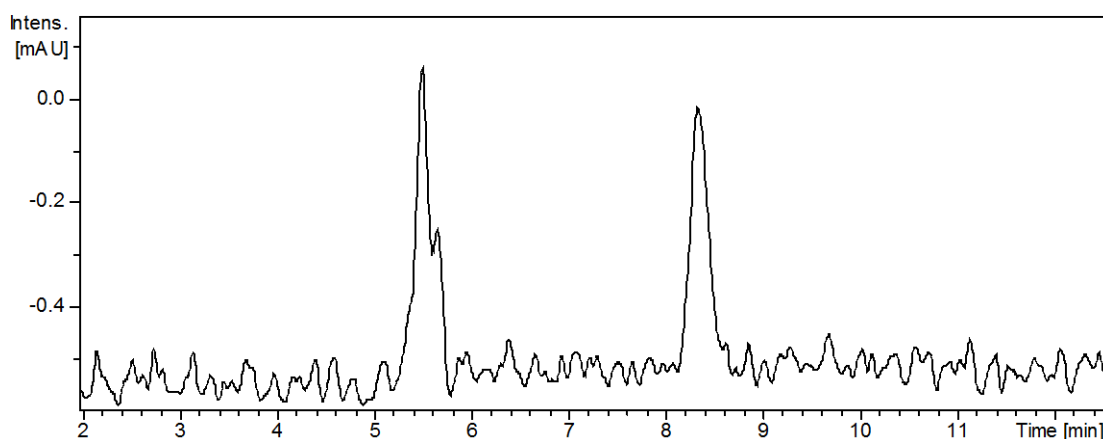


Figure 3.7: A_{533} chromatogram resulting from LC-MS analysis of the mycelial extracts of the *redL* mutant fed with 2-UP analogue **257**

Examination of the mass spectrum for each peak revealed m/z values corresponding to the sulphide, sulphoxide and sulphone, as seen for feeding 2-UP analogue **101**. Extracted ion chromatograms for $m/z = 410$ and $m/z = 342$, the m/z values for $[\text{M}+\text{H}]^+$ derived from **260** and **259** respectively, revealed neither was present, Figure 3.8.

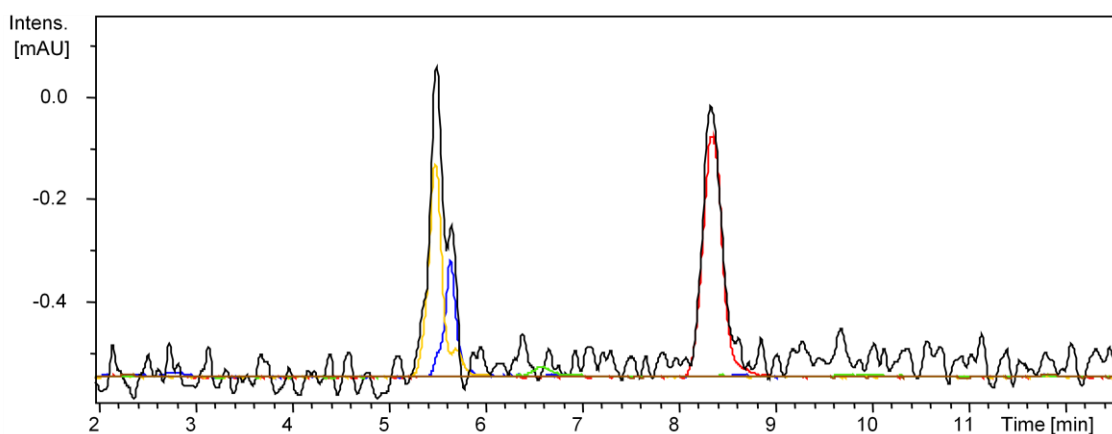


Figure 3.8: A_{533} chromatogram (black) and extracted ion chromatograms at $m/z = 412$ (red), $m/z = 428$ (blue), $m/z = 444$ (yellow), $m/z = 410$ (green) and $m/z = 342$ (brown) from LC-MS analysis of the mycelial extracts of the *redL* mutant fed with 2-UP analogue **257**

To confirm that RedG was responsible for the oxidation products observed, the experiments were repeated with the *redLG* double mutant, Figure 3.9.

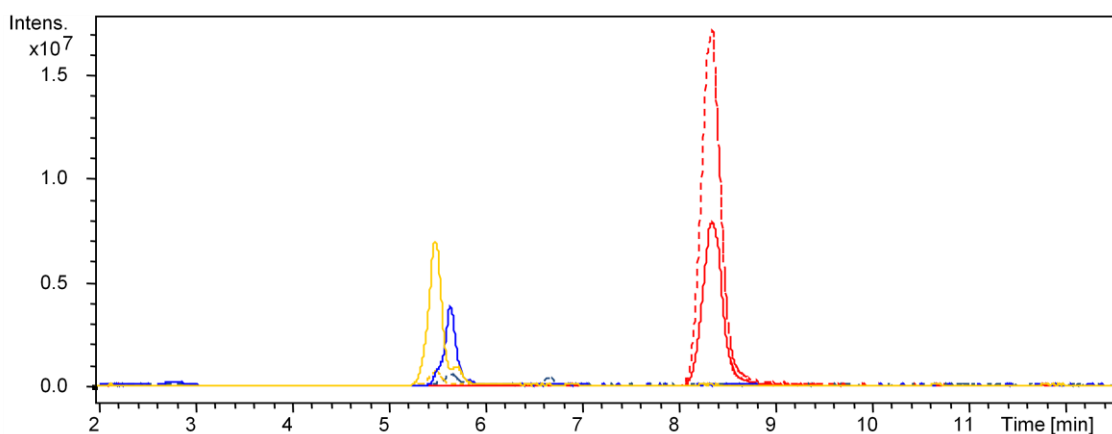
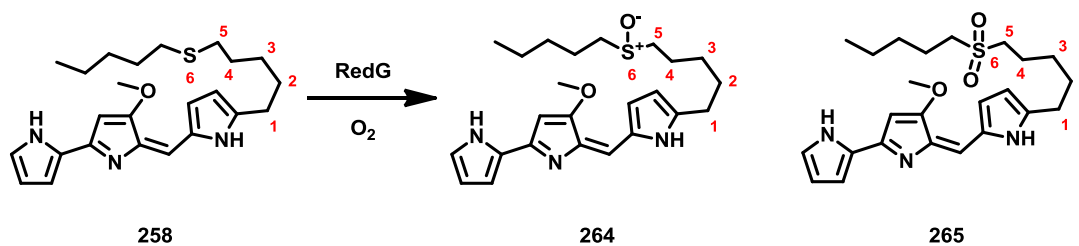


Figure 3.9: Extracted ion chromatograms at $m/z = 412$ (red), $m/z = 428$ (blue) and $m/z = 444$ (yellow) from LC-MS analysis of the mycelial extracts of the *redL* mutant (solid lines) and *redLG* double mutant (dashed lines) fed with 2-UP analogue **257**

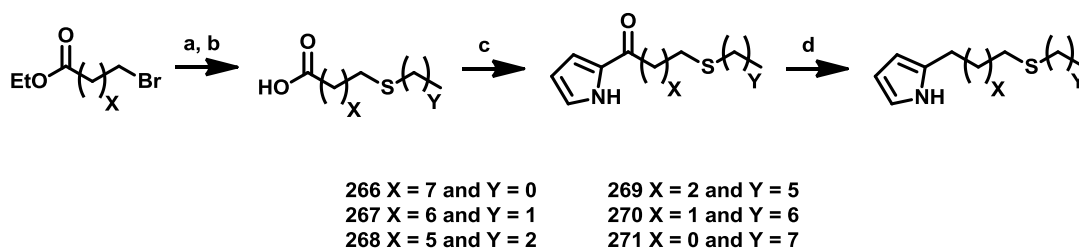
The observation of only sulphoxide **264** and sulphone **265** products, while unexpected, can be explained by the ease with which sulphur can be oxidised compared to carbon. In the case of undecylprodigiosin analogue **258**, the sulphur atom that replaced C-6' presumably remains in close proximity to the activated oxygen species generated at the non-haem iron active site. Thus, the sulphur atom is oxidised more rapidly than the adjacent carbon atom, Scheme 3.6.



Scheme 3.6: The observed products resulting from feeding of 2-UP analogue **257** to the *redL* mutant

3.2.3 Feeding of sulphur containing 2-UP analogues 266 – 270

To further probe this unexpected oxidation process, 2-UP analogues bearing a sulphur atom at other positions of the undecyl chain were synthesised, Scheme 3.7 and Table 3.1. In addition to the sulphur oxidation process catalysed by RedG, it was predicted that the typical oxidative carbocyclisation reaction would occur when the sulphur atom was far enough removed from C-7', resulting in the formation of novel streptorubin B analogues bearing a sulphur atom in the macrocycle, Scheme 3.8.

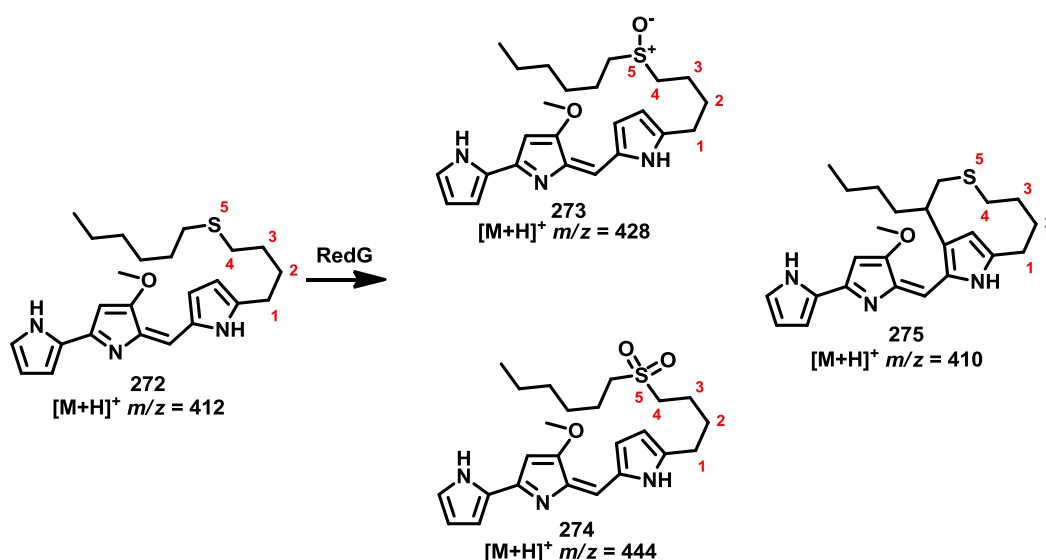


Scheme 3.7: The synthetic route to 2-UP analogues **266** – **271**; **a.** $\text{CH}_3(\text{CH}_2)_Y\text{SH}$, *n*-BuLi, THF, 0 °C; or, NaSCH_3 , DMF, 80 °C; **b.** NaOH, THF:Water, 75 °C; **c.** i. $(\text{PyS})_2$, PPh_3 , toluene, 25 °C
ii. EtMgBr, pyrrole, toluene, -78 °C; **d.** NaBH_4 , IPA, 85 °C

Position of sulphur atom	Step A	Step B	Step C	Step D
10' 266	24% (44%)	90%	49%	95%
9' 267	99%	100%	89%	69%
8' 268	97%	99%	76%	80%
5' 269	99%	99%	76%	83%
4' 270	100%	99%	60%	63%
3' 271	87%	94%	53%	-

Table 3.1: The yields for the synthesis of 2-UP analogues **266** – **271** as outlined in Scheme 3.7;

step A for S-10' **266** resulted in 44% of the corresponding carboxylic acid



Scheme 3.8: The expected undecylprodigiosin analogue **272** and possible oxidation products that might result from feeding 2-UP analogue **269** to the *redL* mutant as a representative example

The 2-UP analogues **266** – **271** were synthesised using an analogues route to that described in Section 2.4.1. In the synthesis of 2-UP analogue **271** that had C-3' replaced with a sulphur atom, no product was isolated from the final reduction, due to extensive degradation *via* an unknown mechanism. In the case of 2-UP analogue **266** that had C-10' replaced with a

sulphur atom, the sodium salt of methanthiol was utilised in place of methanthiol, which is a gas at room temperature and pressure. Interestingly, 44% of the corresponding carboxylic acid was isolated, presumably resulting from a competing transthioesterification reaction or *via* a direct displacement of the carboxylate anion using the sodium methanthiolate.

The results of feeding sulphur containing 2-UP analogues **101**, **257** and **266 – 270** to the *redL* mutant is summarised in Table 3.2 (see Appendix for chromatograms).

Position of sulphur atom	Sulphide analogue	Sulphoxide analogue	Sulphone analogue	Streptorubin B analogue
10' 266	276 ?	277 ?	278 ?	279 ?
9' 267	280 ?	281 ?	282 ?	283 ?
8' 268	284 ?	285 ?	286 ?	287 ?
7' 101	102 ✓	103 ✓	256 ✓	-
6' 257	258 ✓	264 ✓	265 ✓	260 *
5' 269	272 ✓	273 ✓	274 ✓	275 *
4' 270	288 ✓	289 ✓	290 ✓	291?

Table 3.2: The observed products resulting from feeding of 2-UP analogues **101**, **257** and **266 – 270** to the *redL* mutant; ✓ compound was observed; ? inconclusive; * compound was not observed

In the case of 2-UP analogues **269** and **270**, with C-5' and C-4' replaced with sulphur atoms respectively, the corresponding sulphoxides **273** and **289** along with sulphones **274** and **290** were observed. For 2-UP analogue **270**, a trace amount of a compound with the expected *m/z* for the corresponding streptorubin B analogue **291** was barely detected. However, there was no significant difference between the control experiment when 2-UP analogue **270** was fed to the *redLG* double mutant. Interestingly, the amount of sulphur oxidation product observed appeared to decrease as the sulphur atom was moved further from C-7'. This

decrease in sulphur atom oxidation is presumably due to the sulphur atom being too far from the activated oxygen non-haem iron to react.

It was expected that feeding of 2-UP analogues **266**, **267** and **268** to the *redL* mutant would provide analogous results to **270**, **269** and **257**, respectively, since the sulphur atom is the same distance from C-7' except on the other side. Indeed, it was also hypothesised that feeding of 2-UP analogue **266** might result in the formation of a streptorubin B analogue, this time with an exocyclic sulphur atom. However, feeding of these 2-UP analogues yielded unexpected results, Figure 3.10.

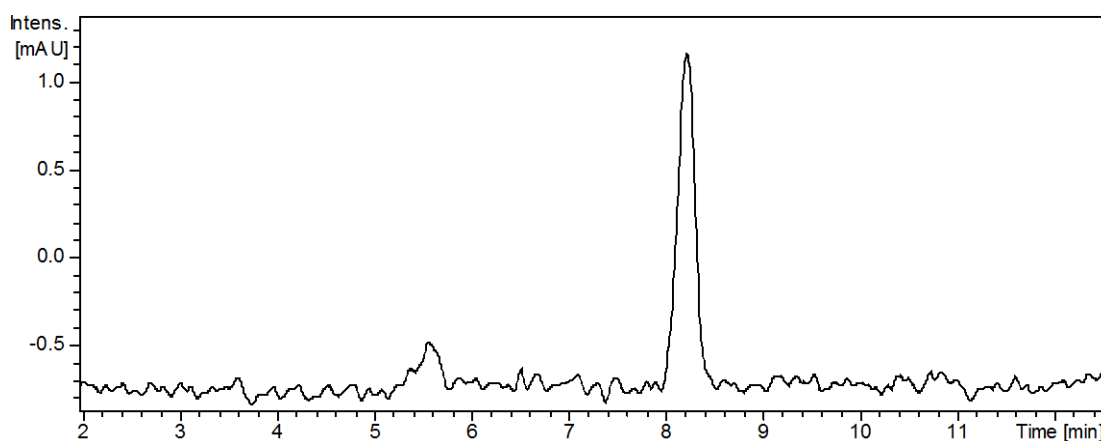


Figure 3.10: A₅₃₃ chromatogram from LC-MS analysis of the mycelial extracts of the *redL* mutant fed with 2-UP analogue **268** as a representative example

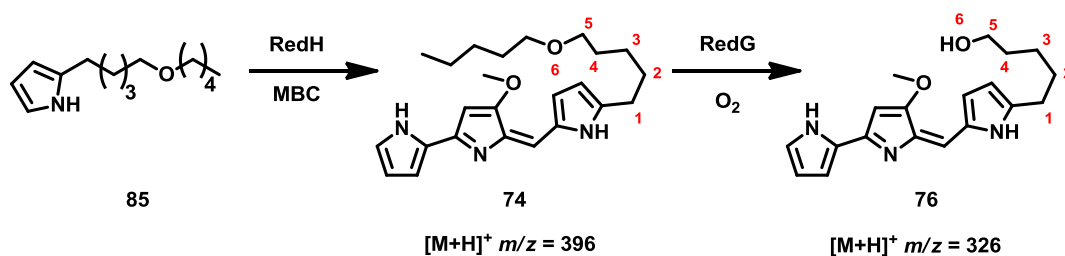
As shown in Figure 3.10, only trace amounts of the expected sulphur oxidised products **285** and **286** were detected. Indeed, comparison with the control experiment in which 2-UP analogue **268** was fed to the *redLG* double mutant revealed that these products were barely attributable to RedG.

Feeding of 2-UP analogue **268** to the *redL* mutant was repeated with 2-UP **20** and 2-UP analogue **101** performed in parallel as a positive control. However, neither feeding experiment provided the expected result. Attempts to reproduce the results of feeding 2-UP analogues **101**, **257**, **269** or **270** were unsuccessful; this will be discussed in more detail in Section 3.4.

3.3 Feeding of ether containing 2-UP analogue to the

Streptomyces coelicolor redL mutant

As discussed in Section 1.12, feeding of a 2-UP analogue **85** containing an ether linkage adjacent C-7' resulted in the apparent formation of a dealkylated undecylprodigiosin analogue **76**, Scheme 3.9. Prior to confirming the exact nature of the predicted dealkylated product, it was decided to ensure that the results observed by Stuart Haynes could be reproduced.



Scheme 3.9: The undecylprodigiosin analogue **74** and dealkylated product **76** expected to result from feeding 2-UP analogue **85** to the *redL* mutant

LC-MS analysis of the mycelial extract resulting from feeding the *redL* mutant with 2-UP analogue **85** revealed a surprising result, Figure 3.11. Examination of the A_{533} chromatogram revealed the presence of only one peak with a retention time of 7 min. This was surprising because two peaks were expected, corresponding to the undecylprodigiosin analogue **74** and the dealkylated product **76**, respectively.

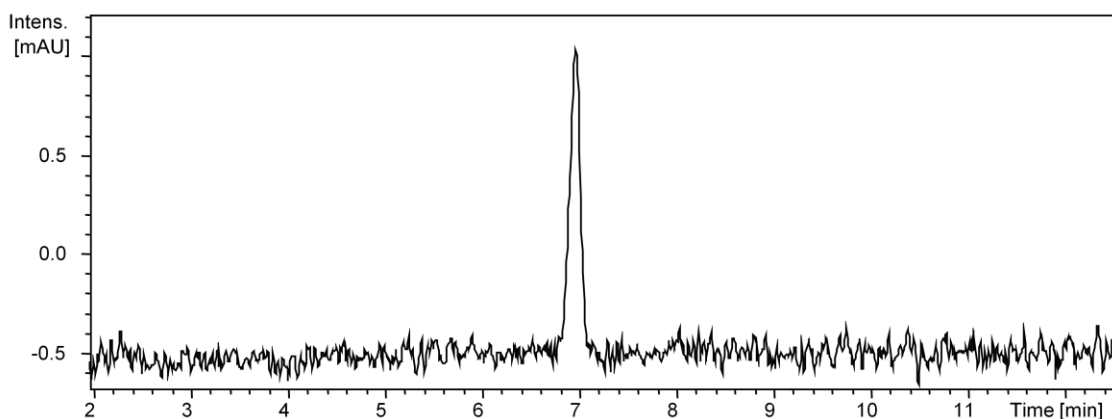


Figure 3.11: A_{533} chromatogram from LC-MS analysis of the mycelial extracts of the *redL* mutant fed with 2-UP analogue **85**

Examination of the mass spectrum corresponding to the single peak in the A_{533} chromatogram showed that it has the m/z value expected for the $[M+H]^+$ ion of undecylprodigiosin analogue **74**. Extracted ion chromatograms for $m/z = 326$ and $m/z = 394$, corresponding to $[M+H]^+$ for the dealkylated product **76** and cyclised product **75**, respectively, did not reveal any additional peaks, Figure 3.12.

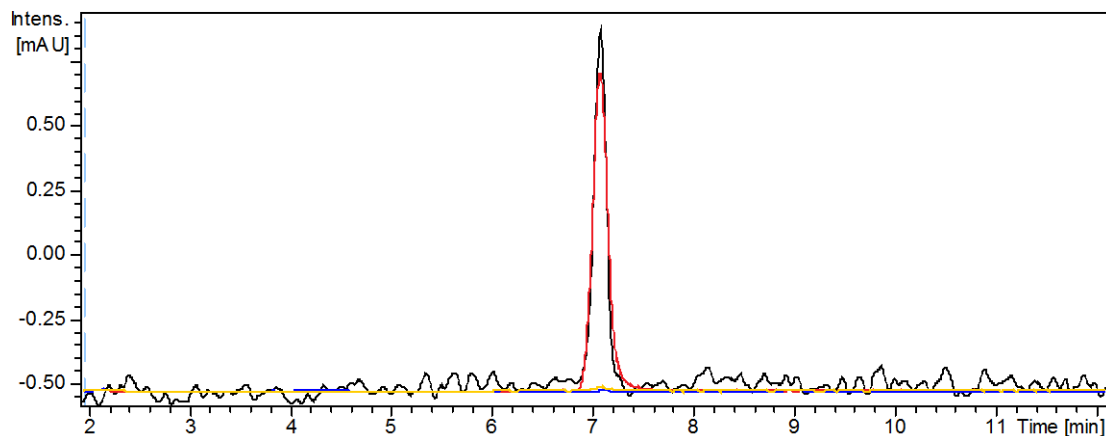


Figure 3.12: A_{533} chromatogram (black) and extracted ion chromatograms at $m/z = 396$ (red), $m/z = 326$ (blue) and $m/z = 394$ (yellow) from LC-MS analysis of the mycelial extracts of the *redL* mutant fed with 2-UP analogue **85**

This failure to reproduce the results reported by Stuart Haynes may have been due to problems with the activity of RedG, as previously observed in the feeding of the sulphur analogues, Section 3.2.4.

3.4 Problems with feeding to the *Streptomyces coelicolor redL*

mutant

As shown in both Section 3.2 and 3.3, the reproducibility of the feeding experiments with the *redL* mutant was poor. Indeed, it was noticed that over the course of several months, the apparent activity of RedG decreased, even when the *redL* mutant strains were fed with the natural substrate 2-UP **20**. This reduced activity of RedG would explain why feeding of ether containing 2-UP analogue **85** did not result in the dealkylated product **76** previously observed by Stuart Haynes.

A possible explanation for this reduced RedG activity could be instability of the plasmid introduced by Paulina Sydor containing the additional copies of *redH* and *redG*. To confirm that the *redL* mutants still contained this plasmid, spores of the *redL* mutant were grown on SFM agar plates containing hygromycin. Since the plasmid containing the additional copies of *redH* and *redG* also contained a hygromycin resistance gene, only spores that still contained the plasmid should survive. A single colony was subsequently picked and used to generate a new spore stock. However, feeding of 2-UP **20** to cultures derived from this fresh spore stock did not result in the ratio of streptorubin B **6** to undecylprodigiosin **4** originally observed when this strain was created.

In a further effort to improve the ratio of streptorubin B **6** to undecylprodigiosin **4**, a range of alternative experimental conditions were investigated, including:

- Changing the growth medium
- Changing the amount of 2-UP / 2-UP analogue fed
- Changing the amount of time the culture was grown for before commencing feeding
- Changing the method of feeding
- Changing the source of water used to make the culture medium¹¹²

None of these factors had a significant impact on the ratio of streptorubin B **6** to undecylprodigiosin **4** observed. Thus, an alternative approach for utilising the mechanistic probes to investigate the catalytic mechanism of RedG was pursued.

**4. Results and discussion: Feeding of 2-undecypyrrole
analogues to *Streptomyces albus* expressing *redHG***

4.1 *Streptomyces albus* as a heterologous host for expression of

redHG

Due to the poor and inconsistent activity of RedG in the *redL* mutant, resulting in a poor ratio of streptorubin B **6** to undecylprodigiosin **4**, an alternative method was required to investigate the oxidative carbocyclisation catalysed by RedG.

Paulina Sydor, a previous member of the Challis group, reported that *Streptomyces albus* expressing *redHG* under the control of the constitutive *ermE** promoter produces an approximate 1:1 ratio of streptorubin B **6** to undecylprodigiosin **4** when fed with chemically synthesised 2-UP **20** and MBC **19**.¹¹³ Fresh transconjugants of *S. albus* expressing *redH* and *redHG* were prepared as described by Paulina Sydor.¹¹⁰

After similar optimisation experiments to those undertaken for *S. coelicolor*, as discussed in Section 3.4, it was found that feeding 2 mg of MBC **19** and 2-UP **20** to *S. albus + redHG* on the third day after inoculation provided the best yield and ratio of streptorubin B **6** to undecylprodigiosin **4**. It was established that premixing a DMSO solution of MBC **19** and a methanol solution of 2-UP **20**, followed by direct addition to the bacterial culture as small droplets, without the addition of water, was essential to achieve good levels of production.

Feeding of chemically synthesised 2-UP **20** and MBC **19** to wild type *S. albus*, *S. albus + redH* and *S. albus + redHG*, showed that almost no red pigment is produced in the absence of *redH*, Figure 4.1.



Figure 4.1: A photograph of wild type *S. albus* (left), *S. albus* + *redH* (middle) and *S. albus* + *redHG* (right) after two days incubation at 30 °C fed with chemically synthesised 2-UP **20** and MBC **19**

LC-MS analyses of the mycelial extracts resulting from feeding chemically synthesised 2-UP **20** and MBC **19** to *S. albus*, *S. albus* + *redH* and *S. albus* + *redHG*, Figure 4.2, revealed that wild type *S. albus* (red chromatogram) only produces a trace amount of undecylprodigiosin **4**, presumably due to non-enzymatic acid-catalysed condensation of 2-UP **20** and MBC **19** during extraction of the mycelia. In contrast, *S. albus* + *redH* produces a substantial amount of undecylprodigiosin **4** (blue chromatogram), and *S. albus* + *redHG* produces a 1:1 ratio of streptorubin B **6** to undecylprodigiosin **4** (yellow chromatogram).

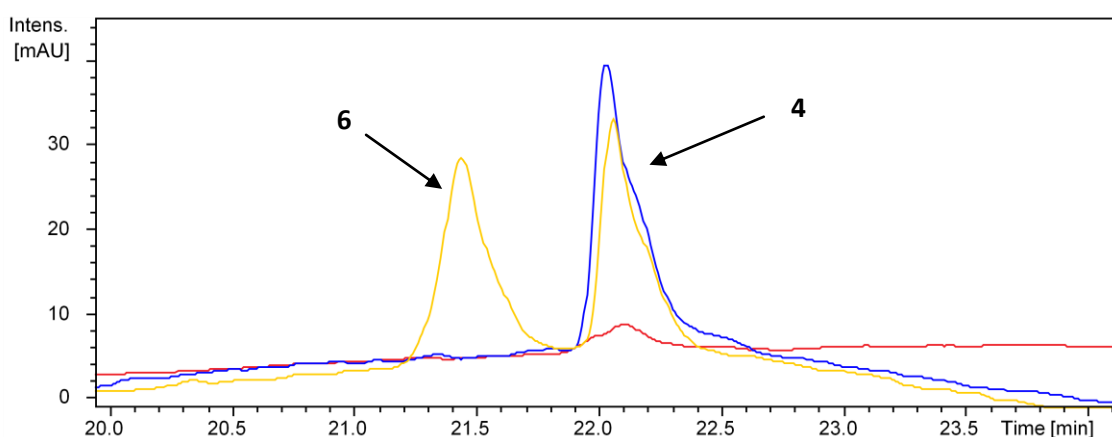


Figure 4.2: A comparison of A_{533} chromatograms resulting from LC-MS analysis of the mycelial extracts of *S. albus* (red), *S. albus* + *redH* (blue) and *S. albus* + *redHG* (yellow) fed with chemically synthesised 2-UP **20** and MBC **19**

Previously, Paulina Sydor had noticed that the ratio of streptorubin B **6** to undecylprodigiosin **4** was improved when RedH and RedG were present. It was not obvious why the ratio of streptorubin B **6** to undecylprodigiosin **4** should be affected by RedH, since it has no direct role in the oxidative carbocyclisation reaction. One possible explanation for this observation is that RedH and RedG form a complex *in vivo*, in which undecylprodigiosin **4** is 'passed' directly from RedH to RedG, preventing undecylprodigiosin **4** from becoming trapped in the cell membrane by its lipophilic undecyl chain, thus preventing RedG from accessing its substrate.

During the feeding of chemically synthesised 2-UP **20** and MBC **19** to *S. albus* + *redHG*, it was noticed that red pigment was visible much sooner than in *S. albus* + *redH*, Figure 4.3. As shown in Figure 4.3, after two hours incubation at 30 °C, *S. albus* + *redHG* (top right) has produced more red pigment than *S. albus* + *redH* (bottom right). Since RedG is not involved in the condensation of 2-UP **20** and MBC **19**, this observation was unexpected. A possible explanation for this unexpected observation could be that the catalytic efficiency of RedH is improved by forming a complex *in vivo* with RedG; thus, undecylprodigiosin **4** is produced more rapidly.

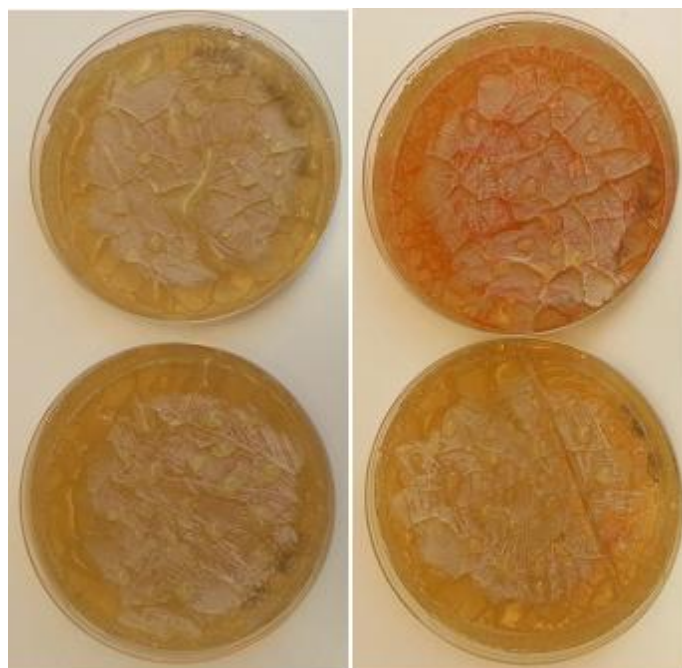


Figure 4.3: A comparison of *S. albus* + *redHG* (top plates) and *S. albus* + *redH* (bottom plates) immediately after feeding chemically synthesised 2-UP **20** and MBC **19** (left) and after two hours incubation at 30 °C (right)

Feeding of MBC **19** and 2-UP analogues was reinvestigated using *S. albus* + *redHG*. However, it was noticed that over the course of several weeks, the level of RedG activity reduced dramatically, Figure 4.4.

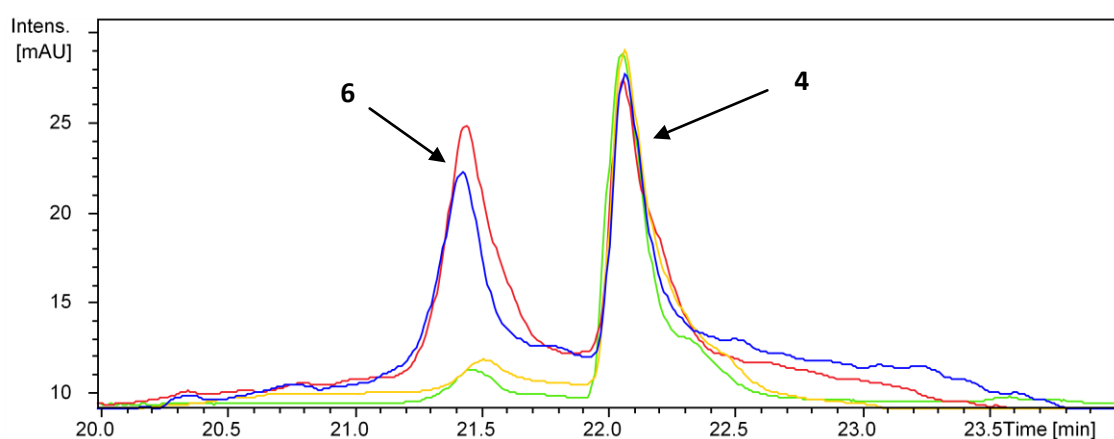


Figure 4.4: A comparison of A_{533} chromatogram resulting from LC-MS analysis of the mycelial extracts of *S. albus* + *redHG* fed with chemically synthesised 2-UP **20** and MBC **19** immediately after conjugation (red) and after spores had been stored at -80 °C for one week (blue), three weeks (yellow) and five weeks (green)

Immediately after conjugation, a 1:1 ratio of streptorubin B **6** to undecylprodigiosin **4** was observed (red chromatogram). However, after one week of storage at -80 °C, this ratio had reduced slightly and after five weeks, only trace amounts of streptorubin B **6** were detected (green chromatogram). During this same time period, undecylprodigiosin **4** production remained constant. Since undecylprodigiosin **4** was still produced, the plasmid containing *redH* and *redG* must still be present in the *S. albus* strain.

A possible explanation for this marked decrease in activity could be a result of an unforeseen toxic effect of RedG on *S. albus*. Since *redG* is constitutively expressed, for large periods of time when no substrate is present in the cells, reactive oxygen species, such as superoxide or hydrogen peroxide, could be generated by RedG, resulting in cell damage. Indeed, it is well known that many iron-containing enzymes that activate molecular oxygen often self-inactivate due to reactions with the reactive oxygen species.^{114,115} It is therefore possible that strains containing mutant *redG* alleles, which no longer express active enzyme are selected for during storage. Due to time constraints, sequencing of the *redG* gene from the samples that had lost enzymatic activity to investigate this hypothesis was not undertaken.

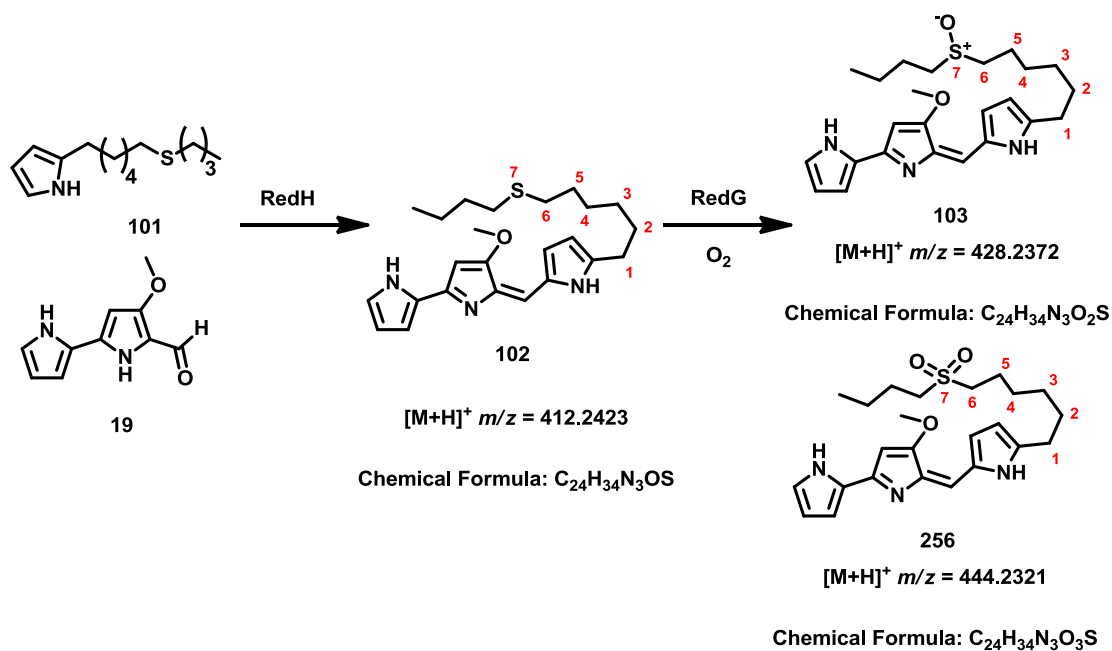
Whatever the cause of this observed decrease in RedG activity, it proved necessary to use freshly conjugated *S. albus* + *redHG* for the feeding experiments with 2-UP analogues.

4.2 Feeding of sulphur containing 2-UP analogues to *Streptomyces albus* + *redHG*

With this new feeding method developed, it was decided to repeat the feeding of the sulphide analogues to confirm the results obtained from feeding in *S. coelicolor*.

4.2.1. Feeding of sulphur containing 2-UP analogue 101

As discussed in Section 3.2.1, feeding of 2-UP analogue **101** with C-7' replaced with a sulphur atom resulted in oxidation of the sulphide to the corresponding sulphoxide **103** and sulphone **256**, Scheme 4.1. This was repeated using *S. albus* + *redHG* to confirm the previous observations, Figure 4.5.



Scheme 4.1: The observed undecylprodigiosin analogue **102** and sulphur oxidation products **103** and **256** resulting from feeding 2-UP analogue **101** to the *S. coelicolor redL* mutant

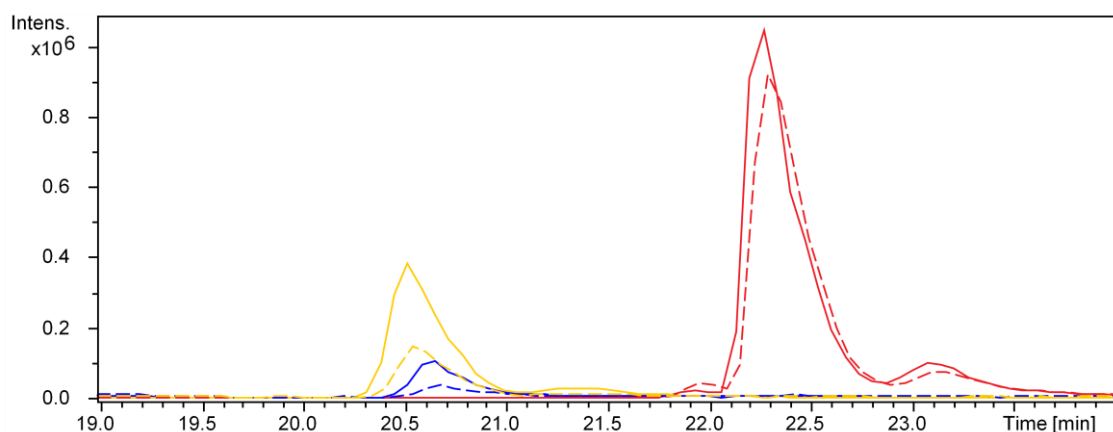
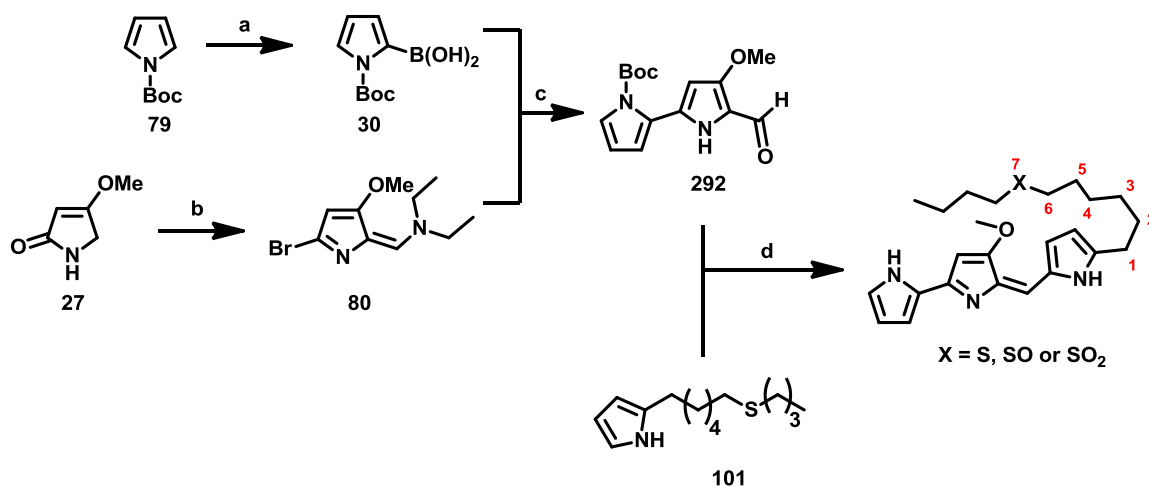


Figure 4.5: Extracted ion chromatograms at $m/z = 412.24$ (red), $m/z = 428.23$ (blue) and $m/z = 444.23$ (yellow) from LC-MS analysis of the mycelial extracts of *S. albus* + *redHG* (solid lines) and *S. albus* + *redH* (dashed lines) fed with 2-UP analogue **101** and MBC **19**

As shown in Figure 4.5, both of the expected sulphur oxidation products **103** and **256** were observed in addition to large amounts of the corresponding sulphide **102**. As a control experiment, 2-UP analogue **101** and MBC **19** were also fed to the *S. albus* + *redH* strain (dashed lines). As expected, a significant decrease in the amount of sulphur oxidation products **103** and **256** was observed.

To confirm the identity of the undecylprodigiosin analogues produced in these experiments, it was decided to synthesise authentic standards of sulphide **102**, sulphoxide **103** and sulphone **256**. Comparison of the retention times and fragmentation patterns of the authentic standards with the compounds produced in the feeding experiment would confirm their structures.

As discussed in Section 1.11.3, Thomson *et al* completed their enantioselective total synthesis of streptorubin B **6** by an acid-catalysed condensation of BOC-protected MBC **292** and monopyrrole **50**. It was envisaged that this procedure could be utilised in the synthesis of the authentic standards with an additional sulphur oxidation step, Scheme 4.2 and Table 4.1.



Scheme 4.2: The synthetic route to the authentic standards of **102**, **103** and **256**; **a.** *n*-BuLi, 2,2,6,6-tetramethylpiperidine, B(OMe)₃, THF, -78 °C, 54%; **b.** POBr₃, Et₂NCHO, CH₂Cl₂, 40 °C, 73%; **c.** i. Pd(OAc)₂, PPh₃, Na₂CO₃, ii. HCl, 54%; **d.** i. 2M HCl, MeOH, ii. Oxidant, iii. NaOMe

	Oxidant	Yield
Sulphide 102	-	38%
Sulphoxide 103	<i>m</i> -CPBA	58% (33%)
Sulphone 256	Oxone	54% (13%)

Table 4.1: The oxidant used for the sulphur oxidation; the yield of different sulphur oxidation products are shown in brackets

After the initial Suzuki coupling reaction, careful addition of 2M HCl to hydrolyse the enamine afforded BOC-protected MBC **292**. Acid-catalysed condensation of BOC-protected MBC **292** and 2-UP analogue **101**, followed by oxidation, deprotection and purification by HPLC provided the authentic standards **102**, **103** and **256**. For sulphoxide **103**, *m*-CPBA was used to oxidise the sulphide to the corresponding sulphoxide, with approximately 33% of sulphide **102** remaining. For sulphone **256**, Oxone was used to oxidise the sulphide to the corresponding sulphone, with approximately 13% of sulphoxide **103** also isolated.

As shown in Figure 4.6, the chemically synthesised authentic standards had the same retention times as the compounds from the mycelial extract. In addition, the authentic standards had identical fragmentation patterns to the corresponding metabolites in the mycelial extract, Figure 4.7.

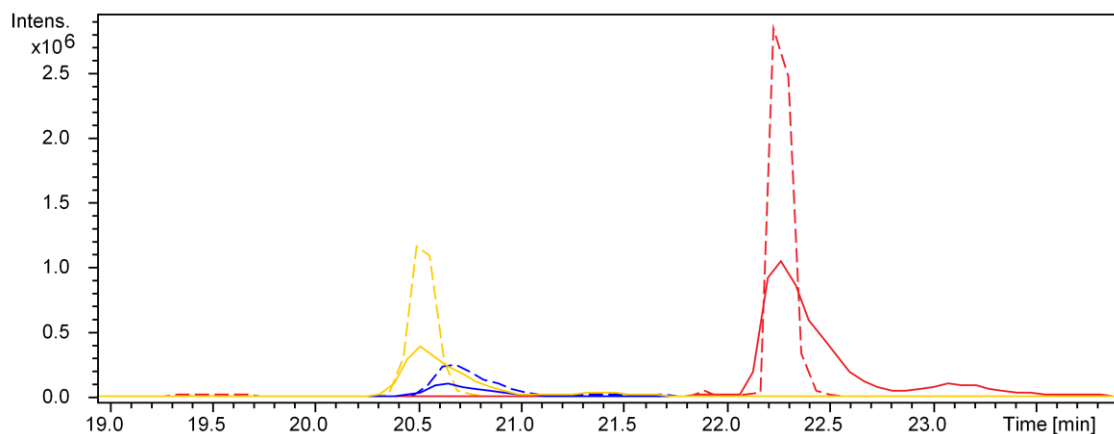


Figure 4.6: Extracted ion chromatograms at $m/z = 412.24$ (red), $m/z = 428.23$ (blue) and $m/z = 444.23$ (yellow) from LC-MS analysis of the mycelial extracts of *S. albus* + *redHG* (solid lines) fed with 2-UP analogue **101** and MBC **19** and solutions of the chemically synthesised authentic standards **102**, **103** and **256** (dashed lines)

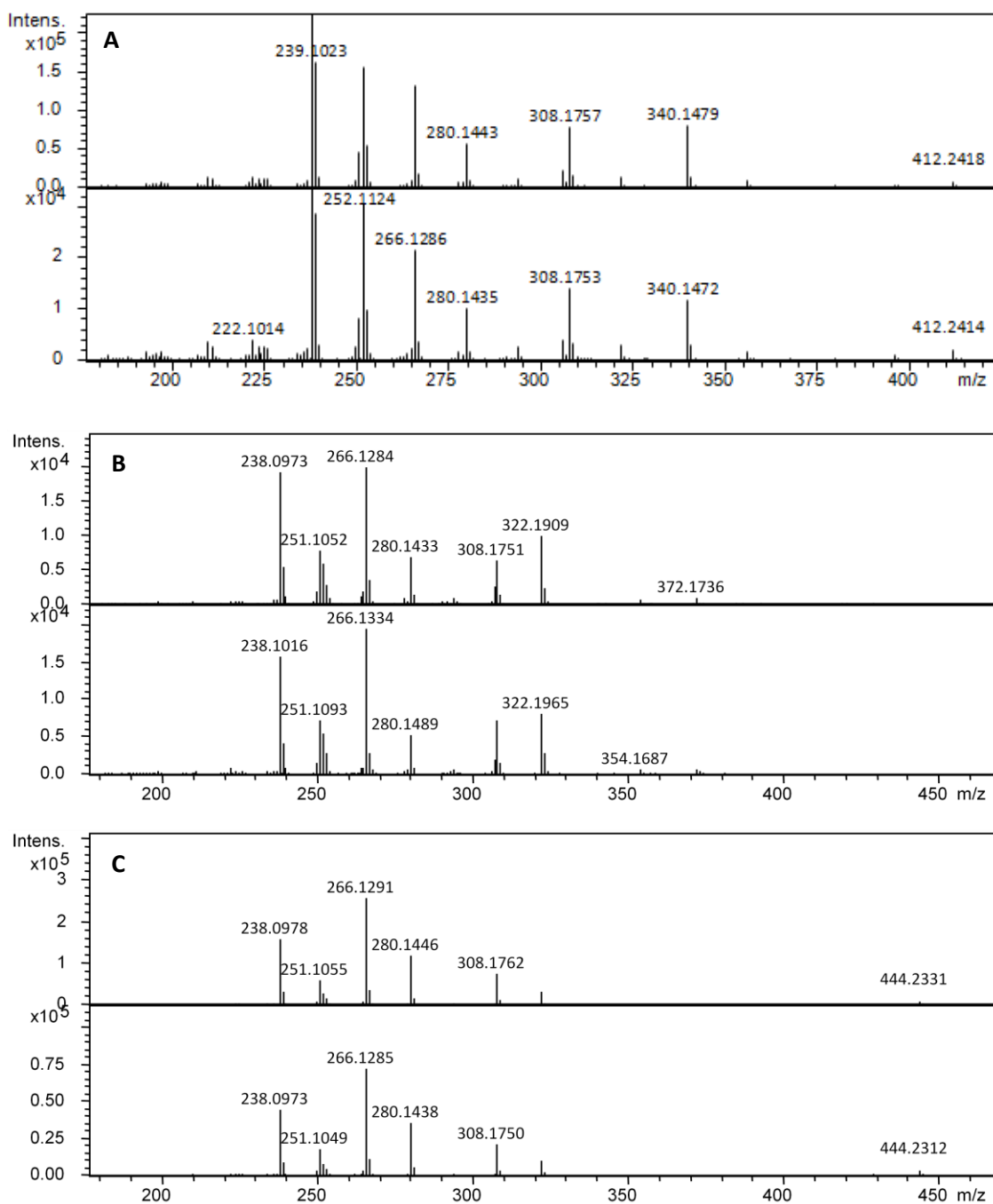
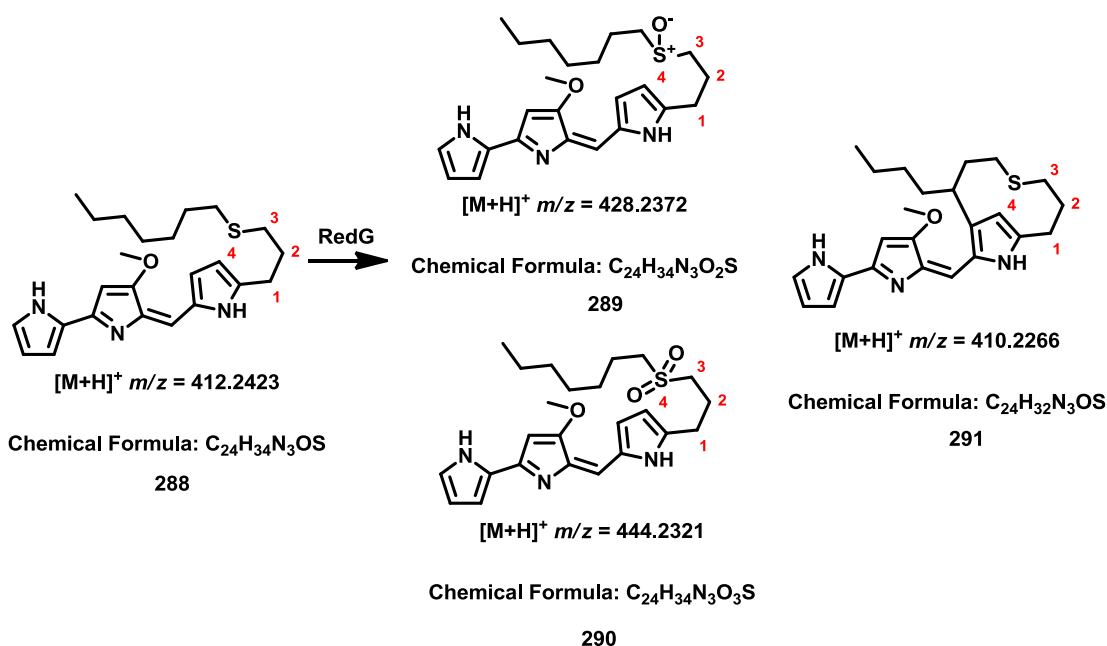


Figure 4.7: A comparison of the MS/MS spectrum observed for the authentic standards (top spectra) and the mycelial extract of sulphide **102** (A), sulphoxide **103** (B) and sulphone **256** (C)

4.2.2 Feeding of other sulphur containing 2-UP analogues

With the successful reproduction of the results observed for the feeding experiments in *S. coelicolor* utilising *S. albus* + *redHG*, feeding of the remaining sulphur containing 2-UP analogues **257** and **266 – 270** was repeated. The results of these feeding experiments are summarised in Table 4.2.



Scheme 4.3: The undecylprodigiosin analogue **288** and oxidised expected to result from feeding *S. albus* + *redHG* with 2-UP analogue **270** and MBC **19**, as a representative example

Position of sulphur atom	Sulphide analogue	Sulphoxide analogue	Sulphone analogue	Streptorubin B analogue
10' 266	276 ✓	277 ✓	278 ✓	279 ✓*
9' 267	280 ✓	281 ✓	282 ✓	283 ✗
8' 268	284 ✓	285 ✓	286 ✓	287 ✗
7' 101	102 ✓	103 ✓	256 ✓	-
6' 257	258 ✓	264 ✓	265 ✓	260 ✗
5' 269	272 ✓	273 ✓	274 ✓	275 ✗
4' 270	288 ✓	289 ✓	290 ✓	291 ✓

Table 4.2: The observed products resulting from feeding of 2-UP analogues **101**, **257** and **266 – 270** with MBC **19** to *S. albus* + *redHG*; ✓ compound was observed; ✗ compound was not observed; * other RedG-derived products were observed

As shown in Table 4.2, feeding of 2-UP analogues **257** and **266 – 270** with chemically synthesised MBC **19** to *S. albus* + *redHG* resulted in the corresponding sulphoxides and

sulphones in all cases. For each oxidation product, HRMS provided molecular formulae consistent with the expected sulphur oxidised products. Control experiments were performed by feeding each 2-UP analogue, along with chemically synthesised MBC **19**, to the *S. albus + redH* strain, resulting in substantially reduced levels of sulphur oxidation products. It should be noted that, as in the case of the *redL* mutant, trace amounts of the corresponding sulfoxides and sulphones were detected in the control experiments, presumably due to non-enzymatic oxidation by air and/or the actions of a non-specific oxidative enzyme in *Streptomyces albus*. The observation that the amount of sulphur oxidised product observed decreased as the sulphur atom was moved further away from C-7' was confirmed using *S. albus + redHG*, with 2-UP analogues **266** and **270** producing the least.

When feeding 2-UP analogue **270** to the *S. coelicolor redL* mutant, trace amounts of the corresponding oxidative cyclised product **291** may have been produced. Repeating this experiment in the *S. albus + redHG* strain, resulted in a substantial amount of the putative oxidative carbocyclised **291** product being observed, Figure 4.8 and 4.9.

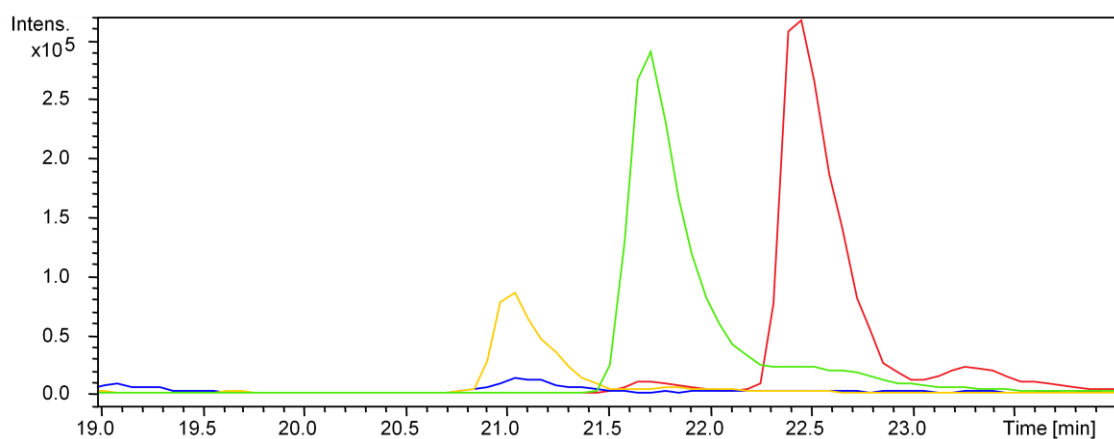


Figure 4.8: Extracted ion chromatograms at $m/z = 412.24$ (red), $m/z = 428.23$ (blue), $m/z = 444.23$ (yellow) and $m/z = 410.22$ (green) from LC-MS analysis of the mycelial extracts of *S. albus* + *redHG* fed with 2-UP analogue **270** and MBC **19**

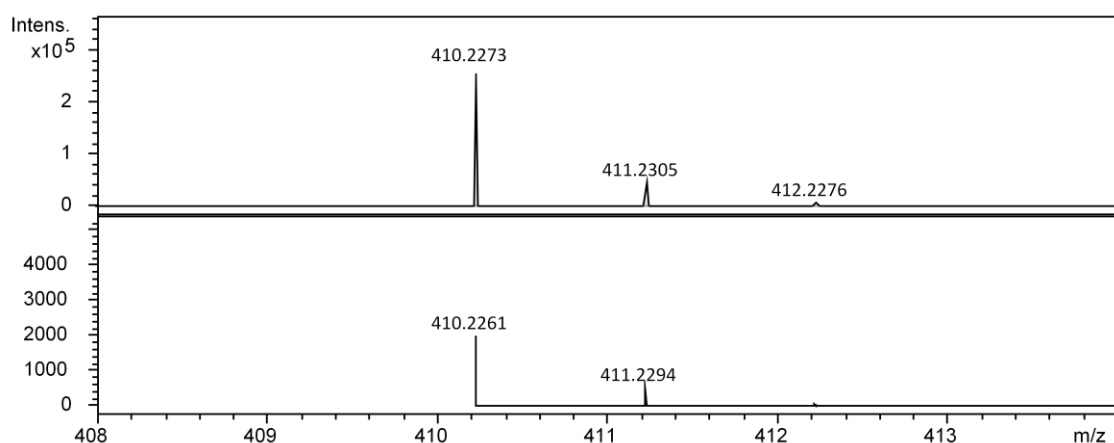


Figure 4.9: A comparison of the HRMS for the compound eluting after 21.7 min in the LC-MS analysis of *S. albus* + *redHG* fed with 2-UP analogue **270** and MBC **19** (top spectrum) and the predicted mass spectrum for $C_{24}H_{32}N_3OS$ (bottom spectrum)

Since the peak at 21.7 min has the correct molecular formula and a similar retention time relative to streptorubin B **6**, it seems likely that this compound is indeed the streptorubin B analogue **291**. However, due to time constraints, this analogue was not isolated to confirm the structure *via* NMR spectroscopy.

Initial analysis of the LC-MS data resulting from the mycelial extracts of *S. albus* + *redHG* fed with 2-UP analogue **266** and chemically synthesised MBC **19** indicated that only a trace amount of the corresponding streptorubin B analogue **279** was produced. This was

unexpected, since the analogous 2-UP analogue **270**, with the sulphur atom the same number of atoms from C-7' but on the other side, resulted in a substantial amount of the corresponding oxidative carbocyclised product **291**. However, examination of the A_{533} chromatogram revealed the presence of an additional broad peak with a retention time of 19.2 min, Figure 4.10.

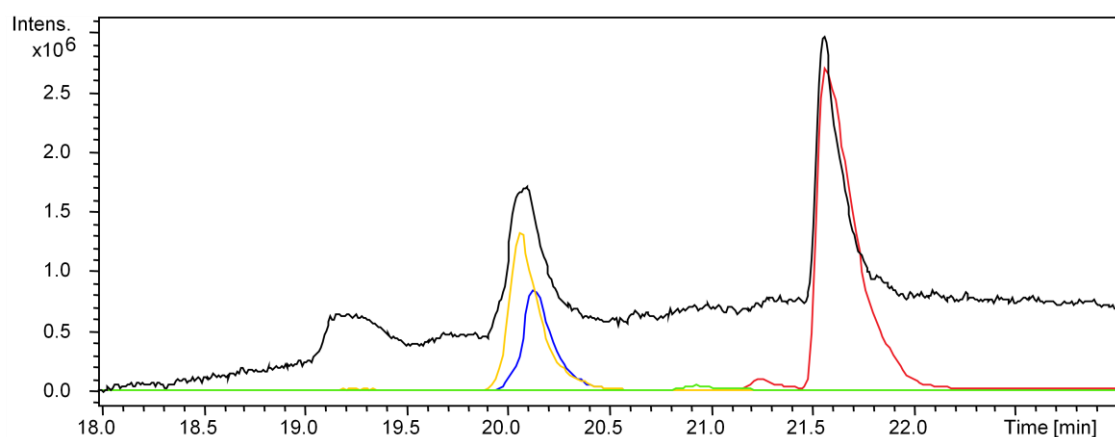


Figure 4.10: A_{533} chromatogram (black) and extracted ion chromatograms at $m/z = 412.24$ (red), $m/z = 428.23$ (blue), $m/z = 444.23$ (yellow) and $m/z = 410.21$ (green) from LC-MS analysis of the mycelial extracts of *S. albus* + *redHG* fed with 2-UP analogue **266** and MBC **19**

Examination of the high resolution mass spectrum for the peak with retention time of 19.2 min revealed the presence of $m/z = 426.2214$ and $m/z = 442.2166$, Figure 4.11 and 4.12.

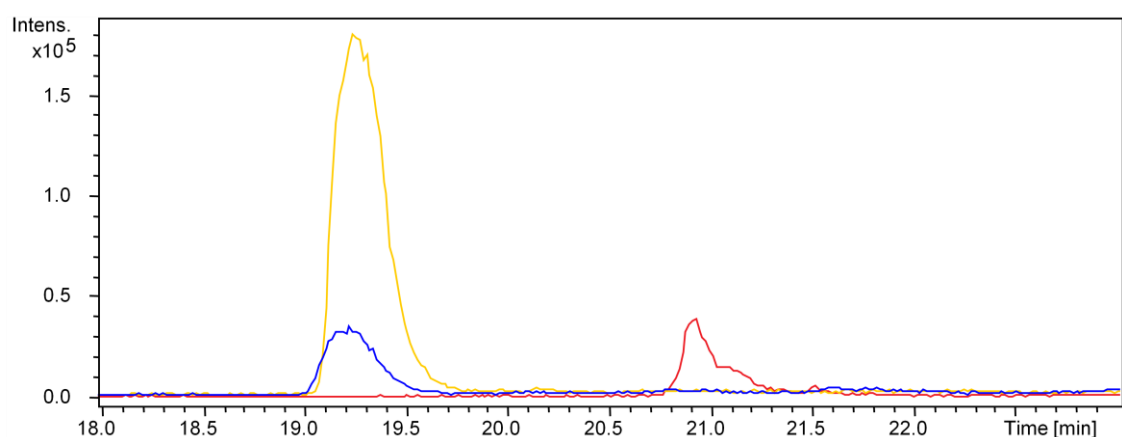


Figure 4.11: Extracted ion chromatograms at $m/z = 412.24$ (red), $m/z = 428.23$ (blue) and $m/z = 444.23$ (yellow) from LC-MS analysis of the mycelial extracts of *S. albus* + *redHG* fed with 2-UP analogue **266** and MBC **19**

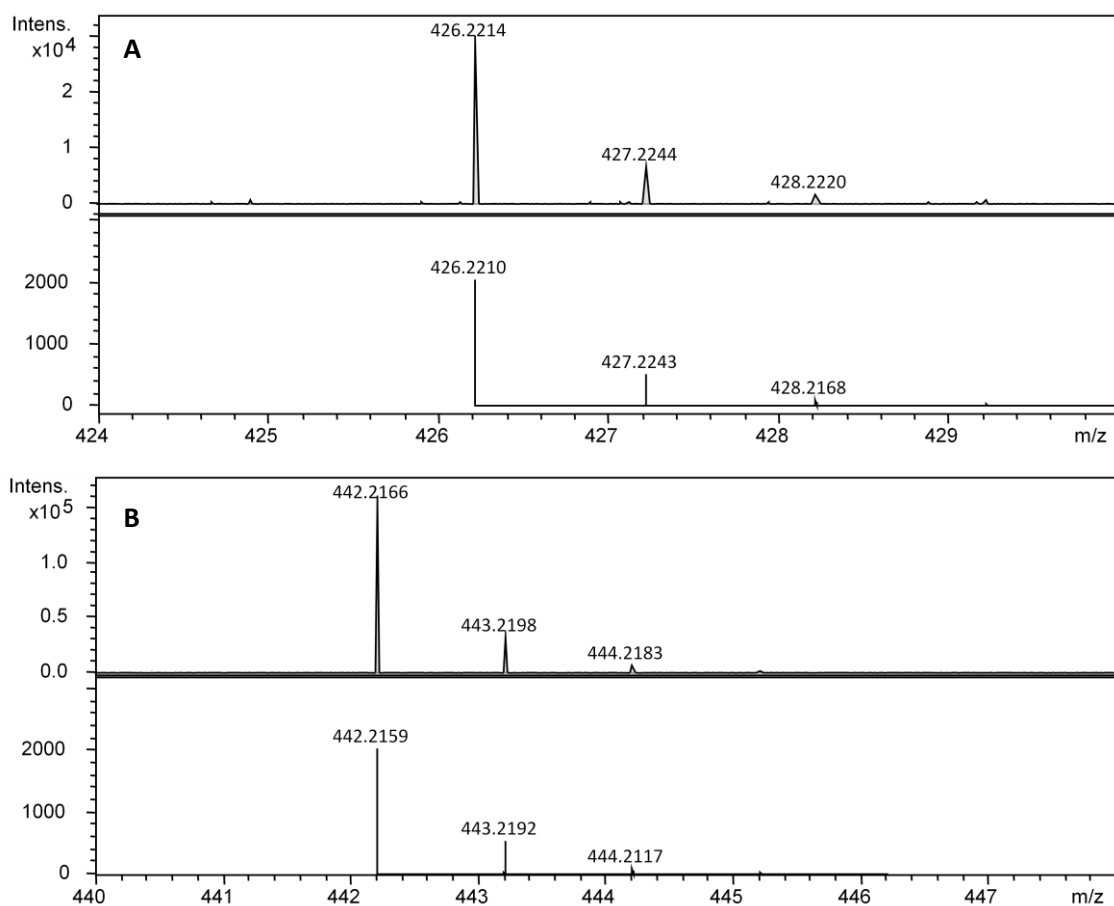
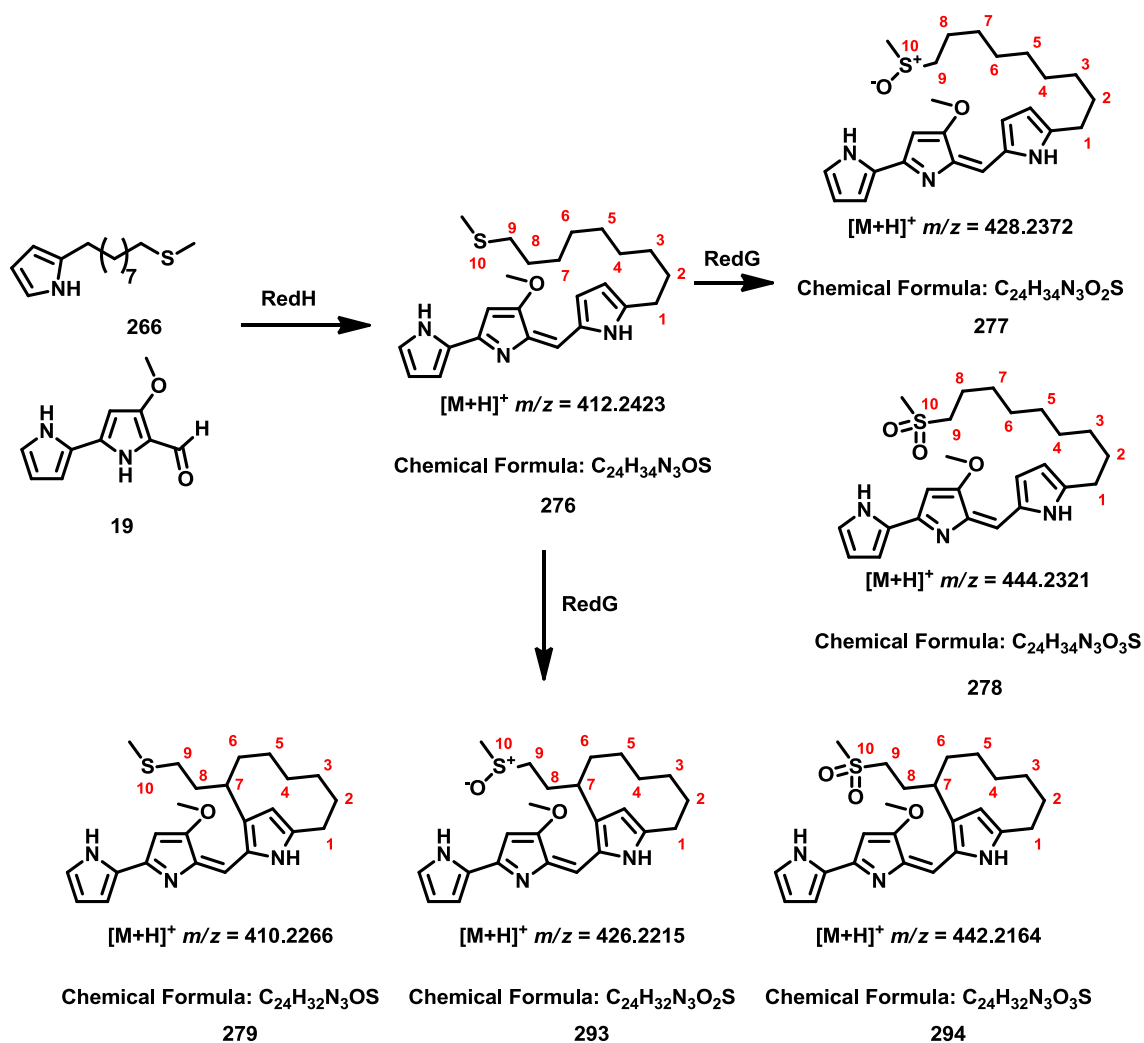


Figure 4.12: A comparison of the HRMS for the compounds eluting after 19.0 min and 19.3 min in the LC-MS analysis (A and B, respectively, top spectrum) and the predicted mass spectrum for $C_{24}H_{32}N_3O_2S$ and $C_{24}H_{32}N_3O_3S$ (A and B, respectively, bottom spectrum)

Given that these two unexpected peaks differ from sulphoxide **277** and sulphone **278** by two mass units, it seems plausible that this broad peak was a result of the corresponding streptorubin B sulphoxide **293** and sulphone **294** analogues, respectively, Scheme 4.4. To confirm these compounds were RedG-derived, 2-UP analogue **266** was fed with MBC **19** to *S. albus* + *redH*. LC-MS analysis indicated that neither of these putative streptorubin B analogues were observed, in addition to reduced levels of the sulphur oxidised products **277** and **278**.



Scheme 4.4: The observed undecylprodigiosin analogue **276**, sulphur oxidation products **277** and **278** and streptorubin B analogues **279**, **293** and **294** resulting from LC-MS analysis of the mycelial extract of *S. albus* + *redHG* fed with 2-UP analogue **266** and MBC **19**

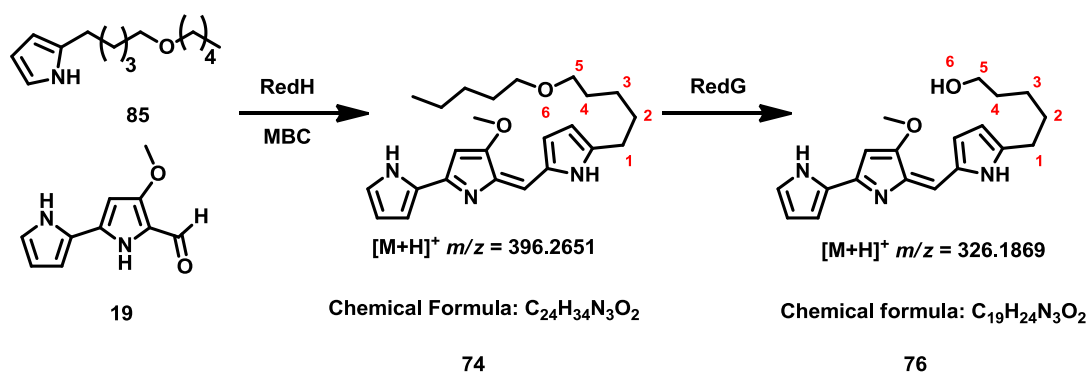
A number of possible explanations can be proposed for the formation of these unexpected sulphur oxidised streptorubin B analogues **293** and **294**. Firstly, sulfoxide **277** and sulphone **278** may be substrates for RedG, in which case sulphur oxidation could occur prior to the oxidative carbocyclisation reaction. Alternatively, oxidative carbocyclisation could occur first followed by sulphur oxidation either catalysed by RedG or a non-specific enzyme present in *S. albus*. To discriminate between these possibilities, chemically synthesised sulfoxide **277**, produced *via* an analogous route to that shown in Scheme 4.2, could be fed to *S. albus* + *redHG* to determine whether oxidative carbocyclisation occurs. However, due to time constraints, this was not pursued further.

4.3 Feeding of ether containing 2-UP analogues to

Streptomyces albus + redHG

4.3.1 Feeding of ether containing 2-UP analogue 85

As discussed in Section 3.3, feeding of 2-UP analogue **85** with an oxygen atom in the 6' position to the *S. coelicolor* redL mutant did not replicate the dealkylation reaction observed by Stuart Haynes. This was therefore reinvestigated by feeding 2-UP analogue **85** with MBC **19** to *S. albus* + redHG, Scheme 4.5. 2-UP analogue **85** and MBC **19** were also fed to *S. albus* + redH as a control, Scheme 4.5.



Scheme 4.5: The undecylprodigiosin analogue **74** and dealkylated product **76** expected to result from feeding 2-UP analogue **85** and MBC **19** to *S. albus* + redHG

The results of the LC-MS analysis of the mycelial extracts resulting from this experiment are shown in Figure 4.13. As shown in Figure 4.13, a large amount of the corresponding undecylprodigiosin analogue **74** was produced (red chromatogram). Examination of the high resolution mass spectrum for this peak provided a molecular formula of $C_{24}H_{34}N_3O_2$, consistent with the expected analogue **74**. In addition, a small peak was observed with the expected $m/z = 326.18$ for the dealkylated product **76** (blue chromatogram). Indeed, examination of the high resolution mass spectrum for this peak provided a molecular formula of $C_{19}H_{24}N_3O_2$, consistent with the expected dealkylated product **76**, Figure 4.14. This

dealkylated product **76**, but not the undecylprodigiosin analogue **74**, was absent from the control experiment employing *S. albus* + *redH*.

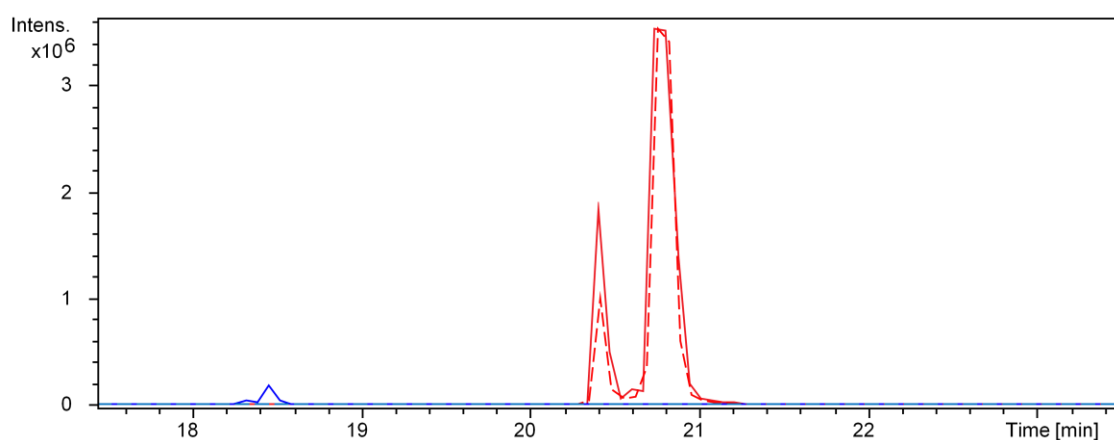


Figure 4.13: Extracted ion chromatograms at $m/z = 396.26$ (red) and $m/z = 326.18$ (blue) from LC-MS analysis of the mycelial extract of *S. albus* + *redHG* (solid lines) and *S. albus* + *redH* (dashed lines) fed with 2-UP analogue **85** and MBC **19**

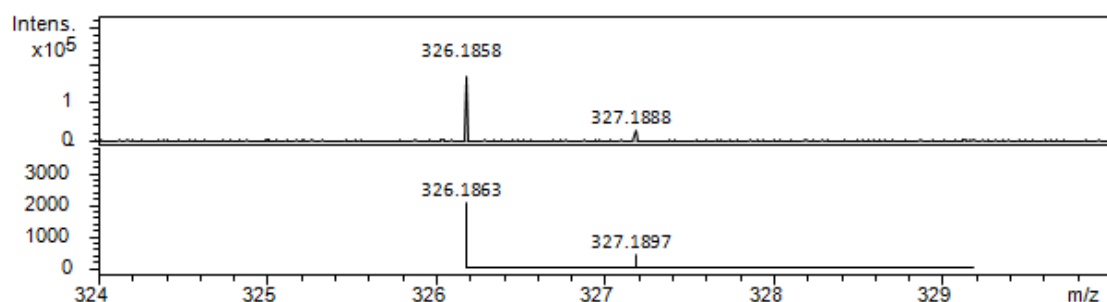
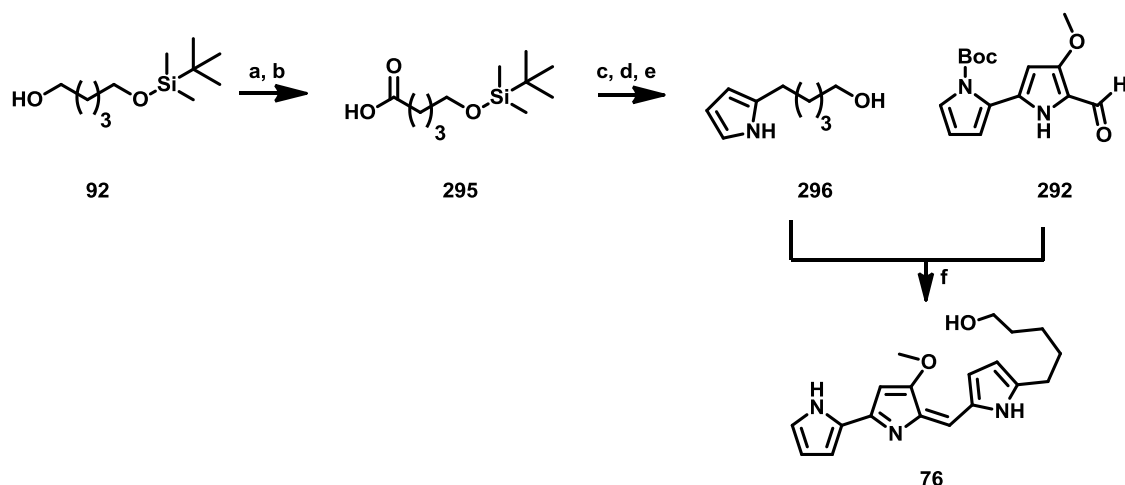


Figure 4.14: A comparison of the HRMS for the compound eluting after 18.5 min in the LC-MS analysis (top spectrum) and the predicted mass spectrum for $C_{19}H_{24}N_3O_2$ (bottom spectrum)

Only small amounts of the putative dealkylated product **76** were produced, thus it was not practical to isolate it from the bacterial culture for NMR spectroscopic analysis. An authentic standard of the proposed dealkylated product was therefore synthesised to confirm the identity of this product, Scheme 4.6.



Scheme 4.6: The synthetic route to the authentic standard of dealkylated product **76**; **a.** $(\text{COCl})_2$, DMSO, CH_2Cl_2 , Et_3N , $-78\text{ }^\circ\text{C}$, 79%; **b.** NaClO_2 , NaH_2PO_4 , 2-Methyl-2-butene, *t*-BuOH, water, 64%; **c.** i. $(\text{PyS})_2$, PPh_3 , toluene, $25\text{ }^\circ\text{C}$ ii. EtMgBr , pyrrole, toluene, $-78\text{ }^\circ\text{C}$, 47%; **d.** NaBH_4 , IPA, $85\text{ }^\circ\text{C}$, 90%; **e.** TBAF, THF, 70%; **f.** i. HCl, MeOH, ii. NaOMe, 80%

Oxidation of monosilyl protected alcohol **92** under Swern conditions, yielded the corresponding aldehyde in 79% yield. It was expected that treatment of this aldehyde with Oxone, as discussed previously, would provide the desired carboxylic acid **295**. However, upon addition of Oxone, a complex mixture of products was obtained, presumably due to the instability of the silyl ether protecting group to the strongly oxidising reaction conditions. Thus, a milder method for the oxidation was required. The Pinnick oxidation was selected due to the wide range of functional groups tolerated by this procedure and provided carboxylic acid **295** in 64% yield.^{116,117} Coupling of carboxylic acid **295** with pyrrole, followed by reduction of the resulting 2-ketopyrrole and silyl deprotection, yielded the corresponding alcohol **296**, which was condensed under acidic conditions with BOC-protected MBC **292** to provide the authentic standard of the dealkylated product **76** in 80% yield after reverse-phase HPLC purification. With the authentic standard of the dealkylated product **76** in hand, an LC-MS comparison with the putative dealkylated product in the mycelial extract was undertaken, Figure 4.15.

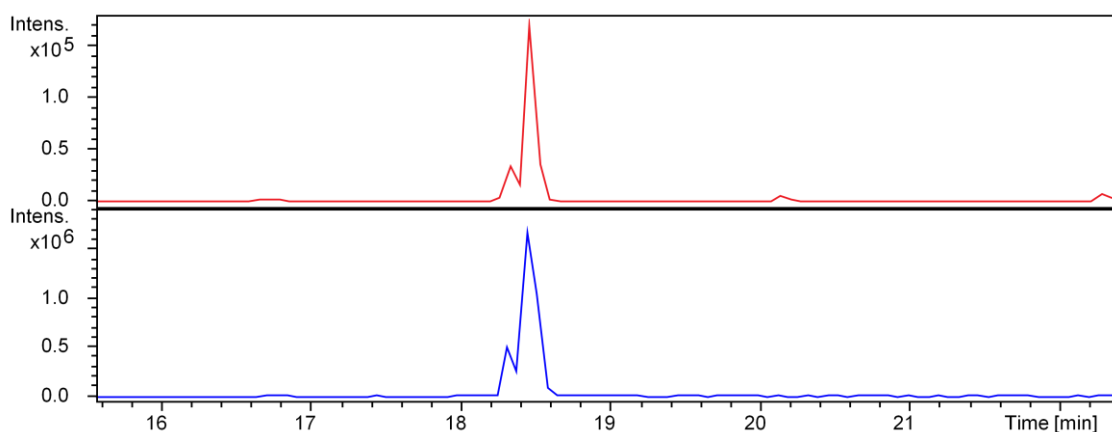


Figure 4.15: Extracted ion chromatograms for $m/z = 326.18$ from LC-MS analysis of the mycelial extracts of *S. albus* + *redHG* fed with 2-UP analogue **85** and MBC **19** (red) and the chemically synthesised authentic standard **76** (blue)

As shown in Figure 4.15, the authentic standard has an identical retention time to that of the putative dealkylated product **76** in the mycelial extract. In addition, the putative dealkylated product in the mycelial extract and the authentic standard give identical high resolution mass spectra and MS/MS fragmentation patterns, Figures 4.16 and 4.17.

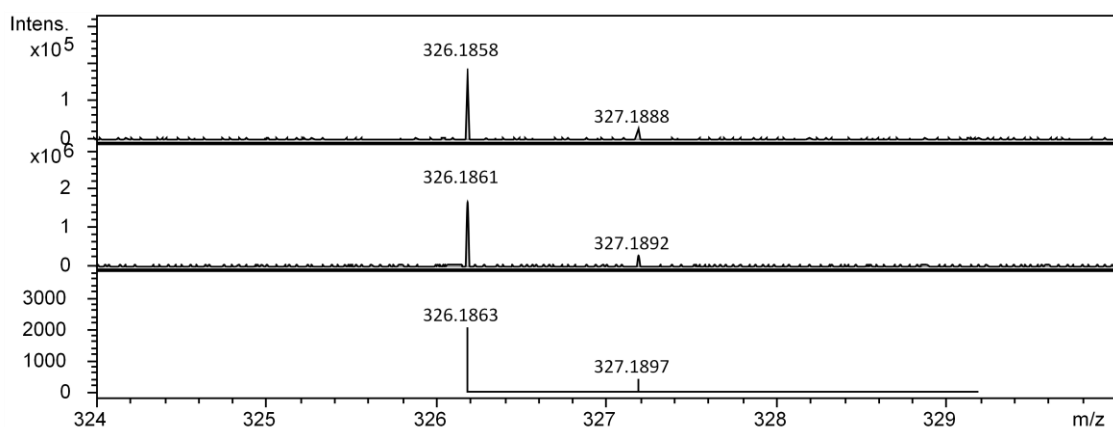


Figure 4.16: A comparison of the HRMS for the compound eluting after 18.5 min in LC-MS analysis of the mycelial extract of *S. albus* + *redHG* fed with 2-UP analogue **85** and MBC **19** (top spectrum), HRMS of the authentic standard **76** (middle spectrum) and the predicted mass spectrum for $C_{19}H_{24}N_3O_2$ (bottom spectrum)

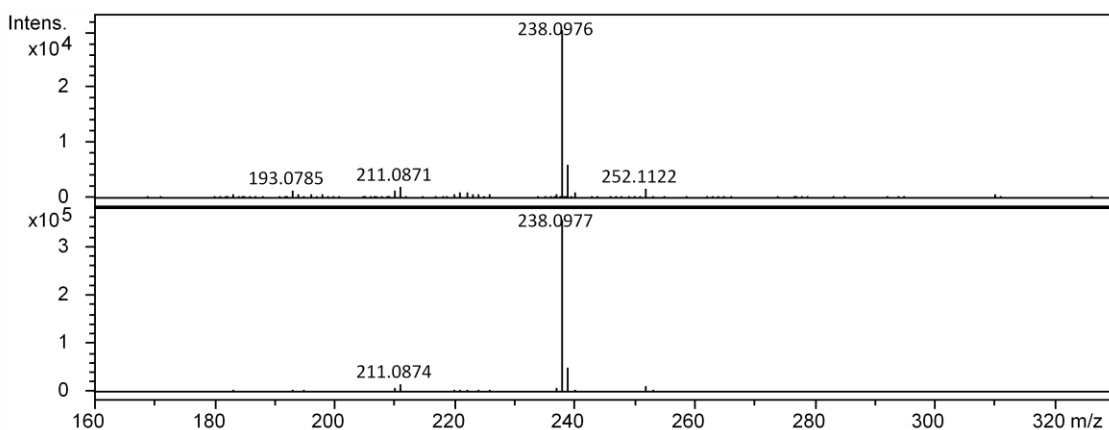
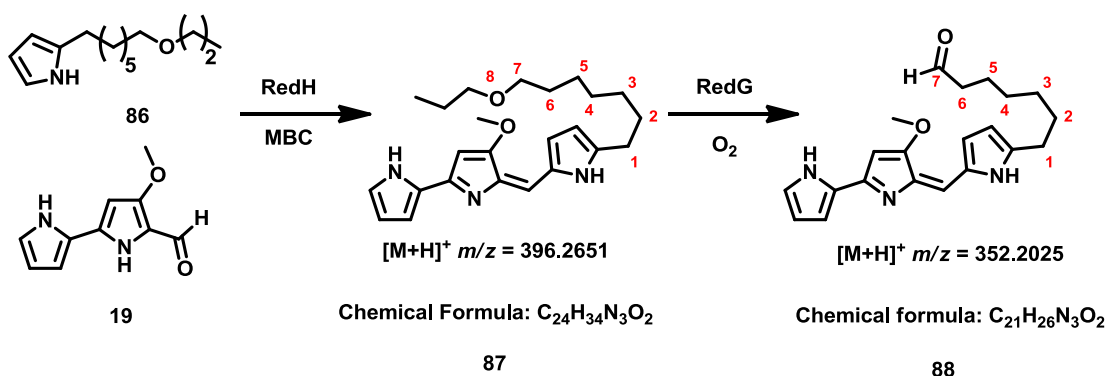


Figure 4.17: A comparison of the MS/MS spectrum observed for the authentic standard of **76** (top spectrum) and **76** in the mycelial extract of *S. albus* + *redHG* fed with MBC **19** and 2-UP analogue **85** (bottom spectrum)

The authentic standard was mixed with the mycelial extract and reanalysed by LC-MS to confirm that the retention time of the authentic standard and **76** in the mycelial extract were identical. Together, these data confirmed that the compound with a retention time of 18.5 min observed in the LC-MS analysis when 2-UP analogue **85** and MBC **19** are fed to *S. albus* + *redHG* is indeed the dealkylated product **76**.

4.3.2 Feeding of ether containing 2-UP analogue **86**

As discussed in Section 2.3, it was hypothesised that undecylprodigiosin analogue **87** would result in the formation of dealkylated aldehyde **88** by the actions of RedG, Scheme 4.7.



Scheme 4.7: The undecylprodigiosin analogue **87** and dealkylated aldehyde product **88** expected to result from feeding 2-UP analogue **86** and MBC **19** to *S. albus* + *redHG*

Unfortunately, analysis of the A_{533} chromatogram from LC-MS analysis of the mycelial extracts of *S. albus* + *redHG* fed with 2-UP analogue **86** and MBC **19** indicated the presence of only one peak, Figure 4.18. Analysis of the HRMS for this peak indicated that the only observed product was the corresponding undecylprodigiosin analogues **87**. LC-MS analysis of did not reveal any RedG-derived products.

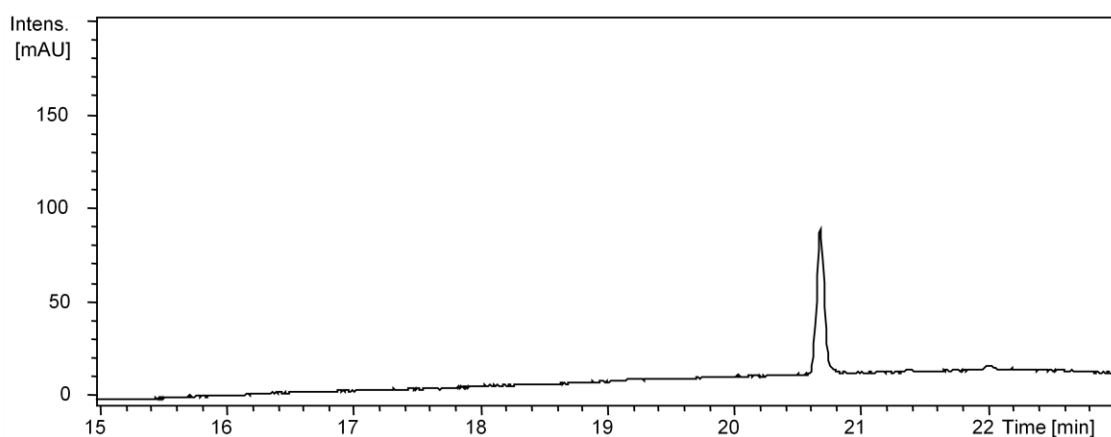


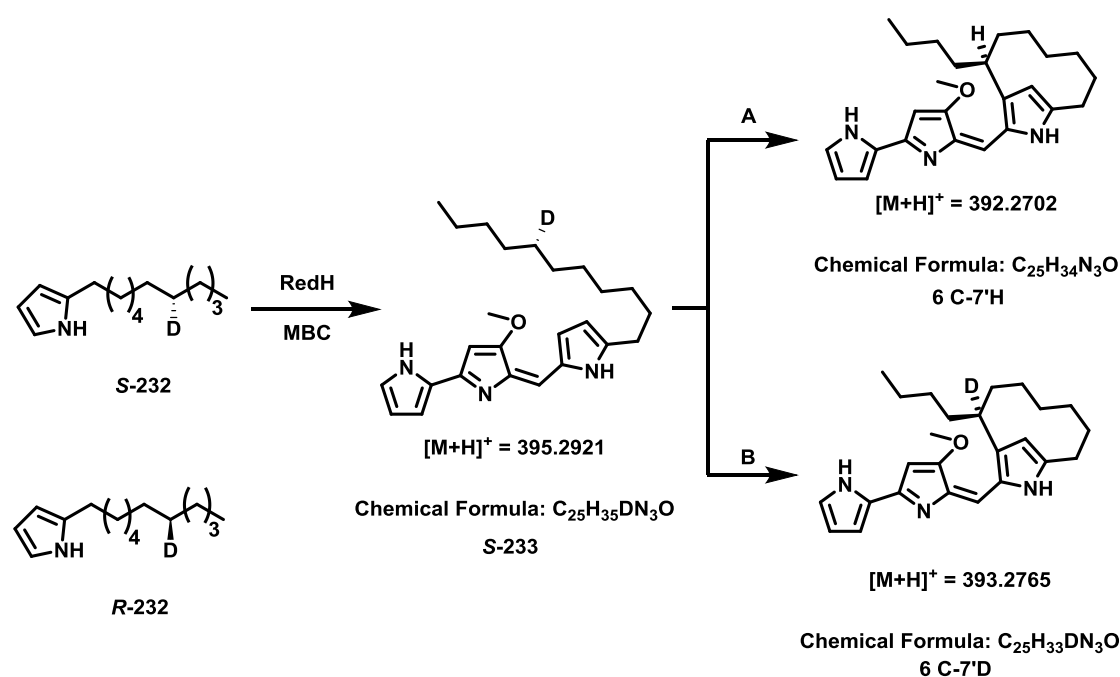
Figure 4.18: A_{533} chromatogram from LC-MS analysis of the mycelial extracts of *S. albus* + *redHG* fed with 2-UP analogue **86** and MBC **19** showing the single peak

This lack of RedG products was surprising since 2-UP analogue **85** had been shown to undergo dealkylation catalysed by RedG. A possible explanation for this lack of observed product could be the instability of the resulting aldehyde **88** *in vivo*. It is well known that aldehyde functional groups are reactive species and, if only trace amounts were generated, the expected aldehyde could have degraded and therefore would not be detected. It is also possible that undecylprodigiosin analogue **87** is not a substrate for RedG.

4.4 Feeding of stereoselectively deuterated 2-UP to *Streptomyces albus* + *redHG*

As discussed in Section 2.9, feeding of 2-UP bearing a deuterium-label at either the *pro-R* or *pro-S* position of C-7' would allow the stereochemical course of the RedG-catalysed oxidative carbocyclisation reaction to be probed. If RedG stereospecifically abstracts the *pro-S* hydrogen atom from C-7', then feeding of 2-UP analogue **S-232** should result in a loss of the deuterium

label, in keeping with other non-haem iron-dependent oxidative cyclases that proceed with retention of configuration (route A, Scheme 4.8). Alternatively, if RedG stereospecifically abstracts the *pro-R* hydrogen atom from C-7', then feeding of 2-UP analogue **S-232** should result in retention of the deuterium label (route B, Scheme 4.8). On the other hand, a non-stereoselective process would result in approximately 50% retention of the deuterium label in both experiments.



Scheme 4.8: The undecylprodigiosin analogue **S-233** expected to result from feeding of stereoselectively deuterium-labelled 2-UP **232** with MBC **19** to *S. albus* + *redHG* and two possible outcomes for the conversion of **233** to streptorubin B **6**

A comparison of the A_{533} chromatograms resulting from LC-MS analysis of the mycelial extracts of *S. albus* + *redHG* fed with either 2-UP **20**, **S-232** and **R-232** and MBC **19** is shown in Figure 4.19.

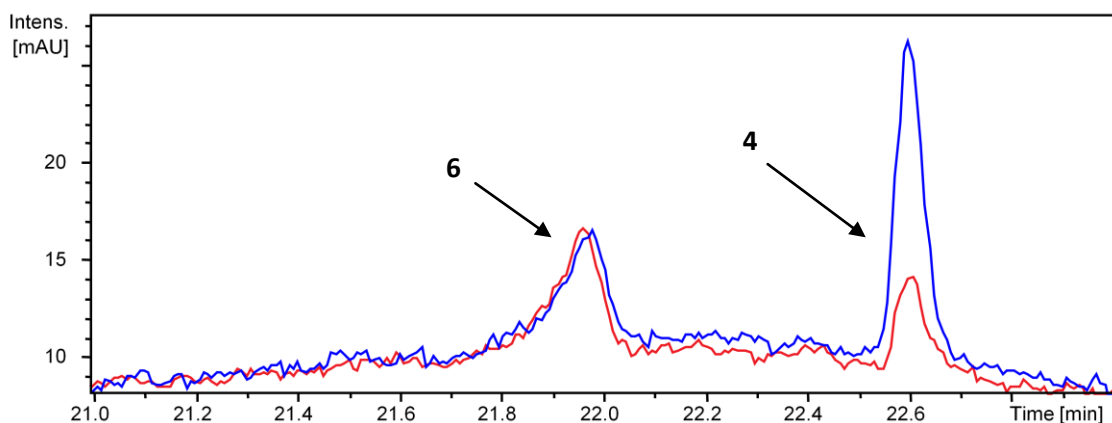


Figure 4.19: A comparison of the A_{533} chromatograms from LC-MS analysis of the mycelial extracts of *S. albus* + *redHG* fed with *pro-S* labelled 2-UP **S-232** (red) and *pro-R* labelled 2-UP **R-232** (blue) with **MBC 19**, respectively

As shown in Figure 4.19, feeding of **R-232** and **MBC 19** to *S. albus* + *redHG* resulted in a lower ratio of unlabelled streptorubin B **6 C-7'H** than the ratio of labelled streptorubin B **6 C-7'D** produced when **S-232** was fed. This difference in ratio of streptorubin B **6** to undecylprodigiosin **232** is consistent with a primary kinetic isotope effect. If RedG abstracts the *pro-R* hydrogen atom from C-7', the position of the deuterium atom in **R-232** would slow this reaction, reducing the ratio of streptorubin B **6** to undecylprodigiosin **4** produced. On the other hand, the position of the deuterium atom in **S-232** would be expected to have little or no effect on the rate of abstraction of the *pro-R* hydrogen atom. It should be noted that, due to time constraints, this experiment was only performed once.

Consistent with the ratio of streptorubin B **6** to undecylprodigiosin **233** produced, feeding of **S-232** resulted in almost complete retention of the deuterium label, whereas feeding of **R-232** appeared to result in an approximately 2:1 mixture of unlabelled to labelled streptorubin B **6**, Figure 4.20.

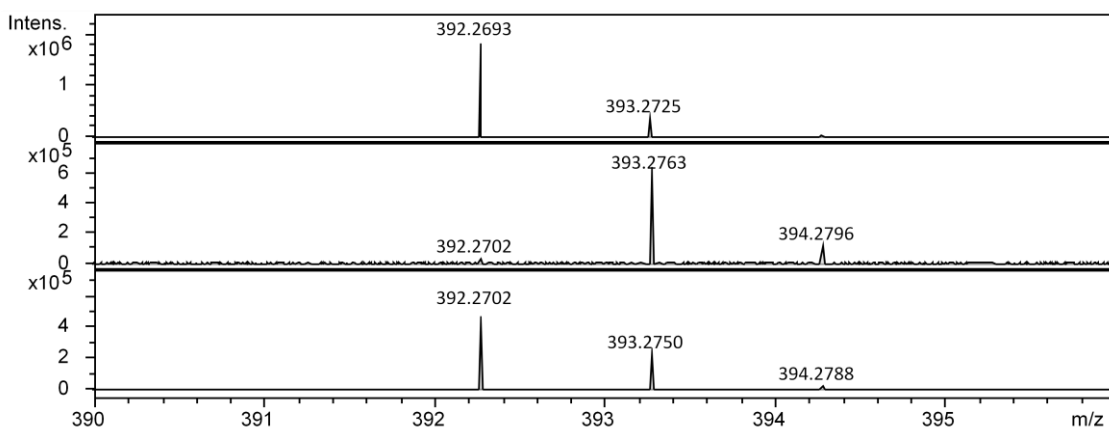


Figure 4.20: A comparison of the HRMS for the compounds with a retention time of at 22.0 min in the LC-MS analyses of the mycelial extract of *S. albus* + *redHG* fed with MBC **19** and either 2-UP **20** (top), **S-232** (middle) or **R-232** (bottom)

The small peak at $m/z = 392.2702$ in the spectrum of streptorubin B **6** arising from feeding of **S-232** to *S. albus* + *redHG* presumably results from the small amount of **R-232** present in the sample. By calculating the area under each peak in the mass spectrum, it was concluded that 92% of the deuterium label is retained when **S-232** is fed to *S. albus* + *redHG*.

A more detailed analysis of the mass spectrum resulting from feeding of **R-232** to *S. albus* + *redHG* was complicated by the inability of the mass spectrometer to distinguish compounds containing a carbon-13 atom from those containing a deuterium atom. The peak at $m/z = 393.2750$ presumably appears more intense than expected because it is a combination of the ^{13}C -isotopomer of unlabelled streptorubin B **6** and the oxidative carbocyclisation product of the small amounts of **S-232** present in the starting material. Using Equation 4.1, it was possible to calculate the proportion of the $m/z = 393.2750$ peak that is due to the ^{13}C -isotopomer.

$$N_c = \frac{100x_{13}}{1.1x_{12}}$$

Equation 4.1: N_c is the number of carbon atoms in the molecule, X_{13} is the area of the carbon-13 isotopomer peak and X_{12} is the area of the carbon-12 isotopomer peak

Thus, it was determined that 48% of the $m/z = 393.2750$ peak is due to the ^{13}C -isotopomer and that 77% of the deuterium label is lost when **R-232** is fed to *S. albus + redHG*. The larger than expected level of deuterium retention resulting in streptorubin B **6** presumably results from consumption of the small amount of **S-232** present in the **R-232** sample, due to the absence of a primary kinetic isotope effect.

From the results of these feeding experiments, it was determined that the RedG-catalysed oxidative carbocyclisation reactions proceeds *via* preferential abstraction of the *pro-R* hydrogen atom from C-7' and proceeds with inversion of configuration at C-7'. Thus, RedG differs from the majority of non-haem iron-dependent oxidative cyclases for which retention of configuration is observed, see Section 2.9. In the case of these other oxidative cyclases, the retention of configuration can be explained by the fact that the incoming heteroatom is bound to the non-haem iron centre, thus is delivered to the same face of the carbon atom that hydrogen atom abstraction occurred from (route A Figure 4.21). However, in the case of RedG, the incoming pyrrole carbon atom is not bound to the non-haem iron centre and so the carbon-centred radical undergoes inversion prior to cyclisation as a result of the specific substrate orientation in the RedG active site (route B Figure 4.21).

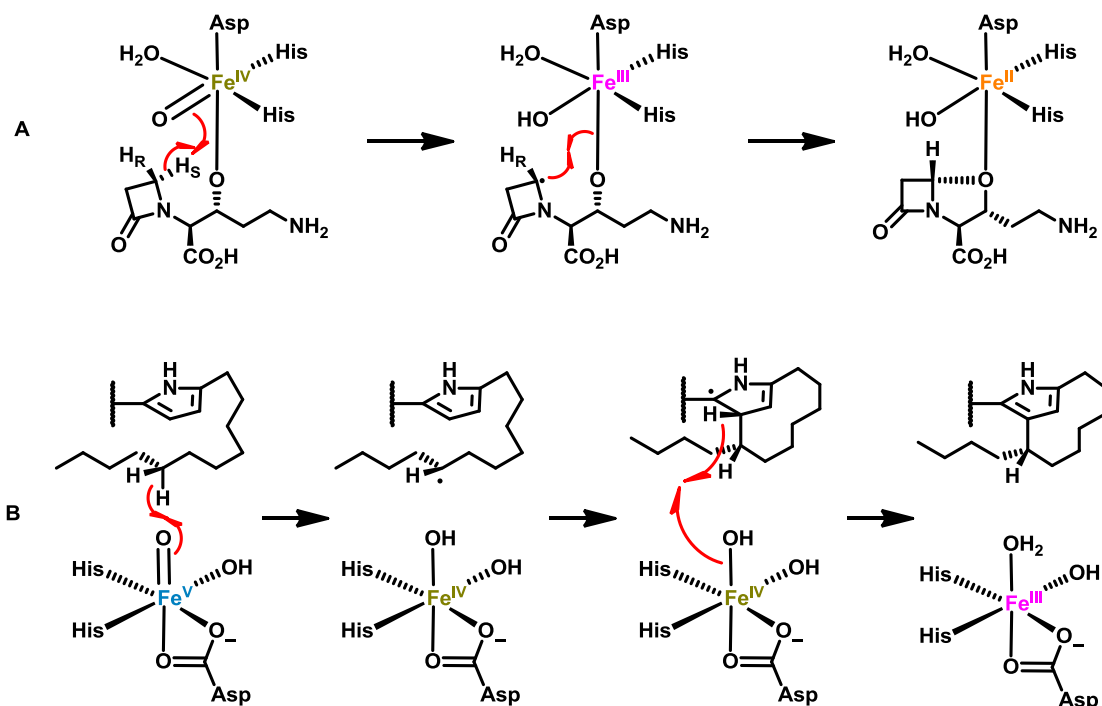


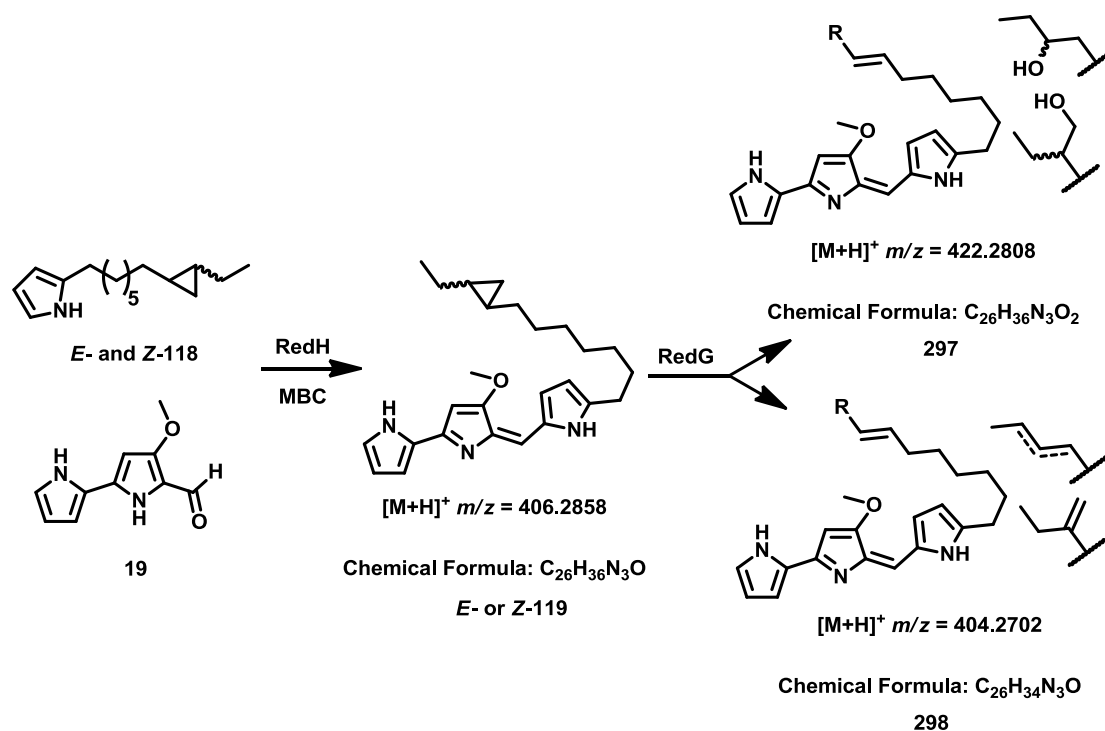
Figure 4.21: An explanation for why most non-haem iron-dependent oxidative cyclases proceed with retention of configuration (route A), whereas the RedG-catalysed carbocyclisation proceeds with inversion of configuration (route B). Only half of the curly arrows are shown for clarity

As discussed in Section 1.10.3, natural streptorubin B **6** is produced as a 9:1 mixture of enantiomers. The mechanism by which the minor enantiomer is produced is not known, but it could be formed either by abstractions of the *pro-S* hydrogen atom from C-7' or by cyclisation of the intermediate carbon-centred radical with retention of configuration. If *R*-streptorubin B **R-6** is generated *via* abstraction of the *pro-S* hydrogen atom from C-7', it would be expected that much less of this enantiomer of the product would have been produced when **S-232** was fed along with MBC **19** to *S. albus* + *redHG*, due to the primary kinetic isotope effect. A preliminary analysis of the mycelial extract from this experiment using a homochiral HPLC column indicated that the ratio of *S*-streptorubin B **6** to *R*-streptorubin B **R-6** is unchanged, suggesting that abstraction of the *pro-S* hydrogen atom is not responsible for the formation of *R*-streptorubin B **R-6**. However, only small amounts of material were available for this analysis and it is not conclusive, because the observed peaks

were very small. This experiment will need to be repeated using more material to provide a definitive answer.

4.5 Feeding of cyclopropyl containing 2-UP analogues to *Streptomyces albus* + redHG

As discussed in Section 2.5, feeding of 2-UP analogue **Z**- and **E-118** containing a cyclopropane adjacent to the site of cyclisation was synthesised to probe the possibility that a carbon-centred radical was generated *via* the actions of RedG. If RedG abstracts a hydrogen atom from C-7', it would be expected that the resulting cyclopropylcarbiny radicals would undergo a skeletal rearrangement, yielding a homoallylic radical. The fate of this homoallylic radical is difficult to predict but in principal, they could undergo hydroxylation, desaturation of carbocyclisation, Scheme 4.9.



Scheme 4.9: The undecylprodigiosin analogues **E**- and **Z-119** and possible hydroxylated and desaturated products **297** and **298** expected to from feeding 2-UP analogues **Z**- and **E-118** to *S. albus* + redHG. Any streptorubin B analogues would have the same expected m/z and chemical formula as the desaturated product

Unfortunately, analysis of the A_{533} chromatogram from LC-MS analysis of the mycelial extracts of *S. albus* + *redHG* fed with either **Z-** or **E-188** and **MBC 19** indicated the presence of only one peak in each case, Figure 4.22 and 4.23. Analysis of the HRMS for these two peaks indicated that the two observed peaks were the corresponding undecylprodigiosin analogues **Z-** and **E-119**, respectively. LC-MS analysis of did not reveal any RedG derived products.

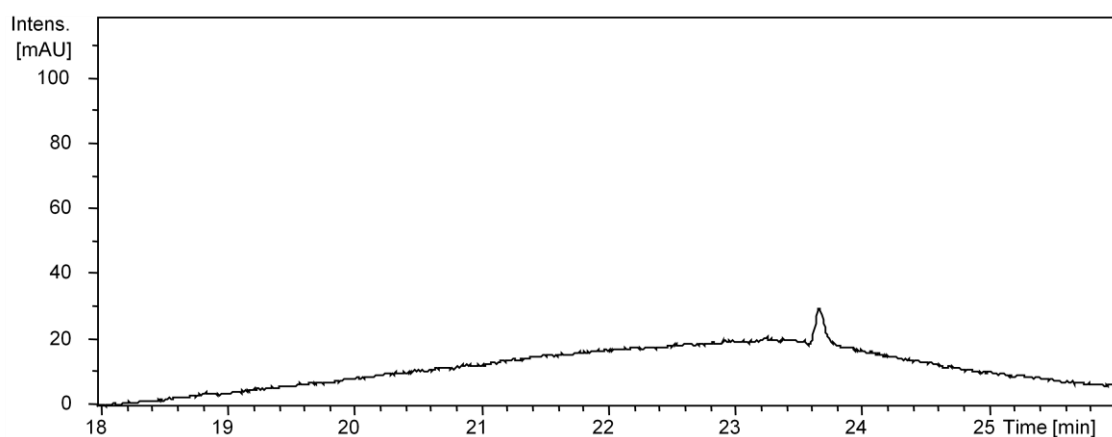


Figure 4.22: A_{533} chromatogram from LC-MS analysis of the mycelial extracts of *S. albus* + *redHG* fed with 2-UP analogue **Z-118** and **MBC 19**

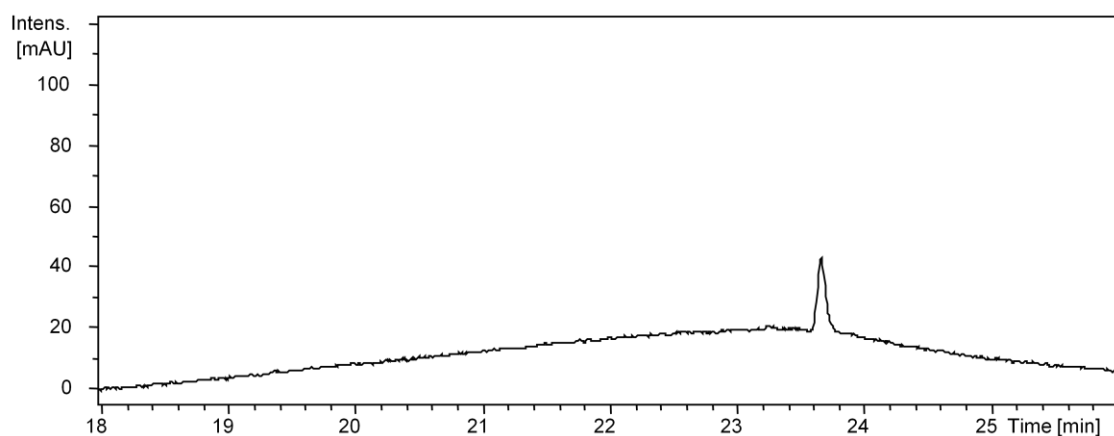


Figure 4.23: A_{533} chromatogram from LC-MS analysis of the mycelial extracts of *S. albus* + *redHG* fed with 2-UP analogue **E-118** and **MBC 19**

A number of possibilities can be proposed to explain the lack of any RedG derived products resulting from feeding *S. albus* + *redHG* with either 2-UP analogues **Z-** or **E-118**. One possible explanation for the lack of RedG derived products could be that neither 2-UP analogues **Z-** or **E-118** are substrates for RedG, potentially as a result of the increased steric bulk of the cyclopropane ring at C-8'. Another possibility is that both 2-UP analogues **Z-** and **E-118** are

toxic to *S. albus* + *redHG* and effect the growth and development of the cells. It was noticed that during the mycelial extraction after feeding 2-UP analogue **Z-118** and MBC **19**, removal of the biomass from the membrane overlay proved problematic. Typically, the biomass was easily removed from the overlay membrane using a scalpel. However, after feeding with 2-UP analogue **Z-118**, the bacteria had become 'watery' and less red pigment was present, Figure 4.24.



Figure 4.24: A comparison of 'typical' *S. albus* + *redHG* fed with 2-UP **20** and MBC **19** (left) and the unusual effect resulting from feeding 2-UP analogue **Z-118** and MBC **19** (right)

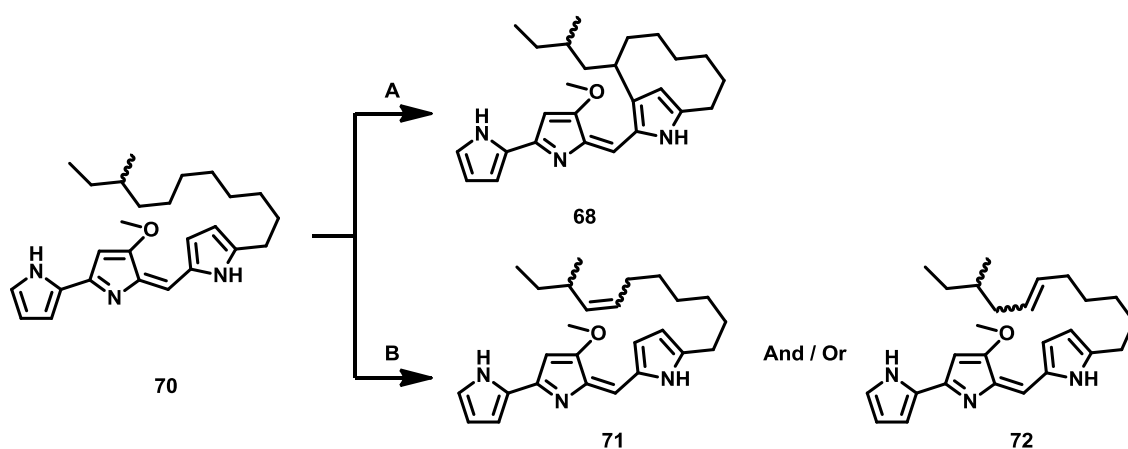
As shown in Figure 4.24, it appears that feeding of 2-UP analogue **Z-118** had a negative effect on the growth of the *S. albus* + *redHG* bacteria. One possible reason for this could be due to the effect that 2-UP analogue **Z-118** has on the cell membrane as a result of embedding in the cell membrane. Since 2-UP analogue **Z-118** is locked in the *cis* configuration, this could lead to structural changes within the membrane affecting the membrane fluidity.

4.6 Feeding of branched methyl analogues to *Streptomyces*

albus + redHG

4.6.1 Feeding of branched methyl 2-UP analogue 185

As discussed in Section 1.12, feeding of 2-UP analogue **185** bearing a methyl substituent at C-9' had previously been shown to result in a mixture of the corresponding streptorubin B analogue **68** in addition to a desaturated product **71** and/or **72**, Scheme 4.10.

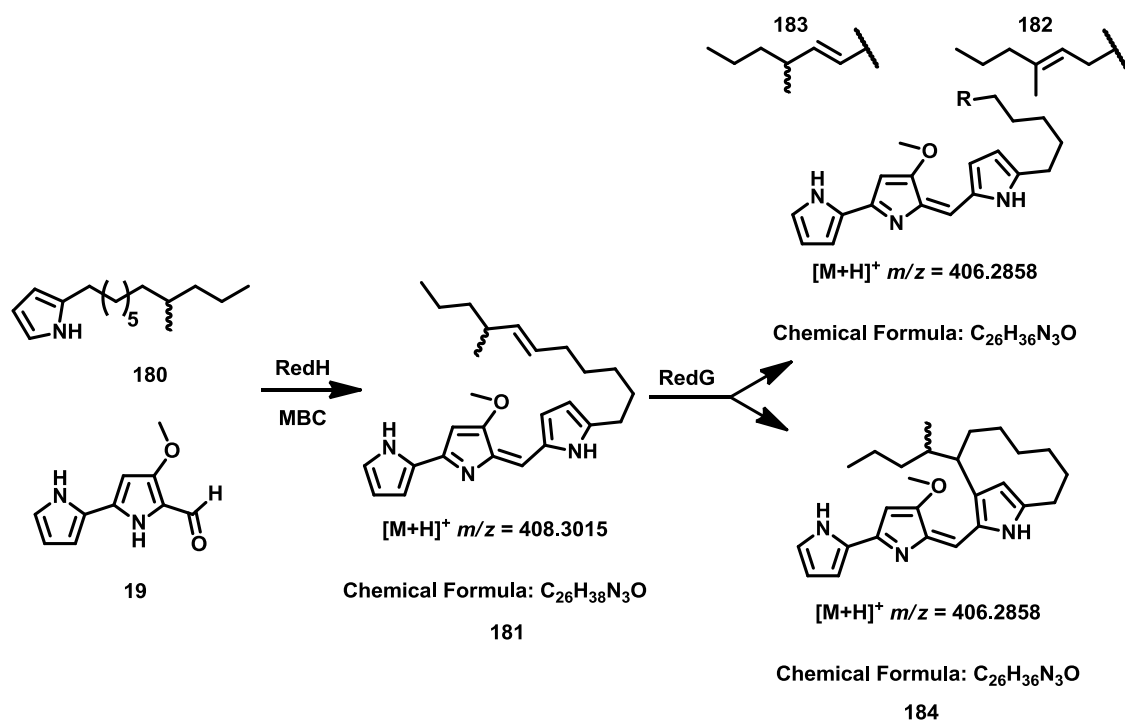


Scheme 4.10: The streptorubin B analogue **68** resulting from oxidative carbocyclisation (route A) and the mixture of desaturated undecylprodigiosin analogues **71** and **72** resulting from a competing desaturation reaction (route B) from feeding *S. albus* + redHG with 2-UP analogue **185** and MBC **19**

However, due to the unforeseen problems in developing an efficient and reproducible feeding method, 2-UP analogue **185** had degraded and there was insufficient time available to synthesise more.

4.6.2 Feeding of branched methyl 2-UP analogue 180

As discussed in Section 2.7, feeding of 2-UP analogue **180** bearing a methyl substituent at C-8' was proposed to increase the amount of desaturated products relative to the oxidative carbocyclised product due to the increase in steric bulk, Scheme 4.11.



Scheme 4.11: The undecylprodigiosin analogue **181** with the proposed desaturated products **182** and **183** in addition to the oxidative carbocyclised product **184** to result from feeding *S. albus* + redHG with 2-UP analogue **180** and MBC **19**

Unfortunately, analysis of the A₅₃₃ chromatogram from LC-MS analysis of the mycelial extracts of *S. albus* + redHG fed with 2-UP analogue **180** and MBC **19** indicated the presence of only one peak, Figure 4.25. Analysis of the HRMS for this peak indicated that it was the corresponding undecylprodigiosin analogue **181**.

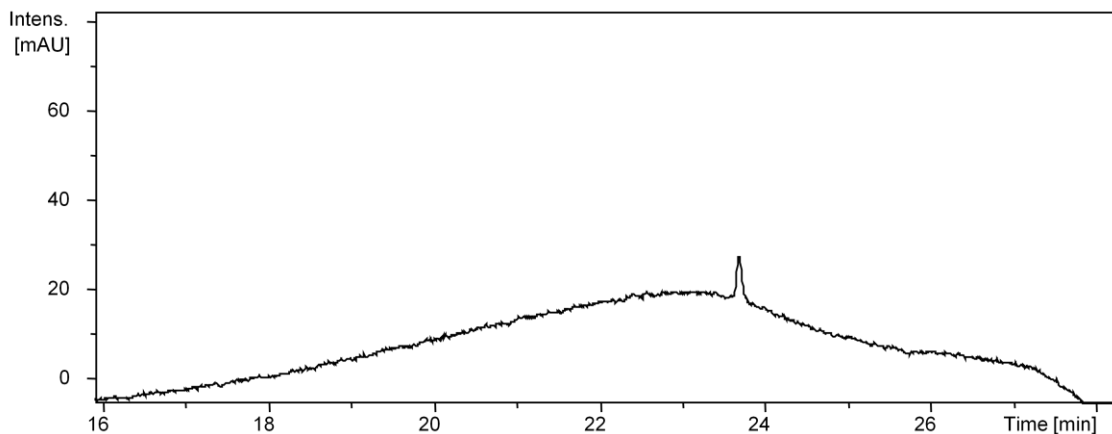
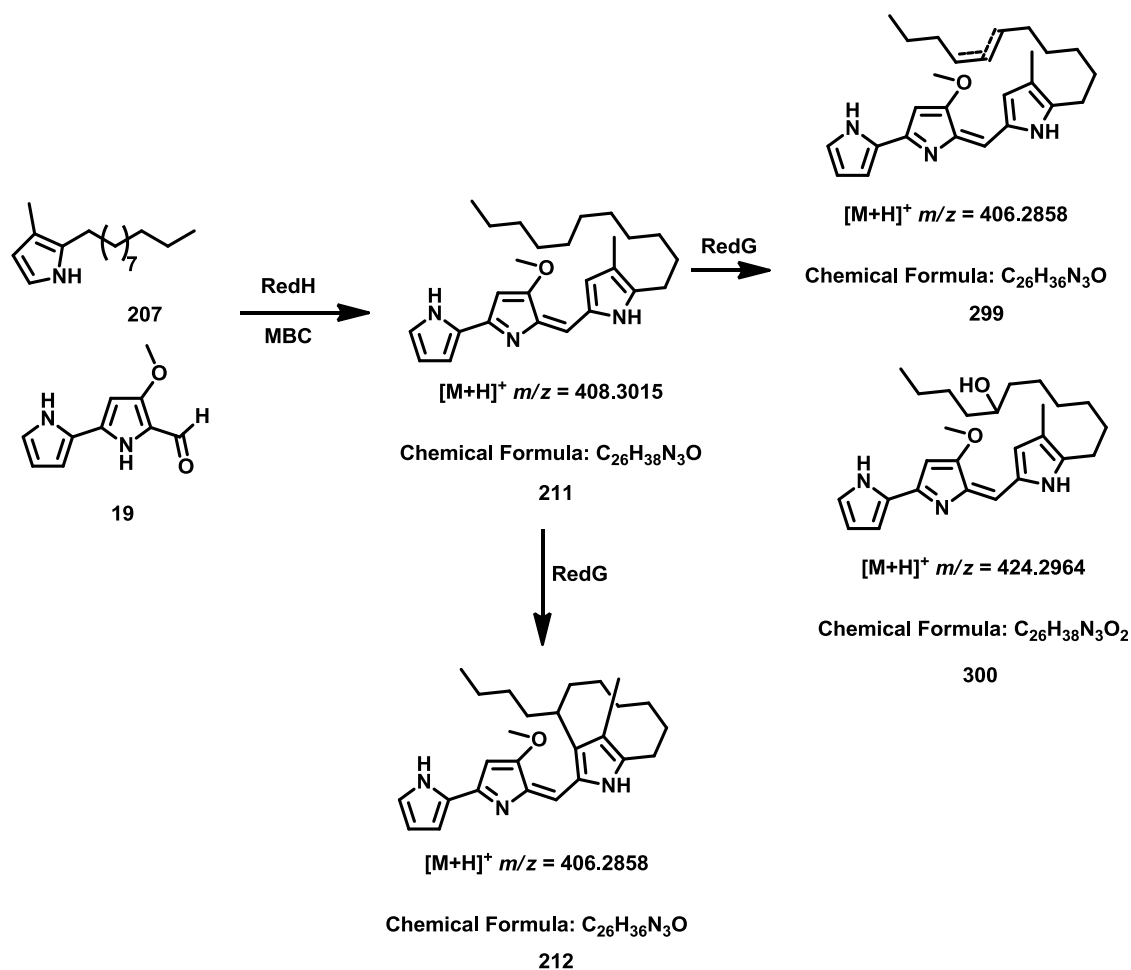


Figure 4.25: A_{533} chromatogram from LC-MS analysis of the mycelial extracts of *S. albus* + *redHG* fed with 2-UP analogue **180** and MBC **19**

The lack of any RedG-derived products is presumably a result of substrates with extra bulk at the C-8' position are not tolerated by RedG. This is consistent with that observation for 2-UP analogues **Z-** and **E-118** to *S. albus* + *redHG*.

4.7 Feeding of a methyl-substituted pyrrole analogue to *Streptomyces albus* + *redHG*

As discussed in Section 2.8, feeding of 2-UP analogue **207** containing an additional methyl group on the dialkylpyrrole would probe the steric tolerance of the RedG-catalysed oxidative carbocyclisation. If the additional methyl group on the pyrrole ring prevents cyclisation, it is possible that the undecyl chain could undergo desaturation or hydroxylation as a shunt product, Scheme 4.12.



Scheme 4.12: The undecylprodigiosin analogue **211** and proposed desaturated product **299**, hydroxylated product **300** in addition to the oxidative carbocyclised product **212** to result from feeding *S. albus* + *redHG* with 2-UP analogue **207** and MBC **19**

During the feeding of 2-UP analogue **207**, it was noticed that the biomass had a much more intense red colour when compared to the natural substrate 2-UP **20**. Comparison of the A_{533} chromatograms from LC-MS analysis of the mycelial extract of *S. albus* + *redHG* fed with MBC **19** and either 2-UP **20** or 2-UP analogue **207** revealed that substantially more of the corresponding undecylprodigiosin analogue **211** was produced, Figure 4.26.

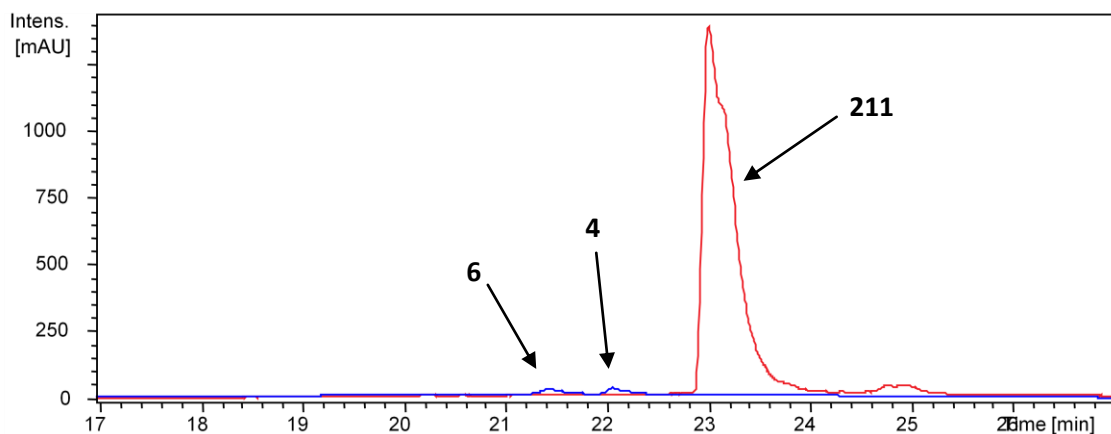


Figure 4.26: A comparison of the A_{533} chromatograms from the LC-MS analysis of the mycelial extracts of *S. albus* + *redHG* fed with MBC **19** and either 2-UP **20** (blue) or 2-UP analogue **207** (red)

Presumably, this increase in production of undecylprodigiosin analogue **211** is a result of the additional electron-donating methyl group increasing the nucleophilicity of the pyrrole, causing the condensation with MBC **19** to occur much more rapidly. To confirm that the additional undecylprodigiosin analogue **211** production was a result of RedH and not non-enzymatic acid-condensation of 2-UP analogue **207** and MBC **18**, the feeding experiment was repeated with wild type *S. albus* and *S. albus* + *redH*, Figure 4.27

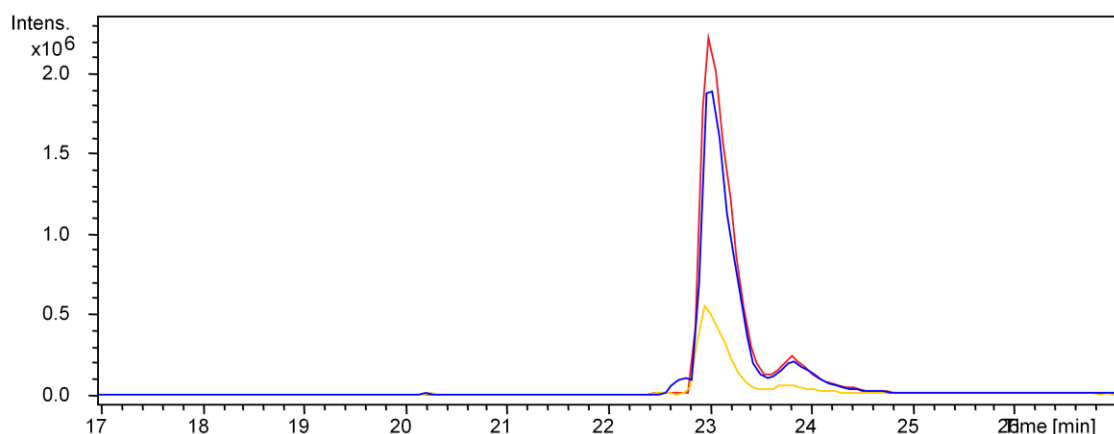


Figure 4.27: A comparison of the extracted ion chromatograms at $m/z = 403.30$ from LC-MS analysis of the mycelial extracts of *S. albus* + *redHG* (red), *S. albus* + *redH* (blue) and *S. albus* wild type (yellow) fed with 2-UP analogue **207** and MBC **19**

As shown in Figure 4.27, significantly more undecylprodigiosin analogue **211** is formed in the presence of RedH. However, even with this substantial increase in substrate, no RedG-derived products were observed.

5. Conclusion and Future Work

In the course of this research, a range of 2-UP analogues bearing specific functional groups have been synthesised in an effort to probe the remarkable oxidative carbocyclisation reaction catalysed by RedG.

Initial feeding experiments were performed in a mutant of *S. coelicolor* blocked in the biosynthesis of 2-UP. During the course of these experiments, it became apparent that the activity of both RedH and RedG decreased over the course of several months. It remains unclear why the activity of this mutant decreased; perhaps mutations accumulated in the *redH* and *redG* gene resulting in inactivation of the corresponding enzyme. Whatever the cause for this decrease in activity, an alternative feeding method was developed in which *redH* and *redG* were heterologously expressed in *S. albus*.

Feeding of 2-UP **20** and MBC **19** to the *S. albus* + *redHG* strain resulted in a 1:1 ratio of streptorubin B **6** to undecylprodigiosin **4**, as previously observed by Paulina Sydor. It was noticed that, over the course of several weeks, the activity of RedG decreased while RedH activity remained constant. The most likely explanation for this decrease in activity is unforeseen toxic effects of *redG* expression on *S. albus*, leading to an accumulation of mutations in the *redG* gene, resulting in inactivation of RedG. To explore this hypothesis further, the *redG* gene from *S. albus* + *redHG* samples that lost activity could be sequenced to determine if any of the codons for catalytically-essential amino acid residues have been mutated.

5.1 Sulphur containing 2-UP analogues

Feeding of 2-UP analogue **101** that replaced the C-7' with a sulphur atom trapped the proposed reactive oxygen species as a sulphoxide. The origin of the sulphoxide oxygen atom was confirmed to originate from molecular oxygen by incorporation of an ^{18}O atom when the experiment was repeated under an atmosphere of $^{18}\text{O}_2$. Interestingly, oxidation to the sulphone, *via* the sulphoxide as shown by the $^{18}\text{O}_2$ incorporation experiment, was also

observed. It is not clear at the moment whether RedG is responsible for this second oxidation reaction, or whether it is a result of another enzyme present in *S. albus*. To discriminate between these possibilities, feeding of sulphoxide **103** to *S. albus* + *redHG* and *S. albus* + *redH* could be undertaken to investigate if sulphone production is RedG-dependent.

Several other sulphur-containing 2-UP analogues were synthesised, in which the sulphur atom was moved away from C-7'. Oxidation of the sulphide to the corresponding sulphoxide and sulphone was observed in each case, with the extent of sulphur oxidation decreasing as the sulphur atom was moved away from C-7'. It was not until C-4' and C-10' were replaced with sulphur atoms that putative streptorubin B analogues were detected. To confirm the structures of these putative streptorubin B analogues, isolation *via* HPLC and structure elucidation using NMR spectroscopy would be required.

5.2 Ether containing 2-UP analogues

Previous work by Stuart Haynes indicated that feeding of 2-UP analogue **85**, in which C-6' is replaced with an oxygen atom, results in dealkylation of the corresponding undecylprodigiosin analogue. Repeating this experiment in *S. albus* + *redHG* resulted in the detection of a compound with the expected *m/z* for the dealkylated product. The identity of this compound was confirmed as the dealkylated undecylprodigiosin analogue **76** by comparison with a synthetic authentic standard.

Feeding of 2-UP analogue **86**, in which C-8' had been replaced with an oxygen atom, resulted in the formation of the corresponding undecylprodigiosin analogue *via* the action of RedH. However, none of the expected dealkylated aldehyde product was observed. This is presumably due to the instability of the aldehyde functional group *in vivo* resulting in degradation of the expected product. It is also possible that the corresponding undecylprodigiosin analogue **87** is not a substrate for RedG.

5.3 Cyclopropane containing 2-UP analogues

Feeding of 2-UP analogues **Z-** and **E-118** bearing cyclopropanes between C-8/9' resulted in the production of the corresponding undecylprodigiosin analogues *via* the action of RedH. However, no products resulting from the action of RedG were detected. It was noticed that feeding of **Z-118** had a detrimental effect on the growth of the *S. albus* + *redHG* strain. This may be responsible for the lack of products of RedG-catalysis. This toxic effect was most probably due to changes in cell membrane fluidity as a result **Z-118** embedding in the membrane. Alternatively, RedG may not tolerate substrates containing extra bulk C-8'.

5.4 Branched methyl containing 2-UP analogues

Feeding of 2-UP analogue **180** bearing a methyl substituent at C-8' resulted in the production of the corresponding undecylprodigiosin analogue **181** *via* the action of RedH. However, no products resulting from the action of RedG were detected, presumably because substrates with extra bulk at C-8' are not tolerated by RedG.

5.5 Methyl-substituted pyrrole containing 2-UP analogue

Feeding of 2-UP analogue **207** resulted in a substantial increase in the amount of undecylprodigiosin analogue produced relative to the natural substrate 2-UP **20**. This increase in activity of RedH is presumably a result of the increased nucleophilicity of the pyrrole ring due to the electron-donating properties of the additional methyl group. However, no products resulting from the actions of RedG were detected.

5.6 Stereoselectively deuterium-labelled 2-UP

Feeding of 2-UP analogues **S-** and **R-232** containing a deuterium-label in place of one of the prochiral hydrogen atoms attached to C-7' resulted in productions of the corresponding undecylprodigiosin analogues *via* the action of RedH. RedG-catalysed oxidative carbocyclisation of *pro-S* labelled undecylprodigiosin resulted in 92% retention of the

deuterium label, whereas 77% loss of the deuterium label was observed for the *pro-R* labelled undecylprodigiosin. This indicates that the RedG-catalysed oxidative carbocyclisation proceeds *via* stereoselective abstraction the *pro-R* hydrogen atom from C-7', followed by inversion of the resulting carbon-centred radical and attack on the pyrrole. This inversion of configuration at the carbon atom undergoing functionalisation is in contrast with the majority of reactions catalysed by other non-haem iron-dependent oxidative cyclases, for which retention of configuration is the norm. In these other non-haem iron-dependent oxidative cyclases, the group that traps the carbon-centred radical tends to be ligated to the non-haem iron atom and so is delivered to the same face of the carbon atom that the hydrogen atom is abstracted from. In the case of RedG, the carbon-centred radical does not react with a ligand of the non-haem iron atom but reacts with a pyrrole carbon, which needs to be shielded from the reactive oxygen species generated at the iron-centre to prevent pyrrole oxidation.

5.7 Implications for RedH

RedH appears to exhibit relatively relaxed substrate specificity with regard to the undecyl chain of 2-UP **20**. All of the 2-UP analogues synthesised in this project, bearing heteroatoms, methyl groups and cyclopropanes were substrates for RedH and resulted in substantial production of the corresponding undecylprodigiosin analogues. RedH was also able to utilise 2-UP analogue **207** bearing a methyl group on the pyrrole, resulting in an increased production of the corresponding undecylprodigiosin analogue **211**.

Comparison of the feeding of 2-UP **20** and MBC **19** to *S. albus* + *redH* and *S. albus* + *redHG* revealed that the RedH-catalysed condensation reaction occurs more rapidly in the presence of RedG. A possible explanation for this increased rate of condensation could be that RedH and RedG form a catalytic complex *in vivo* enhancing the activity of both enzymes. Indeed, previous work by Paulina Sydor had revealed that RedG is more active in the presence of RedH.

5.8 Implications for the RedG mechanism

At the beginning of this work, little was known regarding the mechanism by which RedG converts undecylprodigiosin **4** to streptorubin B **6**. A proposed mechanism, based on another Rieske non-haem iron-dependent enzyme NDO, predicted that RedG would utilise molecular oxygen as the oxidant and would proceed *via* abstraction of a hydrogen atom from C-7' to generate a carbon-centred radical that subsequently cyclises onto the pyrrole, furnishing the macrocycle. Based on other non-haem iron-dependent oxidative cyclases, it was also expected that oxidative carbocyclisation would proceed with retention of configuration at C-7'.

Evidence that RedG does indeed utilise molecular oxygen as the oxidant during the oxidative carbocyclisation has been obtained using sulphur-containing analogues. It has also been demonstrated that RedG stereoselectively abstracts the *pro-R* hydrogen atom from C-7' and that functionalisation of this carbon atom proceeds with inversion of configuration. This stereochemical course contrasts with the majority of reactions catalysed by other oxidative cyclases, which typically proceed with retention of configuration at the carbon atom undergoing functionalisation.

It has also been demonstrated that RedG is capable of catalysing a dealkylation reaction of ether containing substrate analogues. A summary of the insight into the catalytic mechanism of RedG obtained through this work is shown in Figure 5.1.

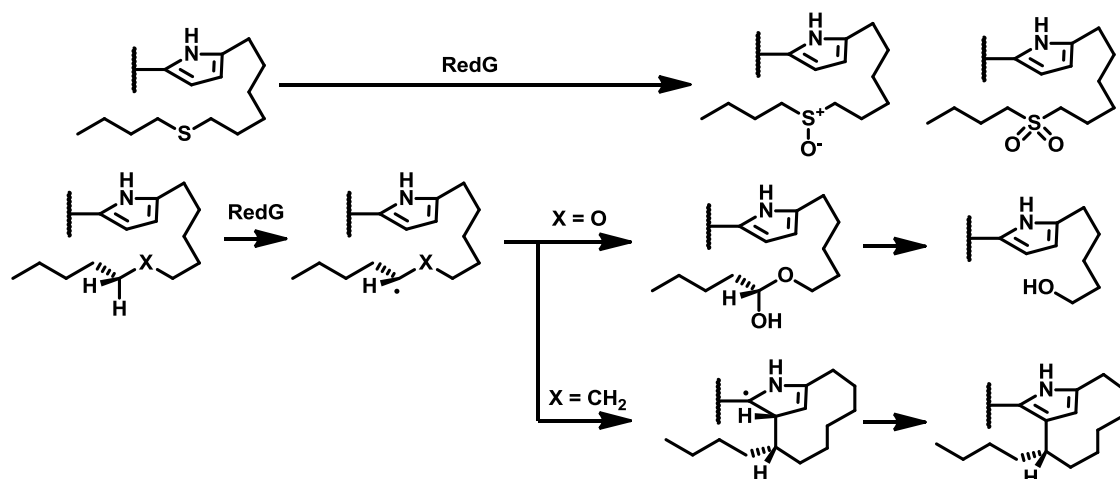


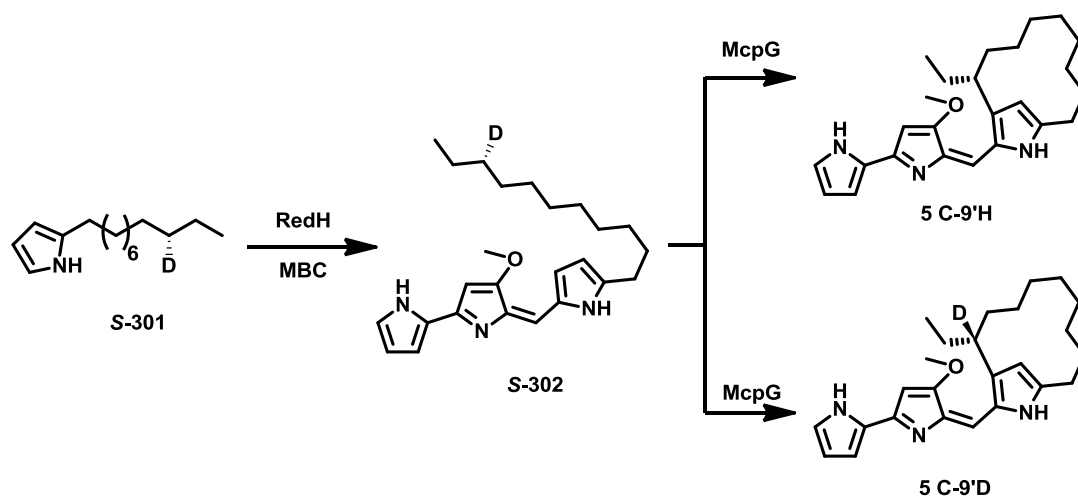
Figure 5.1: A summary of the insight into the catalytic mechanism of RedG obtained through this work

5.9 Future work

To aid in further investigation of the catalytic mechanism of RedG, it would be advantageous if a method to provide functional recombinant RedG could be developed to allow for *in vitro* investigations. The use of recombinant RedG would overcome several of the problems encountered during this work with inconsistent reproducibility and loss of RedG-activity over time. However, efforts to purify recombinant RedG has been unsuccessful because, like many other Rieske non-haem iron-dependent enzymes, recombinant RedG is unstable under aerobic conditions, resulting in rapid loss of the Rieske iron-sulphur cluster, essential for activity. A method that provides recombinant RedG could potentially allow for X-ray crystallographic investigation into the structure of RedG. Such investigations could reveal the orientation of substrate binding within the active site, to help explain why the RedG-catalysed oxidative carbocyclisation proceeds with inversion of configuration at the carbon atom being functionalised.

Very recently, Rebin Salih, a current PhD student in the Challis group, has expressed *mcpH* and *mcpG*, homologues of *redH* and *redG* involved in the biosynthesis of metacycloprodigiosin **5**, in *Streptomyces albus*. He has demonstrated that feeding of chemically synthesised 2-UP **20** and MBC **19** results in the production of undecylprodigiosin **4** and metacycloprodigiosin **5**.

Since McpG is proposed to catalyse the oxidative carbocyclisation of undecylprodigiosin **4** into metacycloprodigiosin **5** *via* an analogous mechanism to that of RedG, several of the 2-UP analogues synthesised in this work could be used to investigate this reaction (e.g. the sulphur-containing 2-UP analogues). The origin of the opposite stereochemistry of metacycloprodigiosin **5** at C-9' could be investigated *via* an analogous stereoselective labelling experiment to that performed for RedG, Scheme 5.1. McpG may yield the opposite stereochemistry to RedG by either stereoselectively abstracting the *pro-S* hydrogen atom from C-9' with subsequent inversion of configuration, or by stereoselectively abstracting the *pro-R* hydrogen atom from C-9' with subsequent retention of configuration. McpG may also tolerate a 2-UP analogue bearing a cyclopropane at C-10'/11' better than RedG to investigate the possibility that a carbon-centred radical is formed.



Scheme 5.1: The analogous stereoselectively deuterium-labelled 2-UP **301** experiment to investigate the stereochemical course of the McpG-catalysed oxidative carbocyclisation in metacycloprodigiosin **5** biosynthesis

6. Experimental

6.1 Chemistry experimental

All reagents were purchased from Sigma Aldrich, Alfa Aesar, Acros Organic, TCI, FluoroChem or VWR and used without further purification unless otherwise stated.

All solvents were purchased from Fischer Scientific and used without further purification unless otherwise stated.

Flash chromatography was conducted on Fluka silica gel (40-63 μm , 60 \AA). TLC was performed on aluminium backed plates pre-coated with Merck silica gel 60 F₂₅₄ and was visualised with UV radiation, potassium permanganate, bromocresol or 2,4-DNP stains.

All ^1H -NMR spectra were obtained using a Bruker DPX400 spectrometer at 400 MHz equipped with a Proton Carbon Dual Probe. 600 MHz and 700 MHz ^1H -NMR spectra were obtained by the University of Warwick NMR service using Bruker AVIII600 or 700 instrument equipped with a BBO probe and TCI cryoprobe respectively. Deuterated solvents were purchased from Sigma Aldrich and used as supplied.

IR spectra were recorded using a Perkin Elmer Avatar 320 Fourier Transformation spectrometer. Selected absorptions are recorded and given in units of wave numbers.

Low resolution ESI mass spectra were recorded using a Bruker Esquire 2000 spectrometer or an Agilent 6130B single quad mass spectrometer. HRMS spectra were measured by the University of Warwick mass spectrometry service on Bruker MaXis or MicroTOF mass spectrometers. GC-MS spectra were obtained using a Varian 4000 instrument fitted with a Varian CP8944 VF (5 μm 30 x 0.25 mm) column.

Melting points were measured using a Stuart Scientific SMP10 melting point apparatus and were uncorrected.

Acetone distillation

Acetone was heated to 50 °C over activated 4Å molecular sieves for 3 hours before being collected by distillation at 65 °C. The dry acetone was stored over activated 4 Å molecular sieves under argon.

Acetonitrile distillation

Acetonitrile was heated to 70 °C over calcium hydride for 2 hours before being collected by distillation at 105 °C. The dry acetonitrile was stored over activated 4 Å molecular sieves under argon.

Dichloromethane distillation

CH₂Cl₂ was heated to 35 °C over calcium hydride for 3 hours before being collected by distillation at 65 °C. The dry CH₂Cl₂ was stored over activated 4 Å molecular sieves under argon.

Diisopropyl amine distillation

Diisopropyl amine was heated to 80 °C over calcium hydride for 2 hours before being collected by distillation at 100 °C. The dry diisopropylamine was stored under argon.

Pyridine distillation

Pyridine was heated to 110 °C over calcium hydride for 2 hours before being collected by distillation at 130 °C. The dry pyridine was stored over dried KOH pellets under argon.

2,2,6,6-Tetramethyl piperidine distillation

2,2,6,6-Tetramethyl piperidine was heated to 100 °C over calcium hydride for 2 hours before being collected by distillation at 155 °C. The dry 2,2,6,6-tetramethyl piperidine was used immediately for reactions.

***n*-Butyl lithium titration**¹¹⁹

To a solution of diphenyl acetic acid (100 mg, 0.50 mmol) in THF (2 ml), under argon, was added enough *n*-butyl lithium solution to give a persistent yellow colour. This was repeated three times and the average titre used to calculate the initial *n*-butyl lithium concentration.

IBX synthesis¹²⁰

To a solution of Oxone (32.50 g, 52.42 mmol) in water (130 ml) was added 2-iodobenzoic acid (10.00 g, 40.32 mmol) and the resulting thick slurry vigorously stirred for 3 hours while being heated to 75 °C. The reaction mixture was cooled to 0 °C and stirred for an additional 1.5 hours before the solid was collected via filtration. The solid was washed with water and acetone to give IBX as a bright white solid. ¹H-NMR of this material was identical to that reported in the literature.

***p*-Toluenesulphonyl chloride recrystallisation**

To a solution of commercially available *p*-toluenesulphonyl chloride (25.00 g) in chloroform (100 ml) was added pet ether (500 ml) and the resulting mixture stirred for 15 mins. The resulting mixture was filtered through celite and solvent removed under vacuum to leave the purified *p*-toluenesulphonyl chloride as a bright white solid.

General procedure for sulphide synthesis¹²¹

To a solution of *n*-butyl lithium (1.25 eq) in THF, under argon cooled to 0 °C, was added the required thiol (1.2 eq) in THF. The resulting white precipitate was stirred for 10 mins before the required bromo ester (1 eq) in THF was added and allowed to warm to RT over 30 mins. Water was added to the reaction mixture and it was extracted with Et₂O. The combined organics were washed with brine, dried (MgSO₄) and concentrated under vacuum to give the desired sulphide.

General procedure for ester hydrolysis

To a solution of the required sulphide ester in THF, under argon, was added 2.35 M sodium hydroxide and the reaction was heated to 75 °C for 16 hours. The THF was removed under vacuum and the aqueous layer acidified with conc HCl to pH 1 before being extracted with EtOAc. The combined organic layers were washed with brine, dried (MgSO₄) and concentrated under vacuum to give the desired carboxylic acid.

General procedure for coupling of carboxylic acid with pyrrole¹²²

A solution of carboxylic acid, 2,2'-dipyridyl disulphide (2 eq) and triphenyl phosphine (2 eq) in toluene, under argon, was stirred for 16 hours. This solution was cooled to -78 °C and pyrrol magnesium bromide (3 eq), prepared by adding ethyl magnesium bromide to freshly distilled pyrrole in toluene at -40 °C, was added and stirred vigorously for 45 mins. Saturated NH₄Cl solution was added and extracted with EtOAc. The combined organics were washed with 5% K₂CO₃, 2M HCl, brine, dried (MgSO₄) and concentrated under vacuum. The crude product was purified by flash column chromatography.

General procedure for the reduction of acyl ketone

A suspension of sodium borohydride (6 eq) in propan-2-ol (under argon for sulphides), was heated to 85 °C for 60 mins before the acyl ketone in propan-2-ol was added and stirred for 16 hours. Water was added to dissolve the solid and the aqueous layer extracted with EtOAc. The combined organics were washed with brine, dried (MgSO₄) and concentrated under vacuum. The crude product was purified by flash column chromatography.

General procedure for Swern Oxidation¹²³

To a solution of oxalyl chloride (1.7 eq) in CH₂Cl₂, cooled to -78 °C under argon, was added DMSO (2.5 eq) in CH₂Cl₂ dropwise and allowed to stir for 10 mins. The desired alcohol (1 eq) in CH₂Cl₂ was added and the reaction stirred for an additional 45 mins. Triethylamine (5 eq)

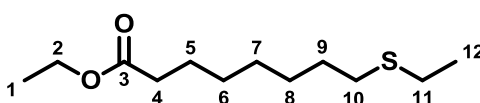
was added and the reaction mixture allowed to warm to RT over 20 mins. Water was added to dissolve the white solid and extracted with CH₂Cl₂. The combined organics were washed with 2M HCl, sat NaCO₃, brine, dried (MgSO₄) and concentrated under vacuum to give the desired aldehyde.

General procedure for Oxone Oxidation¹²⁴

To a solution of aldehyde in DMF was added Oxone (1.5 eq) and the resulting suspension stirred for 30 mins. 2M HCl was added and the aqueous layer extracted with EtOAc. The combined organics were dried (MgSO₄) and concentrated under vacuum. The residue was left under high vacuum for 24 hours to remove residual DMF.

6.1.1 Synthesis of sulphur containing 2-UP analogues

Ethyl (8-ethylsulfanyl)octanoate



Following the general sulphide procedure, work up gave ethyl (8-ethylsulfanyl)octanoate (2.76 g, 99% yield) as a colourless oil.

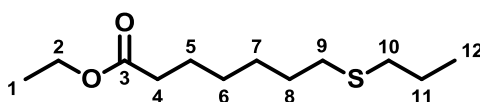
¹H-NMR (CDCl₃, 400 MHz) δ : 4.05 (q, 2H, H-2, J=7.2Hz), 2.49 – 2.43 (m, 4H, H-10 and 11), 2.22 (t, 2H, H-4, J=7.5Hz), 1.59 – 1.47 (m, 4H, H-5 and 9), 1.31 (m, 2H, H-8), 1.25 (m, 4H, H-6 and 7), 1.18 (m, 6H, H-1 and 12)

¹³C-NMR (CDCl₃, 100 MHz) δ : 172.83 (C-3), 59.16 (C-2), 33.32 (C-4), 30.61, 28.55, 27.89, 27.87, 27.72, 24.92, 23.89, 13.79 (C-1 or 12), 13.25 (C-1 or 12)

IR (cm⁻¹): 1733 (C=O stretch)

HRMS: *m/z* calculated for C₁₂H₂₄O₂SNa = 255.1395 [M+Na]⁺; Found 255.1395

Ethyl (7-propylsulfanyl)heptanoate



Following the general sulphide procedure, work up gave ethyl (7-propylsulfanyl)heptanoate (2.84 g, 97% yield) as a pale yellow oil.

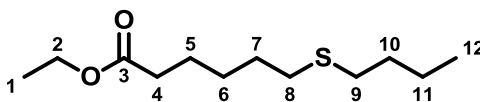
$^1\text{H-NMR}$ (CDCl_3 , 400 MHz) δ : 4.06 (q, 2H, H-2, $J=7.1\text{Hz}$), 2.45 – 2.30 (m, 4H, H-9 and 10), 2.22 (t, 2H, H-4, $J=7.4\text{Hz}$), 1.60 – 1.48 (m, 6H, H-5, 8 and 11), 1.37 – 1.23 (m, 4H, H-6 and 7), 1.19 (t, 3H, H-1, $J=7.2\text{Hz}$), 0.92 (t, 3H, H-12, $J=7.7\text{Hz}$)

$^{13}\text{C-NMR}$ (CDCl_3 , 100 MHz) δ : 173.80 (C-3), 60.21 (C-2), 34.30 (C-4), 34.25, 32.03, 29.54, 28.76, 28.56, 24.86, 23.02, 14.27 (C-1), 13.55 (C-12)

IR (cm^{-1}): 1733 (C=O stretch)

HRMS: m/z calculated for $\text{C}_{12}\text{H}_{24}\text{O}_2\text{SNa} = 255.1395$ [$\text{M}+\text{Na}$] $^+$; Found 255.1390

Ethyl (6-butylsulfanyl)hexanoate



Following the general sulphide procedure, work up gave ethyl (6-butylsulfanyl)hexanoate (1.02 g, 98% yield) as a colourless oil.

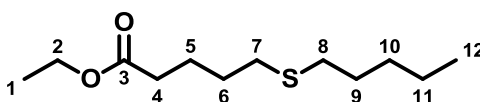
$^1\text{H-NMR}$ (CDCl_3 , 400 MHz) δ : 4.11 (q, 2H, H-2, $J=7.1\text{Hz}$), 2.48 (m, 4H, H-8 and 9), 2.29 (t, 2H, H-4, 7.3Hz), 1.59 (m, 6H, H-5, 7 and 10), 1.40 (m, 4H, H-6 and 11), 1.24 (t, 3H, H-1, 7.0Hz), 0.90 (t, 3H, H-12, 7.3Hz)

$^{13}\text{C-NMR}$ (CDCl_3 , 100 MHz) δ : 173.67 (C-3), 60.24 (C-2), 34.23 (C-4), 31.94 (C-8), 31.86 (C-9), 31.82 (C-10), 29.36 (C-7), 28.40 (C-6), 24.61 (C-5), 22.05 (C-11), 14.27 (C-1), 13.71 (C-12)

IR (cm^{-1}): 1733 (C=O stretch)

HRMS: m/z calculated for $\text{C}_{12}\text{H}_{24}\text{O}_2\text{SNa} = 255.1395$ [$\text{M}+\text{Na}$] $^+$; Found 255.1389

Ethyl (5-pentylsulfanyl)pentanoate



Following the general sulphide procedure, work up gave ethyl (5-pentylsulfanyl)pentanoate (1.07 g, 96% yield) as a colourless oil.

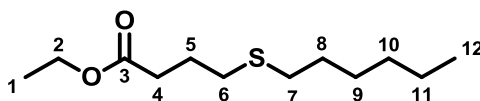
$^1\text{H-NMR}$ (CDCl_3 , 400 MHz) δ : 4.06 (q, 2H, H-2, $J=7.0\text{Hz}$), 2.44 (m, 4H, H-7 and 8), 2.25 (t, 3H, H-4, $J=7.4\text{Hz}$), 1.70 (m, 2H, H-5), 1.63 – 1.59 (m, 4H, H-6 and 9), 1.31 – 1.23 (m, 4H, H-10 and 11), 1.10 (t, 3H, H-1, $J=7.6\text{Hz}$), 0.83 (t, 3H, H-12, $J=7.2\text{Hz}$)

$^{13}\text{C-NMR}$ (CDCl_3 , 100 MHz) δ : 173.80 (C-3), 60.21 (C-2), 34.30 (C-4), 34.25 (C-10), 32.03 (C-9), 29.54 (C-8), 28.76 (C-7), 28.56 (C-6), 24.86 (C-5), 23.02 (C-11), 14.27 (C-1), 13.55 (C-12)

IR (cm^{-1}): 1735 (C=O stretch)

HRMS: m/z calculated for $\text{C}_{12}\text{H}_{24}\text{O}_2\text{SNa}$ = 255.1395 $[\text{M}+\text{Na}]^+$; Found 255.1385

Ethyl (4-hexylsulfanyl)butanoate



Following the general sulphide procedure, the crude product was purified on silica gel (3% EtOAc in pet ether) to give ethyl (4-hexylsulfanyl)butanoate (1.18 g, 99% yield) as a colourless oil.

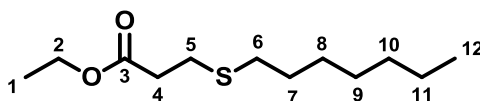
$^1\text{H-NMR}$ (CDCl_3 , 400 MHz) δ : 4.06 (q, 2H, H-2, $J=7.1\text{Hz}$), 2.45 (m, 4H, H-6 and 7), 2.36 (t, 2H, H-4, $J=7.3\text{Hz}$), 1.84 (m, 2H, H-5), 1.50 (m, 2H, H-8), 1.31 (m, 2H, H-9), 1.25 – 1.17 (m, 7H, H-1, 10 and 11), 0.81 (t, 3H, H-12, $J=6.9\text{Hz}$)

$^{13}\text{C-NMR}$ (CDCl_3 , 100 MHz) δ : 173.10 (C-3), 60.39 (C-2), 33.16 (C-4), 32.00 (C-7), 31.46 (C-10), 31.36 (C-6), 29.61 (C-8), 28.61 (C-9), 24.80 (C-5), 22.57 (C-11), 14.25 (C-1), 14.05 (C-11)

IR (cm^{-1}): 1732 (C=O stretch)

HRMS: m/z calculated for $C_{12}H_{24}O_2SNa = 255.1395 [M+Na]^+$; Found 255.1387

Ethyl (3-heptylsulfanyl)propanoate



Following the general sulphide procedure, the crude product was purified on silica gel (4% EtOAc in pet ether) to give ethyl (3-heptylsulfanyl)propanoate (1.28 g, 100% yield) as a colourless oil.

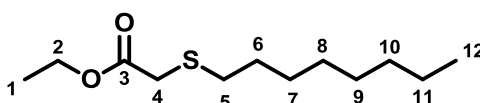
$^1\text{H-NMR}$ (CDCl_3 , 400 MHz) δ : 4.09 (q, 2H, H-2, $J=7.2\text{Hz}$), 2.71 (t, 2H, H-4), 2.51 (m, 4H, H-5 and 6), 1.51 (m, 2H, H-7), 1.31 (m, 2H, H-8), 1.26 – 1.18 (m, 9H, H-1, 9, 10 and 11), 0.81 (t, 3H, H-12, $J=6.6\text{Hz}$)

$^{13}\text{C-NMR}$ (CDCl_3 , 100 MHz) δ : 172.07 (C-3), 60.64 (C-2), 35.00 (C-5), 32.19 (C-6), 31.74 (C-10), 29.58 (C-7), 28.90 (C-8), 28.84 (C-9), 27.02 (C-4), 22.61 (C-11), 14.22 (C-1), 14.08 (C-12)

IR (cm^{-1}): 1735 (C=O stretch)

HRMS: m/z calculated for $C_{12}H_{24}O_2SNa = 255.1395 [M+Na]^+$; Found 255.1391

Ethyl (2-octylsulfanyl)ethanoate



Following the general sulphide procedure, the crude product was purified on silica gel (4% EtOAc in pet ether) to give ethyl (2-octylsulfanyl)ethanoate (2.43 g, 87% yield) as a colourless oil.

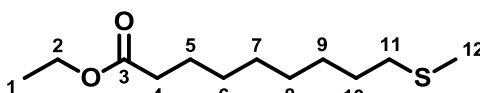
$^1\text{H-NMR}$ (CDCl_3 , 400 MHz) δ : 4.12 (q, 2H, H-2, $J=7.2\text{Hz}$), 3.14 (s, 2H, H-4), 2.56 (t, 2H, H-5, $J=7.2\text{Hz}$), 1.53 (m, 2H, H-6), 1.27 – 1.20 (m, 11H, H-1, 8, 9, 10 and 11), 0.81 (t, 3H, H-12, $J=7.5\text{Hz}$)

¹³C-NMR (CDCl₃, 100 MHz) δ: 170.66 (C-3), 61.28 (C-2), 33.76 (C-4), 32.73 (C-5), 31.81 (C-10), 29.17, 29.15, 29.03 (C-6), 28.78 (C-7), 22.65 (C-11), 14.19 (C-1), 14.10 (C-12)

IR (cm⁻¹): 1732 (C=O stretch)

HRMS: *m/z* calculated for C₁₂H₂₄O₂SNa = 255.1395 [M+Na]⁺; Found 255.1392

Ethyl (9-methylsulfanyl)nonanoate



To a suspension of sodium thiomethoxide (1.59 g, 22.62 mmol) in DMF (20 ml), heated to 80 °C under argon, was added ethyl 9-bromononanoate (2.00 g, 7.75 mmol) and the reaction stirred for 32 hours. The reaction mixture was poured into 2M HCl and extracted with EtOAc. The combined organics were dried (MgSO₄) and concentrated under vacuum. The crude product was purified on silica gel (10% EtOAc increasing to 50% EtOAc in pet ether) to give ethyl (9-methylsulfanyl)nonanoate (411 mg, 24% yield) as a colourless oil and (9-methylsulfanyl)nonanoic acid (684 mg, 44 % yield) as a white solid.

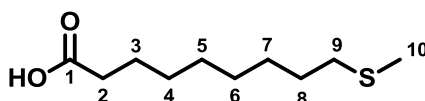
¹H-NMR (CDCl₃, 400 MHz) δ: 4.05 (q, 2H, H-2, J=7.0Hz), 2.41 (t, 2H, H-1, J=7.0Hz), 2.22 (t, 2H, H-4, J=7.2Hz), 2.03 (s, 3H, H-12), 1.58 – 1.48 (m, 4H, H-5 and 10), 1.34 – 1.24 (m, 8H, H-6 to 9), 1.19 (t, 3H, H-1, J=7.2Hz)

¹³C-NMR (CDCl₃, 100 MHz) δ: 172.86 (C-3), 59.15 (C-2), 33.45, 33.27, 28.13, 28.03, 27.72, 23.93, 14.53 (C-12), 13.25 (C-1). 2 signals missing.

IR (cm⁻¹): 1733 (C=O stretch)

HRMS: *m/z* calculated for C₁₂H₂₄O₂SNa = 255.1395 [M+Na]⁺; Found 255.1392

(9-Methylsulfanyl)nonanoic acid



Following the general ester hydrolysis procedure, work up gave (9-methylsulfanyl)nonanoic acid (241 mg, 90% yield) as a brown solid.

$^1\text{H-NMR}$ (CDCl_3 , 400 MHz) δ : 2.42 (t, 2H, H-9, $J=7.0$ Hz), 2.28 (t, 2H, H-2, $J=7.0$ Hz), 2.03 (s, 3H, H-10), 1.60 – 1.48 (m, 4H, H-3 and 8), 1.34 – 1.19 (m, 8H, H-4 to 7)

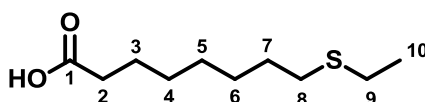
$^{13}\text{C-NMR}$ (CDCl_3 , 100 MHz) δ : 179.82 (C-1), 34.28 (C-9), 33.98 (C-2), 29.13, 29.03, 28.98, 28.73, 24.64 (C-3), 15.55 (C-10). 1 signal missing.

IR (cm^{-1}): 3037 (H-O stretch), 1705 (C=O stretch)

HRMS: m/z calculated for $\text{C}_{10}\text{H}_{20}\text{O}_2\text{SNa} = 227.1076$ [$\text{M}+\text{Na}$] $^+$; Found 277.1075

Melting point ($^\circ\text{C}$): 35 – 36

(8-Ethylsulfanyl)octanoic acid



Following the general ester hydrolysis procedure, work up gave (8-ethylsulfanyl)octanoic acid (2.42 g, 100% yield) as a white waxy solid.

$^1\text{H-NMR}$ (CDCl_3 , 400 MHz) δ : 2.49 (m, 4H, H-8 and 9), 2.28 (t, 2H, H-2, $J=7.5$ Hz), 1.57 (m, 2H, H-3), 1.51 (m, 2H, H-7), 1.34 – 1.28 m, 6H, H-4 to 6), 1.19 (t, 3H, H-10, $J=7.5$ Hz)

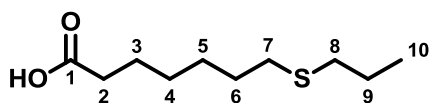
$^{13}\text{C-NMR}$ (CDCl_3 , 100 MHz) δ : 178.90 (C-1), 33.82 (C-2), 31.63, 29.56, 28.93, 28.87, 28.71, 25.95, 24.61 (C-3), 14.94 (C-10)

IR (cm^{-1}): 3035 (H-O stretch), 1703 (C=O stretch)

HRMS: m/z calculated for $\text{C}_{10}\text{H}_{20}\text{O}_2\text{SNa} = 227.1076$ [$\text{M}+\text{Na}$] $^+$; Found 277.1075

Melting point (°C): 34 – 36

(7-Propylsulfanyl)heptanoic acid



Following the general ester hydrolysis procedure, work up gave (7-propylsulfanyl)heptanoic acid (2.48 g, 99% yield) as a dark yellow oil.

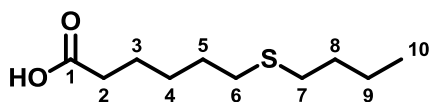
¹H-NMR (CDCl₃, 400 MHz) δ: 2.45 – 2.30 (m, 4H, H-7 and 8), 2.29 (t, 2H, H-2, J=7.6Hz), 1.61 – 1.48 (m, 6H, H-3, 6 and 9), 1.38 – 1.26 (m, 4H, H-4 and 5), 0.92 (t, 3H, H-10, J=7.3Hz)

¹³C-NMR (CDCl₃, 100 MHz) δ: 180.08 (C-1), 34.25 (C-8), 33.98 (C-2), 32.00 (C-7), 29.49 (C-6), 28.66 (C-5), 28.51 (C-4), 24.53 (C-3), 23.01 (C-9), 13.54 (C-10)

IR (cm⁻¹): 3037 (H-O stretch), 1703 (C= stretch)

HRMS: *m/z* calculated for C₁₀H₂₀O₂SNa = 227.1073 [M+Na]⁺; Found 277.1075

(6-Butylsulfanyl)hexanoic acid 105



Following the general ester hydrolysis procedure, work up gave (6-butylsulfanyl)hexanoic acid (788 mg, 88% yield) as a pale yellow oil.

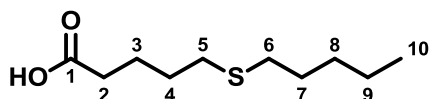
¹H-NMR (CDCl₃, 400 MHz) δ: 2.51 (m, 4H, H-6 and 7), 2.36 (t, 2H, H-2, J=7.6Hz), 1.61 (m, 6H, H-3, 5 and 8), 1.43 (m, 4H, H-4 and 9), 0.91 (t, 3H, H-10, J=7.3Hz)

¹³C-NMR (CDCl₃, 100 MHz) δ: 179.85 (C-1), 34.00 (C-2), 32.02 (C-6), 32.00 (C-7), 31.93 (C-8), 29.44 (C-5), 28.42 (C-4), 22.17 (C-9), 24.42 (C-3), 13.83 (C-10)

IR (cm⁻¹): 3214 (H-O stretch), 1705 (C=O stretch)

HRMS: *m/z* calculated for C₁₀H₁₉O₂S = 203.1111 [M-H]; Found 203.1104

(5-Pentylsulfanyl)pentanoic acid 262



Following the general ester hydrolysis procedure, work up gave (5-pentylsulfanyl)pentanoic acid (859 mg, 91% yield) as a pale yellow oil.

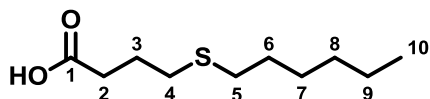
$^1\text{H-NMR}$ (CDCl_3 , 400 MHz) δ : 2.47 – 2.41 (m, 4H, H-5 and 6), 2.31 (t, 2H, H-2, $J=7.0\text{Hz}$), 1.72 (m, 2H, H-3), 1.64 – 1.61 (m, 4H, H-4 and 7), 1.31 – 1.23 (m, 4H, H-8 and 9), 0.83 (t, 3H, H-10, $J=7.0\text{Hz}$)

$^{13}\text{C-NMR}$ (CDCl_3 , 100 MHz) δ : 179.82 (C-1), 33.59 (C-2), 32.14 (C-6), 31.64 (C-5), 31.10 (C-8), 29.36 (C-7), 28.95 (C-4), 23.83 (C-3), 22.31 (C-9), 13.98 (C-10)

IR (cm^{-1}): 3216 (H-O stretch), 1706 (C=O stretch)

HRMS: m/z calculated for $\text{C}_{10}\text{H}_{19}\text{O}_2\text{S} = 203.1111$ [M-H] $^-$; Found 203.1103

(4-Hexylsulfanyl)butanoic acid



Following the general ester hydrolysis procedure, work up gave (4-hexylsulfanyl)butanoic acid (1.18 g, 99% yield) as a pale yellow oil.

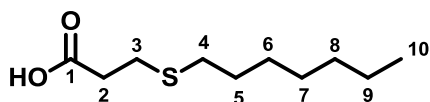
$^1\text{H-NMR}$ (CDCl_3 , 400 MHz) δ : 2.50 (m, 2H, H-4), 2.43 (m, 4H, H-2 and 5), 1.85 (qu, 2H, H-3, $J=7.3\text{Hz}$), 1.50 (qu, 2H, H-6, $J=7.3\text{Hz}$), 1.29 (m, 2H, H-7), 1.25 – 1.17 (m, 4H, H-8 and 9), 0.82 (t, 3H, H-10, $J=6.6\text{Hz}$)

$^{13}\text{C-NMR}$ (CDCl_3 , 100 MHz) δ : 179.21 (C-1), 32.73 (C-2), 31.98 (C-5), 31.45 (C-8), 31.21 (C-4), 29.59 (C-6), 28.59 (C-7), 24.80 (C-3), 22.56 (C-9), 14.05 (C-10)

IR (cm^{-1}): 1705 (C=O stretch)

HRMS: m/z calculated for $\text{C}_{10}\text{H}_{20}\text{O}_2\text{SNa} = 227.1076$ [M+Na] $^+$; Found 227.1076

(3-Heptylsulfanyl)propanoate



Following the general ester hydrolysis procedure, work up gave (3-heptylsulfanyl)propanoic acid (1.12 g, 99% yield) as a colourless oil.

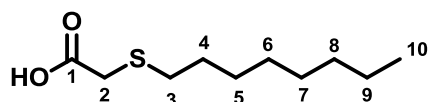
$^1\text{H-NMR}$ (CDCl_3 , 400 MHz) δ : 2.71 (t, 2H, H-2, $J=6.5\text{Hz}$), 2.59 (t, 2H, H-3, $J=6.5\text{Hz}$), 2.47 (t, 2H, H-4, $J=7.4\text{Hz}$), 1.52 (m, 2H, H-5), 1.29 (m, 2H, H-6), 1.24 – 1.18 (m, 6H, H- 7, 8 and 9), 0.81 (t, 3H, H-10, $J=6.9\text{Hz}$)

$^{13}\text{C-NMR}$ (CDCl_3 , 100 MHz) δ : 177.90 (C-1), 34.67 (C-3), 32.23 (C-4), 31.73 (C-8), 29.54 (C-5), 28.89 (C-7), 28.83 (C-6), 26.61 (C-2), 22.61 (C-9), 14.08 (C-10)

IR (cm^{-1}): 1684 (C=O stretch)

HRMS: m/z calculated for $\text{C}_{10}\text{H}_{20}\text{O}_2\text{SNa} = 227.1076$ $[\text{M}+\text{Na}]^+$; Found 227.1073

(2-Octylsulfanyl)ethanoic acid



Following the general ester hydrolysis procedure, work up gave (2-octylsulfanyl)ethanoic acid (2.02 g, 94% yield) as a brown oil.

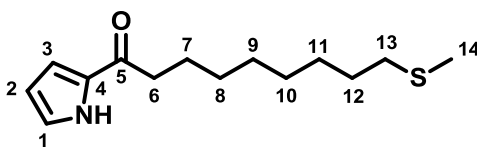
$^1\text{H-NMR}$ (CDCl_3 , 400 MHz) δ : 3.19 (s, 2H, H-2), 2.59 (t, 2H, H-3, $J=7.4\text{Hz}$), 1.54 (m, 2H, H-4), 1.31 (m, 2H, H-5), 1.25 – 1.20 (m, 8H, H- 6, 7, 8 and 9), 0.81 (t, 3H, H-9, $J=6.9\text{Hz}$)

$^{13}\text{C-NMR}$ (CDCl_3 , 100 MHz) δ : 175.66 (C-1), 33.50 (C-2), 32.85 (C-3), 31.80 (C-8), 29.15 (C-7), 28.92 (C-4), 28.83 (C-5), 28.75 (C-6), 22.65 (C-9), 14.10 (C-9)

IR (cm^{-1}): 1703 (C=O stretch)

HRMS: m/z calculated for $\text{C}_{10}\text{H}_{20}\text{O}_2\text{SNa} = 227.1076$ $[\text{M}+\text{Na}]^+$; Found 227.1074

(9-Methylsulfanyl)-1-(pyrrole-2-yl)nonan-1-one



Following the general carboxylic acid coupling procedure, the crude product was purified on silica gel (15% EtOAc in pet ether) to give (9-methylsulfanyl)-1-(pyrrole-2-yl)nonan-1-one (787 mg, 49% yield) as a white solid.

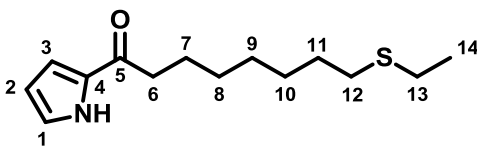
$^1\text{H-NMR}$ (CDCl_3 , 400 MHz): 9.42 (bs, 1H, H-N), 6.95 (m, 1H, H-1), 6.84 (m, 1H, H-3), 6.21 (m, 1H, H-2), 2.69 (t, 2H, H-6, $J=7.2\text{Hz}$), 2.41 (t, 2H, H-13, $J=7.3\text{Hz}$), 2.02 (s, 3H, H-14), 1.64 (m, 2H, H-7), 1.51 (m, 2H, H-8), 1.34 – 1.32 (m, 8H, H-9 to 12)

$^{13}\text{C-NMR}$ (CDCl_3 , 100 MHz): 191.15 (C-5), 132.08 (C-4), 124.32 (C-3), 115.98 (C-1), 110.56 (C-2), 38.01 (C-6), 34.28 (C-13), 29.39, 29.34, 29.15, 29.10, 28.78, 25.24 (C-7), 15.56 (C-14)

IR (cm^{-1}): 3283 (N-H stretch), 1640 (C=O stretch)

HRMS: m/z calculated for $\text{C}_{14}\text{H}_{23}\text{NOSNa} = 276.1392$ $[\text{M}+\text{Na}]^+$; Found 276.1390

(8-Ethylsulfanyl)-1-(pyrrole-2-yl)octan-1-one



Following the general carboxylic acid coupling procedure, the crude product was purified on silica gel (15% EtOAc in pet ether) to give (8-ethylsulfanyl)-1-(pyrrole-2-yl)octan-1-one (2.68 g, 89% yield) as a yellow oil.

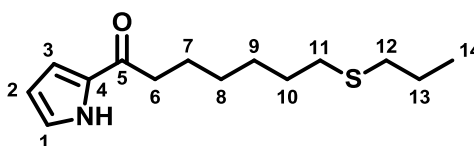
$^1\text{H-NMR}$ (CDCl_3 , 400 MHz) δ : 6.95 (m, 1H, H-1), 6.83 (m, 1H, H-3), 6.75 (m, 1H, H-2), 2.69 (t, 2H, H-6, $J=7.3\text{Hz}$), 2.49 – 2.42 (m, 4H, H-12 and 13), 1.65 (m, 2H, H-7), 1.51 (m, 2H, H-11), 1.36 – 1.29 (m, 6H, H-8 to 10), 1.18 (m, 3H, H-14)

$^{13}\text{C-NMR}$ (CDCl_3 , 100 MHz) δ : 191.07 (C-5), 132.10 (C-4), 124.31 (C-3), 117.69 (C-1), 115.94 (C-2), 37.97 (C-6), 31.64 (C-12), 29.60, 29.33, 29.07, 28.78, 25.94 (C-13), 25.20 (C-7), 14.83 (C-14)

IR (cm^{-1}): 1680 (C=O stretch)

HRMS : m/z calculated for $\text{C}_{14}\text{H}_{23}\text{NOSNa}$ = 276.1398 $[\text{M}+\text{Na}]^+$; Found 276.1396

(7-Propylsulfanyl)-1-(pyrrol-2-yl)heptan-1-one



Following the general carboxylic acid coupling procedure, the crude product was purified on silica gel (10% EtOAc in hexane) to give (7-propylsulfanyl)-1-(pyrrol-2-yl)heptan-1-one (2.34 g, 76% yield) as a colourless oil.

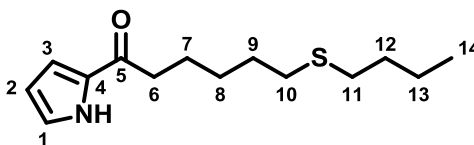
$^1\text{H-NMR}$ (CDCl_3 , 400 MHz) δ : 9.39 (bs, 1H, N-H), 6.94 (m, 1H, H-1), 6.84 (m, 1H, H-3), 6.21 (m, 1H, H-2), 2.69 (t, 2H, H-6, $J=7.0\text{Hz}$), 2.43 (m, 4H, H-11 and 12), 1.66 (m, 2H, H-7), 1.60 – 1.49 (4H, m, H-10 and 13), 1.40 – 1.27 (m, 4H, H-8 and 9), 0.91 (t, 3H, H-14, $J=7.0\text{Hz}$)

$^{13}\text{C-NMR}$ (CDCl_3 , 100 MHz) δ : 190.96 (C-5), 132.07 (C-4), 124.30 (C-3), 115.93 (C-1), 110.58 (C-2), 37.89 (C-6), 34.24, 32.05, 29.58, 29.06, 28.73, 23.02, 25.11 (C-7), 13.55 (C-14)

IR (cm^{-1}): 3280 (N-H stretch), 1633 (C=O stretch)

HRMS : m/z calculated for $\text{C}_{14}\text{H}_{23}\text{NOSNa}$ = 276.1398 $[\text{M}+\text{Na}]^+$; Found 276.1396

(6-Butylsulfanyl)-1-(pyrrol-2-yl)hexan-1-one 106



Following the general carboxylic acid coupling procedure, the crude product was purified on silica gel (15% EtOAc in hexane) to give (6-butylsulfanyl)-1-(pyrrol-2-yl)hexan-1-one (795 mg, 81% yield) as a orange oil.

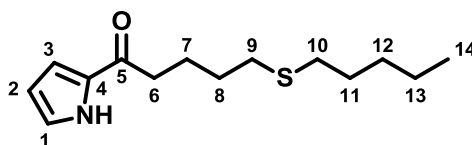
$^1\text{H-NMR}$ (CDCl_3 , 400 MHz) δ : 9.61 (bs, 1H, N-H), 7.03 (m, 1H, H-3), 6.90 (m, 1H, H-1), 6.27 (m, 1H, H-2), 2.77 (t, 2H, H-6, $J=7.2\text{Hz}$), 2.51 (m, 4H, H-10 and 11), 1.74 (m, 2H, H-7), 1.66 – 1.35 (m, 8H, H- 8, 9, 12 and 13), 0.91 (t, 3H, H-14, $J=7.0\text{ Hz}$)

$^{13}\text{C-NMR}$ (CDCl_3 , 100 MHz) δ : 191.10 (C-5), 132.22 (C-4), 124.78 (C-3), 116.34 (C-1), 110.74 (C-2), 37.76 (C-6), 32.16 (C-10), 32.06 (C-11), 32.01 (C-12), 29.74 (C-9), 28.91 (C-8), 25.01 (C-7), 22.24 (C-13), 13.91 (C-14)

IR (cm^{-1}): 1679 (C=O stretch)

HRMS: m/z calculated for $\text{C}_{14}\text{H}_{23}\text{NOSNa} = 276.1398$ [$\text{M}+\text{Na}$] $^+$; Found 276.1392

(5-Pentylsulfanyl)-1-(pyrrol-2-yl)pentan-1-one 263



Following the general carboxylic acid coupling procedure, the crude product was purified on silica gel (15% EtOAc in hexane) to give (5-pentylsulfanyl)-1-(pyrrol-2-yl)pentan-1-one (795 mg, 81% yield) as an orange oil.

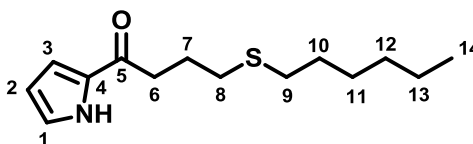
$^1\text{H-NMR}$ (CDCl_3 , 400 MHz) δ : 9.71 (bs, 1H, N-H), 6.96 (m, 1H, H-1), 6.85 (m, 1H, H-3), 6.20 (m, 1H, H-2), 2.72 (t, 2H, H-6, $J=7.3\text{Hz}$), 2.49 – 2.40 (m, 4H, H-9 and 10), 1.76 (m, 2H, H-7), 1.59 (m, 2H, H-8), 1.50 (m, 2H, H-11), 1.26 – 1.20 (m, 4H, H-11 and 12), 0.82 (t, 3H, H-14, $J=7.0\text{Hz}$)

$^{13}\text{C-NMR}$ (CDCl_3 , 100 MHz) δ : 190.63 (C-5), 131.97 (C-4), 124.67 (C-3), 116.22 (C-1), 110.58 (C-2), 37.44 (C-6), 32.16 (C-10), 31.86 (C-9), 31.12 (C-13), 29.40, 24.43 (C-7), 22.33 (C-12), 14.01 (C-14). 1 signal missing.

IR (cm⁻¹): 3285 (N-H), 1678 (C=O stretch)

HRMS: *m/z* calculated for C₁₄H₂₃NOSNa = 276.1398 [M+Na]⁺; Found 276.1393

(4-Hexylsulfanyl)-1-(pyrrol-2-yl)butan-1-one



Following the general carboxylic acid coupling procedure, the crude product was purified on silica gel (10% EtOAc in hexane) to give (4-hexylsulfanyl)-1-(pyrrol-2-yl)butan-1-one (2.34 g, 76% yield) as a colourless oil.

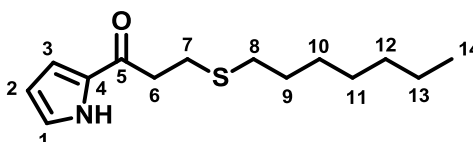
¹H-NMR (CDCl₃, 400 MHz) δ: 9.39 (bs, 1H, H-N), 6.96 (m, 1H, H-1), 6.88 (m, 1H, H-3), 6.21 (m, 1H, H-2), 2.84 (t, 2H, H-6, J=7.3Hz), 2.52 (t, 2H, H-8, J=7.4Hz), 2.44 (t, 2H, H-9, J=7.5Hz), 1.94 (qu, 2H, H-7, J=7.4Hz), 1.50 (qu, 2H, H-10, J=7.3Hz), 1.30 – 1.18 (m, 6H, H-11 to 13), 0.81 (t, 3H, H-14, J=7.1Hz)

¹³C-NMR (CDCl₃, 100 MHz) δ: 189.91 (C-5), 131.92 (C-4), 124.44 (C-1), 116.18 (C-3), 110.69 (C-2), 36.58 (C-6), 31.97 (C-9), 31.68 (C-8), 31.68, 29.63 (C-10), 28.63 (C-11), 24.64 (C-7), 22.58, 14.08 (C-14)

IR (cm⁻¹): 3282 (N-H stretch), 1634 (C=O stretch)

HRMS: *m/z* calculated for C₁₄H₂₃NOSNa = 276.1393 [M+ Na]⁺; Found 276.1391

(3-Heptylsulfanyl)-1-(pyrrol-2-yl)propan-1-one



Following the general carboxylic acid coupling procedure, the crude product was purified on silica gel (15% EtOAc in hexane) to give (3-heptylsulfanyl)-1-(pyrrol-2-yl)propan-1-one (794 mg, 60% yield) as a colourless oil.

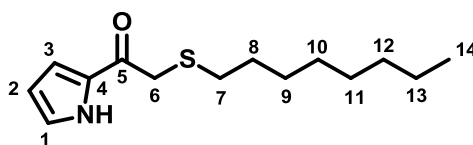
$^1\text{H-NMR}$ (CDCl_3 , 400 MHz) δ : 9.34 (bs, 1H, N-H), 6.97 (m, 1H, H-1), 6.87 (m, 1H, H-3), 6.21 (m, 1H, H-2), 2.99 (t, 2H, H-6, $J=7.4\text{Hz}$), 2.82 (t, 2H, H-7, $J=7.4\text{Hz}$), 2.48 (t, 2H, H-8, $J=7.5\text{Hz}$), 1.52 (m, 2H, H-9), 1.34 – 1.20 (m, 8H, H-10 to 13), 0.81 (t, 3H, H-14, $J=7.0\text{Hz}$)

$^{13}\text{C-NMR}$ (CDCl_3 , 100 MHz) δ : 188.57 (C-5), 131.90 (C-4), 124.74 (C-3), 116.35 (C-1), 110.81 (C-2), 38.23, 32.49, 31.75, 29.63, 28.92, 28.88, 26.97, 22.62, 14.09 (C-14)

IR (cm^{-1}): 3287 (N-H stretch), 1641 (C=O stretch)

HRMS : m/z calculated for $\text{C}_{14}\text{H}_{23}\text{NOSNa}$ = 276.1393 [$\text{M} + \text{Na}$] $^+$; Found 276.1390

(2-Octylsulfanyl)-1-(pyrrol-2-yl)ethan-1-one



Following the general carboxylic acid coupling procedure, the crude product was purified on silica gel (15% EtOAc in hexane) to give (2-octylsulfanyl)-1-(pyrrol-2-yl)ethan-1-one (128 mg, 53% yield) as a dark yellow oil.

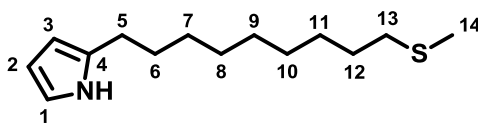
$^1\text{H-NMR}$ (CDCl_3 , 400 MHz) δ : 6.98 (m, 1H, H-3), 6.88 (m, 1H, H-1), 6.23 (m, 1H, H-2), 3.54 (s, 2H, H-6), 2.54 (m, 2H, H-7), 1.51 (m, 2H, H-8), 1.29 (m, 2H, H-9), 1.22 – 1.17 (m, 8H, H-10 to 13), 0.80 (t, 3H, H-14, $J=7.0\text{Hz}$)

$^{13}\text{C-NMR}$ (CDCl_3 , 100 MHz) δ : 185.73 (C-5), 132.24 (C-4), 125.08 (C-3), 116.86 (C-1), 110.98 (C-2), 36.75 (C-6), 32.72 (C-7), 31.80, 29.17, 29.10, 28.82, 22.65, 14.11 (C-14). 1 signal missing.

IR (cm^{-1}): 3283 (N-H stretch), 1640 (C=O stretch)

HRMS : m/z calculated for $\text{C}_{14}\text{H}_{23}\text{NOSNa}$ = 276.1393 [$\text{M} + \text{Na}$] $^+$; Found 276.1391

2-(9-Methylsulfanylnonyl)-pyrrole 266



Following the general acyl ketone reduction procedure, the crude product was purified on silica gel (10% EtOAc in pet ether) to give 2-(9-methylsulfanylnonyl)-pyrrole (700 mg, 95% yield) as a colourless oil.

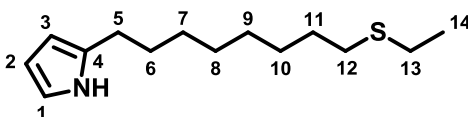
$^1\text{H-NMR}$ (CDCl_3 , 400 MHz) δ : 7.84 (bs, 1H, N-H), 6.60 (m, 1H, H-1), 6.01 (m, H-2), 5.84 (m, 1H, H-3), 2.52 (t, 2H, H-5, $J=7.6\text{Hz}$), 2.42 (t, 2H, H-13, $J=7.3\text{Hz}$), 2.03 (s, 3H, H-14), 1.58 – 1.48 (m, 4H, H-6 and 12), 1.32 – 1.19 (m, 10H, H-7 to 11)

$^{13}\text{C-NMR}$ (CDCl_3 , 100 MHz) δ : 132.61 (C-4), 115.99 (C-1), 108.25 (C-2), 104.86 (C-3), 34.32 (C-13), 29.67, 29.46, 29.39, 29.37, 29.25, 29.18, 28.83, 27.74 (C-5), 15.58 (C-14)

IR (cm^{-1}): 3371 (N-H stretch)

HRMS: m/z calculated for $\text{C}_{14}\text{H}_{26}\text{NS}$ = 240.1780 $[\text{M}+\text{H}]^+$; Found 240.1787

2-(8-Ethylsulfanyloctyl)-pyrrole 267



Following the general acyl ketone reduction procedure, the crude product was purified on silica gel (7% EtOAc in pet ether) to give 2-(8-ethylsulfanyloctyl)-pyrrole (1.74 g, 69% yield) as a colourless oil.

$^1\text{H-NMR}$ (CDCl_3 , 400 MHz) δ : 7.84 (bs, 1H, N-H), 6.59 (m, 1H, H-1), 6.06 (m, 1H, H-2), 5.84 (m, 1H, H-3), 2.52 (t, 2H, H-5, $J=7.5\text{Hz}$), 2.47 – 2.42 (m, 4H, H-12 and 13), 1.58 – 1.47 (m, 4H, H-6 and 11), 1.36 – 1.25 (m, 8H, H-7 to 10), 1.18 (t, 3H, H-14, $J=7.5\text{Hz}$)

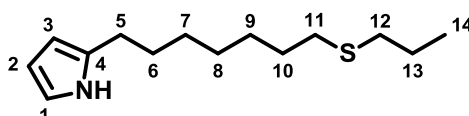
$^{13}\text{C-NMR}$ (CDCl_3 , 100 MHz) δ : 132.71 (C-4), 115.98 (C-1), 108.88 (C-2), 104.88 (C-3), 31.68 (C-12), 29.64, 29.31, 29.17, 28.92, 27.73 (C-5), 25.95 (C-13), 14.83 (C-14). 2 signals missing.

IR (cm⁻¹): 3370 (N-H stretch)

HRMS: *m/z* calculated for C₁₄H₂₆NS = 240.1780 [M+H]⁺ and C₁₄H₂₅NSNa = 262.1605 [M+Na]⁺;

Found 240.1785 and 262.1605

2-(7-Propylsulfanylheptyl)-pyrrole 268



Following the general acyl ketone reduction procedure, the crude product was purified on silica gel (5% EtOAc in pet ether) to give 2-(7-propylsulfanylheptyl)-pyrrole (730 mg, 80% yield) as a yellow oil.

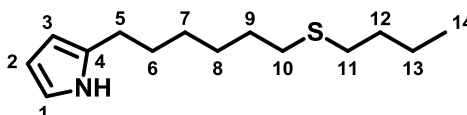
¹H-NMR (CDCl₃, 400 MHz) δ: 7.95 (bs, 1H, N-H), 6.68 (m, 1H, H-1), 6.15 (m, 1H, H-3), 5.93 (m, 1H, H-2), 2.62 (t, 2H, H-5, J=7.2Hz), 2.53 (4H, m, H-11 and 12), 1.68 – 1.56 (m, 6H, H-6, 9 and 10), 1.47 – 1.38 (m, 6H, H-7, 8 and 13), 0.94 (t, 3H, H-14, J=7.1Hz)

¹³C-NMR (CDCl₃, 100 MHz) δ: 132.66 (C-4), 116.02 (C-1), 108.26 (C-3), 104.92 (C-2), 32.12 (C-11), 31.87 (C-12), 31.83 (C-7), 29.57 (C-10), 29.56 (C-6), 28.90 (C-7), 28.66 (C-8), 27.62 (C-5), 22.06 (C-13), 13.73 (C-14)

IR (cm⁻¹): 3379 (N-H stretch)

HRMS: *m/z* calculated for C₁₄H₂₆NS = 240.1780 [M+H]⁺; Found 240.1783

2-(6-Butylsulfanylhexyl)-pyrrole 101



Following the general acyl ketone reduction procedure, the crude product was purified on silica gel (5% EtOAc in hexane) to give 2-(6-butylsulfanylhexyl)-pyrrole (531 mg, 71% yield) as a yellow oil.

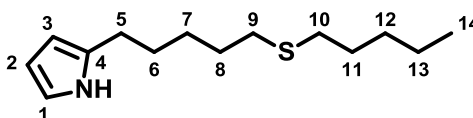
$^1\text{H-NMR}$ (CDCl_3 , 600 MHz) δ : 7.95 (bs, 1H, N-H), 6.68 (m, 1H, H-1), 6.15 (m, 1H, H-3), 5.93 (m, 1H, H-2), 2.62 (t, 2H, H-5, $J=7.2\text{Hz}$), 2.53 (4H, m, H-10 and 11), 1.68 – 1.56 (m, 6H, H-6, 9 and 12), 1.47 – 1.38 (m, 6H, H-7, 8 and 13), 0.94 (t, 3H, H-14, $J=7.1\text{Hz}$)

$^{13}\text{C-NMR}$ (CDCl_3 , 150 MHz) δ : 132.66 (C-4), 116.02 (C-1), 108.26 (C-3), 104.92 (C-2), 32.12 (C-11), 31.87 (C-10), 31.83 (C-7), 29.57 (C-12), 29.56 (C-6), 28.90 (C-7), 28.66 (C-8), 27.62 (C-5), 22.06 (C-13), 13.73 (C-14)

IR (cm^{-1}): 3379 (N-H stretch)

HRMS: m/z calculated for $\text{C}_{14}\text{H}_{26}\text{NS}$ = 240.1780 $[\text{M}+\text{H}]^+$ and $\text{C}_{14}\text{H}_{25}\text{NSNa}$ = 262.1605 $[\text{M}+\text{Na}]^+$;
Found 240.1785 and 262.1605

2-(5-Pentylsulphanyl)pentyl-pyrrole 257



Following the general acyl ketone reduction procedure, the crude product was purified on silica gel (5% EtOAc in hexane) to give 2-(5-pentylsulphanyl)pentyl-pyrrole (154 mg, 52% yield) as a yellow oil.

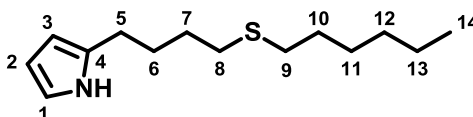
$^1\text{H-NMR}$ (CDCl_3 , 400 MHz) δ : 7.85 (bs, 1H, N-H), 6.59 (m, 1H, H-1), 6.06 (m, 1H, H-2), 5.84 (m, 1H, H-3), 2.54 (t, 2H, H-5, $J=7.3\text{Hz}$), 2.44 (m, 4H, H-9 and 10), 1.59 – 1.50 (m, 6H, H-6, 8 and 11), 1.38 (m, 2H, H-7), 1.31 – 1.23 (m, 4H, H-12 and 13), 0.83 (t, 3H, H-14, $J=7.0\text{Hz}$)

$^{13}\text{C-NMR}$ (CDCl_3 , 100 MHz) δ : 132.52 (C-4), 116.08 (C-1), 108.29 (C-2), 104.98 (C-3), 32.21 (C-9), 32.08 (C-10), 31.15 (C-12), 29.49 (C-6), 29.44 (C-11), 29.32 (C-8), 28.60 (C-7), 27.61 (C-5), 22.35 (C-13), 14.02 (C-14)

IR (cm^{-1}): 3384 (N-H stretch)

HRMS: m/z calculated for $\text{C}_{14}\text{H}_{26}\text{NS}$ = 240.1780 $[\text{M}+\text{H}]^+$; Found 240.1781

2-(4-Hexylsulphanylbutyl)-pyrrole 269



Following the general acyl ketone reduction procedure, the crude product was purified on silica gel (5% EtOAc in hexane) to give 2-(4-hexylsulphanylbutyl)-pyrrole (671 mg, 83% yield) as a yellow oil.

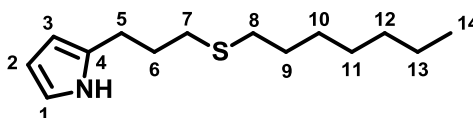
$^1\text{H-NMR}$ (CDCl_3 , 400 MHz) δ : 7.87 (bs, 1H, N-H), 6.59 (m, 1H, H-1), 6.06 (m, 1H, H-2), 5.85 (m, 1H, H-3), 2.56 (t, 2H, H-5, $J=7.3\text{Hz}$), 2.47 – 2.40 (m, 4H, H-8 and 9), 1.70 – 1.46 (m, 6H, H-6, 7 and 10), 1.34 – 1.19 (m, 6H, H-11, 12 and 13), 0.82 (t, 3H, H-14, $J=7.0\text{Hz}$)

$^{13}\text{C-NMR}$ (CDCl_3 , 100 MHz) δ : 132.18 (C-4), 116.16 (C-1), 108.32 (C-2), 105.13 (C-3), 32.23 (C-9), 31.48 (C-12), 29.69, 29.22, 28.79, 28.64, 27.32, 22.58, 14.06 (C-14). 1 signal missing.

IR (cm^{-1}): 3382 (N-H stretch)

HRMS: m/z calculated for $\text{C}_{14}\text{H}_{26}\text{NSNa} = 262.1600$ [$\text{M}+\text{Na}$] $^+$; Found 262.1604

2-(3-Heptylsulphanylpropyl)-pyrrole 270



Following the general acyl ketone reduction procedure, the crude product was purified on silica gel (7% EtOAc in hexane) to give 2-(3-heptylsulphanylpropyl)-pyrrole (474 mg, 63% yield) as a colourless oil.

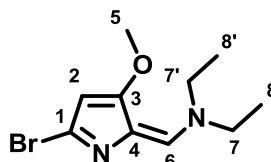
$^1\text{H-NMR}$ (CDCl_3 , 400 MHz) δ : 7.95 (bs, 1H, N-H), 6.60 (m, 1H, H-1), 6.06 (m, 1H, H-2), 5.86 (m, 1H, H-3), 2.66 (t, 2H, H-5, $J=6.9\text{Hz}$), 2.53 – 2.39 (m, 4H, H-7 and 8), 1.84 (m, 2H, H-6), 1.50 (m, 2H, H-9), 1.31 – 1.20 (m, 8H, H-10 to 13), 0.81 (t, 3H, H-14, $J=7.0\text{Hz}$)

$^{13}\text{C-NMR}$ (CDCl_3 , 100 MHz) δ : 132.14 (C-4), 108.38 (C-2), 105.25 (C-3), 32.11 (C-8), 31.48 (C-7), 31.76, 29.70, 29.39, 28.93, 26.50, 22.62, 14.10 (C-14). 2 signals missing.

IR (cm⁻¹): 3380 (N-H stretch)

HRMS: *m/z* calculated for C₁₄H₂₆NSNa = 262.1600 [M+Na]⁺ ; Found 262.1600

N-(5-Bromo-3-methoxy-pyrrol-2-ylidene-methyl)-diethylamine 80



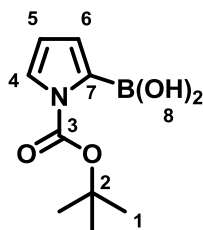
To a solution of diethyl formamide (1.63 ml, 14.59 mmol) in CH₂Cl₂ (10 ml), cooled to 0 °C under argon, was added phosphorous oxybromide (4.18 g, 14.59 mmol) in CH₂Cl₂ (10 ml). The resulting solution was stirred for 25 mins until a white precipitate formed to which 4-methoxy-3-pyrroli-2-one (750 mg, 6.63 mmol) in CH₂Cl₂ (10 ml) was added and heated to 40 °C for 6 hours. Water (80 ml) was added, the pH adjusted to 8 with 2.35M NaOH before EtOAc (100 ml) was added and filtered through a pad of celite. The aqueous layer was separated and extracted with EtOAc (2 x 75 ml). The combined organics were washed with brine, dried (MgSO₄) and concentrated under vacuum to give (1.26 g, 73% yield) as a brown oil.

¹H-NMR (CDCl₃, 400 MHz): 6.99 (s, 1H, H-2), 5.58 (s, 1H, H-6), 4.11 (q, 2H H-7 or 7', J=7.1Hz), 3.75 (s, 3H, H-5), 3.39 (q, 2H, H-7 or 7', 7.1Hz), 1.28 (m, 6H, Proton 8 and 8')

¹³C-NMR (CDCl₃, 100 MHz) δ: 165.45 (C-3), 138.72 (C-2), 133.80 (C-4), 120.92 (C-1), 96.58 (C-6), 58.11 (C-5), 51.23 (C-7 or 7'), 44.65 (C-7 or 7'), 14.72 (C-8 or 8'), 12.61 (C-8 or 8')

HRMS: *m/z* calculated for C₁₀H₁₆N₂OBr = 259.0446 and 261.0426 [M+H]⁺; Found 259.0434 and 261.0416

N-Boc pyrrole-2-boronic acid 30



To a solution of 2,2,6,6-tetramethyl piperidine (2.23 ml, 13.16 mmol) in THF (20 ml), cooled to -78 °C under argon, was added *n*-butyl lithium (9.77 ml, 14.95 mmol) cautiously and the resulting yellow solution allowed to warm to RT over 30 mins. This solution was cooled back to -78 °C before N-Boc pyrrole (2.00 ml, 11.96 mmol) in THF (20 ml) was added and stirred for 2 hours. Trimethyl borate (35.88 mmol, 3.99 ml) in THF (20 ml) was added and the reaction mixture allowed to warm to RT overnight. 0.5M HCl (30 ml) was added to the reaction before the THF removed under vacuum. Water (30 ml) was added and extracted with Et₂O (4 x 20 ml). The combined organic were washed with brine, dried (MgSO₄) and concentrated under vacuum until a white precipitate began to form. This was cooled to -78 °C for 10 mins and the precipitate filtered off; this was repeated four times to give N-Boc pyrrole-2-boronic acid (1.36g, 54% yield) as an off-white solid.

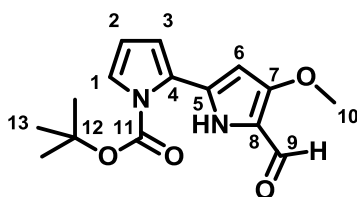
¹H-NMR (CDCl₃, 400 MHz): 7.72 (bs, 2H, H-8), 7.45 (dd, 1H, H-6, J₁=3.1Hz, J₂=1.7Hz), 7.12 (dd, 1H, H-4, J₁=3.3Hz, J₂=1.7Hz), 6.26 (t, 1H, H-5, J=3.2Hz), 1.62 (s, 9H, H-1)

¹³C-NMR (CDCl₃, 100 MHz) δ: 152.48 (C-3), 128.94 (C-4), 127.21 (C-6), 112.24 (C-5), 85.75 (C-2), 28.12 (C-1). 1 signal missing

IR (cm⁻¹): 3373 (H-O stretch), 1705 (C=O stretch)

HRMS: *m/z* calculated for C₉H₁₄NO₄Na = 234.0914 [M+Na]⁺; Found 234.0902

3-Methoxy-5-(1-BOC-pyrrol-2-yl)-1H-pyrrole-2-carboxaldehyde¹²⁵

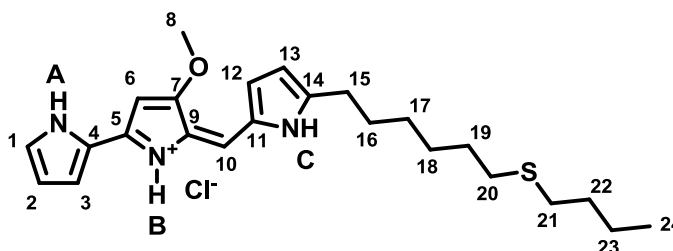


A suspension of palladium(II) acetate (68 mg, 0.30 mmol) and triphenyl phosphine (388 mg, 1.48 mmol) in degassed toluene (4 ml), under argon, was heated to 70 °C for 20 mins. To this was added N-(5-bromo-3-methoxy-pyrrol-2-ylidene)methyl)-diethyl-amine (767 mg, 2.96 mmol) and N-Boc pyrrole-2-boronic acid (625 mg, 2.96 mmol) in degassed 10% water:1,4-dioxane (10 ml) and sodium carbonate (941 mg, 8.88 mmol). The reaction was heated to 85 °C for a further 3 hours. The reaction mixture was diluted with CH₂Cl₂ and water before 2M HCl was added to neutralise the mixture with vigorous stirring. The aqueous layer was separated and extracted several times with CH₂Cl₂. The combined organics were dried (MgSO₄) and concentrated under vacuum. The crude product was purified on silica gel (30% EtOAc in pet ether) to give 3-methoxy-5-(1-BOC-pyrrol-2-yl)-1H-pyrrole-2-carboxaldehyde (464 mg, 54% yield) as an orange solid.

¹H-NMR (d₆-DMSO, 400 MHz δ: 10.65 (bs, 1H, N-H), 9.46 (s, 1H, H-9), 7.27 (m, 1H, H-1), 6.60 (m, 1H, H-3), 6.18 (m, 1H, H-2), 6.00 (m, 1H, H-6), 3.82 (s, 3H, H-10), 1.54 (s, 9H, H-13)

HRMS: *m/z* calculated for C₁₅H₁₈N₂O₄ = 291.1339 [M+H]⁺; Found 291.1341

2-[[5-(6-Butylsulfanylhexyl)-1H-pyrrol-2-yl]methylene]-3-methoxy-5-(1H-pyrrol-2-yl)pyrrole hydrochloride salt⁴⁷ 102



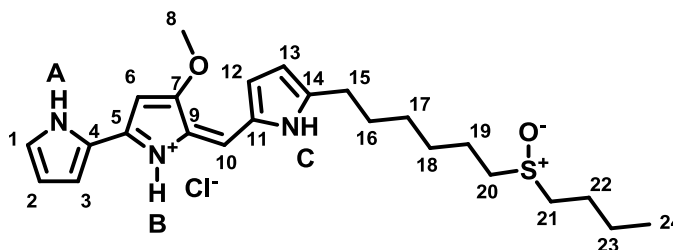
To a solution of 3-methoxy-5-(1-BOC-pyrrol-2-yl)-1H-pyrrole-2-carboxaldehyde (25 mg, 0.09 mmol) and 2-(6-butylsulfanylhexyl)-pyrrole (23 mg, 0.10 mmol) in methanol (1.5 ml) was added 2M HCl in methanol (0.05 ml) and the resulting red solution stirred for 30 mins. Sodium methoxide (29 mg, 0.54 mmol) was added and the resulting yellow/brown solution stirred for a further 45 mins. The reaction mixture was poured into water and the yellow colour extracted with EtOAc. The combined organics were dried (MgSO_4) and concentrated under vacuum. The crude product was purified on reverse phase HPLC (Table 6.2). The required fractions were combined and the methanol removed under vacuum. The remaining solution was poured into sat NaHCO_3 and the yellow colour extracted with EtOAc. The combined organics were washed with 2M HCl, dried (MgSO_4) and concentrated under vacuum to give 2-[[5-(6-butylsulfanylhexyl)-1H-pyrrol-2-yl]methylene]-3-methoxy-5-(1H-pyrrol-2-yl)pyrrole hydrochloride salt (14 mg, 38% yield) as a red solid.

$^1\text{H-NMR}$ (CDCl_3 , 700 MHz) δ : 12.63 (bs, 1H, N-H B), 12.55 (bs, 1H, N-H C), 12.45 (bs, 1H, N-H A), 7.14 (m, 1H, H-1), 6.88 (s, 1H, H-6), 6.87 (s, 1H, H-6), 6.74 (m, 1H, H-12), 6.25 (m, 1H, H-2), 6.10 (m, 1H, H-13), 6.00 (s, 1H, H-10), 3.92 (s, 3H, H-8), 2.86 (t, 2H, H-15), 2.41 (m, 4H, H-20 and 21), 1.68 (m, 2H, H-16), 1.52 – 1.45 (m, 4H, H-19 and 22), 1.34 – 1.29 (m, 6H, H-17, 18 and 23), 0.83 (t, 3H, H-24)

$^{13}\text{C-NMR}$ (CDCl_3 , 125 MHz) δ : 165.32 (C-7), 151.72 (C-14), 147.93 (C-9), 128.17 (C-12), 126.72 (C-1), 125.06 (C-11), 120.99 (C-4), 120.54 (C-5), 117.06 (C-3), 115.26 (C-6), 111.43 (C-13), 111.01 (C-2), 92.16 (C-10), 57.85 (C-8), 31.09, 30.82, 28.64, 28.09, 27.91, 27.68, 27.29 (C-15), 21.08, 12.69 (C-24). 1 signal missing.

HRMS: m/z calculated for $\text{C}_{24}\text{H}_{34}\text{N}_3\text{OS}$ = 412.2417 $[\text{M}+\text{H}]^+$; Found 412.2420

2-[[5-(6-Butylhexylsulphoxide)-1H-pyrrol-2-yl]methylene]-3-methoxy-5-(1H-pyrrol-2-yl)pyrrole hydrochloride salt^{47,125} 103



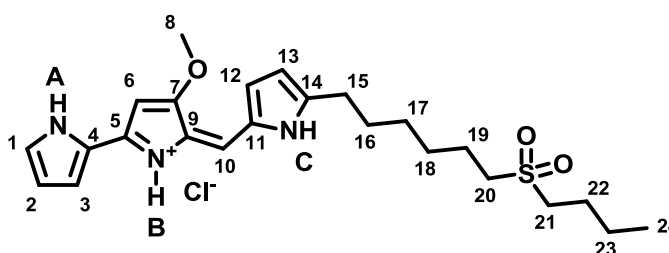
To a solution of 3-methoxy-5-(1-BOC-pyrrol-2-yl)-1H-pyrrole-2-carboxaldehyde (50 mg, 0.17 mmol) and 2-(6-butylsulfanylhexyl)-pyrrole (45 mg, 0.19 mmol) in methanol (3 ml) was added 2M HCl in methanol (0.10 ml) and the resulting red solution stirred for 15 mins. 3 Chloroperbenzoic acid (33 mg, 0.19 mmol) in methanol (1 ml) was added and stirred for a further 15 mins. Sodium methoxide (55 mg, 1.02 mmol) was added and the resulting yellow/brown solution stirred for a further 45 mins. The reaction mixture was poured into water and the yellow colour extracted with EtOAc. The combined organics were dried (MgSO_4) and concentrated under vacuum. The crude product was purified on reverse phase HPLC (Table 6.3). The required fractions were combined and the methanol removed under vacuum. The remaining solution was poured into sat NaHCO_3 and the yellow colour extracted with EtOAc. The combined organics were washed with 2M HCl, dried (MgSO_4) and concentrated under vacuum to give 2-[[5-(6-butylhexylsulphoxide)-1H-pyrrol-2-yl]methylene]-3-methoxy-5-(1H-pyrrol-2-yl)pyrrole hydrochloride salt (42 mg, 58% yield) as a red solid and 2-[[5-(6-Butylsulfanylhexyl)-1H-pyrrol-2-yl]methylene]-3-methoxy-5-(1H-pyrrol-2-yl)pyrrole hydrochloride salt (23 mg, 33% yield).

$^1\text{H-NMR}$ (CDCl_3 , 700 MHz) δ : 12.74 (bs, 1H, N-H B), 12.62 (bs, 1H, N-H C), 12.56 (bs, 1H, N-H A), 7.23 (m, 1H, H-1), 6.99 (s, 1H, H-6), 6.95 (m, 1H, H-3), 6.83 (m, 1H, H-12), 6.35 (m, 1H, H-2), 6.19 (m, 1H, H-13), 6.08 (s, 1H, H-10), 4.01 (s, 3H, H-8), 2.93 (t, 2H, H-15), 2.74 (m, 2H, H-20a and 21b), 2.64 (m, 2H, H-20b and 21b), 1.80 – 1.72 (m, 6H, H-16, 19 and 22), 1.55 – 1.42 (m, 6H, H-17, 18 and 23), 0.94 (t, 3H, H-24, $J=6.9\text{Hz}$)

$^{13}\text{C-NMR}$ (CDCl_3 , 125 MHz) δ : 166.38 (C-7), 152.41 (C-14), 149.01 (C-9), 129.20 (C-12), 127.71 (C-1), 126.03 (C-11), 122.03 (C-4), 121.58 (C-5), 112.03 (C-2), 118.10 (C-3), 116.35 (C-6), 112.52 (C-13), 93.14 (C-10), 58.83 (C-8), 51.96, 51.87, 28.91, 28.59, 28.29, 28.19, 24.62, 22.35, 22.05, 13.68 (C-24)

HRMS: m/z calculated for $\text{C}_{24}\text{H}_{34}\text{N}_3\text{O}_2\text{S}$ = 428.2366 $[\text{M}+\text{H}]^+$; Found 428.2365

2-[[5-(6-Butylhexylsulphone)-1H-pyrrol-2-yl]methylene]-3-methoxy-5-(1H-pyrrol-2-yl)pyrrole hydrochloride salt^{47,125} **256**



To a solution of 3-methoxy-5-(1-BOC-pyrrol-2-yl)-1H-pyrrole-2-carboxaldehyde (50 mg, 0.17 mmol) and 2-(6-butylsulfanylhexyl)-pyrrole (45 mg, 0.19 mmol) in methanol (3 ml) was added 2M HCl in methanol (0.10 ml) and the resulting red solution stirred for 15 mins. Oxone (261 mg, 0.43 mmol) in methanol (1 ml) was added and stirred for a further 15 mins. Sodium methoxide (64 mg, 1.19 mmol) was added and the resulting yellow/brown solution stirred for a further 45 mins. The reaction mixture was poured into water and the yellow colour extracted with EtOAc. The combined organics were dried (MgSO_4) and concentrated under vacuum. The crude product was purified on reverse phase HPLC (Table 6.3). The required fractions were combined and the methanol removed under vacuum. The remaining solution was poured into sat NaHCO_3 and the yellow colour extracted with EtOAc. The combined organics were washed with 2M HCl, dried (MgSO_4) and concentrated under vacuum to give 2-[[5-(6-butylhexylsulphone)-1H-pyrrol-2-yl]methylene]-3-methoxy-5-(1H-pyrrol-2-yl)pyrrole hydrochloride salt (40 mg, 53% yield) as a red solid and 2-[[5-(6-butylhexylsulphoxide)-1H-pyrrol-2-yl]methylene]-3-methoxy-5-(1H-pyrrol-2-yl)pyrrole hydrochloride salt (15 mg).

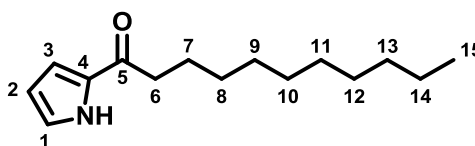
$^1\text{H-NMR}$ (CDCl_3 , 700 MHz δ): 12.87 (bs, 1H, N-H B), 12.71 (bs, 1H, N-H C), 12.66 (bs, 1H, N-H A), 7.26 (m, 1H, H-1), 7.03 (s, 1H, H-6), 6.98 (m, 1H, H-3), 6.85 (m, 1H, H-12), 6.38 (m, 1H, H-2), 6.21 (m, 1H, H-13), 6.11 (s, 1H, H-10), 4.04 (s, 3H, H-8), 2.98 – 2.94 (m, 4H, H-15, 20 and 21), 1.87 – 1.79 (m, 6H, H-16, 19 and 22), 1.53 – 1.44 (m, 6H, H-17, 18 and 23), 0.96 (t, 3H, H-24)

$^{13}\text{C-NMR}$ (CDCl_3 , 125 MHz δ): 166.42 (C-7), 152.24 (C-14), 149.07 (C-9), 129.14 (C-12), 127.66 (C-1), 126.04 (C-11), 122.09 (C-4), 121.63 (C-5), 118.07 (C-3), 116.39 (C-6), 112.52 (C-13), 112.10 (C-2), 93.10 (C-10), 58.84 (C-8), 52.70, 52.41, 28.90, 28.52, 28.03, 23.88, 21.89, 21.77 (C-15 to 19, 22 and 23), 13.53 (C-24). 1 signal missing.

HRMS: m/z calculated for $\text{C}_{24}\text{H}_{34}\text{N}_3\text{O}_3\text{S}$ = 444.2315 $[\text{M}+\text{H}]^+$; Found 444.2316

6.1.2 Synthesis of 2-UP 20

1-(Pyrrol-2-yl)undecan-1-one 84



Following the general carboxylic acid coupling procedure, the crude product was purified on silica gel (5% EtOAc in pet ether) to give 1-(pyrrol-2-yl)undecan-1-one (841 mg, 83% yield) as a white solid.

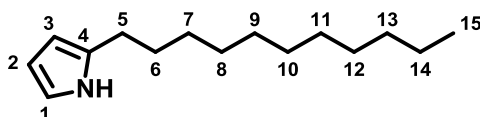
$^1\text{H-NMR}$ (CDCl_3 , 400 MHz δ): 9.32 (bs, 1H, H-N), 6.94 (m, 1H, H-1), 6.83 (m, 1H, H-3), 6.21 (m, 1H, H-2), 2.68 (t, 2H, H-6, $J=7.1\text{Hz}$), 1.64 (m, 2H, H-7), 1.59 – 1.30 (m, 14H, 6 to 14), 0.81 (t, 3H, H-15, $J=6.5\text{Hz}$)

$^{13}\text{C-NMR}$ (CDCl_3 , 100 MHz δ): 191.19 (C-4), 124.18 (C-1), 115.86 (C-3), 110.55 (C-2), 38.06 (C-6), 31.91, 22.69, 14.13 (C-15). 7 signals missing.

IR (cm^{-1}): 3282 (N-H stretch), 1642 (C=O stretch)

HRMS: m/z calculated for $\text{C}_{15}\text{H}_{25}\text{NO}$ = 258.1834 $[\text{M}+\text{Na}]^+$; Found 258.1832

2-Undecylpyrrole 20



Following the general acyl ketone procedure, the crude product was purified on silica gel (5% EtOAc in pet ether) to give 2-undecylpyrrole (487 mg, 61% yield) as a white solid.

$^1\text{H-NMR}$ (CDCl_3 , 400 MHz) δ : 7.91 (bs, 1H, H-N), 6.68 (m, 1H, H-1), 6.14 (m, 1H, H-2), 5.93 (m, 1H, H-3), 2.61 (t, 2H, H-5, $J=7.1\text{Hz}$), 1.63 (m, 2H, H-6), 1.38 – 1.28 (m, 16H, H-8 to 14), 0.90 (t, 3H, H-15, $J=6.7\text{Hz}$)

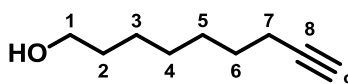
$^{13}\text{C-NMR}$ (CDCl_3 , 100 MHz) δ : 132.90 (C-4), 115.95 (C-1), 108.24 (C-2), 104.84 (C-3), 31.93, 22.70, 14.13 (C-15). 8 signals missing.

IR (cm^{-1}): 3365 (N-H stretch)

HRMS: m/z calculated for $\text{C}_{15}\text{H}_{26}\text{DN}$ = 223.2279 $[\text{M}+\text{H}]^+$; Found 223.2288

6.1.3 Synthesis of cyclopropane containing 2-UP analogues

8-Nonyn-1-ol 123



A suspension of sodium hydride (857 mg, 35.70 mmol) in ethylene diamine (25 ml), under argon, was heated to 60 °C for 45 mins, after which it turned purple. 3-Nonyn-1-ol (1.13 ml, 7.14 mmol) was added and again heated to 60 °C for 2 hours. The reaction mixture was cooled to 0 °C before 2M HCl (30 ml) was added cautiously followed by water (100 ml). The aqueous layer was extracted with Et_2O (3 x 30 ml). The combined organic layers were washed with brine, dried (MgSO_4) and concentrated under vacuum. The crude product was purified on silica gel (15% EtOAc in hexane) to give 8-nonyn-1-ol (0.69 g, 67% yield) as a pale yellow oil.

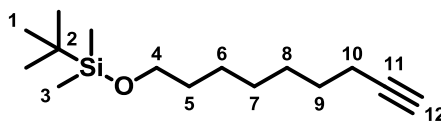
$^1\text{H-NMR}$ (CDCl_3 , 700 MHz) δ : 3.64 (t, 2H, H-1, $J=6.5\text{Hz}$), 2.18 (td, 2H, H-7, $J_1=6.8\text{Hz}$, $J_2=2.7\text{Hz}$), 1.94 (t, 1H, H-9, $J=2.6\text{Hz}$), 1.57 (m, 2H, H-2), 1.53 (m, 2H, H-6), 1.44 – 1.31 (m, 6H, H-3, 4 and 5)

$^{13}\text{C-NMR}$ (CDCl_3 , 175 MHz) δ : 84.67 (C-8), 68.13 (C-9), 62.95 (C-1), 32.68 (C-2), 28.86 (C-3), 28.65 (C-5), 28.36 (C-6), 25.59 (C-4), 18.35 (C-7)

IR (cm^{-1}): 3300 (O-H stretch), 2114 ($\text{C}\equiv\text{C}$ stretch)

HRMS: m/z calculated for $\text{C}_9\text{H}_{16}\text{ONa}$ = 163.1099 $[\text{M}+\text{Na}]^+$; Found 163.1096

8-Nonyn-1-oxy(*t*-butyldimethylsilyl)



To a solution of 8-nonyn-1-ol (3.22 g, 22.98 mmol) and *t*-butyldimethylsilylchloride (4.48 g, 29.87 mmol) in CH_2Cl_2 (100 ml), cooled to 0 °C under argon, was added imidazole (2.03 g, 29.87 mmol) and the resulting solution stirred for 3 hours. Water (150 ml) was added to dissolve the precipitate and the organics separated. The organics were washed with brine, dried (MgSO_4) and concentrated under vacuum. The crude product was purified on silica gel (5% EtOAc in hexane) to give 8-nonyn-1-oxy(*t*-butyldimethylsilyl) (5.48 g, 94% yield) as a pale yellow oil.

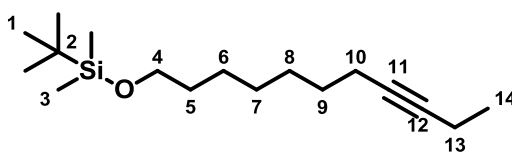
$^1\text{H-NMR}$ (CDCl_3 , 700 MHz) δ : 3.60 (t, 2H, H-4, $J=6.5\text{Hz}$), 2.18 (td, 2H, H-10, $J_1=6.9\text{Hz}$, $J_2=2.6\text{Hz}$), 1.94 (t, 1H, H-12, $J=2.7\text{Hz}$), 1.55 – 1.50 (m, 4H, H-5 and 9), 1.40 (m, 2H, H-6), 1.36 – 1.31 (m, 4H, H-7 and 8), 0.90 (s, 9H, H-1), 0.05 (s, 6H, H-3)

$^{13}\text{C-NMR}$ (CDCl_3 , 175 MHz) δ : 84.72 (C-11), 68.05 (C-12), 63.05 (C-4), 32.79 (C-9), 28.89 (C-8), 28.72 (C-6), 28.43 (C-5), 27.94 (C-2), 25.97 (C-1), 25.67 (C-7), 18.37 (C-10), -5.28 (C-3)

IR (cm^{-1}): 3315 (C-H alkyne stretch), 2120 ($\text{C}\equiv\text{C}$ stretch), 1254 (C-O stretch), 1098 (O-C stretch)

HRMS: m/z calculated for $\text{C}_{15}\text{H}_{31}\text{OSi}$ = 255.2144 $[\text{M}+\text{H}]^+$; Found 255.2135

1-(*t*-Butyldimethylsilyl)-oxy-undec-8-yne 124



To a solution of 8-nonyn-1-oxy(*t*-butyldimethylsilyl) (1.00 g, 3.93 mmol) in THF (20 ml), cooled to -30 °C under argon, was added *n*-butyl lithium (3.45 ml, 5.11 mmol) and the resulting yellow solution stirred for 30 mins. Ethyl iodide (1.5 ml, 18.87 mmol) in THF (10 ml) was added and stirred at RT for 24 hours. A small amount of water was added to quench the reaction. This was loaded directly onto silica gel and eluted with 10% EtOAc in hexane to give 1-(*t*-butyldimethylsilyl)-oxy-undec-8-yne (0.97 g, 88% yield) as a colourless oil.

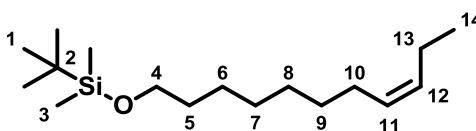
$^1\text{H-NMR}$ (CDCl_3 , 400 MHz) δ : 3.55 (t, 2H, H-4, $J=6.5\text{Hz}$), 2.14 – 2.07 (m, 4H, H-10 and 13), 1.48 (m, 4H, H-5 and 9), 1.34 – 1.21 (m, 6H, H-6, 7 and 8), 1.07 (t, 3H, H-14, $J=7.3\text{Hz}$), 0.85 (s, 9H, H-1), 0.00 (s, 6H, H-3)

$^{13}\text{C-NMR}$ (CDCl_3 , 100 MHz) δ : 81.46 (C-12), 79.43 (C-11), 63.30 (C-4), 32.84 (C-5), 29.12 (C-9), 28.98 (C-6), 28.86 (C-8), 25.99 (C-1), 25.72 (C-7), 18.73 (C-10), 18.39 (C-2), 14.40 (C-14), 12.43 (C-13), -5.25 (C-3)

IR (cm^{-1}): 2169 (C \equiv C stretch), 1253 (C-O stretch), 1099 (O-Si stretch)

HRMS: m/z calculated for $\text{C}_{17}\text{H}_{34}\text{OSiNa} = 305.2277$ [$\text{M}+\text{Na}$] $^+$; Found 305.2271

1-(*t*-Butyldimethylsilyl)-oxy-undec-8-(*Z*)-ene Z-125



To a solution of 1-(*t*-butyldimethylsilyl)-oxy-undec-8-yne (1.00 g, 3.54 mmol) and quinoline (0.21 ml, 1.77 mmol) in THF (20 ml) was added Lindlar's catalyst (20 mg) and the flask purged with hydrogen gas five times before being left to stir for 2 hours. The reaction mixture was filtered through celite and concentrated under vacuum. The crude material was purified on

silica gel (2% EtOAc in pet ether) to give 1-(*t*-butyldimethylsilyl)-oxy-undec-8-(*Z*)-ene (981 mg, 98% yield) as a colourless oil.

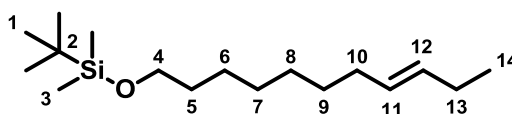
$^1\text{H-NMR}$ (CDCl_3 , 400 MHz) δ : 5.38 – 5.24 (m, 2H, H-11 and 12), 3.55 (t, 2H, H-4, $J=6.5\text{Hz}$), 1.99 (m, 4H, H-10 and 13), 1.46 (m, 2H, H-5), 1.30 – 1.25 (m, 8H, H-6, 7, 8 and 9), 0.97 (t, 3H, H-14, $J=7.3\text{Hz}$), 0.85 (s, 9H, H-1), 0.00 (s, 6H, H-1)

$^{13}\text{C-NMR}$ (CDCl_3 , 100 MHz) δ : 131.55 (C-12), 129.32 (C-11), 63.35 (C-4), 32.89 (C-5), 29.73, 29.35, 29.27, 27.09 (C-10), 26.00 (C-1), 25.79, 20.52 (C-13), 18.71 (C-2), 14.40 (C-14), -5.24 (C-3)

IR (cm^{-1}): 1253 (C-O stretch), 1098 (O-Si stretch)

HRMS : m/z calculated for $\text{C}_{17}\text{H}_{36}\text{OSi}$ = 285.2608 $[\text{M}+\text{H}]^+$; Found 285.2606

1-(*t*-Butyldimethylsilyl)-oxy-undec-8-(*E*)-ene E-125



Ammonia (100 ml) was condensed into a flask fitted with a dry ice/acetone condenser containing a solution of 1-(*t*-butyldimethylsilyl)-oxy-undec-8-yne (1.00 g, 3.54 mmol) in diethyl Et_2O (10 ml) under argon. Sodium (500 mg) was added in portions until the deep blue colour remained and allowed to stir for a further 5 hours. Solid NH_4Cl was cautiously added to quench the blue colour and the ammonia allowed to evaporate before water was added and extracted with Et_2O . The combined organics were dried (MgSO_4) and concentrated under vacuum. The crude product was purified on silica gel (1% EtOAc in pet ether) to give 1-(*t*-butyldimethylsilyl)-oxy-undec-8-(*E*)-ene (885 mg, 89% yield) as a yellow oil.

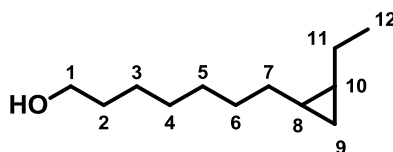
$^1\text{H-NMR}$ (CDCl_3 , 400 MHz) δ : 5.43 – 5.30 (m, 2H, H-11 and 12), 3.55 (t, 2H, H-4, $J=6.6\text{Hz}$), 1.99 (m, 4H, H-10 and 13), 1.46 (m, 2H, H-5), 1.30 – 1.21 (m, 8H, H-6, 7, 8 and 9), 0.91 (t, 3H, H-14, $J=7.4\text{Hz}$), 0.85 (s, 9H, H-1), 0.00 (s, 6H, H-1)

$^{13}\text{C-NMR}$ (CDCl_3 , 100 MHz) δ : 131.90 (C-12), 129.36 (C-11), 63.35 (C-4), 32.89 (C-5), 32.55 (C-10), 29.61, 29.32, 29.16, 26.00 (C-1), 25.77, 25.61, 18.71 (C-2), 14.42 (C-14), -5.25 (C-3)

IR (cm^{-1}): 1250 (C-O stretch), 1090 (O-Si stretch)

HRMS: m/z calculated for $\text{C}_{17}\text{H}_{36}\text{OSi}$ = 285.2608 [$\text{M}+\text{H}^+$]; Found 285.2609

7-(2-Ethylcyclopropyl)-(Z)-heptan-1-ol Z-126



To a solution of 1-(*t*-butyldimethylsilyl)-oxy-undec-8-(*Z*)-ene (738 mg, 2.60 mmol) in CH_2Cl_2 (45 ml), cooled to -20°C under argon in the dark, was added 1M diethyl zinc (12.98 ml, 12.98 mmol). Diiodomethane (1.04 ml, 12.98 mmol) was added dropwise and the reaction allowed to warm to RT over 24 hours. Once GC-MS indicated the complete consumption of the starting material, 2.35M NaOH (12 ml) was cautiously added and the resulting white solid removed by filtration. The combined organics were dried (MgSO_4) and concentrated under vacuum.

To a solution of this crude product in THF (15 ml), cooled to 0°C , was added tetrabutylammonium fluoride (946 mg, 7.80 mmol) and stirred for 5 hours. The majority of the THF was removed under vacuum before the residual was loaded onto silica gel. This was eluted with 20% EtOAc in pet ether to give 7-(2-ethylcyclopropyl)-(Z)-heptan-1-ol (425 mg, 89% yield) as a colourless oil.

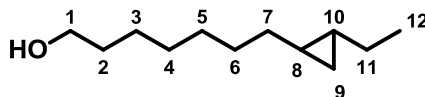
$^1\text{H-NMR}$ (CDCl_3 , 700 MHz) δ : 3.59 (t, 2H, H-1, $J=6.4\text{Hz}$), 1.52 (m, 2H, H-2), 1.38 – 1.28 (m, 10H, H-3 to 6, 7a and 11a), 1.18 – 1.07 (m, 2H, H-7b and 11b), 0.98 (t, 3H, H-12, $J=7.3\text{Hz}$) 0.60 (m, 2H, 8 and 10), 0.52 (m, 1H, H-9a), -0.38 (m, 1H, H-9b)

$^{13}\text{C-NMR}$ (CDCl_3 , 175 MHz) δ : 62.07 (C-1), 31.79 (C-2), 29.12, 28.58, 28.46, 27.56, 24.72, 20.90, 16.67, 14.90, 13.45 (C-12), 9.66 (C-9)

IR (cm⁻¹): 3319 (O-H stretch)

HRMS: *m/z* calculated for C₁₂H₂₄ONa = 207.1719 [M+Na]⁺; Found 207.1717

7-(2-Ethylcyclopropyl)-(E)-heptan-1-ol E-126



To a solution of 1-(*t*-butyldimethylsilyl)-oxy-undec-8-(*E*)-ene (485 mg, 1.71 mmol) in CH₂Cl₂ (30 ml), cooled to -20°C under argon in the dark, was added 1M diethyl zinc (8.53 ml, 8.53 mmol). Diiodomethane (0.68 ml, 8.53 mmol) was added dropwise and the reaction allowed to warm to RT over 24 hours. Once GC-MS indicated the complete consumption of the starting material, 2.35M NaOH (6 ml) was cautiously added and the resulting white solid removed by filtration. The combined organics were dried (MgSO₄) and concentrated under vacuum.

To a solution of this crude product in THF (10 ml), cooled to 0°C, was added tetrabutylammonium fluoride (1.08 g, 3.42 mmol) and stirred for 5 hours. The majority of the THF was removed under vacuum before the residual was loaded onto silica gel. This was eluted with 15% EtOAc in pet ether to give 7-(2-ethylcyclopropyl)-(E)-heptan-1-ol (181 mg, 58% yield) as a colourless oil.

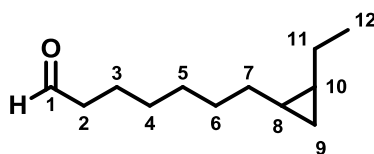
¹H-NMR (CDCl₃, 700 MHz) δ: 3.57 (t, 2H, H-1, J=6.5Hz), 1.50 (m, 2H, H-2), 1.30 – 1.24 (m, 8H, H-3 to 6), 1.18 (m, 2H, H-7a and 11a), 1.09 (m, 1H, H-11b), 1.03 (m, 1H, H-7b), 0.87 (t, 3H, H-12, J=7.3Hz), 0.32 – 0.26 (m, 2H, H-8 and 10), 0.08 (m, 2H, H-9)

¹³C-NMR (CDCl₃, 175 MHz) δ: 63.11 (C-1), 34.29 (C-7), 32.81 (C-2), 29.62, 29.47, 29.44, 27.31 (C-11), 25.74, 20.64 (C-10), 18.52 (C-8), 13.78 (C-12), 11.56 (C-9)

IR (cm⁻¹): 3320 (O-H stretch)

HRMS: *m/z* calculated for C₁₂H₂₄ONa = 207.1719 [M+Na]⁺; Found 207.1718

7-(2-Ethylcyclopropyl)-(Z)-heptanal



Following the general Swern procedure, the crude material was purified on silica gel (5% EtOAc in pet ether) to give 7-(2-ethylcyclopropyl)-(Z)-heptanal (693 mg, 87% yield) as a colourless oil.

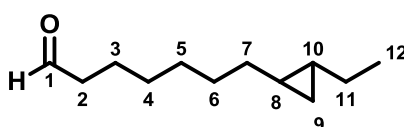
$^1\text{H-NMR}$ (CDCl_3 , 400 MHz) δ : 9.70 (t, $J=1.9\text{Hz}$, 1H, H-1), 2.35 (td, 2H, H-2, $J_1=7.2\text{Hz}$, $J_2=1.9\text{Hz}$), 1.57 (m, 2H, H-3), 1.34 – 1.27 (m, 8H, H-4 to 7a and 11b), 1.20 – 1.07 (m, 2H, 7b and 11b), 0.91 (t, 3H, H-12, $J=7.3\text{Hz}$), 0.57 (m, 2H, H-8 and 10), 0.52 (m, 1H, H-9a), -0.40 (m, 1H, H-9b)

$^{13}\text{C-NMR}$ (CDCl_3 , 100 MHz) δ : 203.04 (C-1), 43.95 (C-2), 30.00, 29.36, 29.23, 28.28, 22.12, 21.94, 17.69, 15.88, 14.49 (C-12), 10.71 (C-9)

IR (cm^{-1}): 2713 (C(O)-H stretch), 1725 (C=O stretch)

HRMS: m/z calculated for $\text{C}_{12}\text{H}_{22}\text{ONa}$ = 205.1563 ; Found 205.1563

7-(2-Ethylcyclopropyl)-(E)-heptanal



Following the general Swern procedure, the crude material was purified on silica gel (5% EtOAc in pet ether) to give 7-(2-ethylcyclopropyl)-(E)-heptanal (300 mg, 70% yield) as a pale yellow oil.

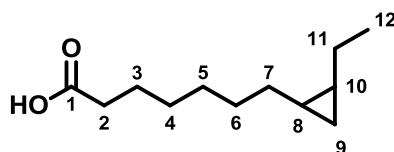
$^1\text{H-NMR}$ (CDCl_3 , 400 MHz) δ : 9.62 (t, 1H, H-1, $J=1.8\text{Hz}$), 2.27 (td, 2H, H-2, $J_1=7.4\text{Hz}$, $J_2=1.8\text{Hz}$), 1.49 (m, 2H, H-3), 1.19 (m, 6H, H-4, 5 and 6), 1.11 (m, 2H, 7a and 11a), 0.99 (m, 2H, H-7b and 11b), 0.79 (t, 3H, H-12, $J=7.4\text{Hz}$), 0.20 (m, 2H, H-8 and 10), 0.00 (m, 2H, H-9)

$^{13}\text{C-NMR}$ (CDCl_3 , 100 MHz) δ : 202.96 (C-1), 43.93 (C-2), 34.22, 29.48, 29.22, 29.19, 27.31, 22.10, 20.66, 18.52, 13.78 (C-12), 11.58 (C-9)

IR (cm^{-1}): 2710 (CO-H stretch), 1725 (C=O stretch)

HRMS: m/z calculated for $\text{C}_{12}\text{H}_{23}\text{O}$ = 183.1743, $[\text{M}+\text{H}]^+$; Found 183.1749

7-(2-Ethylcyclopropyl)-(Z)-heptanoic acid Z-127



Following the general Oxone procedure gave 7-(2-ethylcyclopropyl)-(Z)-heptanoic acid (632 mg, 91% yield) was a colourless oil.

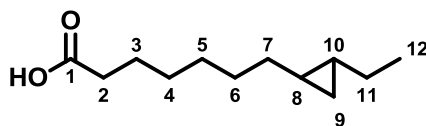
$^1\text{H-NMR}$ (CDCl_3 , 400 MHz) δ : 2.28 (t, 2H, H-2, $J=7.6\text{Hz}$), 1.57 (m, 2H, H-3), 1.34 – 1.28 (m, 8H, H-4, 5, 6, 7a and 11a), 1.19 – 1.07 (m, 2H, H-7b and 11b), 0.91 (t, 3H, H-12, $J=7.6\text{Hz}$), 0.56 – 0.49 (m, 3H, H-8, 9a and 10), -0.40 (m, 1H, H-9b)

$^{13}\text{C-NMR}$ (CDCl_3 , 100 MHz) δ : 179.48 (C-1), 33.95, 29.98, 29.23, 21.93, 29.11 (C-11), 28.52 (C-7), 17.69, 15.88, 24.70 (C-2), 14.48 (C-12), 10.70 (C-9)

IR (cm^{-1}): 1706 (C=O stretch)

HRMS: m/z calculated for $\text{C}_{12}\text{H}_{21}\text{O}$ = 197.1547 $[\text{M}-\text{H}]^-$; Found 197.1552

7-(2-Ethylcyclopropyl)-(E)-heptanoic acid E-127



Following the general Oxone procedure gave 7-(2-ethylcyclopropyl)-(E)-heptanoic acid (310 mg, 95% yield) as a colourless oil.

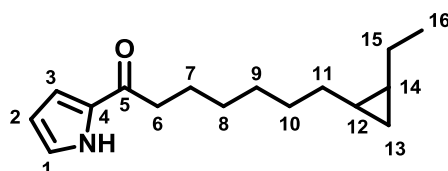
$^1\text{H-NMR}$ (CDCl_3 , 400 MHz) δ : 2.21 (t, 2H, H-2, $J=7.6\text{Hz}$), 1.50 (m, 2H, H-3), 1.19 (m, 6H, H-4 to 6), 1.09 (m, 2H, H-7a and 11a), 1.04 – 0.93 (m, 2H, H-7b to 11b), 0.79 (t, , 3H, H-12 $J=7.6\text{Hz}$), 0.20 (m, 2H, H-8 and 10), 0.00 (m, 2H, H-9)

$^{13}\text{C-NMR}$ (CDCl_3 , 100 MHz) δ : 179.59 (C-1), 34.23, 29.48, 29.11, 29.08, 27.31, 24.70, 20.65, 18.55, 13.79 (C-12), 11.58 (C-9). 1 signal missing.

IR (cm^{-1}): 1707 (C=O stretch)

HRMS: m/z calculated for $\text{C}_{12}\text{H}_{22}\text{ONa}$ = 221.1512 $[\text{M}+\text{Na}]^+$; Found 221.1513

7-(2-(Z)-Ethylcyclopropyl)-1-(pyrrol-2-yl)heptan-1-one Z-128



Following the general carboxylic acid coupling procedure, the crude product was purified on silica gel (10% EtOAc in pet ether) to give 7-(2-(Z)-ethylcyclopropyl)-1-(pyrrol-2-yl)heptan-1-one (548 mg, 69% yield) as a pale yellow oil.

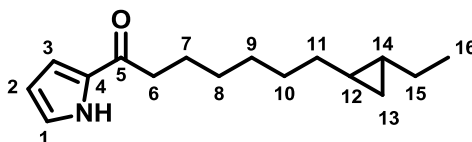
$^1\text{H-NMR}$ (CDCl_3 , 400 MHz) δ : 9.29 (bs, 1H, N-H), 6.94 (m, 1H, H-1), 6.83 (m, 1H, H-3), 6.20 (m, 1H, H-2), 2.96 (t, 2H, H-6, $J=7.8\text{Hz}$), 1.65 (m, 2H, H-7), 1.30 (m, 8H, H-8, 9, 10, 11a and 15a), 1.12 (m, 2H, H-11b and 15b), 0.90 (t, 3H, H-16, $J=7.1\text{Hz}$), 0.58 (m, 2H, H-12 and 14), 0.50 (m, 1H, H-13a), -0.40 (m, 1H, 13b)

$^{13}\text{C-NMR}$ (CDCl_3 , 100 MHz) δ : 191.10 (C-5), 132.30 (C-4), 124.14 (C-3), 115.82 (C-1), 110.56 (C-2), 38.05 (C-6), 30.06, 29.53, 29.45, 28.56, 25.31 (C-7), 21.93 14.48 (C-16), 10.70 (C-13), 17.70, 15.91

IR (cm^{-1}): 3271 (N-H stretch), 1635 (C=O stretch)

HRMS: m/z calculated for $\text{C}_{16}\text{H}_{25}\text{NO}$ = 248.2009 $[\text{M}+\text{H}]^+$ and $\text{C}_{16}\text{H}_{25}\text{NONa}$ = 270.1828 $[\text{M}+\text{Na}]^+$; Found 248.2007 and 270.1825

7-(2-(E)-Ethylcyclopropyl)-1-(pyrrol-2-yl)heptan-1-one E-128



Following the general carboxylic acid coupling procedure, the crude product was purified on silica gel (10% EtOAc in pet ether) to give 7-(2-(E)-ethylcyclopropyl)-1-(pyrrol-2-yl)heptan-1-one (169 mg, 44% yield) as a colourless oil.

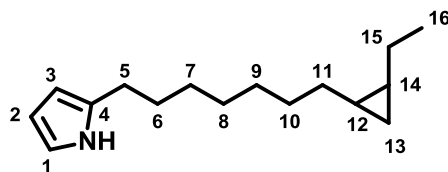
$^1\text{H-NMR}$ (CDCl_3 , 400 MHz) δ : 9.26 (bs, 1H, N-H), 6.94 (m, 1H, H-1), 6.83 (m, 1H, H-3), 6.20 (m, 1H, H-2), 2.68 (t, 2H, H-6, $J=7.8\text{Hz}$), 1.65 (m, 2H, H-7), 1.28 (m, 6H, H-6 to 8), 1.21 – 1.01 (m, 4H, H-11 and 15), 0.86 (t, 3H, H-16, $J=7.3\text{Hz}$), 0.27 (m, 2H, H-12 and 14), 0.07 (m, 2H, H-13)

$^{13}\text{C-NMR}$ (CDCl_3 , 100 MHz) δ : 192.20 (C-5), 128.47 (C-4), 124.14 (C-1), 115.82 (C-3), 110.56 (C-2), 38.06 (C-6), 30.04, 29.50, 29.47, 28.56, 25.30 (C-7), 21.90, 20.66, 18.56, 13.80 (C-16), 11.58 (C-13)

IR (cm^{-1}): 3270 (N-H stretch), 1630 (C=O stretch)

HRMS: m/z calculated for $\text{C}_{16}\text{H}_{25}\text{NO}$ = 248.2009 [$\text{M}+\text{H}$] $^+$; Found 248.2007

2-[7-(2-(Z)-Ethylcyclopropyl)heptyl]-pyrrole Z-118



Following the general acyl ketone reduction procedure, the crude product was purified on silica gel (3% EtOAc in pet ether) to give 2-[7-(2-(Z)-ethylcyclopropyl)heptyl]-pyrrole (415 mg, 60% yield) as a purple oil.

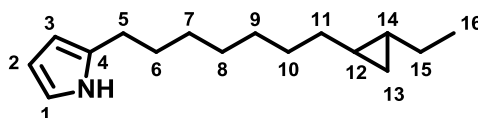
$^1\text{H-NMR}$ (CDCl_3 , 700 MHz) δ : 7.90 (bs, 1H, N-H), 6.67 (m, 1H, H-1), 6.14 (m, 1H, H-2), 5.92 (m, 1H, H-3), 2.61 (t, 2H, H-5, $J=7.7\text{Hz}$), 1.64 (m, 2H, H-6), 1.41 – 1.32 (m, 10H, H-7 to 10, 11a and 15a), 1.24 – 1.14 (m, 2H, H-11b and 15b), 0.99 (t, 3H, H-16, $J=7.3\text{Hz}$), 0.65 (m, 2H, H-12 and 14), 0.56 (m, 1H, H-13a), -0.31 (m, 1H, H-13b)

$^{13}\text{C-NMR}$ (CDCl_3 , 175 MHz) δ : 132.87 (C-4), 115.92 (C-1), 108.24 (C-2), 104.84 (C-3), 30.18, 29.66, 29.55, 29.47, 29.38, 28.57, 27.73 (C-5), 21.91 (C-15), 17.69, 15.91, 14.45 (C-16), 10.68 (C-13)

IR (cm^{-1}): 3380 (N-H stretch)

HRMS : m/z calculated for and $\text{C}_{16}\text{H}_{27}\text{N}$ = 234.2216 $[\text{M}+\text{H}]^+$; Found 234.2216

2-[7-(2-(E)-Ethylcyclopropyl)heptyl]-pyrrole E-118



Following the general acyl ketone reduction procedure, the crude product was purified on silica gel (3% EtOAc in pet ether) to give 2-[7-(2-(E)-ethylcyclopropyl)heptyl]-pyrrole (103 mg, 65% yield) as a colourless oil.

$^1\text{H-NMR}$ (CDCl_3 , 700 MHz) δ : 7.91 (bs, 1H, N-H), 6.68 (m, 1H, H-1), 6.14 (m, 1H, H-2), 6.14 (m, 1H, H-3), 2.61 (t, 3H, H-5, $J=7.6\text{Hz}$), 1.64 (m, 2H, H-6), 1.43 – 1.22 (m, 10H, H-7 to 10, 11a and 15a), 1.18 (m, 1H, H-15b), 1.11 (m, 1H, H-11b), 0.95 (t, 3H, H-16, $J=7.4\text{Hz}$), 0.38 (m, 2H, H-12 and 14), 0.16 (m, 2H, H-13)

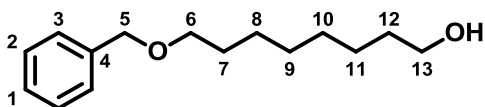
$^{13}\text{C-NMR}$ (CDCl_3 , 175 MHz) δ : 132.89 (C-4), 115.94 (C-1), 108.24 (C-2), 104.84 (C-3), 34.31 (C-11), 29.68, 29.57, 29.49, 29.42, 29.40, 27.74 (C-5), 27.33 (C-15), 20.65, 18.58, 13.80 (C-16), 11.57 (C-13)

IR (cm^{-1}): 3376 (N-H stretch)

HRMS : m/z calculated for and $\text{C}_{16}\text{H}_{27}\text{N}$ = 234.2216 $[\text{M}+\text{H}]^+$; Found 234.2213

6.1.4 Synthesis of branched methyl containing 2-UP analogues

8-Benzyloxyoctan-1-ol 154⁷⁵



To a solution of octan-1,8-diol (3.00 g, 20.52 mmol) in CH₂Cl₂ (30 ml), under argon, was added silver (I) oxide (7.13 g, 30.78 mmol) and the resulting suspension stirred for 20 mins. Benzyl bromide (0.90 ml, 7.52 mmol) was added and the reaction mixture stirred for 16 hours. The reaction mixture was filtered and concentrated under vacuum. The crude product was purified on silica gel (35% EtOAc in pet ether) to give 8-benzyloxyoctan-1-ol (3.61 g, 74% yield) as a colourless oil.

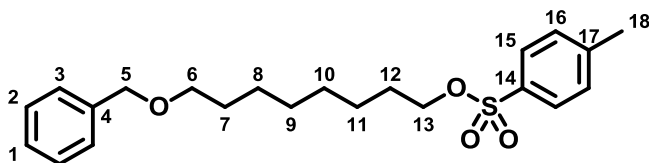
¹H-NMR (CDCl₃, 400 MHz) δ : 7.26 – 7.21 (m, 5H, H-1, 2 and 3), 4.43 (s, 2H, H-5), 3.56 (t, 2H, H-13, J=6.6Hz), 3.39 (t, 2H, H-6, J=6.6Hz), 1.58 – 1.45 (m, 4H, H-7 and 12), 1.31 – 1.25 (m, 8H, H-8 to 11)

¹³C-NMR (CDCl₃, 100 MHz) δ : 138.71 (C-4), 128.35, 127.64, 127.49, 72.88 (C-5), 70.49 (C-6), 63.05 (C-13), 32.78 (C-12), 29.75 (C-7), 29.43, 29.36, 26.14, 25.68

IR (cm⁻¹): 3290 (H-O stretch)

HRMS: m/z calculated for and C₁₅H₂₄O₂Na = 259.1669 [M+Na]⁺; Found 259.1676

8-Benzyloxyoctyl 4-methylbenzenesulfonate



To a solution of 8-benzyloxyoctan-1-ol (1.00 g, 4.23 mmol), 4-dimethylaminopyridine (155 mg, 1.27 mmol) and triethylamine (1.29 ml, 10.58 mmol) in CH₂Cl₂ (15 ml), under argon, was added *p*-toluenesulfonyl chloride and the resulting mixture was stirred for 24 hours. CH₂Cl₂ was added to dilute the reaction mixture and was washed with 2M HCl, sat NaHCO₃, dried (MgSO₄) and concentrated under vacuum. The crude product was purified on silica gel (15%

EtOAc in pet ether) to give 8-benzyloxyoctyl 4-methylbenzenesulfonate (1.40 g, 85% yield) as a colourless oil.

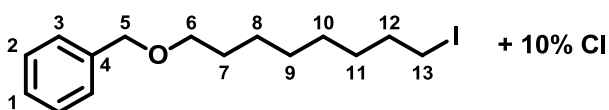
$^1\text{H-NMR}$ (CDCl_3 , 400 MHz) δ : 7.71 (m, 2H, H-15), 7.27 – 7.20 (m, 7H, H-1 to 3 and 16), 4.42 (s, 2H, H-5), 3.94 (t, 2H, H-13, $J=6.6\text{Hz}$), 3.37 (t, 2H, H-6, $J=6.4\text{Hz}$), 2.37 (s, 3H, H-18), 1.59 – 1.47 (m, 4H, H-7 and 12), 1.28 – 1.15 (m, 8H, H-8 to 11)

$^{13}\text{C-NMR}$ (CDCl_3 , 100 MHz) δ : 144.63 (C-17), 138.68 (C-4), 133.26 (C-14), 129.81 (C-16), 128.36, 127.90, 127.64, 127.50, 72.89 (C-5), 70.67 (C-13), 70.41 (C-6), 29.71, 29.21, 28.87, 28.80, 26.06, 25.28, 21.69 (C-18)

IR (cm^{-1}): 1357 (S=O stretch)

HRMS : m/z calculated for $\text{C}_{22}\text{H}_{30}\text{O}_4\text{S}$ = 413.1757 $[\text{M}+\text{H}]^+$; Found 413.1762

8-Benzyloxy-1-iodooctane 189



To a solution of 8-benzyloxyoctyl 4-methylbenzenesulfonate (1.40 g, 3.58 mmol) in acetone (20 ml), under argon, was added potassium iodide (11.90 g, 71.70 mmol) and the resulting suspension heated to 65 °C for 24 hours. The reaction mixture was poured into water and extracted with EtOAc. The combined organics were dried (MgSO_4) and concentrate under vacuum to give a mixture of 8-benzyloxy 1-iodooctane (1.07 g, 90% yield) and 8-benzyloxy 1-chlorooctane (79 mg, 10% yield) as a yellow/brown oil; ratio estimated by $^1\text{H-NMR}$ integration of triplets adjacent to the halogen.

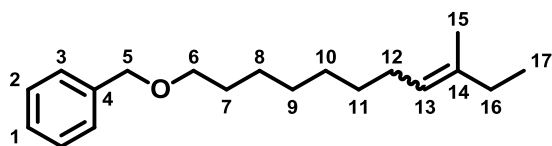
$^1\text{H-NMR}$ (CDCl_3 , 400 MHz) δ : 7.26 – 7.20 (m, 5H, H-1 to 3), 4.43 (s, 2H, H-5), 3.45 (t, 0.2H, H-13 Cl, $J=6.9\text{Hz}$), 3.39 (t, 2H, H-6, $J=6.5\text{Hz}$), 3.11 (t, 1.8H, H-13 I, $J=6.9\text{Hz}$), 1.74 (m, 2H, H-12), 1.54 (m, 2H, H-7), 1.33-1.24 (m, 8H, H-8 to 11)

$^{13}\text{C-NMR}$ (CDCl_3 , 100 MHz) δ : 138.70 (C-4), 128.37, 127.64, 127.50 (C-1 to 3), 72.89 (C-5), 70.43 (C-6), 45.34 (C-13 Cl), 33.54 (C-12), 30.45, 29.73, 29.25, 28.49, 26.12, 7.30 (C-13 I)

IR (cm⁻¹): 1098 (C-O stretch)

HRMS: *m/z* calculated for C₁₅H₂₃OI = 369.0686 [M+Na]⁺; Found 369.0686

1-Benzoyloxy-9-methylundec-8-ene 190



To a solution of 8-benzyloxy-1-iodooctane (1.03 g, 2.97 mmol) in toluene (20 ml) was added triphenyl phosphine (1.17 g, 4.46 mmol) and the resulting solution heated to 120 °C for 48 hours. The toluene was removed under vacuum before dissolving the residue in THF (40 ml) under argon. This was cooled to -78 °C before *n*-butyl lithium (2.23 ml, 3.56 mmol) was added and the bright orange solution stirred for 30 mins. Butanone (0.40 ml, 4.46 mmol) was added and stirred for a further 16 hours while warming to RT. The reaction was quenched with sat NH₄Cl and extracted with Et₂O. The combined organics were dried (MgSO₄) and concentrated under vacuum. The crude product was purified on silica gel (3% Et₂O in pet ether) to give 1-benzyloxy-9-methylundec-8-ene (600 mg*, 85% yield) as a colourless oil.

*Product co-purified with Ph₃PO so yield is based on ¹H-NMR integrals.

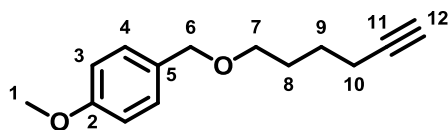
¹H-NMR (CDCl₃, 400 MHz) δ: 7.27 – 7.20 (m, H-1 to 3 plus Ph₃PO), 5.01 (m, 1H, H-13), 4.43 (s, 2H, H-5), 3.39 (t, 2H, H-6), 1.97 – 1.88 (m, 4H, H-12 and 16), 1.58 – 1.48 (m, 5H, H-7 and 15), 1.30 – 1.18 (m, 8H, H-8 to 11), 0.89 (m, 3H, H-17)

¹³C-NMR (CDCl₃, 100 MHz) δ: *

HRMS: *

* No data due to triphenylphosphine oxide impurity

1-(4-Methoxybenzyloxy)hex-5-yne 178



To a solution of 5-hexyn-1-ol (1.00 g, 10.19 mmol) in DMF (20 ml), cooled to 0 °C under argon, was added sodium hydride (240 mg, 12.23 mmol) and the suspension stirred for 30 mins. 4-Methoxybenzyl chloride (1.66 ml, 12.23 mmol) was added and the reaction mixture heated to 60 °C for 16 hours. The reaction mixture was poured into water and extracted with EtOAc. The combined organics were dried (MgSO₄) and concentrated under vacuum. The crude product was purified on silica gel (7% Et₂O in pet ether) to give 1-(4-methoxybenzyloxy)hex-5-yne (1.89 g, 95% yield) as a colourless oil.

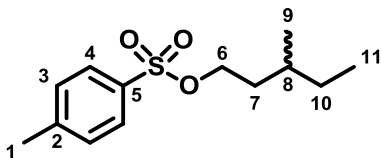
¹H-NMR (CDCl₃, 400 MHz) δ: 7.18 (d, 2H, H-4, J=8.6Hz), 6.80 (d, 2H, H-3, J=8.6Hz), 4.36 (s, 2H, H-6), 3.73 (s, 3H, H-1), 3.40 (t, 2H, H-7, J=6.2Hz), 2.14 (td, 2H, H-10, J=7.1, 2.6Hz), 1.87 (t, 1H, H-12, J=2.6Hz), 1.65 (m, 2H, H-8), 1.55 (m, 2H, H-9)

¹³C-NMR (CDCl₃, 100 MHz) δ: 159.30 (C-2), 130.68 (C-5), 129.23 (C-4), 113.78 (C-3), 84.40 (C-12), 72.55 (C-6), 69.44 (C-7), 68.37 (C-11), 55.30 (C-1), 28.78 (C-8), 25.26 (C-9), 18.23 (C-10)

IR (cm⁻¹): 3290 (C-H alkyne stretch), 2935 (C-H stretch)

HRMS: *m/z* calculated for and C₁₄H₁₈O₂Na = 241.1199 [M+Na]⁺; Found 241.1197

3-Methylpentyl *p*-toluenesulphonate



To a solution of 3-methylpentan-1-ol (2.00 g, 19.58 mmol), 4-dimethylaminopyridine (717 mg, 5.87 mmol) and triethylamine (6.73 ml, 48.95 mmol) in CH₂Cl₂ (100 ml), under argon, was added *p*-toluenesulphonyl chloride (4.11 g, 21.54 mmol) and the resulting mixture stirred for 4 hours. The reaction mixture was poured into water and extracted with CH₂Cl₂. The organics

were washed with water, 2M HCl, sat NaHCO₃, dried (MgSO₄) and concentrated under vacuum. The crude product was purified on silica gel (10% EtOAc in pet ether) to give 3-methylpentyl *p*-toluenesulphonate (4.50 g, 90% yield) as a colourless oil.

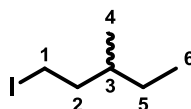
¹H-NMR (CDCl₃, 400 MHz) δ: 7.72 (d, 2H, H-4, J=8.3Hz), 7.27 (d, 2H, H-3, J=8.3Hz), 3.99 (m, 2H, H-6), 2.38 (s, 3H, H-1), 1.59 (m, 1H, H-7a), 1.37 (m, 2H, H-7b and 8), 1.20 (m, 1H, H-10a), 1.05 (m, 1H, H-10b), 0.75 (t, 3H, H-11, J=7.4Hz), 0.72 (d, 3H, H-9, J=6.3Hz)

¹³C-NMR (CDCl₃, 100 MHz) δ: 143.60 (C-5), 133.41 (C-2), 128.77 (C-3), 126.87 (C-4), 68.13 (C-6), 34.29 (C-7), 29.69 (C-8), 28.11 (C-10), 20.62 (C-1), 17.65 (C-9), 10.06 (C-11)

IR (cm⁻¹): 1358 (S=O stretch)

HRMS: *m/z* calculated for C₁₃H₂₀O₃S = 279.1025 [M+Na]⁺; Found 279.1027

1-iodo-3-methyl pentane 193

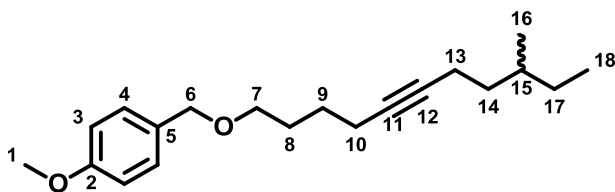


To a solution of 3-methylpentyl *p*-toluenesulphonate (2.00 g, 7.80 mmol) in acetone (40 ml) was added potassium iodide (26.00 g, 156 mmol) and the reaction heated to 60 °C for 48 hours. The reaction mixture was poured into water and extracted with Et₂O. The combined organics were washed with sat NaHCO₃, dried (MgSO₄) and concentrated under vacuum to give 1-iodo-3-methyl pentane (1.40 g, 100% yield) as a colourless oil.

¹H-NMR (CDCl₃, 400 MHz) δ: 3.21 – 3.07 (m, 2H, H-1), 1.81 (m, 1H, H-2a), 1.58 (m, 1H, H-2b), 1.42 (m, 1H, H-3), 1.28 (m, 1H, H-5a), 1.11 (m, 1H, H-5b), 0.83 – 0.79 (m, 6H, H-4 and 6)

¹³C-NMR (CDCl₃, 100 MHz) δ: 39.54 (C-2), 34.41 (C-3), 27.71 (C-5), 17.22 (C-4), 10.13 (C-6), 4.34 (C-1)

1-(4-Methoxybenzyloxy)-9-methyl-undec-5-yne 194



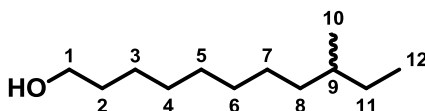
To a solution of 1-(4-methoxybenzyloxy)hex-5-yne (2.65 g, 12.16 mmol) in THF (40 ml), cooled to $-78\text{ }^{\circ}\text{C}$ under argon, was added *n*-butyl lithium (8.62 ml, 13.97 mmol) and the solution stirred for 15 mins. 1-Iodo-3-methyl pentane (1.72 g, 8.11 mmol) in THF (20 ml) was added and the reaction heated to $75\text{ }^{\circ}\text{C}$ to 48 hours. The reaction mixture was poured into water and extracted with EtOAc. The combined organics were dried (MgSO_4) and concentrated under vacuum. The crude product was purified on silica gel (3% EtOAc in pet ether) to give 1-(4-methoxybenzyloxy)-9-methyl-undec-5-yne (1.35 g, 75% yield) as a colourless oil.

$^1\text{H-NMR}$ (CDCl_3 , 400 MHz) δ : 7.20 (d, 2H, H-3, $J=8.4\text{Hz}$), 6.81 (d, 2H, H-4, $J=8.2\text{Hz}$), 4.36 (s, 2H, H-6), 3.73 (s, 3H, H-1), 3.39 (t, 2H, H-7, $J=6.4\text{Hz}$), 2.11 – 2.03 (m, 4H, H-10 and 13), 1.63 (m, 2H, H-8), 1.52 – 1.03 (m, 7H, H-9, 14, 15 and 17), 0.79 (m, 6H, H-16 and 18)

$^{13}\text{C-NMR}$ (CDCl_3 , 100 MHz) δ : 159.41 (C-2), 130.76 (C-5), 129.21 (C-3), 113.77 (C-4), 72.51 (C-6), 69.66 (C-7), 55.29 (C-1), 35.92, 33.60, 29.11, 28.89, 25.85, 18.59 (C-16), 16.54 (C-8), 11.32 (C-18). 3 signals missing.

HRMS: m/z calculated for $\text{C}_{20}\text{H}_{30}\text{O}_2\text{Na} = 325.2138$ $[\text{M}+\text{Na}]^+$; Found 325.2137

9-Methylundecan-1-ol 191



From 1-benzyloxy-9-methylundec-8-ene: To a solution of naphthalene (1.68 g, 13.14 mmol) in THF (13 ml), under argon, was added lithium (76 mg, 10.95 mmol) and the resulting mixture sonicated for 60 sec until a dark green solution appeared. This was stirred for a further 4 hours before 1-benzyloxy-9-methylundec-8-ene (600 mg, 2.19 mmol) in THF (7 ml) was added and heated to $50\text{ }^{\circ}\text{C}$ for 48 hours. Sat NH_4Cl solution was cautiously added and

extracted with EtOAc. The combined organics were washed with brine, dried (MgSO_4) and concentrated under vacuum. The crude product was purified on silica gel (15% EtOAc in pet ether).

The purified material from the previous step was dissolved in THF (7 ml) before 10% palladium on carbon (50 mg) was added and flushed with hydrogen gas ten times. The resulting mixture was allowed to stir for 16 hours before being filtered through celite and concentrated under vacuum to give 9-methylundecan-1-ol (393 mg, 96% yield) as a colourless oil.

From 1-(4-methoxybenzyloxy)-9-methyl-undec-5-yne: To a solution of 1-(4-methoxybenzyloxy)-9-methyl-undec-5-yne (1.35 g, 4.47 mmol) in THF (40 ml) was added 10% palladium on carbon (70 mg) and the flask flushed with hydrogen gas ten times and stirred for 24 hours. The reaction mixture was filtered through celite and concentrated under vacuum. The crude product was purified on silica gel (10% EtOAc in pet ether) to give 9-methylundecan-1-ol (591 mg, 71% yield) as a colourless oil.

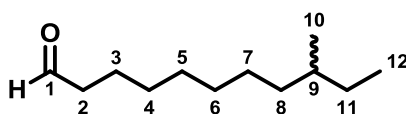
$^1\text{H-NMR}$ (CDCl_3 , 400 MHz) δ : 3.57 (t, 2H, H-1, $J=6.7\text{Hz}$), 1.50 (m, 2H, H-2), 1.29 – 1.14 (m, 13H, H-3 to 7, 8a, 9 and 11a), 1.08 – 0.99 (m, 2H, H-8b and 11b), 0.81 – 0.77 (m, 6H, H-10 and 12)

$^{13}\text{C-NMR}$ (CDCl_3 , 100 MHz) δ : 63.13 (C-1), 36.63, 34.41 (C-9), 32.83 (C-2), 29.95, 29.66, 29.51, 29.46, 27.09, 25.76, 19.23 (C-10), 11.42 (C-12)

IR (cm^{-1}): 3349 (H-O stretch)

HRMS : m/z calculated for and $\text{C}_{12}\text{H}_{26}\text{ONa} = 209.1876$ $[\text{M}+\text{Na}]^+$; Found 209.1873

9-Methylundecanal



Following the general IBX procedure, the crude product was purified on silica gel (10% EtOAc in pet ether) to give 9-methylundecanal (437 mg, 73% yield) as a colourless oil.

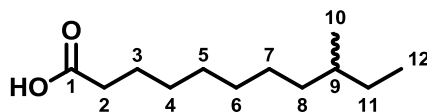
$^1\text{H-NMR}$ (CDCl_3 , 400 MHz) δ : 9.70 (t, 1H, H-1, $J=1.9\text{Hz}$), 2.35 (td, 2H, H-2, $J_1=7.3\text{Hz}$, $J_2=1.9\text{Hz}$), 1.56 (m, 2H, H-3), 1.30 – 1.15 (m, 10H, H-4 to 7, 8a, 9 and 11a), 1.08 – 0.99 (m, 2H, H-8b and 11b), 0.78 (m, 6H, H-10 and 12)

$^{13}\text{C-NMR}$ (CDCl_3 , 100 MHz) δ : 202.99 (C-1), 43.94 (C-2), 36.59, 34.39 (C-9), 29.78, 29.49, 29.41, 29.19, 27.01, 19.22 (C-10), 11.42 (C-12). 1 signal missing.

IR (cm^{-1}): 2712 (OC-H stretch), 1725 (C=O stretch)

HRMS : m/z calculated for and $\text{C}_{12}\text{H}_{24}\text{ONa} = 207.1717$ $[\text{M}+\text{Na}]^+$; Found 207.1715

9-Methylundecanoic acid 188



Following the general procedure gave 9-methylundecanoic acid (468 mg, 99% yield) as a pale yellow oil.

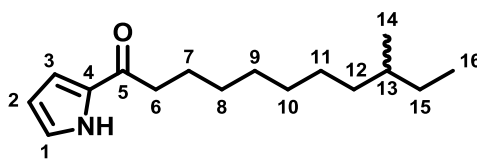
$^1\text{H-NMR}$ (CDCl_3 , 400 MHz) δ : 2.28 (t, 2H, H-2, $J=7.5\text{Hz}$), 1.57 (m, 2H, H-3), 1.28 – 1.15 (m, 11H, H-4 to 8a, 9 and 11a), 1.10 – 0.99 (m, 2H, H-8b and 11b), 0.80 – 0.76 (m, 6H, H-10 and 12)

$^{13}\text{C-NMR}$ (CDCl_3 , 100 MHz) δ : 179.14 (C-1), 36.59, 34.39 (C-9), 33.80 (C-2), 29.78, 29.50, 29.28, 29.07, 27.02, 24.70 (C-3), 19.22 (C-10), 11.42 (C-12)

IR (cm^{-1}): 1706 (C=O stretch)

HRMS : m/z calculated for and $\text{C}_{12}\text{H}_{24}\text{O}_2\text{Na} = 223.1666$ $[\text{M}+\text{Na}]^+$; Found 223.1669

9-Methyl-1-(1H-pyrrol-2-yl)undecan-1-one



Following the general carboxylic acid coupling procedure, the crude product was purified on silica gel (7% EtOAc in pet ether) to give 9-methyl-1-(1H-pyrrol-2-yl)undecan-1-one (485 mg, 83% yield) as a pale yellow oil.

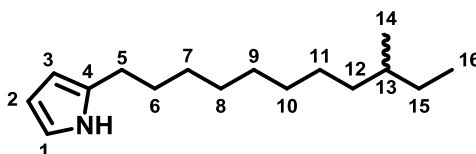
$^1\text{H-NMR}$ (CDCl_3 , 400 MHz) δ : 9.30 (bs, 1H, H-N), 6.94 (m, 1H, H-1), 6.83 (m, 1H, H-3), 6.12 (m, 1H, H-2), 2.68 (t, 2H, H-6, $J=7.2\text{Hz}$), 1.65 (m, 2H, H-7), 1.27 – 1.19 (m, 11H, H-8 to 12a, 13 and 15a), 1.08 – 0.98 (m, 2H, H-12b and 15b), 0.80 – 0.76 (m, 6H, H-14 and 16)

$^{13}\text{C-NMR}$ (CDCl_3 , 100 MHz) δ : 191.16 (C-5), 132.00 (C-4), 124.16 (C-3), 115.83 (C-1), 110.55 (C-2), 38.06 (C-6), 36.61, 34.39 (C-13), 29.85, 29.50, 27.06, 25.31 (C-7), 19.22 (C-14), 11.42 (C-16). 2 signals missing.

IR (cm^{-1}): 3277 (N-H stretch), 1634 (C=O stretch)

HRMS : m/z calculated for $\text{C}_{16}\text{H}_{27}\text{NONa}$ = 272.1985 $[\text{M}+\text{Na}]^+$; Found 272.1994

2-(9-Methylundecyl)-1H-pyrrole 185



Following the general acyl ketone reduction, the crude product was purified on silica gel (5% EtOAc in pet ether) to give 2-(9-methylundecyl)-1H-pyrrole (298 mg, 66% yield) as a colourless oil.

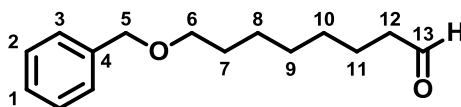
$^1\text{H-NMR}$ (CDCl_3 , 400 MHz) δ : 7.82 (bs, 1H, N-H), 6.59 (m, 1H, H-1), 6.06 (m, 1H, H-2), 5.84 (m, 1H, H-3), 2.52 (t, 2H, H-5, $J=7.5\text{Hz}$), 1.55 (m, 2H, H-6), 1.29 – 1.12 (m, 13H, H-7 to 11, 12a, 13 and 15a), 1.08 – 1.01 (m, 2H, H-12b and 15b), 0.80 – 0.76 (m, 6H, H-14 and 16)

$^{13}\text{C-NMR}$ (CDCl_3 , 100 MHz) δ : 132.77 (C-4), 115.95 (C-1), 108.26 (C-2), 104.86 (C-3), 36.63, 34.42 (C-13), 30.01, 29.69, 29.64, 29.52, 29.48, 29.42, 27.76 (C-5), 27.10, 19.24 (C-14), 11.43 (C-16)

IR (cm^{-1}): 3383 (N-H stretch)

HRMS : m/z calculated for and $\text{C}_{16}\text{H}_{29}\text{N}$ = 236.2373 $[\text{M}+\text{H}]^+$; Found 236.2369

8-Benzyloxyoctanal 155



Following the general Swern oxidation procedure, the crude product was purified on silica gel (15% Et_2O in pentane) to give 8-benzyloxyoctanal (910 mg, 81% yield) as a colourless oil.

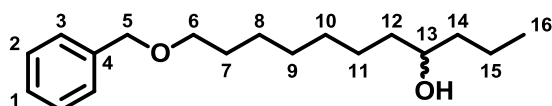
$^1\text{H-NMR}$ (CDCl_3 , 400 MHz) δ : 9.69 (t, 1H, H-13, $J=1.9\text{Hz}$), 7.27 – 7.18 (m, 5H, H-1 to 3), 4.43 (s, 2H, H-5), 3.39 (t, 2H, H-6, $J=6.6\text{Hz}$), 2.34 (td, 2H, H-12, $J_1=7.4\text{Hz}$, $J_2=1.9\text{Hz}$), 1.59 – 1.50 (m, 4H, H-7 and 11), 1.34 – 1.24 (m, 6H, H-8 to 10)

$^{13}\text{C-NMR}$ (CDCl_3 , 100 MHz) δ : 202.87 (C-13), 138.68 (C-4), 128.36, 127.64, 127.50, 72.90 (C-5), 70.38 (C-6), 43.89 (C-12), 29.69 (C-7), 29.19 (C-8), 29.10 (C-10), 26.01 (C-9), 22.02 (C-11)

IR (cm^{-1}): 2717 (OC-H stretch), 1722 (C=O stretch), 1621 and 1453 (benzene), 1097 (C-O stretch)

HRMS : m/z calculated for and $\text{C}_{15}\text{H}_{22}\text{O}_2\text{Na}$ = 257.1512 $[\text{M}+\text{Na}]^+$; Found 257.1513

11-Benzyloxyundecan-4-ol 151



To a solution of 8-benzyloxyoctanal (3.19 g, 13.62 mmol) in THF (100 ml), cooled to $-78\text{ }^\circ\text{C}$ under argon, was added dropwise propylmagnesium chloride solution (10.22 ml 2M solution).

The resulting solution was allowed to warm to RT over 16 hours before water was cautiously

added and extracted with EtOAc. The combined organics were dried (MgSO_4) and concentrated under vacuum. The crude product was purified on silica gel (20% EtOAc in pet ether) to give 11-benzyloxyundecan-4-ol (3.46 g, 91% yield) as a colourless oil.

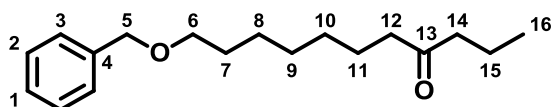
$^1\text{H-NMR}$ (CDCl_3 , 400 MHz) δ : 7.26 – 7.21 (m, 5H, H-1 to 3), 4.43 (s, 2H, H-5), 3.52 (m, 1H, H-13), 3.39 (t, 2H, H-6, $J=6.6\text{Hz}$), 1.54 (m, 2H, H-7), 1.39 – 1.19 (m, 14H, H-8 to 12 and 14 to 15), 0.86 (t, 3H, H-16, $J=7.1\text{Hz}$)

$^{13}\text{C-NMR}$ (CDCl_3 , 100 MHz) δ : 138.72 (C-4), 128.35, 127.63, 127.48, 72.88 (C-5), 71.72 (C-13), 70.50 (C-6), 39.69, 37.49, 29.76, 29.65, 29.46, 26.16, 25.60, 18.85, 14.15 (C-16)

IR (cm^{-1}): 3342 (H-O stretch)

HRMS: m/z calculated for and $\text{C}_{18}\text{H}_{30}\text{O}_2\text{Na} = 301.2138$ [$\text{M}+\text{Na}$] $^+$; Found 301.2140

11-Benzyloxyundecan-4-one 152



Following the general Swern procedure, the crude product was purified on silica gel (7% EtOAc in pet ether) to give 11-benzyloxyundecan-4-one (761 mg, 82% yield) as a colourless oil.

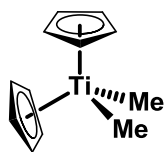
$^1\text{H-NMR}$ (CDCl_3 , 400 MHz) δ : 7.27 – 7.20 (m, 5H, H-1 to 3), 4.43 (s, 2H, H-5), 3.39 (t, 2H, H-6, $J=6.6\text{Hz}$), 2.29 (m, 4H, H-12 and 14), 1.57 – 1.45 (m, 6H, H-7, 11 and 15), 1.31 – 1.17 (m, 6H, H-8 to 10), 0.84 (t, 3H, H-16, $J=7.4\text{Hz}$)

$^{13}\text{C-NMR}$ (CDCl_3 , 100 MHz) δ : 210.14 (C-13), 138.73 (C-4), 128.35, 127.48, 127.48, 72.88 (C-5), 70.44 (C-6), 44.73, 42.81, 29.71, 29.29, 29.21, 26.05, 23.80, 17.32, 13.79 (C-16)

IR (cm^{-1}): 1709 (C=O stretch)

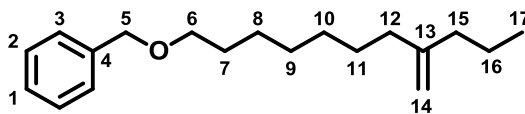
HRMS: m/z calculated for and $\text{C}_{18}\text{H}_{28}\text{O}_2\text{Na} = 299.1982$ [$\text{M}+\text{Na}$] $^+$; Found 299.1980

Dimethyl titanocene¹²⁶



To a suspension of titanocene dichloride (5.00 g, 20.08 mmol) in toluene (100 ml), cooled to 0 °C under argon, was added methylmagnesium chloride (14.7 ml 3M solution) dropwise over 30 mins. This was stirred for a further 10 mins before ¹H-NMR showed the reaction was complete. 6% NH₄Cl solution was added dropwise and the aqueous layer extracted with EtOAc. The combined organics were washed with water and dried (MgSO₄). The remaining solution was concentrated to approximately 30 ml to give a bright orange solution (4.09 g, 98% yield, ~0.5M in toluene and THF).

4-Methylene-11-benzyloxyundecane¹²⁷



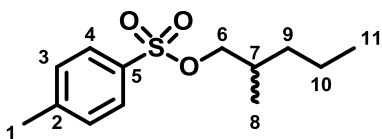
To a solution of 11-benzyloxyundecan-4-one (855 mg, 3.10 mmol) and titanocene dichloride (40 mg, 0.16 mmol) in THF (15 ml), under argon, was added dimethyl titanocene (15.5 ml ~0.5M solution) and heated to 85 °C for 72 hours. The THF was removed under vacuum before 5% EtOAc in pet ether (100 ml) was added and the precipitate filtered. This was concentrated under vacuum before being purified on silica gel (2% EtOAc in pet ether) to give 4-methylene-11-benzyloxyundecane (646 mg, 76% yield) as a yellow oil.

¹H-NMR (CDCl₃, 400 MHz) δ: 7.26 – 7.20 (m, 5H, H-1 to 3), 4.62 (m, 2H, H-14), 4.43 (s, 2H, H-5), 3.39 (t, 2H, H-6, J=6.6Hz), 1.91 (m, 4H, H-12 and 15), 1.55 (m, 2H, H-7), 1.12 – 1.19 (m, 10H, H-8 to 11 and 16), 0.83 (t, 3H, H-17, J=7.2Hz)

¹³C-NMR (CDCl₃, 100 MHz) δ: 150.10 (C-13), 138.74 (C-4), 128.35, 127.47, 127.47, 72.88 (C-5), 70.52 (C-6), 38.23, 36.03, 29.78, 29.40, 27.77, 26.19, 20.19, 13.91 (C-17). 2 signals missing.

HRMS: m/z calculated for and $C_{19}H_{30}ONa = 297.2189 [M+Na]^+$; Found 297.2193

2-Methylpentyl *p*-toluenesulphonate



To a solution of 2-methylpentan-1-ol (2.00 g, 19.58 mmol), 4-dimethylaminopyridine (717 mg, 5.87 mmol) and triethyl amine (6.73 ml, 48.95 mmol) in CH_2Cl_2 (100 ml) was added *p*-toluenesulphonyl chloride (4.11 g, 21.54 mmol) and the reaction stirred for 4 hours. The reaction mixture was diluted with CH_2Cl_2 . The organics were washed with water, 2M, HCl, sat $NaHCO_3$, dried ($MgSO_4$) and concentrated under vacuum. The crude product was purified on silica gel (10% EtOAc in pet ether) to give 2-methylpentyl *p*-toluenesulphonate (4.95 g, 98% yield) as a colourless oil.

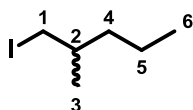
1H -NMR ($CDCl_3$, 400 MHz) δ : 7.71 (d, 2H, H-4, $J=8.3$ Hz), 7.27 (d, 2H, H-3, $J=8.1$ Hz), 3.80 (dd, 1H, H-6a, $J_1=9.4$, $J_2=5.7$ Hz), 3.72 (dd, 1H, H-6b, $J_1=9.4$ Hz, $J_2=6.5$ Hz), 2.38 (s, 3H, H-1), 1.71 (m, 1H, H-7), 1.27 – 0.97 (m, 4H, H-9 and 10), 0.82 (d, 3H, H-8, $J=6.7$ Hz), 0.76 (t, 3H, H-11, $J=7.2$ Hz)

^{13}C -NMR ($CDCl_3$, 100 MHz) δ : 144.62 (C-5), 133.19 (C-2), 129.79 (C-3), 127.90 (C-4), 75.19 (C-6), 34.87 (C-9), 32.57 (C-7), 21.64 (C-1), 19.71 (C-10), 16.40 (C-8), 14.09 (C-11)

IR (cm^{-1}): 1355 (S=O stretch)

HRMS: m/z calculated for and $C_{13}H_{20}O_3SNa = 279.1025 [M+Na]^+$; Found 279.1024

1-Iodo-2-methyl pentane 196



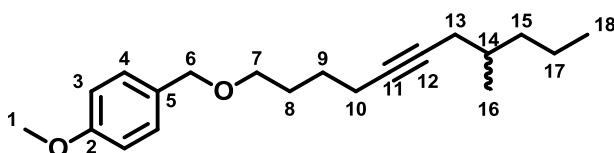
To a solution of 2-methylpentyl *p*-toluenesulphonate (2.00 g, 7.80 mmol) in acetone (40 ml) was added potassium iodide (26.00 g, 156.00 mmol) and the reaction heated to 60 °C for 48 hours. The reaction mixture was poured into water and extracted with Et_2O . The

combined organics were washed with sat NaHCO_3 , dried (MgSO_4) and concentrated under vacuum to give 1-iodo-2-methyl pentane (1.32 g, 80% yield) as a colourless oil.

$^1\text{H-NMR}$ (CDCl_3 , 400 MHz) δ : 3.15 (dd, 1H, H-1a, $J_1=9.6\text{Hz}$, $J_2=4.6\text{Hz}$), 3.09 (dd, 1H, H-1b, $J_1=9.3\text{Hz}$, $J_2=6.1\text{Hz}$), 1.39 (m, 1H, H-2), 1.31 – 1.19 (m, 3H, H-4a and 5), 1.13 (m, 1H, H-4b), 0.90 (d, 3H, H-3, $J=6.6\text{Hz}$), 0.84 (t, 3H, H-6, $J=7.1\text{Hz}$)

$^{13}\text{C-NMR}$ (CDCl_3 , 100 MHz) δ : 38.68 (C-4), 34.48 (C-2), 20.59 (C-3), 20.09 (C-5), 18.11 (C-1), 14.11 (C-6)

1-(4-Methoxybenzyloxy)-8-methyl-undec-5-yne 197



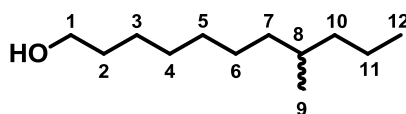
To a solution of 1-(4-methoxybenzyloxy)hex-5-yne (2.90 g, 13.30 mmol) in THF (40 ml), cooled to -78°C under argon, was added *n*-butyl lithium (9.14 ml, 14.63 mmol) and the solution stirred for 15 mins. 1-Iodo-2-methyl pentane (1.41 g, 6.65 mmol) in THF (20 ml) was added and the reaction heated to 75°C to 48 hours. The reaction mixture was poured into water and extracted with EtOAc. The combined organics were dried (MgSO_4) and concentrated under vacuum. The crude product was purified on silica gel (5% EtOAc in pet ether) to give 1-(4-methoxybenzyloxy)-8-methyl-undec-5-yne (1.31 g, 65% yield) as a colourless oil.

$^1\text{H-NMR}$ (CDCl_3 , 400 MHz) δ : 7.19 (d, 2H, H-3, $J=8.4\text{Hz}$), 6.80 (d, 2H, H-4, $J=8.3\text{Hz}$), 4.36 (s, 2H, H-6), 3.74 (s, 3H, H-1), 3.39 (t, 2H, H-7, $J=6.4\text{Hz}$), 2.13 (m, 2H, H-10), 2.02 (m, 1H, H-13a), 1.95 (m, 1H, H-13b), 1.64 (m, 2H, H-8), 1.55 – 1.40 (m, 3H, H-8 and 14), 1.32 – 1.04 (m, 4H, H-16 and 17), 0.87 (d, 3H, H-15, $J=6.7\text{Hz}$), 0.82 (t, 3H, H-18, $J=7.2\text{Hz}$)

$^{13}\text{C-NMR}$ (CDCl_3 , 100 MHz) δ : 159.50 (C-2), 130.73 (C-5), 129.24 (C-4), 113.75 (C-3), 80.71, 79.29, 72.51 (C-6), 69.65 (C-7), 55.30 (C-1), 38.38, 26.17, 25.89, 20.21, 32.59 (C-14), 28.90 (C-8), 19.52 (C-15), 18.61 (C-10), 14.31 (C-18)

HRMS: m/z calculated for $C_{20}H_{30}O_2Na = 325.2138 [M+Na]^+$; Found 325.2134

8-Methylundecan-1-ol 198



From 4-methylene-11-benzyloxyundecane: A solution of 4-methylene-11-benzyloxyundecane (646 mg, 2.36 mmol) and palladium on carbon (10%) was flushed with hydrogen gas five times and heated to 70 °C for 15 days. The reaction mixture was filtered through celite and concentrated under vacuum. The crude product was purified on silica gel (20% EtOAc in pet ether) to give 8-methylundecan-1-ol (345 mg, 79% yield) as a colourless oil. The benzyl protected alcohol was also isolated in 15% yield.

From 1-(4-methoxybenzyloxy)-8-methyl-undec-5-yne: To a solution of 1-(4-methoxybenzyloxy)-8-methyl-undec-5-yne (489 mg, 1.62 mmol) in THF (10 ml) was added 10% palladium on carbon (30 mg) and the flask flushed with hydrogen gas ten times and stirred for 24 hours. The reaction mixture was filtered through celite and concentrated under vacuum. The crude product was purified on silica gel (20% EtOAc in pet ether) to give 9 methylundecan-1-ol (143 mg, 48% yield) as a colourless oil.

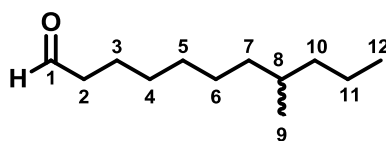
1H -NMR ($CDCl_3$, 400 MHz) δ : 3.57 (t, 2H, H-1, $J=6.7$ Hz), 1.50 (m, 2H, H-2), 1.32 – 1.14 and 1.00 (m, 16H, H-3 to 8, 10 and 11), 0.81 (t, 3H, H-12, $J=7.0$ Hz), 0.76 (d, 3H, H-9, $J=6.5$ Hz)

^{13}C -NMR ($CDCl_3$, 100 MHz) δ : 63.13 (C-1), 39.43, 37.07, 32.84 (C-2), 32.48 (C-8), 29.98, 29.50, 27.01, 25.77, 20.15, 19.68 (C-9), 14.42 (C-12)

IR (cm^{-1}): 3309 (H-O stretch)

HRMS: m/z calculated for $C_{12}H_{26}ONa = 209.1876 [M+Na]^+$; Found 209.1877

8-Methylundecanal



Following the general Swern procedure, the crude product was purified on silica gel (7% EtOAc in pet ether) to give 8-methylundecanal (338 mg, 68% yield) as a colourless oil.

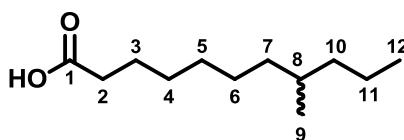
$^1\text{H-NMR}$ (CDCl_3 , 400 MHz) δ : 9.70 (t, 1H, H-1, $J=1.6\text{Hz}$), 2.35 (td, 2H, H-2, $J_1=7.4\text{Hz}$, $J_2=1.6\text{Hz}$), 1.56 (m, 2H, H-3), 1.38 – 1.17 (m, 12H, H-4 to 7a, 8, 10a and 11), 1.02 (m, 2H, H-7b and 10b), 0.80 (t, 3H, H-12, $J=6.7\text{Hz}$), 0.77 (d, 3H, H-9, $J=6.5\text{Hz}$)

$^{13}\text{C-NMR}$ (CDCl_3 , 100 MHz) δ : 202.98 (C-1), 43.94 (C-2), 39.39, 36.98, 32.46 (C-8), 29.71, 29.22, 27.64, 26.84, 22.12 (C-3), 19.65 (C-9), 14.41 (C-12)

IR (cm^{-1}): 2710 (OC-H stretch), 1726 (C=O stretch)

HRMS : m/z calculated for and $\text{C}_{12}\text{H}_{24}\text{ONa} = 207.1719$ $[\text{M}+\text{Na}]^+$; Found 207.1727

8-Methylundecanoic acid 199



Following the general Oxone procedure gave 8-methylundecanoic acid (350 mg, 95% yield) as a colourless oil.

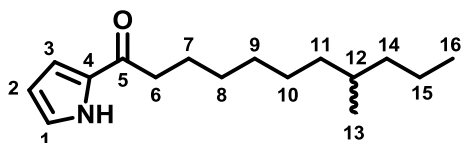
$^1\text{H-NMR}$ (CDCl_3 , 400 MHz) δ : 2.28 (t, 2H, H-2, $J=7.4\text{Hz}$), 1.57 (m, 2H, H-3), 1.32 – 1.13 (m, 11H, H-4 to 7a, 8, 10a and 11), 1.02 (m, 2H, H-7b and 10b), 0.80 (t, 3H, H-12, $J=6.8\text{Hz}$), 0.76 (d, 3H, H-9, $J=6.5\text{Hz}$)

$^{13}\text{C-NMR}$ (CDCl_3 , 100 MHz) δ : 178.83 (C-1), 39.40, 36.99 (C-2), 33.86, 32.46 (C-8), 29.60, 29.12, 26.85, 24.71 (C-3), 20.14, 19.66 (C-9), 14.42 (C-12)

IR (cm^{-1}): 1707 (C=O stretch)

HRMS: m/z calculated for $C_{12}H_{24}O_2Na = 223.1666 [M+Na]^+$; Found 223.1670

8-Methyl-1-(1H-pyrrol-2-yl)undecan-1-one



Following the general carboxylic acid coupling procedure, the crude product was purified on silica gel (7% EtOAc in pet ether) to give 8-methyl-1-(1H-pyrrol-2-yl)undecan-1-one (310 mg, 71% yield) as a brown oil.

1H -NMR ($CDCl_3$, 400 MHz) δ : 9.30 (bs, 1H, N-H), 6.94 (m, 1H, H-1), 6.83 (m, 1H, H-3), 6.21 (m, 1H, H-2), 2.68 (t, 2H, H-6, $J=7.5$ Hz), 1.65 (m, 2H, H-7), 1.31 – 1.12 (m, 13H, H-8 to 11a, 12, 14a and 15), 0.99 (m, 2H, H-11b and 14b), 0.80 (t, 3H, H-16, $J=6.9$ Hz), 0.76 (d, 3H, H-13, $J=6.6$ Hz)

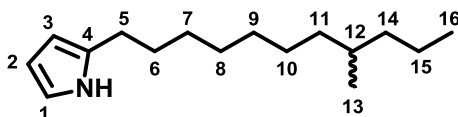
^{13}C -NMR ($CDCl_3$, 100 MHz) δ : 191.20 (C-5), 131.90 (C-4), 124.15 (C-1), 115.83 (C-3), 110.55 (C-2), 38.06 (C-6), 36.68, 34.39, 32.47 (C-12), 29.50, 27.10, 25.31, 19.67 (C-13), 14.42 (C-16).

2 signals missing

IR (cm^{-1}): 3274 (N-H stretch), 1635 (C=O stretch)

HRMS: m/z calculated for and $C_{16}H_{27}NONa = 272.1985 [M+Na]^+$; Found 272.1984

2-(8-Methylundecyl)-1H-pyrrole 180



Following the general acyl ketone reduction procedure, the crude product was purified on silica gel (5% EtOAc in pet ether) to give 2-(8-methylundecyl)-1H-pyrrole (171 mg, 59% yield) as a colourless oil.

1H -NMR ($CDCl_3$, 400 MHz) δ : 7.82 (bs, 1H, N-H), 6.59 (m, 1H, H-1), 6.06 (m, 1H, H-2), 5.84 (m, 1H, H-3), 2.52 (t, 2H, H-5, $J=7.7$ Hz), 1.55 (m, 2H, H-6), 1.32 – 1.14 (m, 13H, H-7 to 11a, 12, 13a and 14), 1.02 (m, 2H, H-11b and 13b), 0.81 (t, 3H, H-16, $J=6.9$ Hz), 0.76 (t, 3H, H-13, $J=6.5$ Hz)

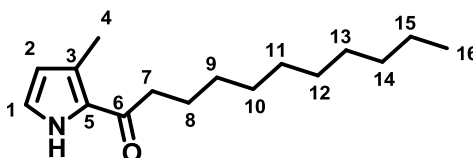
$^{13}\text{C-NMR}$ (CDCl_3 , 100 MHz) δ : 132.80 (C-4), 115.95 (C-1), 108.26 (C-2), 104.86 (C-3), 39.43, 37.08, 32.48 (C-12), 29.93, 29.69, 29.51, 29.42, 27.75 (C-5), 27.06, 20.15, 19.68 (C-13), 14.43 (C-16)

IR (cm^{-1}): 3384 (N-H stretch)

HRMS : m/z calculated for and $\text{C}_{16}\text{H}_{29}\text{N}$ = 236.2373 $[\text{M}+\text{H}]^+$; Found 236.2370

6.1.5 Synthesis of methy-substituted pyrrole containing 2-UP analogues

1-(3-Methylpyrrolyl)undecan-1-one 206



Following the general carboxylic acid coupling procedure with 3-methyl pyrrole, the crude product was purified on silica gel (10% EtOAc in pet ether) to give 1-(3-methylpyrrolyl)undecan-1-one (355 mg, 53% yield) as a white solid.

$^1\text{H-NMR}$ (CDCl_3 , 400 MHz) δ : 9.28 (bs, 1H, N-H), 6.88 (t, 1H, H-1, $J=2.7\text{Hz}$), 6.10 (t, 1H, H-2, $J=2.6\text{Hz}$), 2.74 (t, 2H, H-7, $J=7.4\text{Hz}$), 2.41 (s, 3H, H-4), 1.71 (qu, 2H, H-8, $J=7.5\text{Hz}$), 1.39 – 1.27 (m, 14H, H-6 to 12), 0.90 (t, 3H, H-13, $J=7.0\text{Hz}$)

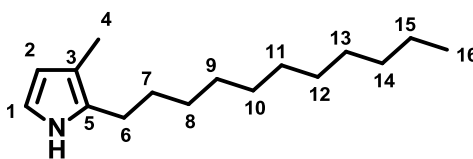
$^{13}\text{C-NMR}$ (CDCl_3 , 100 MHz) δ : 190.80 (C-6), 129.49 (C-5), 126.23 (C-3), 122.55 (C-1), 113.56 (C-2), 39.88 (C-7), 31.89, 29.58, 29.53, 29.32, 22.67, 14.44 (C-1), 14.10 (C-4). 3 signals missing.

IR (cm^{-1}): 3281 (N-H stretch), 1619 (C=O stretch)

HRMS : m/z calculated for $\text{C}_{16}\text{H}_{27}\text{NO}$ = 250.2165 $[\text{M}+\text{H}]^+$; Found 250.2164

Melting point ($^{\circ}\text{C}$): 39 – 40

3-Methyl-2-undecylpyrrole 207



Following the general acyl ketone reduction procedure, the crude product was purified on silica gel (5% EtOAc in pet ether) to give 3-methyl-2-undecylpyrrole (228 mg, 68% yield) as a brown oil.

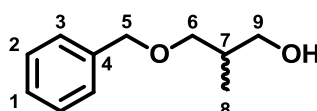
$^1\text{H-NMR}$ (CDCl_3 , 400 MHz) δ : 7.75 (bs 1H, N-H), 6.62 (t, 1H, H-1, $J=2.6\text{Hz}$), 6.01 (t, 1H, H-2, $J=2.7\text{Hz}$), 2.57 (t, 2H, H-6, $J=7.5\text{Hz}$), 2.08 (s, 3H, H-4), 1.59 (m, 2H, H-7), 1.34 – 1.30 (m, 16H, H-8 to 15), 0.93 (t, 3H, H-16, $J=6.6\text{Hz}$)

$^{13}\text{C-NMR}$ (CDCl_3 , 100 MHz) δ : 128.58 (C-5), 114.76 (C-1), 113.68 (C-3), 109.94 (C-2), 31.94, 30.01, 29.74, 29.68, 29.66, 29.64, 29.51, 29.45, 25.84 (C-6), 22.72, 14.14 (C-16), 10.90 (C-4)

IR (cm^{-1}): 3382 (N-H stretch)

HRMS: m/z calculated for $\text{C}_{16}\text{H}_{29}\text{N}$ = 236.2373 $[\text{M}+\text{H}]^+$; Found 236.2373

3-Benzyloxy-2-methyl propan-1-ol



To a solution of 2-methyl-1,3-propanediol (500 mg, 5.55 mmol) in CH_2Cl_2 (30 ml), under argon, was added silver (I) oxide (1.91 g, 8.25 mmol) and the resulting suspension stirred for 30 mins. Benzyl bromide (0.73 ml, 6.16 mmol) was added and the reaction mixture allowed to stir for a further 16 hours. The reaction mixture was filtered and concentrated under vacuum. The crude product was purified on silica gel (60% Et_2O in pentane) to give 3-benzyloxy-2-methylpropan-1-ol (902 mg, 90% yield) as a colourless oil.

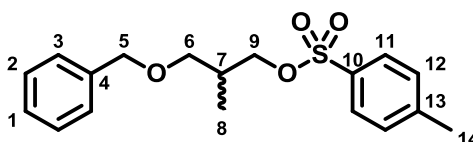
¹H-NMR (CDCl₃, 400 MHz) δ: 7.26 (m, 5H, H-1 to 3), 4.45 (s, 2H, H-5), 3.56 (m, 2H, H-9), 3.49 (dd, 1H, H-6a, J₁=9.1Hz, J₂=4.5Hz), 3.36 (m, 1H, H-6b), 2.00 (m, 1H, H-7), 0.81 (d, 3H, H-8, J=7.0Hz)

¹³C-NMR (CDCl₃, 100 MHz) δ: 138.05 (C-4), 128.48, 127.75, 127.63, 75.52 (C-6), 73.43 (C-5), 67.95 (C-9), 35.60 (C-7), 13.47 (C-8)

IR (cm⁻¹): 3345 (H-O stretch)

HRMS: *m/z* calculated for C₁₁H₁₆O₂ = 203.1043 [M+Na]⁺; Found 203.1047

(3-Benzyloxy-2-methyl propyl) 4-methylbenzenesulfonate



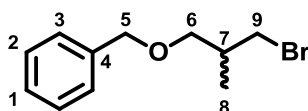
To a solution of 3-benzyloxy-2-methylpropan-1-ol (902 mg, 5.00 mmol), 4-dimethylamino pyridine (183 mg, 1.50 mmol) and triethylamine (1.53 ml, 12.50 mmol) in CH₂Cl₂ (20 ml), under argon, was added *p*-toluene sulfonylchloride (1.05 g, 5.50 mmol) and the resulting solution stirred for 24 hours. The reaction mixture was diluted with CH₂Cl₂ and washed with 2M HCl. The organics were dried (MgSO₄) and concentrated under vacuum to give (3-benzyloxy-2-methyl propyl) 4-methylbenzenesulfonate (1.59 g, 95% yield) as a yellow oil.

¹H-NMR (CDCl₃, 400 MHz) δ: 7.70 (d, 2H, H-11, J=8.3Hz), 7.27 – 7.15 (m, 7H, H-1 to 3 and 12), 4.32 (s, 2H, H-5), 3.95 (m, 2H, H-9), 3.26 (m, 2H, H-6), 2.35 (s, 3H, H-14), 2.03 (m, 1H, H-7), 0.87 (d, 3H, H-8, J=6.9Hz)

¹³C-NMR (CDCl₃, 100 MHz) δ: 144.66 (C-10), 138.23 (C-4), 133.05 (C-13), 129.81, 128.35, 127.59, 127.45, 127.93 (C-11), 73.08 (C-5), 72.25 (C-9), 71.11 (C-6), 33.70 (C-7), 21.64 (C-14), 13.64 (C-8)

HRMS: *m/z* calculated for C₁₈H₂₂O₄Na = 357.1131 [M+Na]⁺; Found 357.1135

3-Benzyloxy-2-methyl 1-bromopropane 214



To a solution of (3-benzyloxy-2-methyl propyl) 4-methylbenzenesulfonate (3.51 g, 10.49 mmol) in acetone (40 ml), under argon, was added lithium bromide (18.22 g, 209.80 mmol) and the resulting suspension heated to 65 °C for 24 hours. The reaction mixture was poured into water and extracted with EtOAc. The combined organics were dried (MgSO₄) and concentrated under vacuum. The crude product was purified on silica gel (7% EtOAc in pet ether) to give 3-benzyloxy-2-methyl 1-bromopropane (2.20 g, 87% yield) as a colourless oil.

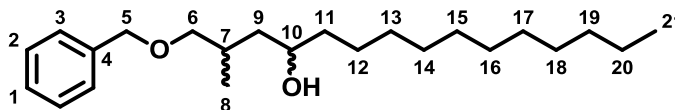
¹H-NMR (CDCl₃, 400 MHz) δ: 7.30 – 7.20 (m, 5H, H-1 to 3), 4.45 (s, 2H, H-5), 3.44 (m, 2H, H-9), 3.34 (m, 2H, H-6), 2.07 (m, 1H, H-7), 0.96 (d, 3H, H-8, J=6.8Hz)

¹³C-NMR (CDCl₃, 100 MHz) δ: 138.36 (C-4), 128.40, 127.60, 73.21 (C-5), 72.78 (C-6), 38.21 (C-9), 35.68 (C-7), 15.89 (C-8). 1 signal missing.

IR (cm⁻¹): 1094 (C-O stretch), 696 (C-Br stretch)

HRMS: *m/z* calculated for C₁₁H₁₅BrO = 265.0198 and 267.0178 [M+Na]⁺; Found 265.0198 and 267.0179

1-Benzyloxy-2-methyl pentadecan-4-ol



Magnesium turnings (93 mg, 3.86 mmol), under argon, was heated with a heat gun for 10 mins before THF (5 ml) was added. 3-Benzyloxy-2-methyl 1-bromopropane (890 mg, 3.68 mmol) in THF (2 ml) was added and heated to 50 °C for 3 hours. The reaction mixture was allowed to cool to RT before dodecanal (690 mg, 4.05 mmol) in THF (2 ml) was added and stirred for a further 16 hours. 2M HCl was added cautiously and extracted with EtOAc. The

combined organics were dried (MgSO_4) and concentrated under vacuum. The crude product was purified on silica gel (15% EtOAc in pet ether to give 1-benzyloxy-2-methyl pentadecan-4-ol (733 mg, 60% yield) as a colourless oil.

Note: the mixture of diastereoisomers was not separated

$^1\text{H-NMR}$ (CDCl_3 , 400 MHz) δ : 7.30 – 7.21 (m, 5H, H-1 to 3), 4.46 (s, 2H, H-5), 3.67 – 3.55 (m, 1H, H-10), 3.33 – 3.19 (m, 2H, H-6), 2.00 – 1.87 (m, 1H, H-7), 1.45 – 1.19 (m, 22H, H-9 and 11 to 20), 0.87 (d, 3H, H-8, $J=6.9\text{Hz}$), 0.81 (t, 3H, H-21, $J=6.5\text{Hz}$)

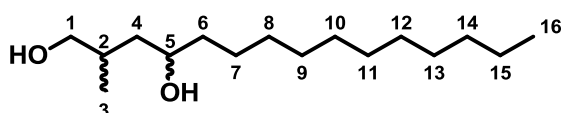
$^{13}\text{C-NMR}$ (CDCl_3 , 100 MHz) δ : 138.05 (C-4), 128.44, 127.74, 127.71, 76.64, 75.93 (C-6), 73.28, 73.18 (C-5), 70.52, 69.23 (C-10), 43.46, 42.95, 37.55, 31.95, 31.79, 30.21, 29.77, 29.67, 29.39, 25.86, 25.81, 22.72, 18.17, 18.07 (C-8), 14.16 (C-21)

Note: multiple signals for several of the carbons due to the mixture of diastereoisomers

IR (cm^{-1}): 3398 (H-O stretch), 1092 (C-O stretch), 1072 (C-O stretch)

HRMS : m/z calculated for $\text{C}_{23}\text{H}_{40}\text{O}_2\text{Na} = 371.2921$ $[\text{M}+\text{Na}]^+$; Found 371.2925

2-Methyl-pentadecane-1,4-diol 215



To a solution of 1-benzyloxy-2-methyl pentadecan-4-ol (633 mg, 1.82 mmol) in THF (15 ml) was added 10% palladium on carbon and the flask flushed with hydrogen gas ten times before being allowed to stir for 16 hours. The reaction mixture was filtered through celite and concentrated under vacuum to give 2-methyl-pentadecane-1,4-diol (417 mg, 89% yield) as a colourless oil.

$^1\text{H-NMR}$ (CDCl_3 , 400 MHz) δ : 3.72 – 3.63 (m, 1H, H-5), 3.54 – 3.32 (m, 2H, H-1), 1.91 – 1.73 (m, 1H, H-2), 1.46 – 1.35 (m, 4H, H-4 and 6), 1.25 – 1.19 (m, 18H, H-7 to 15), 0.88 – 0.79 (m, 6H, H-3 and 16)

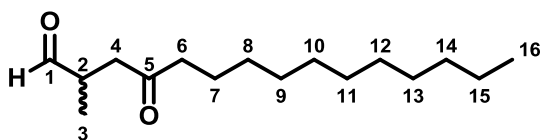
$^{13}\text{C-NMR}$ (CDCl_3 , 100 MHz) δ : 71.18, 69.47 (C-5), 68.95, 68.05 (C-1), 43.06, 41.84, 38.64, 37.63, 34.57, 32.19 (C-2), 31.93, 29.07, 29.64, 29.36, 25.81, 25.69, 22.70, 18.01, 17.51 (C-3), 14.13 (C-16). 2 signals missing.

Note: multiple signals for several carbons due to mixture of several diastereoisomers

IR (cm^{-1}): 3300 (H-O stretch)

HRMS : m/z calculated for $\text{C}_{16}\text{H}_{35}\text{O}_2 = 259.2632$ $[\text{M}+\text{H}]^+$; Found 259.2630

2-Methyl-4-oxo-pentadecanal 216



To a solution of oxalyl chloride (0.31 ml, 3.54 mmol) in CH_2Cl_2 (2 ml), cooled to -78°C under argon, was added DMSO (0.50 ml, 7.08 mmol) and stirred for 15 mins. 2-Methylpentadecane-1,4-diol (417 mg, 1.61 mmol) in CH_2Cl_2 (6 ml) was added and allowed to stir for a further 20 mins. Triethylamine (1.96 ml, 16.10 mmol) was added and stirred for 20 mins. Water was added and extracted with CH_2Cl_2 . The combined organics were washed with 2M HCl, sat NaHCO_3 , brine, dried (MgSO_4) and concentrated under vacuum. The crude product was purified on silica gel (15% EtOAc on pet ether) to give 2-methyl-4-oxo-pentadecanal (306 mg, 75% yield) as a waxy white solid.

$^1\text{H-NMR}$ (CDCl_3 , 400 MHz) δ : 9.62 (s, 1H, H-1), 2.91 – 2.77 (m, 2H, H-2 and 4a), 2.43 – 2.30 (m, 3H, H-4b and 6), 1.51 (m, 2H, H-7), 1.25 – 1.14 (m, 16H, H-8 to 15), 1.08 (d, 3H, H-3, $J=7.4\text{Hz}$), 0.81 (t, 3H, H-16, $J=6.8\text{Hz}$)

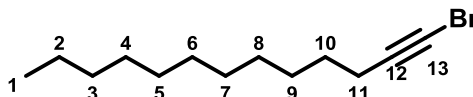
$^{13}\text{C-NMR}$ (CDCl_3 , 100 MHz) δ : 208.81 (C-5), 203.38 (C-1), 43.11, 41.56 (C-2), 31.91, 29.61, 29.47, 29.40, 29.34, 29.20, 22.69, 23.82 (C-7), 14.13 (C-16), 13.54 (C-3). 2 signals missing.

IR (cm^{-1}): 2350 (C(O)-H stretch), 1694 (C=O stretch)

HRMS: m/z calculated for $C_{16}H_{31}O_2 = 255.2319$ $[M+H]^+$; Found 255.2308

Melting point ($^{\circ}C$): 65 – 67

1-Bromotridec-1-yne 223



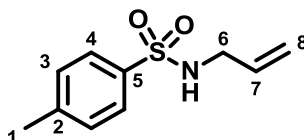
To a solution of 1-tridecyne (1.00 g, 5.55 mmol) in acetone (120 ml), in the dark under argon, was added silver nitrate (0.28 g, 1.67 mmol) followed by *N*-bromo succinimide (1.38 g, 7.77 mmol) and the resulting mixture stirred for 6 hours. Water was added and the acetone removed under vacuum. The aqueous layer was extracted with Et_2O . The combined organics were dried ($MgSO_4$) and concentrated under vacuum. The crude product was purified on silica gel (pet ether) to give 1-bromotridec-1-yne (1.17 g, 82% yield) as a colourless oil.

1H -NMR ($CDCl_3$, 400 MHz) δ : 2.13 (t, 2H, H-11, $J=7.2Hz$), 1.44 (m, 2H, H-10), 1.29 (m, 2H, H-9), 1.23 – 1.19 (m, 14H, H-2 to 8), 0.81 (t, 3H, H-1, $J=7.0Hz$)

^{13}C -NMR ($CDCl_3$, 100 MHz) δ : 80.52 (C-12), 37.41, 31.92, 29.62, 29.50, 29.35, 29.09, 28.80, 28.31, 22.70, 19.69 (C-11), 14.13 (C-1). 1 signal missing.

HRMS: m/z calculated for $C_{13}H_{22}Br = 257.0899$ and 259.0879 $[M-H]^-$; Found 257.0895 and 259.0874

N-Allyl *p*-toluenesulfonylamide 221



To a solution of *p*-toluenesulfonylamide (3.00 g, 17.52 mmol) in acetone (90 ml), under argon, was added potassium carbonate (2.66 g, 19.72 mmol) and the reaction mixture heated to 60 $^{\circ}C$ for 3 hours. Sodium iodide (0.26g g, 1.75 mmol) followed by allyl bromide (3.03 ml, 35.04 mmol) in acetone (10 ml) was added and stirred at 60 $^{\circ}C$ for an additional 16 hours. The reaction mixture was cooled to RT and water added. The acetone was removed under vacuum and the residual aqueous extracted with $EtOAc$. The combined organics were dried

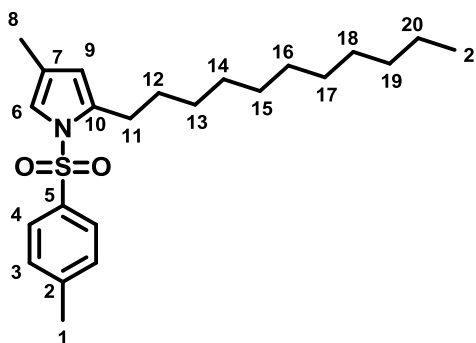
(MgSO₄) and concentrated under vacuum. The crude product was purified on silica gel (25% EtOAc in pet ether) to give *N*-allyl *p*-toluenesulfonylamide (1.15 g, 32% yield) as a white solid.

¹H-NMR (CDCl₃, 400 MHz) δ: 7.79 (d, 2H, H-4, J=8.4Hz), 7.24 (d, 2H, H-3, J=8.3Hz), 5.65 (m, 1H, H-7), 5.06 (m, 2H, H-8), 4.43 (t, 1H, N-H, J=5.9Hz), 3.52 (m, 2H, H-6), 2.36 (s, 3H, H-1)

¹³C-NMR (CDCl₃, 100 MHz) δ: 143.54 (C-2), 136.97 (C-5), 133.00 (C-7), 129.75 (C-3), 127.17 (C-4), 117.75 (C-8), 45.80 (C-6), 21.55 (C-1)

HRMS: *m/z* calculated for C₁₆H₃₁O₂ = 255.2319 [M+H]⁺; Found 255.2308

1-(*p*-Tolylsulfonyl)-2-undecyl-4-methyl pyrrole 225



To a solution of 1-bromotridec-1-yne (1.17 g, 4.53 mmol) and *N*-allyl *p*-toulenesulfonylamide (1.91 g, 9.06 mmol) in DMF (10 ml), under argon, was added potassium phosphate tribasic (1.44 g, 6.80 mmol) and the reaction mixture heated to 120 °C for 2 hours. The reaction mixture was cooled to RT before *n*-tetrabutylammonium bromide (2.19 g, 6.80 mmol) was added and stirred for 10 mins. Palladium(II) acetate (0.10 g, 0.45 mmol) was added and the mixture again heated to 120 °C for 3 hours. After cooling to RT, the reaction was diluted with EtOAc and filtered through celite and the solvent removed under vacuum. The crude product was purified on silica gel (4% EtOAc in pet ether) to give 1-(*p*-tolylsulfonyl)-2-undecyl-4-methyl pyrrole (525 mg, 30% yield) as a brown oil.

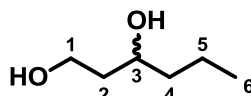
¹H-NMR (CDCl₃, 400 MHz) δ: 7.55 (d, 2H, H-3, J=7.6Hz), 7.20 (d, 2H, H-4, J=7.5Hz), 6.92 (s, 1H, H-6), 5.76 (s, 1H, H-9), 2.54 (t, 2H, H-11, J=7.8Hz), 2.32 (s, 3H, H-1), 1.93 (s, 3H, H-8), 1.43 (m, 2H, H-12), 1.23 – 1.18 (m, 16H, H-13 to 20), 0.81 (t, 3H, H-21, J=6.7Hz)

$^{13}\text{C-NMR}$ (CDCl_3 , 100 MHz) δ : 144.29 (C-2), 136.82 (C-5), 136.17 (C-10), 129.85 (C-4), 126.64 (C-3), 121.90 (C-7), 119.03 (C-6), 114.27 (C-9), 29.65, 29.56, 29.43, 29.37, 29.31, 28.71, 27.21, 26.42, 22.70, 21.59 (C-1), 14.14 (C-21), 11.84 (C-8). 1 signal missing.

HRMS: m/z calculated for $\text{C}_{23}\text{H}_{36}\text{NO}_2\text{S}$ = 390.2461 $[\text{M}+\text{H}]^+$; Found 390.2462

6.1.6 Synthesis of fluorine containing 2-UP analogues

1,3-Hexan-diol



To a suspension of lithium aluminium hydride (1.44 g, 27.93 mmol) in THF (100 ml), under argon, was added ethyl 3-oxohexanoate (5.05 ml, 31.61 mmol) in THF (20 ml) and the resulting mixture heated to 70 °C for 48 hours. The reaction mixture was cooled to 0 °C before water was cautiously added and filtered through celite. The combined organics were dried (MgSO_4) and concentrated under vacuum. The crude product was purified on silica gel (40% EtOAc in pet ether) to give 1,3-hexan-diol (2.77 g, 75% yield) as a colourless oil.

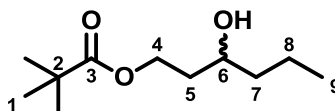
$^1\text{H-NMR}$ (CDCl_3 , 400 MHz) δ : 3.86 – 3.74 (m, 3H, H-1 and 3), 1.93 (bs, 2H, H-O), 1.70 – 1.56 (m, 2H, H-2), 1.49 – 1.24 (m, 4H, H-4 and 5), 0.87 (t, 22H, H-6)

$^{13}\text{C-NMR}$ (CDCl_3 , 100 MHz) δ : 72.17 (C-3), 61.98 (C-1), 40.04 (C-4), 38.31 (C-2), 18.70 (C-5), 14.06 (C-6)

IR (cm^{-1}): 3316 (O-H stretch)

HRMS: m/z calculated for $\text{C}_6\text{H}_{14}\text{O}_2\text{Na}$ = 141.0886 $[\text{M}+\text{Na}]^+$; Found 141.0888

3-Hydroxyhexyl-2,2-dimethylpropanoate



To a solution of 1,3-hexan-diol (1.31 g, 11.09 mmol) in pyridine (15 ml) and CH_2Cl_2 (8 ml), cooled to -20 °C under argon, was added trimethylacetyl chloride (1.78 ml, 14.42 mmol)

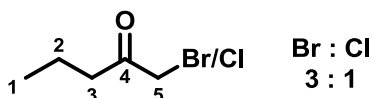
dropwise. The resulting mixture was allowed to stir for 30 mins. An additional 0.2 ml of trimethylacetyl chloride was required to complete the reaction after which EtOAc was added. The organics were washed with 2M HCl, sat NaHCO₃, dried (MgSO₄) and concentrated under pressure. The crude product was purified on silica gel (15% EtOAc in pet ether).

¹H-NMR (CDCl₃, 400 MHz) δ: 4.36 (m, 1H, H-4a), 4.14 (m, 1H, H-4b), 3.67 (m, 1H, H-6), 1.82 (m, 1H, H-5a), 1.68 (m, 1H, H-5b), 1.50 – 1.43 (m, 3H, H-7a and 8), 1.37 (m, 1H, H-7b), 1.21 (s, 9H, H-1), 0.94 (t, 3H, H-9, J=7.0Hz)

¹³C-NMR (CDCl₃, 100 MHz) δ: 178.95 (C-3), 68.47 (C-6), 61.69 (C-4), 39.55, 38.75 (C-2), 36.44 (C-5), 27.18 (C-1), 18.78, 13.96 (C-9)

HRMS: *m/z* calculated for C₁₁H₂₆O₂SiNa = 241.1600 [M+Na]⁺; Found 241.1596

1-Bromopentan-2-one 175



To a solution of butyryl chloride (0.97 ml, 9.39 mmol) in acetonitrile (20 ml), under argon, was added 2M trimethylsilyl diazomethane solution (4.90 ml, 9.80 mmol) dropwise over 15 mins and the resulting yellow solution stirred for 30 mins. The reaction mixture was cooled to -20 °C and 33% hydrobromic acid in acetic acid (2.50 ml, 12.21 mmol) was added dropwise over 10 mins. The resulting colourless solution was allowed to warm to RT over 16 hours. The solvent was removed under vacuum and diluted with Et₂O. The combined organics were washed with water, 2M HCl, sat NaHCO₃, dried (MgSO₄) and concentrated under pressure to give a mixture of 1-bromopentan-2-one and 1-chloropentan-2-one (Br: 69%, Cl 25%; 94% total yield) as a colourless oil.

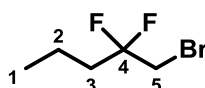
¹H-NMR (CDCl₃, 400 MHz) δ: 4.00 (s, 0.3H, H-5 Cl), 3.81 (s, 1.7H, H-5 Br), 2.57 (t, 1.7H, H-3 Br, J=7.3Hz), 2.51 (t, 0.3H, H-3 Cl, J=7.3Hz), 1.58 (m, 2H, H-2), 0.88 (t, 3H, H-1, J=7.4Hz)

¹³C-NMR (CDCl₃, 100 MHz) δ: 201.95 (C-4), 48.23 (C-5 Cl), 41.71 (C-3 Br), 41.58 (C-3 Cl), 34.30 (C-5 Br), 17.35 (C-2 Br), 17.11 (C-2 Cl), 13.57 (C-1)

IR (cm⁻¹): 1712 (C=O stretch)

HRMS: *m/z* calculated for C₅H₁₀Br = 164.9910 and 166.9889 [M+H]⁺; Found 164.9908 and 166.9887. *m/z* calculated for C₅H₁₀Cl = 121.0415 and 123.0385 [M+H]⁺; Found 121.0414 and 123.0415

1-Bromo-2,2-difluoropentane 176



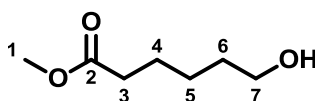
To a solution of 1-bromopentan-2-one and 1-chloropentan-2-one mixture (1.00 g, 6.34 mmol) in CH₂Cl₂ (10 ml), cooled to 0 °C under argon, was added DAST (1.67 ml, 12.68 mmol) dropwise. The reaction mixture was allowed to warm to RT over 16 hours. A further 0.1 ml of DAST was required to complete the reaction. The reaction mixture was poured in sat NaHCO₃ and extracted with Et₂O. The combined organics were washed with sat NaHCO₃, 2M HCl, dried (MgSO₄) and concentrated under vacuum without heating to give 1-bromo-2,2-difluoropentane (490 mg, 42% yield) as a brown oil.

¹H-NMR (CDCl₃, 400 MHz) δ: 3.44 (t, 2H, H-5, J=13.0Hz), 1.94 (m, 2H, H-3), 1.47 (m, 2H, H-2), 0.92 (t, 3H, H-1, J=7.4Hz)

¹³C-NMR (CDCl₃, 100 MHz) δ: 121.39 (C-4), 35.52 (C-3, t, J=24.1Hz), 30.35 (C-5, t, 34.4Hz), 14.53 (C-2, t, 14.4Hz), 12.75 (C-1)

¹⁹F-NMR (CDCl₃, 300 MHz) δ: 99.03

Methyl 6-hydroxyhexanoate



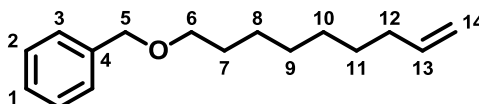
To a solution of ϵ -caprolactone (1.94 ml, 17.52 mmol) in methanol (60 ml), under argon, was added Dowex 50W-X8 (40 mg) and heated to 65 °C for 16 hours. The reaction mixture was filtered and concentrated under vacuum to give methyl 6-hydroxyhexanoate (2.56 g, 100% yield) as a colourless oil.

$^1\text{H-NMR}$ (CDCl_3 , 400 MHz) δ : 3.61 – 3.58 (m, 5H, H-1 and 7), 2.26 (t, 2H, H-3, $J=7.0\text{Hz}$), 1.60 (m, 2H, H-4), 1.52 (m, 2H, H-6), 1.34 (m, 2H, H-5)

$^{13}\text{C-NMR}$ (CDCl_3 , 100 MHz) δ : 174.08 (C-2), 61.65 (C-7), 50.50 (C-1), 32.96 (C-3), 31.30 (C-6), 24.27 (C-5), 23.61 (C-4)

HRMS: m/z calculated for $\text{C}_7\text{H}_{14}\text{O}_3\text{Na} = 169.0835$ [$\text{M}+\text{Na}$] $^+$; Found 169.0832

1-Benzyloxy-non-8-ene 171

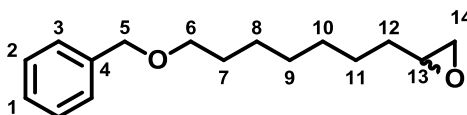


To a solution of 8-benzyloxyoctanal (2.82 g, 12.04 mmol) in THF (15 ml), under argon, was added titanocene dichloride (150 mg, 0.60 mmol) followed by dimethyl titanocene (49.4 ml, $\sim 0.5\text{M}$ solution) and the mixture heated to 85 °C for 72 hours. The reaction mixture was cooled to RT and poured into 5% EtOAc in pet ether. The precipitate was removed by filtration through celite and the solvent removed under vacuum. The crude product was purified on silica gel (3% EtOAc in pet ether) to give 1-benzyloxy-non-8-ene (1.58 g, 57% yield) as a yellow oil.

$^1\text{H-NMR}$ (CDCl_3 , 400 MHz) δ : 7.27 – 7.20 (m, 5H, H-1 to 3), 5.79 – 5.69 (m, 1H, H-13), 4.94 – 4.85 (m, 2H, H-14), 4.43 (s, 2H, H-5), 3.39 (t, 2H, H-6, $J=6.0\text{Hz}$), 1.95 (m, 2H, H-12), 1.54 (m, 2H, H-17), 1.32 – 1.21 (m, 8H, H-8 to 11)

$^{13}\text{C-NMR}$ (CDCl_3 , 100 MHz) δ : 139.20 (C-13), 138.73 (C-4), 128.35, 127.47, 114.15 (C-14), 72.88 (C-5), 70.51 (C-6), 33.79 (C-12), 29.77, 29.33, 29.08, 28.87, 26.16 (C-7 to 11). 1 signal missing.

1-Benzyloxy-non-8-ene oxide 168



To a solution of 1-benzyloxy-non-8-ene (1.58 g, 6.81 mmol) in CH_2Cl_2 (60 ml), cooled to 0°C under argon, was added *m*-chloroperbenzoic acid (1.29 g, 7.49 mmol) and the reaction allowed to warm to RT over 16 hours. A further 400 mg of *m*-chloroperbenzoic acid was required to complete the reaction. The reaction mixture was poured into sat NaHCO_3 and the organics separated. The organic layer was dried (MgSO_4) and concentrated under vacuum. The crude product was purified on silica gel (10% EtOAc in pet ether) to give 1-benzyloxy-8-ene oxide (1.41 g, 84% yield) as a colourless oil.

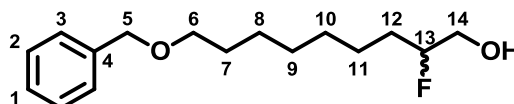
$^1\text{H-NMR}$ (CDCl_3 , 400 MHz) δ : 7.28 – 7.20 (m, 5H, H-1 to 3), 4.43 (s, 2H, H-5), 3.93 (t, 2H, H-6, $J=6.6\text{Hz}$), 2.82 (m, 1H, H-13), 2.67 (dd, 1H, H-14a, $J_1=5.1\text{Hz}$, $J_2=4.1\text{Hz}$), 2.39 (dd, 1H, H-14b, $J_1=5.1\text{Hz}$, $J_2=2.8\text{Hz}$), 1.55 (m, 2H, H-7), 1.45 (m, 2H, H-12), 1.43 – 1.23 (m, 8H, H-8 to 11)

$^{13}\text{C-NMR}$ (CDCl_3 , 100 MHz) δ : 139.10 (C-4), 128.35, 127.63, 127.45, 72.89 (C-5), 70.46 (C-6), 52.40 (C-13), 47.14 (C-14), 32.48 (C-12), 29.74, 29.38, 26.11, 25.92. 1 signal missing.

IR (cm^{-1}): 3031 (C-H stretch epoxide), 1099 (C-O stretch ether)

HRMS: m/z calculated for $\text{C}_{16}\text{H}_{24}\text{O}_2\text{Na} = 271.1669$ $[\text{M}+\text{Na}]^+$; Found 271.1669

9-Benzyloxy-2-fluoro-nonan-1-ol 172



To pyridinium polyhydrofluoride (0.12 ml, 10eq), in a polypropylene tube cooled to 0°C under argon, was added 1-benzyloxy-non-8-ene oxide (100 mg, 0.40 mmol) in CH_2Cl_2 (0.3 ml) and allowed to warm to RT over 16 hours. The reaction mixture was poured into ice cold 2M ammonia and neutralised with conc ammonia. The aqueous layer was extracted with EtOAc. The combined organics were washed with 2M HCl, dried (MgSO_4) and concentrated under

vacuum. The crude product was purified on silica gel (25% EtOAc in pet ether) to give 9-benzyloxy-2-fluoro-nonan-1-ol (52 mg, 49% yield) as a colourless oil.

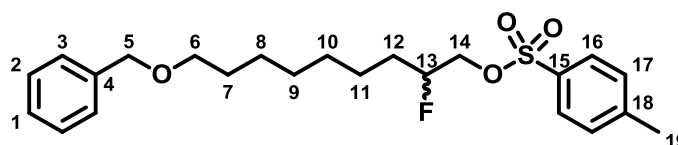
$^1\text{H-NMR}$ (CDCl_3 , 400 MHz) δ : 7.18 – 7.28 (m, 5H, H-1 to 3), 4.53 (m, 0.5H, H-13), 4.42 – 4.38 (m, 2.5Hz, H-5 and 13), 3.66 – 3.51 (m, 2H, H-14), 3.39 (t, 2H, H-6, $J=6.6\text{Hz}$), 2.00 (bs, 1H, H-O), 1.62 – 1.47 (m, 4H, H-7 and 12), 1.41 – 1.25 (m, 8H, H-8 and 11)

$^{13}\text{C-NMR}$ (CDCl_3 , 100 MHz) δ : 138.67 (C-4); 128.37, 127.65, 95.60, 93.94 (C-13), 72.89 (C-5), 70.44 (C-6), 65.14, 64.93 (C-14), 31.05, 30.84 (C-12), 29.72, 29.37, 29.28, 26.09, 24.90, 24.85 (C-7 to 11)

IR (cm^{-1}): 3403 (H-O stretch), 1093 (C-O stretch)

HRMS: m/z calculated for $\text{C}_{16}\text{H}_{26}\text{OFNa} = 269.1911$ [$\text{M}+\text{Na}$] $^+$; Found 269.1916

(9-Benzyloxy-2-fluoro-nonyl)-4-methylbenzenesulphonate 173



To a solution of 9-benzyloxy-2-fluoro-nonan-1-ol (1.28 g, 4.77 mmol), 4-dimethylamino pyridine (175 mg, 1.43 mmol) and triethylamine (0.87 ml, 7.16 mmol) in CH_2Cl_2 (15 ml), cooled to 0 °C under argon, was added *p*-toluenesulphonyl chloride (1.09 g, 5.73 mmol) and stirred for 16 hours. The reaction mixture was poured into water and extracted with CH_2Cl_2 . The combined organics were washed with 2M HCl, sat NaHCO_3 , dried (MgSO_4) and concentrated under vacuum. The crude product was purified on silica gel (10% EtOAc in pet ether) to give (9-benzyloxy-2-fluoro-nonyl)-4-methylbenzenesulphonate (1.18 g, 59 %yield).

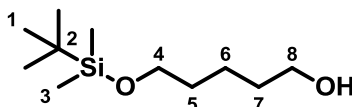
$^1\text{H-NMR}$ (CDCl_3 , 400 MHz) δ : 7.73 (d, 2H, H-17, $J=8.4\text{Hz}$), 7.29 – 7.20 (m, 7H, H-1 to 3 and 16), 4.51 (dm, 1H, H-13, $J=48.8\text{Hz}$), 4.43 (s, 2H, H-5), 4.10 – 3.94 (m, 2H, H-14), 3.38 (t, 2H, H-6, $J=6.6\text{Hz}$), 2.38 (s, 3H, H-19), 1.52 (m, 4H, H-7 and 12), 1.36 – 1.18 (m, 8H, H-8 to 11)

$^{13}\text{C-NMR}$ (CDCl_3 , 100 MHz) δ : 145.05 (C-8), 138.68 (C-4), 129.92, 128.36, 127.99, 127.64, 127.5, 91.38, 89.64 (C-13), 72.89 (C-5), 70.77, 70.54 (C-14), 70.38 (C-6), 30.99, 30.79 (C-12), 29.70, 29.18, 26.06, 24.54, 24.50, 21.68 (C-19)

HRMS: m/z calculated for $\text{C}_{23}\text{H}_{32}\text{O}_4\text{F}$ = 423.2000 $[\text{M}+\text{H}]^+$; Found 423.2004

6.1.7 Synthesis of ether containing 2-UP analogues

1-(*t*-Butyldimethyl silyl)oxypentan-5-ol



To a suspension of sodium hydride (460 mg, 19.20 mmol) in THF (30 ml), cooled to 0 °C under argon, was slowly added 1,5-pentadiol (2.01 ml, 19.20 mmol) in THF (10 ml) and the resulting white precipitate stirred for 30 mins. *t*-Butyldimethylsilyl chloride (2.88 g, 19.20 mmol) in THF (10 ml) was slowly added over 10 mins and allowed to stir for a further 45 mins. Water was cautiously added, the THF removed under vacuum and the aqueous layer extracted with EtOAc (3 x 40 ml). The combined organics were washed with brine, dried (MgSO_4) and concentrated under vacuum. The crude product was purified on silica gel (20% EtOAc in hexane) to give 1-(*t*-butyldimethyl silyl)oxypentan-5-ol (2.93 g, 70% yield) as a colourless oil.

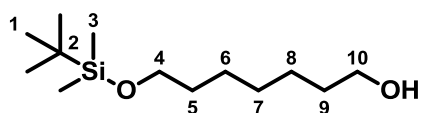
$^1\text{H-NMR}$ (CDCl_3 , 400 MHz) δ : 3.59 (m, 4H, H-4 and 8), 1.58 – 1.46 (m, 4H, H-5 and 7), 1.32 (m, 2H, H-6), 0.85 (s, 9H, H-1), 0.00 (s, 6H, H-3)

$^{13}\text{C-NMR}$ (CDCl_3 , 100 MHz) δ : 63.12 (C-4), 62.99 (C-8), 32.51 (C-5), 32.33 (C-7), 25.98 (C-1), 22.04 (C-6), 18.39 (C-2), -5.27 (C-3)

IR (cm^{-1}): 3367 (H-O stretch), 1095 (O-Si stretch)

HRMS: m/z calculated for $\text{C}_{11}\text{H}_{26}\text{O}_2\text{SiNa}$ = 241.1600 $[\text{M}+\text{Na}]^+$; Found 241.1596

1-(*t*-Butyldimethyl silyl)oxyheptan-7-ol



To a solution of 1,7-heptandiol (3.00 g, 22.71 mmol) in THF (70 ml), cooled to 0 °C under argon, was added sodium hydride (572 mg, 23.85 mmol) and stirred for 15 mins. *T*-Butyldimethylsilyl chloride (3.40 g, 22.71 mmol) was added and stirred for a further 60 mins. The reaction was poured into water and extracted with EtOAc. The combined organics were dried (MgSO₄) and concentrated under vacuum. The crude product was purified on silica gel (20% EtOAc in pet ether) to give 1-(*t*-butyldimethyl silyl)oxyheptan-7-ol (2.23 g, 45% yield) as a colourless oil.

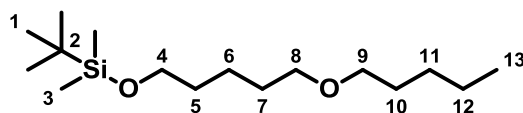
¹H-NMR (CDCl₃, 700 MHz) δ : 3.63 (t, 2H, H-10, J=6.6Hz), 3.60 (t, 2H, H-4, J=6.5Hz), 1.57 (m, 2H, H-9), 1.51 (m, 2H, H-5), 1.45 (bs, 1H, H-O), 1.37 – 1.33 (m, 6H, H-6 to 8), 0.90 (s, 9H, H-10), 0.05 (s, 6H, H-8)

¹³C-NMR (CDCl₃, 175 MHz) δ : 63.28 (C-4), 62.99 (C-10), 32.80, 32.75, 29.25, 29.18, 25.80 (C-1), 25.76, 18.38 (C-2), -5.26 (C-3)

IR (cm⁻¹): 3325 (H-O stretch), 1253 (C-O stretch), 1096 (O-Si stretch)

HRMS: m/z calculated for C₁₃H₃₀O₂SiNa = 269.1913 [M+Na]⁺; Found 269.1907

t-Butyldimethyl-(5-pentoxypentoxysilane 93



To a solution of 1-(*t*-butyldimethyl silyl)oxypentan-5-ol (2.93 g, 13.42 mmol) in DMF (50 ml), cooled to 0 °C under argon, was added sodium hydride (483 mg, 20.14 mmol) and allowed to stir for 30 mins. 1-Bromopentane (4.12 ml, 33.50 mmol) was added and allowed to warm to RT over 24 hours. TLC showed the presence of 1-(*t*-butyldimethyl silyl)oxypentan-5-ol so another equivalent of sodium hydride and 1-bromopentane was added and stirred for a

further 16 hours. Water was cautiously added and extracted with EtOAc (3 x 30 ml). The combined organics were washed with brine, dried (MgSO₄) and concentrated under vacuum. The crude product was purified on silica gel (3% EtOAc in pet ether) to give *t*-butyldimethyl-(5-pentoxypentoxysilane (3.09 g, 80% yield) as a colourless oil.

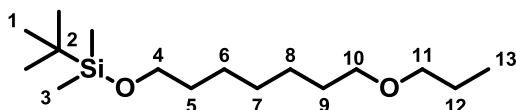
¹H-NMR (CDCl₃, 600 MHz) δ: 3.46 (t, 2H, H-4, J=6.4Hz), 3.35 (m, 4H, H-8 and 9), 1.56 – 1.47 (m, 6H, H-5, 7 and 10), 1.33 (m, 2H, H-6), 1.27 (m, 4H, H-11 and 12), 0.85 (m, 12H, H-1 and 13), 0.00 (s, 6H, H-3)

¹³C-NMR (CDCl₃, 150 MHz) δ: 69.97 (C-9), 69.82 (C-8), 62.16 (C-4), 31.68 (C-5), 28.55 (C-7), 28.46 (C-10), 27.37 (C-11), 24.96 (C-1), 21.55 (C-6), 21.44 (C-12), 17.35 (C-13), 13.03 (C-13), -6.37 (C-3)

IR (cm⁻¹): 1254 (C-O stretch), 1095 (O-Si stretch)

HRMS: *m/z* calculated for C₁₆H₃₆O₂SiNa = 311.2377 [M+Na]⁺; Found 311.2375

***t*-Butyldimethyl-(7-propoxy-heptanoxy)silane 96**



To a solution of 1-(*t*-butyldimethyl silyl)oxyheptan-7-ol (875 mg, 3.55 mmol) in DMF (15 ml), cooled to 0 °C under argon, was added sodium hydride (170 mg, 7.11 mmol) and stirred for 20 mins. 1-Bromopropane (0.96 ml, 10.65 mmol) in DMF (5 ml) was added and stirred for a further 16 hours. Water was added and extracted with EtOAc. The combined organics were dried (MgSO₄) and concentrated under vacuum. The crude product was purified on silica gel (5% EtOAc in pet ether) to give *t*-butyldimethyl-(7-propoxy-heptanoxy)silane (853 mg, 84% yield) as a colourless oil.

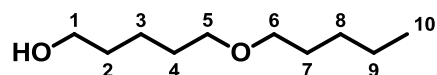
¹H-NMR (CDCl₃, 400 MHz) δ: 3.55 (t, 2H, H-4, J=6.6Hz), 3.34 (m, 4H, H-10 and 11), 1.59 – 1.43 (m, 6H, H-5, 9 and 12), 1.32 – 1.23 (m, 6H, H-6 to 8), 0.87 (t, 3H, H-13, J=7.4Hz), 0.85 (s, 9H, H-1), 0.00 (s, 6H, H-2)

$^{13}\text{C-NMR}$ (CDCl_3 , 100 MHz) δ : 72.57, 70.91, 63.31 (C-4), 32.84, 29.75, 29.33, 26.21, 25.80, 22.95, 26.00 (C-1), 18.39 (C-2), 10.60 (C-13), -5.25 (C-3)

IR (cm^{-1}): 1096 (O-Si stretch)

HRMS : m/z calculated for $\text{C}_{16}\text{H}_{36}\text{O}_2\text{SiNa}$ = 311.2377 $[\text{M}+\text{Na}]^+$; Found 311.2370

5-Pentoxypentan-1-ol



To a solution of *t*-butyldimethyl-(5-pentoxypentanoxy)silane (3.09 g, 10.72 mmol) in THF (40 ml), cooled to 0 °C, was added tetrabutylammonium fluoride (6.76 g, 21.44 mmol) and stirred for 2 hours. The THF was removed under vacuum and the crude product purified on silica gel (15% EtOAc in pet ether) to give 5-pentoxypentan-1-ol (1.81 g, 97% yield) as a pale yellow oil.

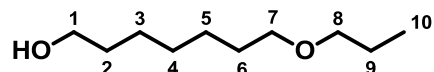
$^1\text{H-NMR}$ (CDCl_3 , 700 MHz) δ : 3.66 (t, 2H, H-1, $J=6.3\text{Hz}$), 3.41 (m, 4H, H-5 and 6), 1.63 – 1.56 (m, 6H, H-2, 4 and 7), 1.44 (m, 2H, H-3), 1.32 (m, 4H, H-8 and 9), 0.90 (t, 3H, H-10, $J=7.0\text{Hz}$)

$^{13}\text{C-NMR}$ (CDCl_3 , 175 MHz) δ : 71.04 (C-6), 70.74 (C-5), 62.87 (C-1), 32.50 (C-2), 29.69 (C-4), 29.43 (C-7), 28.35 (C-8), 22.54 (C-9), 22.45 (C-3), 14.04 (C-10)

IR (cm^{-1}): 3386 (H-O stretch), 1113 (C-O stretch)

HRMS : m/z calculated for $\text{C}_{10}\text{H}_{22}\text{O}_2\text{Na}$ = 197.1512 $[\text{M}+\text{Na}]^+$; Found 197.1515

7-Propoxyheptan-1-ol



To a solution of *t*-butyldimethyl-(7-propoxyheptanoxy)silane (1.60 g, 5.55 mmol) in THF (25 ml) was added tetrabutylammonium fluoride (3.51 g, 11.10 mmol) and stirred for 4 hours. TLC showed no starting material so the reaction was concentrated under vacuum. The crude

product was purified on silica gel (20% EtOAc in pet ether) to give 7-propyloxyheptan-1-ol (900 mg, 93% yield) as a colourless oil.

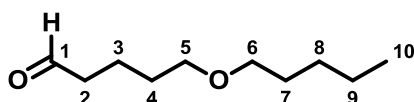
$^1\text{H-NMR}$ (CDCl_3 , 400 MHz) δ : 3.54 (t, 2H, H-1, $J=6.6\text{Hz}$), 3.30 (t, 2H, H-7, $J=6.7\text{Hz}$), 3.26 (t, 2H, H-8, $J=6.8\text{Hz}$), 1.54 – 1.44 (m, 6H, H-2, 6 and 9), 1.28 – 1.23 (m, 6H, H-3 to 5), 0.82 (t, 3H, H-10, $J=7.5\text{Hz}$)

$^{13}\text{C-NMR}$ (CDCl_3 , 100 MHz) δ : 72.59 (C-8), 70.86 (C-7), 63.05 (C-1), 32.73 (C-2), 29.71, 29.28, 26.19, 25.70, 22.95 (C-9), 10.61 (C-10)

IR (cm^{-1}): 3380 (H-O stretch), 1113 (C-O stretch)

HRMS : m/z calculated for $\text{C}_{10}\text{H}_{22}\text{O}_2\text{Na} = 197.1512$ [$\text{M}+\text{Na}$] $^+$; Found 197.1516

5-Pentoxypentanal



To a solution of 5-pentoxypentanol (1.00 g, 5.74 mmol) in DMSO (20 ml) was added IBX (2.41 g, 8.61 mmol) and the resulting solution stirred for 4 hours. Water was added and the resulting white precipitate was filtered off and washed with Et_2O (3 x 50 ml). The combined organics were washed with NaHCO_3 , (3 x 20 ml), brine, dried (MgSO_4) and concentrated under vacuum. The crude product was purified on silica gel (10% EtOAc in pet ether) to give 5-pentoxypentanal (0.79 g, 80% yield) as a colourless oil.

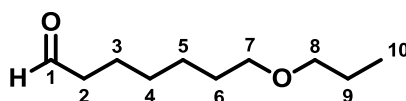
$^1\text{H-NMR}$ (CDCl_3 , 400 MHz) δ : 9.70 (t, 1H, H-1, $J=1.8\text{Hz}$), 3.43 (m, 4H, H-5 and 6), 2.40 (td, 2H, H-2, $J_1=7.1\text{Hz}$, $J_2=1.7\text{Hz}$), 1.66 (m, 2H, H-3), 1.57 – 1.46 (m, 4H, H-4 and 7), 1.25 (m, 4H, H-8 and 9), 0.83 (t, 3H, H-10, $J=6.7\text{Hz}$)

$^{13}\text{C-NMR}$ (CDCl_3 , 100 MHz) δ : 202.62 (C-1), 71.08 (C-6), 70.23 (C-5), 43.66 (C-2), 29.44 (C-7), 29.18 (C-4), 28.37 (C-8), 22.55 (C-9), 19.00 (C-3), 14.05 (C-10)

IR (cm^{-1}): 1725 (C=O stretch), 1112 (C-O stretch)

HRMS: m/z calculated for $C_{10}H_{20}O_2Na = 195.1356 [M+Na]^+$; Found 195.1356

7-Propyloxyheptanal



To a solution of 7-propyloxyheptan-1-ol (900 mg, 5.17 mmol) in DMSO (10 ml) was added IBX (2.18 g, 7.78 mmol) and stirred for 16 hours. The reaction mixture was diluted with EtOAc and filtered. The organic layer was washed with water, dried ($MgSO_4$) and concentrated under vacuum. The crude product was purified on silica gel (10% EtOAc in pet ether) to give 7-propyloxyheptanal (597 mg, 67% yield) as a colourless oil.

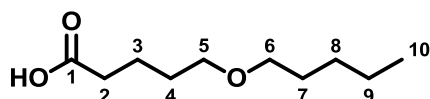
1H -NMR ($CDCl_3$, 400 MHz) δ : 9.69 (t, 1H, H-1, $J=1.8$ Hz), 3.33 (t, 2H, H-7, $J=6.5$ Hz), 3.29 (t, 2H, H-8, $J=6.7$ Hz), 2.36 (td, 2H, H-2, $J_1=7.3$ Hz, $J_2=1.9$ Hz), 1.59 (m 2H, H-3), 1.50 – 1.47 (m, 4H, H-6 and 9), 1.30 (m, 4H, H-4 and 5), 0.85 (t, 3H, H-10, $J=7.4$ Hz)

^{13}C -NMR ($CDCl_3$, 100 MHz) δ : 202.84 (C-1), 72.58 (C-8), 70.66 (C-7), 43.82 (C-2), 29.55, 29.00, 25.98, 22.91, 22.03 (C-3), 14.19 (C-10)

IR (cm^{-1}): 2719 (C-H stretch aldehyde), 1724 (C=O stretch), 1112 (C-O stretch)

HRMS: m/z calculated for $C_{10}H_{20}O_2Na = 195.1356 [M+Na]^+$; Found 195.1353

5-Pentoxypentanoic acid 90



To a solution of 5-pentoxypentanal (785 mg, 4.56 mmol) in DMF (10 ml) was added Oxone (3.64 g, 5.93 mmol) and the resulting suspension stirred for 4 hours. Water was added and acidified with 2M HCl before being extracted with EtOAc (3 x 40 ml). The combined organics were dried ($MgSO_4$) and concentrated under vacuum. The crude product was left under high-vacuum for 24 hours to give 5-pentoxypentanoic acid (0.75 g, 88% yield) as a colourless oil.

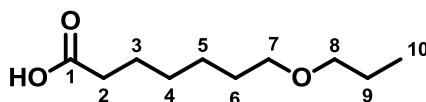
$^1\text{H-NMR}$ (CDCl_3 , 400 MHz) δ : 3.34 (m, 4H, H-5 and 6), 2.33 (t, 2H, H-2, $J=7.0\text{Hz}$), 1.65 (m, 2H, H-3), 1.56 (m, 2H, H-4), 1.50 (m, 2H, H-7), 1.28 – 1.21 (m, 4H, H-8 and 9), 0.83 (t, 3H, H-10, $J=6.9\text{Hz}$)

$^{13}\text{C-NMR}$ (CDCl_3 , 100 MHz) δ : 178.69 (C-1), 71.10 (C-6), 70.28 (C-5), 33.67 (C-2), 29.41 (C-7), 28.99 (C-4), 28.35 (C-8), 22.54 (C-9), 21.63 (C-3), 14.05 (C-10)

IR (cm^{-1}): 1703 (C=O stretch), 1110 (C-O stretch)

HRMS: m/z calculated for $\text{C}_{10}\text{H}_{21}\text{O}_3 = 189.1485$ [$\text{M}+\text{H}$] $^+$; Found 189.1484

7-Propyloxyheptanoic acid 97



To a solution of 7-propyloxyheptanal (597 mg, 3.47 mmol) in DMF (10 ml) was added Oxone (2.77 g, 4.51 mmol) and the resulting suspension stirred for 4 hours. Water was added and acidified with 2M HCl before being extracted with EtOAc (3 x 40 ml). The combined organics were dried (MgSO_4) and concentrated under vacuum. The crude product was left under high-vacuum for 24 hours to give 7-propyloxyheptanoic acid (0.62 g, 94% yield) as a colourless oil.

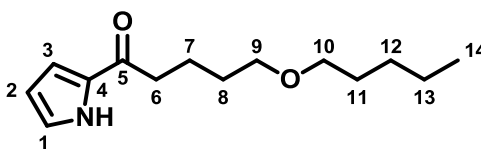
$^1\text{H-NMR}$ (CDCl_3 , 400 MHz) δ : 3.31 (t, 2H, H-7, $J=6.5\text{Hz}$), 3.29 (t, 2H, H-8, $J=6.7\text{Hz}$), 2.28 (t, 2H, H-2, $J=7.4\text{Hz}$), 1.59 (m, 2H, H-3), 1.50 – 1.47 (m, 4H, H-6 and 9), 1.30 (m, 4H, H-5 and 5), 0.84 (t, 3H, H-10, $J=7.4\text{Hz}$)

$^{13}\text{C-NMR}$ (CDCl_3 , 100 MHz) δ : 179.37 (C-1), 72.59 (C-8), 70.71 (C-7), 33.91 (C-2), 29.54 (C-6), 28.90 (C-5), 25.86 (C-9), 24.65 (C-3), 22.90 (C-4), 10.58 (C-10)

IR (cm^{-1}): 1707 (C=O stretch), 1107 (C-O stretch)

HRMS: m/z calculated for $\text{C}_{10}\text{H}_{20}\text{O}_3\text{Na} = 211.1305$ [$\text{M}+\text{Na}$] $^+$; Found 211.1307

5-Pentyloxy-1-(1H-pyrrol-2-yl)-pentan-1-one



Following the general carboxylic acid coupling procedure, the crude product was purified on silica gel (20% EtOAc in hexane) to give 5-pentyloxy-1-(1H-pyrrol-2-yl)-pentan-1-one (384 mg, 40% yield) as a pink oil.

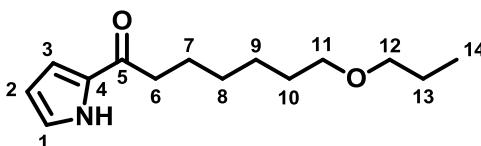
$^1\text{H-NMR}$ (CDCl_3 , 400 MHz) δ : 9.52 (bs, 1H, N-H), 7.01 (m, 1H, H-1), 6.91 (m, 1H, H-3), 6.27 (m, 1H, H-2), 3.43 (t, 2H, H-9, $J=6.4\text{Hz}$), 3.39 (t, 2H, H-10, $J=6.7\text{Hz}$), 2.79 (t, 2H, H-6, $J=7.1\text{Hz}$), 1.79 (m, 2H, H-7), 1.64 (m, 2H, H-8), 1.56 (m, 2H, H-11); 1.31 (m, 4H, H-12 and 13), 0.89 (t, 3H, H-14, $J=6.8\text{Hz}$)

$^{13}\text{C-NMR}$ (CDCl_3 , 100 MHz) δ : 190.94 (C-5), 132.31 (C-4), 124.43 (C-3), 116.12 (C-1), 110.67 (C-2), 71.16 (C-10), 70.61 (C-9), 37.79 (C-6), 29.57 (C-8), 29.54 (C-11), 28.49 (C-12), 22.67 (C-13), 22.10 (C-7), 14.16 (C-14)

IR (cm^{-1}): 3279 (N-H stretch), 1632 (C=O stretch), 1110 (C-O stretch)

HRMS: m/z calculated for $\text{C}_{14}\text{H}_{23}\text{NO}_2\text{Na} = 260.1621$ [$\text{M}+\text{Na}$] $^+$; Found 260.1626

7-Propyloxy-1-(1H-pyrrol-2-yl)-heptan-1-one



Following the general carboxylic acid coupling procedure, the crude product was purified on silica gel (20% EtOAc in hexane) to give 7-propyloxy-1-(1H-pyrrol-2-yl)-heptan-1-one (384 mg, 40% yield) as a pink oil.

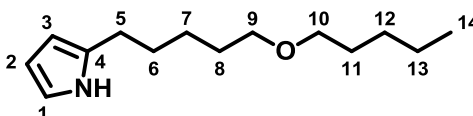
$^1\text{H-NMR}$ (CDCl_3 , 400 MHz) δ : 9.47 (bs, 1H, N-H), 6.95 (m, 1H, H-1), 6.83 (m, 1H, H-3), 6.20 (m, 1H, H-2), 3.33 (t, 2H, H-11, $J=6.7\text{Hz}$), 3.29 (t, 2H, H-12, $J=6.7\text{Hz}$), 2.69 (t, 2H, H-6, $J=7.6\text{Hz}$), 1.68 (m, 2H, H-7), 1.50 (m, 4H, H-10 and 13), 1.32 (m, 4H, H-8 and 9), 0.84 (t, 2H, H-14, $J=7.4\text{Hz}$)

$^{13}\text{C-NMR}$ (CDCl_3 , 100 MHz) δ : 191.09 (C-5), 132.23 (C-4), 124.33 (C-3), 115.97 (C-1), 110.54 (C-2), 72.58 (C-12), 70.77 (C-11), 37.95 (C-6), 29.63 (C-10), 29.31 (C-8), 26.05 (C-9), 25.23 (C-7), 22.94 (C-13), 10.60 (C-14)

IR (cm^{-1}): 3277 (N-H stretch), 1630 (C=O stretch), 1111 (C-O stretch)

HRMS : m/z calculated for $\text{C}_{14}\text{H}_{23}\text{NO}_2\text{Na} = 260.1621$ [$\text{M}+\text{Na}$] $^+$; Found 260.1618

2-(5-Pentoxypentyl)-pyrrole 85



Following the general acyl ketone reduction procedure, the crude product was purified on silica gel (10% EtOAc in pet ether) to give 2-(5-pentoxypentyl)-pyrrole (206 mg, 85% yield) as a yellow oil.

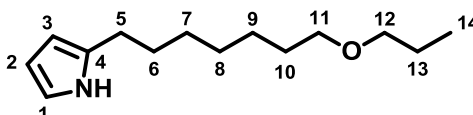
$^1\text{H-NMR}$ (CDCl_3 , 400 MHz) δ : 7.90 (bs, 1H, N-H), 6.59 (m, 1H, H-1), 6.05 (m, 1H, H-2), 5.84 (m, 1H, H-3), 3.33 (m, 4H, H-9 and 10), 2.54 (t, 2H, H-5, $J=7.4\text{Hz}$), 1.62 – 1.49 (m, 6H, H-6, 8 and 11), 1.35 (m, 2H, H-7), 1.25 (m, 4H, H-12 and 13), 0.84 (t, 3H, H-14, $J=6.8\text{Hz}$)

$^{13}\text{C-NMR}$ (CDCl_3 , 100 MHz) δ : 116.03 (C-1), 108.25 (C-2), 104.94 (C-3), 71.05 (C-9), 70.77 (C-10), 29.48, 28.39 (C-13), 27.58 (C-5), 25.88 (C-7), 22.57 (C-12), 14.07 (C-14). 1 signal missing)

IR (cm^{-1}): 3380 (N-H stretch), 1099 (C-O) stretch

HRMS : m/z calculated for $\text{C}_{14}\text{H}_{26}\text{NO} = 224.2009$ [$\text{M}+\text{H}$] $^+$ and $\text{C}_{14}\text{H}_{25}\text{NONa} = 246.1834$ [$\text{M}+\text{Na}$] $^+$; Found 224.2006 and 246.1828

2-(7-Propoxyheptyl)-pyrrole 86



Following the general acyl ketone reduction procedure, the crude product was purified on silica gel (10% EtOAc in pet ether) to give 2-(7-propoxyheptyl)-pyrrole (206 mg, 85% yield) as a yellow oil.

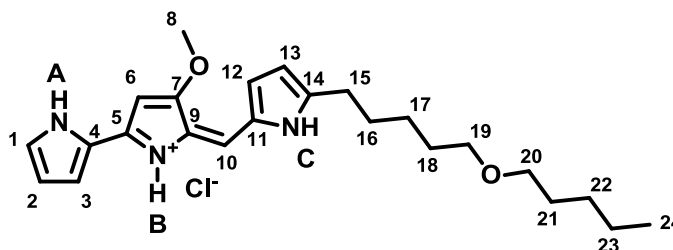
$^1\text{H-NMR}$ (CDCl_3 , 400 MHz) δ : 7.84 (bs, 1H, N-H), 6.59 (m, 1H, H-1), 6.08 (m, 1H, H-2), 5.84 (m, 1H, H-3), 3.34 – 3.27 (m, 4H, H-11 and 12), 2.52 (t, 2H, H-5, $J=7.5\text{Hz}$), 1.59 – 1.46 (m, 6H, H-6, 10 and 13), 1.27 (m, 6H, H-7 to 9), 0.85 (t, 3H, H-14, $J=7.4\text{Hz}$)

$^{13}\text{C-NMR}$ (CDCl_3 , 100 MHz) δ : 132.24 (C-4), 115.98 (C-1), 108.26 (C-2), 104.88 (C-3), 72.60 (C-12), 70.90 (C-11), 29.76 (C-10), 29.62 (C-6), 29.31, 27.71 (C-5), 26.15 (C-9), 22.96 (C-13), 10.61 (C-14). 1 signal missing.

IR (cm^{-1}): 3382 (N-H stretch), 1097 (C-O stretch)

HRMS : m/z calculated for $\text{C}_{14}\text{H}_{25}\text{NONa} = 246.1828$ [$\text{M}+\text{Na}$] $^+$; Found 246.1826

2-[[5-(5-Pentoxypentyl)-1H-pyrrol-2-yl]methylene]-3-methoxy-5-(1H-pyrrol-2-yl)pyrrole hydrochloride salt⁴⁷



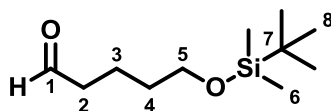
To a solution of 3-methoxy-5-(1-BOC-pyrrol-2-yl)-1H-pyrrole-2-carboxaldehyde (50 mg, 0.17 mmol) and 2-(5-pentoxypentyl)-pyrrole (42 mg, 0.19 mmol) in methanol (3 ml) was added 2M HCl in methanol (0.10 ml) and the resulting red solution stirred for 15 mins. Sodium methoxide (55 mg, 1.02 mmol) was added and the resulting yellow/brown solution stirred for a further 45 mins. The reaction mixture was poured into water and the yellow colour extracted with EtOAc. The combined organics were washed with brine, dried (MgSO_4) and concentrated under vacuum. The crude product was purified *via* reverse phase HPLC (Table 6.2). The required fractions were combined and the methanol removed under vacuum.

The remaining solution was poured into sat NaHCO₃ and the yellow colour extracted with EtOAc. The combined organics were washed with 2M HCl, dried (MgSO₄) and concentrated under vacuum to give 2-[[5-(5-pentoxypentyl)-1H-pyrrol-2-yl]methylene]-3-methoxy-5-(1H-pyrrol-2-yl)pyrrole hydrochloride salt (58 mg, 87% yield) as a red solid.

¹H-NMR (CDCl₃, 700 MHz) δ : 12.82 (bs, 1H, N-H B), 12.68 (bs, 1H, N-H C), 12.63 (bs, 1H, N-H A), 7.22 (m, 1H, H-1), 6.96 (s, 1H, H-6), 6.93 (m, 1H, H-3), 6.82 (m, 1H, H-12), 6.34 (m, 1H, H-2), 6.19 (m, 1H, H-13), (s, 1H, H-10), 3.99 (s, 3H, H-9), 3.41 (t, 2H, H-19, J=6.7Hz), 3.38 (t, 2H, H-20, J=6.7Hz), 2.94 (t, 2H, H-15, J=7.7Hz), 1.80 (m, 2H, H-16), 1.63 (m, 2H, H-18), 1.55 (m, 2H, H-21), 1.46 (m, 2H, H-17), 1.33 – 1.29 (m, 4H, H-22 and 23), 0.88 (t, 3H, H-24, J=6.9Hz)

¹³C-NMR (CDCl₃, 125 MHz) δ : 166.29 (C-7), 152.64 (C-14), 148.86 (C-9), 129.14 (C-12), 127.48 (C-1), 125.99 (C-11), 122.08 (C-4), 121.47 (C-5), 117.95 (C-3), 116.31 (C-6), 112.50 (C-13), 112.00 (C-2), 93.09 (C-10), 70.94 (C-20), 70.70 (C-19), 58.85 (C-8), 29.47, 29.45, 29.07 (C-16), 28.35 (C-15), 25.93, 22.54 (C-17), 14.05 (C-24). 1 signal missing.

5-(*t*-Butyldimethylsilyl)oxypentanal



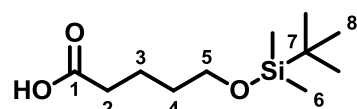
Following the general Swern procedure, the crude product was purified on silica gel (10% EtOAc in pet ether) to give 5-(*t*-butyldimethylsilyl)oxypentanal (1.16 g, 79% yield) as a colourless oil.

¹H-NMR (CDCl₃, 400 MHz) δ : 9.72 (t, 1H, H-1, J=1.8Hz), 3.58 (t, 2H, H-5, J=6.2Hz), 2.41 (td, 2H, H-2, J₁=7.3Hz, J₂=1.8Hz), 1.66 (m, 2H, H-3), 1.51 (m, 2H, H-4), 0.84 (s, 9H, H-8), 0.00 (s, 6H, H-6)

¹³C-NMR (CDCl₃, 100 MHz) δ : 202.78 (C-1), 62.61 (C-5), 43.64 (C-2), 32.12 (C-4), 25.95 (C-8), 18.63 (C-3), -5.33 (C-6). 1 signal missing.

HRMS: *m/z* calculated for C₁₁H₂₄O₂Si = 239.1443 [M+Na]⁺; Found 239.1432

5-(*t*-Butyldimethylsilyl)oxypentanoic acid



To a solution of 5-(*t*-butyldimethylsilyl)oxypentanal (1.02 g, 4.72 mmol) and 2-methyl-2-butene (2 ml) in *t*-butanol (14 ml) was added sodium chlorite (642 mg, 7.09 mmol) and sodium dihydrophosphate (115 mg, 0.95 mmol) in water (4 ml) before being stirred for 60 mins. The reaction mixture was poured into 1M HCl and extracted with EtOAc. The combined organics were dried (MgSO₄) and concentrated under vacuum. The crude product was purified on silica gel (30% EtOAc in pet ether) to give 5-(*t*-butyldimethylsilyl)oxypentanoic acid (700 mg, 64% yield) as a colourless oil.

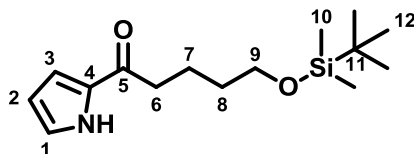
¹H-NMR (CDCl₃, 400 MHz) δ: 3.59 (t, 2H, H-5, J=6.3Hz), 2.34 (t, 2H, H-2, J=7.3Hz), 1.65 (m, 2H, H-3), 1.54 (m, 2H, H-4), 0.84 (s, 9H, H-8), 0.00 (s, 6H, H-6)

¹³C-NMR (CDCl₃, 100 MHz) δ: 178.55 (C-1), 62.66 (C-5), 33.60 (C-2), 31.97 (C-4), 25.95 (C-8), 21.27 (C-3), 18.29 (C-7), -3.59 (C-6)

IR (cm⁻¹): 1708 (C=O stretch)

HRMS: *m/z* calculated for C₁₁H₂₄O₃Si = 231.1422 [M-H]⁻; Found 231.1418

5-(*t*-Butyldimethylsilyl)oxy-1-(1H-pyrrol-2-yl)pentan-1-one

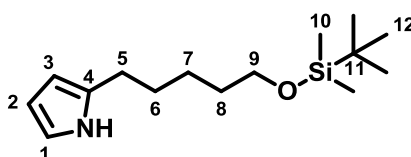


Following the general carboxylic acid coupling procedure, the crude product was purified on silica gel (15% EtOAc in pet ether) to give 5-(*t*-butyldimethylsilyl)oxy-1-(1H-pyrrol-2-yl)pentan-1-one (398 mg, 47% yield) as a colourless oil.

$^1\text{H-NMR}$ (CDCl_3 , 400 MHz) δ : 9.38 (bs, 1H, H-N), 6.97 (m, 1H, H-1), 6.86 (m, 1H, H-3), 6.62 (m, 1H, H-2), 3.60 (t, 2H, H-9, $J=6.4\text{Hz}$), 2.74 (t, 2H, H-6, $J=7.5\text{Hz}$), 1.74 (m, 2H, H-7), 1.55 (m, 2H, H-8), 0.84 (s, 9H, H-12), 0.00 (s, 6H, H-10)

$^{13}\text{C-NMR}$ (CDCl_3 , 100 MHz) δ : 190.72 (C-5), 124.24 (C-1), 115.91 (C-3), 110.57 (C-2), 62.87 (C-9), 37.71 (C-6), 32.47 (C-8), 25.98 (C-12), 21.66 (C-7), 18.33 (C-11), -5.28 (C-10). 1 signal missing.

2-((5-*t*-Butyldimethylsilyl)oxypentyl)-pyrrole

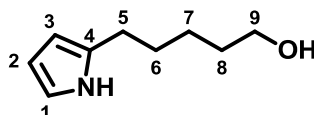


Following the general acyl ketone procedure, the crude product was purified on silica gel (10% EtOAc in pet ether) to give 2-((*t*-butyldimethylsilyl)oxypentyl)-pyrrole (338 mg, 90% yield) as a colourless oil.

$^1\text{H-NMR}$ (CDCl_3 , 400 MHz) δ : 7.88 (bs, 1H, H-N), 6.61 (m, 1H, H-1), 6.08 (m, 1H, H-2), 5.86 (m, 1H, H-3), 3.56 (t, 2H, H-9, $J=6.5\text{Hz}$), 2.56 (t, 2H, H-5, $J=7.5\text{Hz}$), 1.59 (m, 2H, H-6), 1.50 (m, 2H, H-8), 1.35 (m, 2H, H-7), 0.85 (s, 9H, H-12), 0.00 (s, 6H, H-10)

$^{13}\text{C-NMR}$ (CDCl_3 , 100 MHz) δ : 116.03 (C-1), 108.27 (C-2), 104.95 (C-3), 63.16 (C-9), 32.59 (C-8), 29.50 (C-6), 27.68 (C-5), 26.00 (C-12), 25.53 (C-7), 18.31 (C-11), -5.25 (C-10). 1 signal missing.

2-(5-Hydroxypentyl)-pyrrole



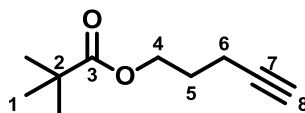
To a solution of 2-((5-*t*-butyldimethylsilyl)oxypentyl)-pyrrole (100 mg, 0.37 mmol) in THF (5 ml) was added tetrabutylammonium fluoride (177 mg, 0.56 mmol) and stirred for 16 hours. The THF was removed under vacuum and the residue loaded onto silica gel. The product was

6.14 (m, 1H, H-13), 6.02 (s, 1H, H-10), 3.95 (s, 3H, H-8), 3.60 (t, 2H, H-19, J=6.4Hz), 2.88 (t, 2H, H-15, J=7.7Hz), 1.77 (m, 2H, H-16), 1.59 (m, 2H, H-18), 1.43 (m, 2H, H-17)

¹³C-NMR (CDCl₃, 125 MHz) δ: 166.55 (C-7), 152.80 (C-14), 149.17 (C-8), 129.40 (C-12), 127.89 (C-1), 126.23 (C-11), 122.28 (C-4), 121.73 (C-5), 118.23 (C-3), 116.57 (C-6), 112.79 (C-13), 112.26 (C-2), 93.40 (C-10), 62.82 (C-11), 59.03 (C-9), 32.35 (C-18), 29.22 (C-16), 28.44 (C-18), 25.44 (C-17)

6.1.8 Synthesis of stereoselectively deuterium-labelled 2-UP analogue

Pent-4-ynyl-2,2-dimethylpropanoate



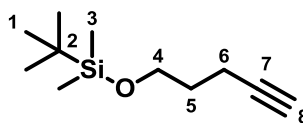
To a solution of 4-pentyne-1-ol (2.00 g, 23.78 mmol), triethyl amine (4.38 ml, 30.91 mmol) and 4-dimethylamino pyridine (140 mg, 1.19 mmol) in CH₂Cl₂ (40 ml), cooled to 0 °C under argon, was added trimethylacetyl chloride (3.22 ml, 26.16 mmol) dropwise. The reaction mixture was allowed to warm to RT over 16 hours. The reaction mixture was diluted with CH₂Cl₂, washed with water, 2M HCl, sat NaHCO₃, dried (MgSO₄) and concentrated under vacuum. The crude product was purified on silica gel (5% EtOAc in pet ether) to give pent-4-ynyl-2,2-dimethylpropanoate (3.86 g, 97% yield) as a colourless oil.

¹H-NMR (CDCl₃, 400 MHz) δ: 4.09 (t, 2H, H-4, J=6.3Hz), 2.22 (td, 2H, H-6, J₁=7.1Hz, J₂=2.6Hz), 1.90 (t, 1H, H-8, J=2.6Hz), 1.80 (qu, 2H, H-5, J=6.7Hz), 1.13 (s, 9H, H-1)

¹³C-NMR (CDCl₃, 100 MHz) δ: 178.50 (C-3), 82.98 (C-8), 68.93 (C-7), 62.84 (C-4), 27.63 (C-5), 27.19 (C-1), 26.52 (C-2), 15.22 (C-6)

HRMS: *m/z* calculated for C₁₀H₁₆O₂ = 169.1223 [M+H]⁺; Found 169.1223

4-Pentyn-1-oxy-(*t*-butyldimethylsilyl)



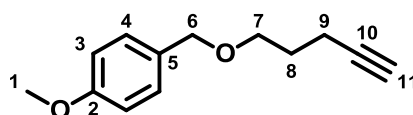
To a solution of 4-pentyn-1-ol (3.00 g, 35.66 mmol) and *t*-butyldimethyl silyl chloride (6.99 g, 46.36 mmol) in CH₂Cl₂ (150 ml), cooled to 0 °C under argon, was added imidazole (3.16 g, 46.36 mmol) and the reaction mixture allowed to stir for 2 hours. TLC showed no starting material so the reaction mixture was diluted with CH₂Cl₂. The organics were washed with water, 2M HCl, sat NaHCO₃, dried (MgSO₄) and concentrated under vacuum to give 4-pentyn-1-oxy-(*t*-butyldimethylsilyl) (7.07 g, 100% yield) as a colourless oil.

¹H-NMR (CDCl₃, 400 MHz) δ: 3.64 (t, 2H, H-4, J=6.0Hz), 2.22 (td, 2H, H-6, J₁=7.0Hz, J₂=2.7Hz), 1.87 (t, 1H, H-8, J=2.6Hz), 1.67 (qu, 2H, H-5, J=6.5Hz), 0.84 (s, 9H, H-1), 0.00 (s, 6H, H-3)

¹³C-NMR (CDCl₃, 100 MHz) δ: 84.01 (C-7), 68.23 (C-8), 61.44 (C-4), 31.53 (C-5), 25.66 (C-1), 18.41 (C-6), 14.85 (C-6), -5.36 (C-3)

HRMS: *m/z* calculated for C₁₁H₂₃OSi = 199.1513 [M+H]⁺; Found 199.1511

1-(4-Methoxybenzyloxy)-pent-4-yne 240



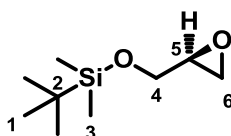
To a suspension of sodium hydride (1.71 g, 71.33 mmol) in DMF (70 ml), cooled to 0 °C under argon, was added 4-pentyn-1-ol (5.00 g, 59.44 mmol) in DMF (50 ml) and stirred for 30 mins. 4-Methoxybenzyl chloride (9.67 ml, 71.33 mmol) was added and the reaction mixture heated to 70 °C for 24 hours. The reaction mixture was poured into water and extracted with EtOAc. The combined organics were washed with water, dried (MgSO₄) and concentrated under vacuum. The crude product was purified on silica gel (7% Et₂O in pet ether) to give 1-(4-methoxybenzyloxy)-pent-4-yne (9.92 g, 83% yield) as a colourless oil.

$^1\text{H-NMR}$ (CDCl_3 , 400 MHz) δ : 7.19 (d, 2H, H-3, $J=8.7\text{Hz}$), 6.80 (d, 2H, H-4, $J=8.6\text{Hz}$), 4.38 (s, 2H, H-6), 3.73 (s, 3H, H-1), 3.47 (t, 2H, H-7, $J=6.1\text{Hz}$), 2.23 (td, 2H, H-9, $J_1=7.1$, $J_2=2.7\text{Hz}$), 1.86 (t, 1H, H-11, $J=2.6\text{Hz}$), 1.80 (qu, 2H, H-8, $J=6.4\text{Hz}$)

$^{13}\text{C-NMR}$ (CDCl_3 , 100 MHz) δ : 159.18 (C-2), 130.58 (C-5), 129.58 (C-3), 113.79 (C-4), 84.03 (C-10), 72.67 (C-6), 68.41 (C-7), 55.30 (C-1), 28.68 (C-8), 15.34 (C-9). 1 signal missing.

HRMS: m/z calculated for $\text{C}_{13}\text{H}_{16}\text{O}_2\text{Na} = 227.1043$ $[\text{M}+\text{H}]^+$; Found 227.1039

(2S)-Oxiran-2-yl-methoxy-1-(*t*-butyldimethylsilyl) S-238



To a solution of *R*(+)-glycidol (1.00 g, 13.50 mmol), 4-dimethylamino pyridine (1.65 g, 13.50 mmol) and triethylamine (3.76 ml, 27.00 mmol) in CH_2Cl_2 (40 ml), cooled to 0°C under argon, was added *t*-butyldimethylsilyl chloride (3.06 g, 20.30 mmol) dropwise over 60 mins. The reaction mixture was allowed to warm to RT over 16 hours. TLC showed no starting material so the reaction mixture was washed with water, 2M HCl, sat NaHCO_3 , dried (MgSO_4) and concentrated under vacuum. The crude product was purified on silica gel (5% EtOAc in pet ether) to give (2S)-oxiran-2-yl-methoxy-1-(*t*-butyldimethylsilyl) (2.18 g, 86% yield) as a colourless oil.

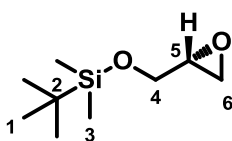
$^1\text{H-NMR}$ (CDCl_3 , 400 MHz) δ : 3.77 (dd, 1H, H-4a, $J_1=11.8\text{Hz}$, $J_2=3.2\text{Hz}$), 3.58 (dd, 1H, H-4b, $J_1=11.8\text{Hz}$, $J_2=4.8\text{Hz}$), 3.01 (m, 1H, H-3), 2.69 (m, 1H, H-6a), 2.55 (1H, H-6b, $J_1=5.1\text{Hz}$, $J_2=2.6\text{Hz}$), 0.83 (s, 9H, H-1), 0.00 (2, 6H, H-3)

$^{13}\text{C-NMR}$ (CDCl_3 , 100 MHz) δ : 63.76 (C-4), 52.44 (C-5), 44.49 (C-6), 25.88 (C-1), 0.05 (C-2), -5.29 (C-3)

IR (cm^{-1}): 1250 (C-O stretch)

HRMS: m/z calculated for $\text{C}_9\text{H}_{20}\text{O}_2\text{SiNa} = 211.1125$ $[\text{M}+\text{H}]^+$; Found 211.1126]

(2R)-Oxiran-2-yl-methoxy-1-(t-butyl dimethylsilyl) R-238



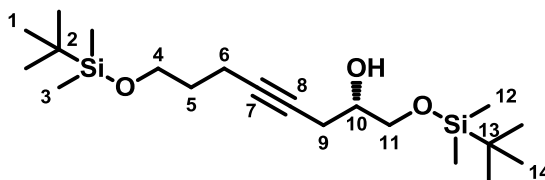
To a solution of *S*-(-)-glycidol (2.00 g, 26.99 mmol), 4-dimethylaminopyridine (4.95 g, 40.50 mmol) and triethylamine (7.51 ml, 53.98 mmol) in CH₂Cl₂ (70 ml), cooled to 0 °C under argon, was added *t*-butyldimethylsilyl chloride (6.10 g, 40.50 mmol) in CH₂Cl₂ (60 ml) dropwise over 60 mins. The reaction was allowed to warm to RT over 4 hours. TLC showed no starting material so the reaction was diluted with CH₂Cl₂ (100 ml). The organics were washed with water, 2M HCl, sat NaHCO₃, dried (MgSO₄) and concentrated under vacuum. The crude product was purified on silica gel (5% EtOAc in pet ether) to give (2*R*)-oxiran-2-yl-methoxy-1-(*t*-butyldimethylsilyl) (4.62 g, 91% yield) as a colourless oil.

¹H-NMR (CDCl₃, 400 MHz) δ: 3.70 (dd, 1H, H-4a, J₁=11.9Hz, J₂=3.2 Hz), 3.61 (dd, 1H, H-4a, J₁=11.9Hz, J₂=4.9Hz), 3.01 (m, 1H, H-5), 2.69 (m, 1H, H-6b), 2.56 (m, 1H, H-6b, J₁=5.2Hz, J₂=2.5Hz), 0.83 (s, 9H, H-1), 0.00 (s, 6H, H-3)

¹³C-NMR (CDCl₃, 100 MHz) δ: 63.76 (C-4), 52.44 (C-5), 44.49 (C-6), 25.88 (C-1), 0.01 (C-2), -5.34 (C-3)

HRMS: *m/z* calculated for C₉H₂₀O₂SiNa = 211.1125 [M+H]⁺; Found 211.1120

(2S)-1,8-bis((t-Butyldimethylsilyl)oxy)oct-4-yn-2-ol



To a solution of 4-pentyn-1-oxy-(*t*-butyldimethylsilyl) (263 mg, 1.33 mmol) in THF (2 ml), cooled to -78 °C under argon, was added *n*-butyl lithium (0.79 ml, 1.17 mmol) dropwise and stirred for 30 mins. Boron trifluoride diethyletherate (0.14 ml, 1.17 mmol) was added followed by (2*S*)-oxiran-2-yl-methoxy-1-(*t*-butyldimethylsilyl) (100 mg, 0.53 mmol) in THF

(1 ml) and stirred for a further 30 mins. TLC showed no SM so the THF was removed under vacuum and loaded onto silica gel. The product was eluted with 10% EtOAc in pet ether to give (2S)-1,8-bis((*t*-butyldimethylsilyl)oxy)oct-4-yn-2-ol (106 mg, 52% yield) as a colourless oil.

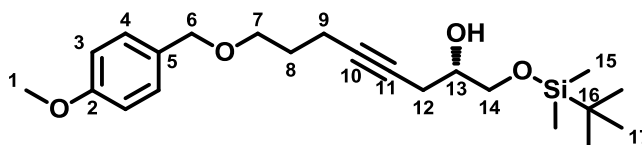
$^1\text{H-NMR}$ (CDCl_3 , 400 MHz) δ : 3.71 (m, 1H, H-10), 3.62 (t, 2H, H-4, $J=6.1\text{Hz}$), 3.53 (dd, 2H, H-11, $J_1=9.6\text{Hz}$, $J_2=5.7\text{Hz}$), 2.33 (m, 2H, H-9), 2.19 (tt, 2H, H-6, $J_1=7.1\text{Hz}$, $J_2=2.4\text{Hz}$), 1.63 (qu, 2H, H-5, $J=6.5\text{Hz}$), 0.86 (s, 9H, H-1 or 14), 0.84 (s, 9H, H-1 or 14), 0.03 (s, 6H, H-3 or 12), 0.00 (s, 6H, H-3 or 12)

$^{13}\text{C-NMR}$ (CDCl_3 , 100 MHz) δ : 81.15 (C-7), 75.85 (C-8), 70.50 (C-10), 65.67 (C-11), 61.70 (C-4), 32.03 (C-5), 25.94, 25.88, 23.44 (C-9), 18.34, 18.08, 15.18 (C-6), -5.31, -5.40

IR (cm^{-1}): 3450 (H-O stretch), 1252 (C-O stretch), 1103 (O-Si stretch)

HRMS : m/z calculated for $\text{C}_{20}\text{H}_{42}\text{O}_3\text{Si}_2\text{H} = 387.2745$ $[\text{M}+\text{H}]^+$; Found 387.2746

(2S)-1-(*t*-Butyldimethylsilyl)oxy-8-((4-methoxyphenyl)methoxy)oct-4-yn-2-ol S-241



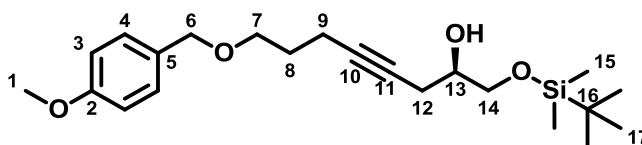
To a solution of 1-(4-methoxybenzyloxy)-pent-4-yne (6.11 g, 29.94 mmol) in THF (150 ml), cooled to -78°C under argon, was added *n*-butyl lithium (16.2 ml, 25.95 mmol) and stirred for 15 mins. (2S)-Oxiran-2-yl-methoxy-1-(*t*-butyldimethylsilyl) (3.76 g, 19.96 mmol) in THF (50 ml) followed by boron trifluoride diethyletherate (3.16 ml, 25.95 mmol) was added and stirred for a further 3 hours. TLC showed no starting material so the reaction mixture was poured into water and extracted with EtOAc. The combined organics were washed with water, dried (MgSO_4) and concentrated under vacuum. The crude product was purified on silica gel (12% EtOAc in pet ether) to give (2S)-1-(*t*-butyldimethylsilyl)oxy-8-((4-methoxyphenyl)methoxy)oct-4-yn-2-ol (7.00 g, 89% yield) as a colourless oil.

$^1\text{H-NMR}$ (CDCl_3 , 400 MHz) δ : 7.18 (d, 2H, H-4, $J=8.6\text{Hz}$), 6.79 (d, 2H, H-3, $J=8.6\text{Hz}$), 4.35 (s, 2H, H-6), 3.72 (s, 3H, H-1), 3.67 – 3.59 (m, 2H, H-13 and 14a), 3.50 (dd, 1H, H-14b, $J_1=9.6\text{Hz}$, $J_2=5.7\text{Hz}$), 3.44 (t, 2H, H-7, $J=6.3\text{Hz}$), 2.37 (m, 1H, H-12a), 2.29 (m, 1H, H-12b), 2.19 (m, 2H, H-9), 1.69 (qu, 2H, H-8, $J=6.5\text{Hz}$), 0.82 (s, 9H, H-17), 0.00 (s, 6H, H-15)

$^{13}\text{C-NMR}$ (CDCl_3 , 100 MHz) δ : 159.10 (C-2), 130.60 (C-5), 129.23 (C-4), 113.78 (C-3), 81.91 (C-10), 72.62 (C-6), 76.06 (C-11), 70.48 (C-13), 68.67 (C-7), 65.67 (C-14), 55.29 (C-1), 29.14 (C-8), 25.88 (C-17), 23.45 (C-12), 18.54 (C-16), 15.67 (C-9), -5.91 (C-15)

HRMS: m/z calculated for $\text{C}_{22}\text{H}_{36}\text{O}_4\text{SiNa}$ = 415.2275 $[\text{M}+\text{Na}]^+$; Found 415.2276

(2R)-1-(*t*-Butyldimethylsilyl)oxy-8-((4-methoxyphenyl)methoxy)oct-4-yn-2-ol R-241



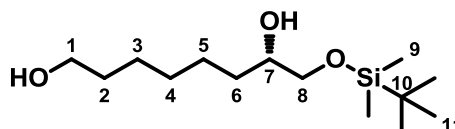
To a solution of 1-(4-methoxybenzyloxy)-pent-4-yne (2.58 g, 12.66 mmol) in THF (80 ml), cooled to -78°C under argon, was added *n*-butyl lithium (7.39 ml, 11.82 mmol) and stirred for 15 mins. (2R)-Oxiran-2-yl-methoxy-1-(*t*-butyldimethylsilyl) (1.59 g, 8.44 mmol) in THF (20 ml) followed by boron trifluoride diethyletherate (1.43 ml, 11.82 mmol) was added and stirred for a further 4 hours. TLC showed no starting material so the reaction mixture was poured into water and extracted with EtOAc. The combined organics were washed with water, dried (MgSO_4) and concentrated under vacuum. The crude product was purified on silica gel (15% EtOAc in pet ether) to give (2R)-1-(*t*-butyldimethylsilyl)oxy-8-((4-methoxyphenyl)methoxy)oct-4-yn-2-ol (2.09 g, 63% yield) as a colourless oil.

$^1\text{H-NMR}$ (CDCl_3 , 400 MHz) δ : 7.24 (d, 2H, H-4, $J=8.6\text{Hz}$), 6.85 (d, 2H, H-3, $J=8.6\text{Hz}$), 4.41 (s, 2H, H-6), 3.78 (s, 3H, H-1), 3.71 (m, 1H, H-13), 3.65 – 3.57 (m, 2H, H-14), 3.50 (t, 2H, H-7, $J=6.2\text{Hz}$), 2.44 (m, 1H, H-12a), 2.34 (m, 1H, H-12b), 2.25 (tt, 2H, H-9, $J_1=7.1\text{Hz}$, $J_2=2.4\text{Hz}$), 1.75 (qu, 2H, H-8, $J=6.8\text{Hz}$), 0.88 (s, 9H, H-17), 0.06 (s, 6H, H-15)

$^{13}\text{C-NMR}$ (CDCl_3 , 100 MHz) δ : 159.09 (C-2), 130.61 (C-5), 129.23 (C-4), 113.77 (C-3), 81.91 (C-10), 76.00 (C-11), 72.62 (C-6), 70.47 (C-13), 68.66 (C-7), 65.66 (C-14), 55.29 (C-1), 29.13 (C-8), 25.89 (C-17), 23.44 (C-12), 18.40 (C-16), 15.67 (C-9), -5.89 (C-15)

HRMS: m/z calculated for $\text{C}_{22}\text{H}_{36}\text{O}_4\text{SiNa}$ = 415.2275 $[\text{M}+\text{Na}]^+$; Found 415.2271

(7S)-8-(*t*-Butyldimethylsilyl)oxyoctan-1,7-diol S-242



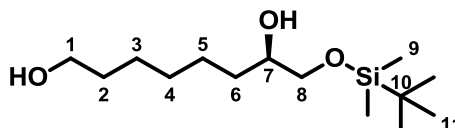
To a solution of (2S)-1-(*t*-butyldimethylsilyl)oxy-8-((4-methoxyphenyl)methoxy)oct-4-yn-2-ol (7.00 g, 17.85 mmol) in THF (150 ml) was added 10% palladium on carbon (300 mg). The reaction flask was flushed with hydrogen gas ten times before being allowed to stir for 24 hours. The reaction mixture was filtered through celite and concentrated under vacuum. The crude product was purified on silica gel (45% EtOAc in pet ether) to give (7S)-8-(*t*-butyldimethylsilyl)oxyoctan-1,7-diol (2.55 g, 52% yield) as a colourless oil.

$^1\text{H-NMR}$ (CDCl_3 , 400 MHz) δ : 3.58 – 3.53 (m, 3H, H-1, 7 and 8a), 3.31 (dd, 1H, H-8b, $J_1=10.1\text{Hz}$, $J_2=8.5\text{Hz}$), 1.61 (m, 2H, H-2), 1.47 – 1.18 (m, 8H, H-3 to 6), 0.83 (s, 9H, H-11), 0.00 (s, 6H, H-9)

$^{13}\text{C-NMR}$ (CDCl_3 , 100 MHz) δ : 71.87 (C-7), 67.29 (C-8), 63.02 (C-1), 32.81, 32.70, 31.79, 29.40, 25.90 (C-11), 25.56, 22.61 (C-10). 1 signal missing.

HRMS: m/z calculated for $\text{C}_{14}\text{H}_{32}\text{O}_3\text{SiNa}$ = 299.2018 $[\text{M}+\text{Na}]^+$; Found 299.2010

(7R)-8-(*t*-Butyldimethylsilyl)oxyoctan-1,7-diol R-242



To a solution of (2R)-1-(*t*-butyldimethylsilyl)oxy-8-((4-methoxyphenyl)methoxy)oct-4-yn-2-ol (2.09 g, 5.33 mmol) in THF (40 ml) was added 10% palladium on carbon (100 mg). The reaction flask was flushed with hydrogen gas ten times before being allowed to stir for 48

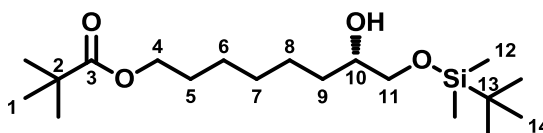
hours. The reaction mixture was filtered through celite and concentrated under vacuum. The crude product was purified on silica gel (45% EtOAc in pet ether) to give (7R)-8-(*t*-butyldimethylsilyl)oxyoctan-1,7-diol (987 mg, 67% yield) as a colourless oil.

$^1\text{H-NMR}$ (CDCl_3 , 400 MHz) δ : 3.57 (m, 4H, H-1, 7 and 8a), 3.31 (m, 1H, H-8b), 1.50 (m, 3H, H-2 and 6a), 1.38 – 1.28 (m, 7H, H-3 to 6b), 0.83 (s, 9H, H-11), 0.00 (s, 6H, H-9)

$^{13}\text{C-NMR}$ (CDCl_3 , 100 MHz) δ : 71.81 (C-7), 67.29 (C-8), 63.01 (C-1), 32.69 (C-6); 29.46, 25.65, 25.56 (C-2 to 5); 32.69 (C-6), 25.90 (C-11). 2 signals missing.

HRMS: m/z calculated for $\text{C}_{14}\text{H}_{32}\text{O}_3\text{SiNa}$ = 299.2018 $[\text{M}+\text{Na}]^+$; Found 299.2013

((7S)-8-(*t*-Butyldimethylsilyl)oxy-7-hydroxy-octyl)-2,2-dimethylpropanoate



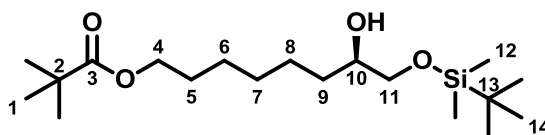
To a solution of (7S)-8-(*t*-butyldimethylsilyl)oxyoctan-1,7-diol (2.55 g, 9.23 mmol) in pyridine (20 ml), cooled to $-20\text{ }^\circ\text{C}$ under argon, was added trimethylacetyl chloride (1.50 ml, 12.00 mmol) in CH_2Cl_2 (15 ml) and stirred for 60 mins. TLC showed no starting material so the reaction was poured into water and extracted with CH_2Cl_2 . The combined organics were washed with water, 2M HCl, sat NaHCO_3 , dried (MgSO_4) and concentrated under vacuum. The crude product was purified on silica gel (10% EtOAc in pet ether) to give ((7S)-8-(*t*-butyldimethylsilyl)oxy-7-hydroxy-octyl)-2,2-dimethylpropanoate (2.56 g, 77% yield) as a colourless oil.

$^1\text{H-NMR}$ (CDCl_3 , 400 MHz) δ : 3.97 (t, 2H, H-4, $J=6.6\text{Hz}$), 3.55 (m, 2H, H-10 and 11a), 3.31 (dd, 1H, H-11b, $J_1=10.1\text{Hz}$, $J_2=8.4\text{Hz}$), 2.34 (m, 1H, H-10), 1.55 (m, 2H, H-5), 1.44 – 1.24 (m, 8H, H-6 to 9), 1.12 (s, 9H, H-1), 0.83 (s, 9H, H-14), 0.00 (s, 6H, H-12)

$^{13}\text{C-NMR}$ (CDCl_3 , 100 MHz) δ : 178.56 (C-3), 71.78 (C-10), 67.28 (C-11), 64.39 (C-4), 38.80 (C-2), 32.70, 29.34, 28.57 (C-5), 27.22 (C-1), 25.90 (C-14), 25.87, 25.50, 18.24 (C-13), -5.30 (C-12)

HRMS: m/z calculated for $C_{19}H_{39}O_4Si$ = 359.2623 $[M+H]^+$; Found = 359.2628

((7R)-8-(*t*-Butyldimethylsilyl)oxy-7-hydroxy-octyl)-2,2-dimethylpropanoate



To a solution of (*7R*)-8-(*t*-butyldimethylsilyl)oxyoctan-1,7-diol (1.05 g, 3.80 mmol) in pyridine (10 ml), cooled to $-20\text{ }^{\circ}\text{C}$ under argon, was added trimethylacetyl chloride (0.61 ml, 4.94 mmol) in CH_2Cl_2 (7 ml) and stirred for 60 mins. TLC showed no starting material so the reaction was poured into water and extracted with CH_2Cl_2 . The combined organics were washed with water, 2M HCl, sat NaHCO_3 , dried (MgSO_4) and concentrated under vacuum. The crude product was purified on silica gel (10% EtOAc in pet ether) to give ((*7R*)-8-(*t*-butyldimethylsilyl)oxy-7-hydroxy-octyl)-2,2-dimethylpropanoate (1.10 g, 80% yield) as a colourless oil.

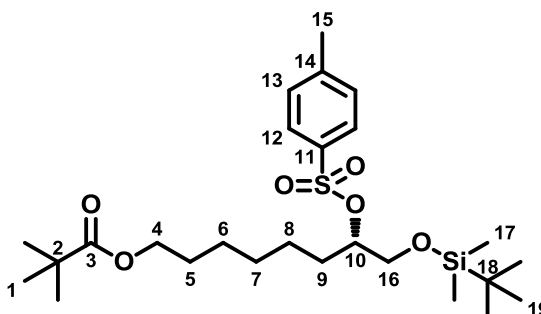
$^1\text{H-NMR}$ (CDCl_3 , 400 MHz) δ : 4.05 (t, 2H, H-4, $J=6.6\text{Hz}$), 3.64 – 3.61 (m, 2H, H-10 and 11a), 3.39 (dd, 1H, H-11b, $J_1=10.6\text{Hz}$, $J_2=8.3\text{Hz}$), 2.39 (bs, 1H, H-O), 1.60 (m, 2H, H-5), 1.45 – 1.36 (m, 8H, H-6 to 9), 1.20 (s, 9H, H-1), 0.91 (s, 9H, H-14), 0.07 (s, 6H, H-12)

$^{13}\text{C-NMR}$ (CDCl_3 , 100 MHz) δ : 178.57 (C-3), 71.78 (C-10), 67.26 (C-11), 64.39 (C-4), 38.81 (C-2), 32.76, 29.35, 28.54 (C-5), 27.23 (C-1), 25.91 (C-14), 25.88, 25.50, 18.25 (C-13), -5.28 (C-12)

HRMS: m/z calculated for $C_{19}H_{39}O_4Si$ = 359.2623 $[M+H]^+$; Found = 359.2621

((7S)-8-(*t*-Butyldimethylsilyl)oxy-7-(*p*-tolylsulphonyloxy)octyl)-2,2-dimethylpropanoate

S-243



To a solution of ((7S)-8-(*t*-butyldimethylsilyl)oxy-7-hydroxy-octyl)-2,2-dimethylpropanoate (2.46 g, 6.83 mmol), 4-dimethylaminopyridine (250 mg, 2.05 mmol) and triethylamine (2.36 ml, 17.08 mmol) in chloroform (35 ml), under argon, was added *p*-toluenesulphonyl chloride (1.69 g, 8.88 mmol) and the reaction heated to 70 °C for 16 hours. The reaction mixture was poured into water and extracted with CH₂Cl₂. The combined organics were washed with water, 2M HCl, sat NaHCO₃ and concentrated under vacuum. The crude product was purified on silica gel (5% EtOAc in pet ether) to give ((7S)-8-(*t*-butyldimethylsilyl)oxy-7-(*p*-tolylsulphonyloxy)octyl)-2,2-dimethylpropanoate (2.82 g, 81% yield) as a colourless oil.

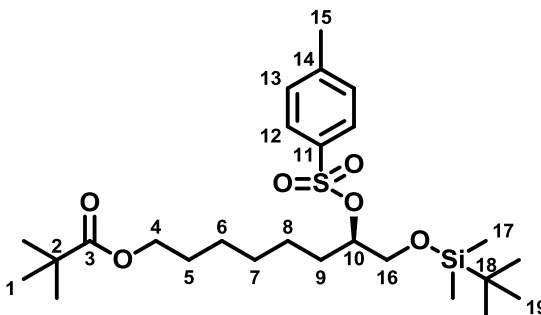
¹H-NMR (CDCl₃, 400 MHz) δ: 7.80 (d, 2H, H-12, J=8.3Hz), 7.33 (dd, 2H, H-13, J=8.2Hz), 4.48 (m, 1H, H-10), 4.02 (t, 2H, H-4, J=6.6Hz), 3.64 (dd, 2H, H-16, J₁=10.9Hz, J₂=4.7Hz), 2.45 (s, 3H, H-15), 1.72 – 1.52 (m, 4H, H-5 and 9), 1.30 – 1.15 (m, 15H, H-6 to 8 and 1), 0.85 (s, 9H, H-19), 0.00 (s, 6H, H-17)

¹³C-NMR (CDCl₃, 100 MHz) δ: 178.57 (C-3), 144.47 (C-14), 134.47 (C-11), 129.67 (C-13), 127.82 (C-12), 83.17 (C-10), 64.30 (C-4), 63.99 (C-16), 38.64 (C-2), 30.99 (C-9), 28.91 (C-5), 28.45, 27.22 (C-1), 25.79 (C-19), 25.70, 24.54, 21.61 (C-15), -5.70 (C-17). 1 signal missing.

HRMS: *m/z* calculated for C₂₆H₄₆O₆SSi = 537.2677 [M+Na]⁺; Found = 537.2678

((7R)-8-(*t*-Butyldimethylsilyl)oxy-7-(*p*-tolylsulphonyloxy)octyl)-2,2-dimethylpropanoate

R-243



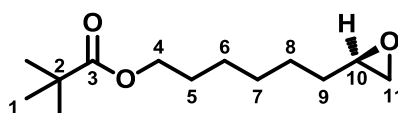
To a solution of ((7R)-8-(*t*-butyldimethylsilyl)oxy-7-hydroxy-octyl)-2,2-dimethylpropanoate (1.96 g, 5.44 mmol), 4-dimethylaminopyridine (200 mg, 1.63 mmol) and triethylamine (1.90 ml, 13.60 mmol) in chloroform (35 ml), under argon, was added *p*-toluenesulphonyl chloride (1.35 g, 7.07 mmol) and the reaction heated to 70 °C for 16 hours. The reaction mixture was poured into water and extracted with CH₂Cl₂. The combined organics were washed with water, 2M HCl, sat NaHCO₃ and concentrated under vacuum. The crude product was purified on silica gel (5% EtOAc in pet ether) to give ((7R)-8-(*t*-butyldimethylsilyl)oxy-7-(*p*-tolylsulphonyloxy)octyl)-2,2-dimethylpropanoate (2.19 g, 79% yield) as a colourless oil.

¹H-NMR (CDCl₃, 400 MHz) δ: 7.79 (d, 2H, H-12, J=8.4Hz), 7.31 (d, 2H, H-13, J=8.3Hz), 4.47 (m, 1H, H-10), 4.02 (t, 2H, H-4, J=6.6Hz), 3.64 (m, 2H, H-16), 2.44 (s, 3H, H-15), 1.67 – 1.54 (m, 4H, H-5 and 9), 1.29 – 1.23 (m, 6H, H-6 to 8), 1.19 (s, 9H, H-1), 0.84 (s, 9H, H-19), 0.00 (s, 6H, H-17)

¹³C-NMR (CDCl₃, 100 MHz) δ: 178.54 (C-3), 144.47 (C-14), 134.47 (C-11), 129.67 (C-13), 127.82 (C-12), 83.18 (C-10), 64.36 (C-4), 63.99 (C-16), 38.65 (C-2), 31.01 (C-9), 28.94 (C-5), 28.43, 27.22 (C-1), 25.74 (C-19), 25.71, 24.54, 21.62 (C-15), -5.69 (C-7). 1 signal missing.

HRMS: *m/z* calculated for C₂₆H₄₆O₆SSi = 537.2677 [M+Na]⁺; Found = 537.2674

6-(2R)-Oxiranhexyl-2,2-dimethylpropanoate R-244



To a solution of ((7S)-8-(*t*-butyldimethylsilyl)oxy-7-(*p*-tolylsulphonyloxy)octyl)-2,2-dimethylpropanoate (2.82 g, 5.48 mmol) in THF (35 ml), under argon, was added tetrabutylammonium fluoride (2.08 g, 6.58 mmol) and stirred for 3 hours. TLC showed no UV active spots and so the solvent was removed under vacuum. The crude product was purified on silica gel (10% EtOAc in pet ether) to give 6-(2R)-oxiranhexyl-2,2-dimethylpropanoate (1.07 g, 86% yield) as a colourless oil.

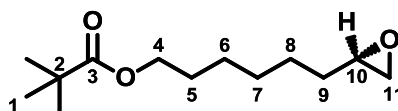
$^1\text{H-NMR}$ (CDCl_3 , 400 MHz) δ : 3.95 (t, 2H, H-4, $J=6.5\text{Hz}$), 2.81 (m, 1H, H-10), 2.65 (dd, 1H, H-11a, $J_1=5.0\text{Hz}$, $J_2=4.2\text{Hz}$), 2.37 (dd, 1H, H-11b, $J_1=5.0\text{Hz}$, $J_2=2.6\text{Hz}$), 1.53 (m, 2H, H-5), 1.45 – 1.25 (m, 8H, H-6 to 9), 1.10 (s, 9H, H-1)

$^{13}\text{C-NMR}$ (CDCl_3 , 100 MHz) δ : 178.46 (C-3), 64.33 (C-4), 52.31 (C-10), 47.10 (C-11), 38.73 (C-2), 32.40 (C-9); 29.05, 28.53 (C-5), 27.22 (C-1), 25.87, 25.66

IR (cm^{-1}): 2930 (C-H stretch), 1725 (C=O stretch), 1152 (C-O epoxide stretch)

HRMS : m/z calculated for $\text{C}_{13}\text{H}_{24}\text{O}_3\text{Na} = 251.1618$ [$\text{M}+\text{Na}$] $^+$; Found = 251.1619

6-(2S)-Oxiranhexyl-2,2-dimethylpropanoate S-244



To a solution of ((7R)-8-(*t*-butyldimethylsilyl)oxy-7-(*p*-tolylsulphonyloxy)octyl)-2,2-dimethylpropanoate (2.19 g, 4.26 mmol) in THF (30 ml), under argon, was added tetrabutylammonium fluoride (1.61 g, 5.11 mmol) and stirred for 3 hours. TLC showed no UV active spots and so the solvent was removed under vacuum. The crude product was purified on silica gel (10% EtOAc in pet ether) to give 6-(2R)-oxiranhexyl-2,2-dimethylpropanoate (696 mg, 72% yield) as a colourless oil.

¹H-NMR (CDCl₃, 400 MHz) δ: 3.95 (t, 2H, H-4, J=6.7Hz), 2.81 (m, 1H, H-10), 2.65 (m, 1H, H-11a), 2.36 (dd, 1H, H-11b, J₁=5.0Hz, J₂=2.7Hz), 1.53 (m, 2H, H-5), 1.45 – 1.27 (m, 8H, H-6 to 9), 1.10 (s, 9H, H-1)

¹³C-NMR (CDCl₃, 100 MHz) δ: 178.59 (C-3), 64.33 (C-3), 52.31 (C-10), 47.11 (C-11), 38.75 (C-2), 32.40, 29.05, 28.53, 27.22 (C-1), 25.87, 25.66

IR (cm⁻¹): 2932 (C-H stretch), 1726 (C=O stretch), 1152 (C-O epoxide stretch)

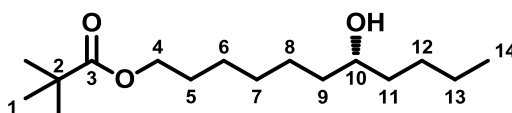
HRMS: *m/z* calculated for C₁₃H₂₄O₃Na = 251.1618 [M+Na]⁺; Found = 251.1619

***n*-Propyl lithium**

To a dried flask was added 25% lithium dispersion in mineral oil (19.45 g, 70.00 mmol) before the flask was flushed with argon. The lithium suspension was washed with hexane (5 x 50 ml), each time allowing time for the lithium to rise to the surface before decanting off the washings.

The clean lithium was suspended in hexane (100 ml) and cooled to 0 °C. To this solution was added 1-chloropropane (28.15 ml, 31.83 mmol) in hexane (25 ml) dropwise over a period of 60 mins. The reaction mixture was stirred for 2 hours before being allowed to warm to RT and stirred for a further 3 hours. After this time, the stirring was stopped and the mixture allowed to stand overnight. The reaction mixture was filtered through a sintered glass funnel *via* a cannula and stored under argon at 4 °C for 3 days. During this time, a fine white precipitate formed and so the mixture was again filtered through a sintered glass funnel and stored under argon. The concentration of *n*-propyl lithium was determined using the method outlined above for *n*-butyl lithium.

(7R)-7-Hydroxyundecyl-2,2-dimethylpropanoate R-247



To a suspension of copper(I) cyanide (467 mg, 5.22 mmol) in Et₂O (50 ml), cooled to -78 °C under argon, was added *n*-propyl lithium (2.44 ml, 6.26 mmol). The reaction mixture was allowed to warm to 0 °C for 15 mins, ensuring that all the solid had dissolved. This was cooled back to -78 °C before 6-(2*R*)-oxiranhexyl-2,2-dimethylpropanoate (596 mg, 2.61 mmol) in Et₂O (20 ml) was added followed by boron trifluoride diethyletherate (0.35 ml, 2.87 mmol). The resulting solution was stirred for 30 mins until TLC showed no starting material. The reaction was quenched by addition of NH₄Cl, poured into water and extracted with EtOAc. The combined organics were washed with 2M HCl, dried (MgSO₄) and concentrated under vacuum. The crude product was purified on silica gel (15% EtOAc in pet ether) to give (7*R*)-7-hydroxyundecyl-2,2-dimethylpropanoate (533 mg, 75% yield) as a colourless oil.

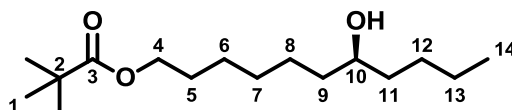
¹H-NMR (CDCl₃, 400 MHz) δ: 3.98 (t, 2H, H-4, J=6.6Hz), 3.52 (m, 1H, H-10), 1.56 (m, 2H, H-5), 1.40 – 1.19 (m, 12H, H-7 to 9, 11 to 13), 1.13 (s, 9H, H-1), 0.84 (t, 3H, H-14, J=7.0Hz)

¹³C-NMR (CDCl₃, 100 MHz) δ: 178.54 (C-3), 71.96 (C-10), 64.40 (C-4), 37.37, 37.24, 29.30, 28.58, 27.86, 27.23 (C-1), 25.92, 25.55, 22.77, 14.09 (C-14). 1 signal missing.

IR (cm⁻¹): 3415 (H-O stretch); 295, 2929, 2857 (C-H stretch); 1728 (C=O stretch)

HRMS: *m/z* calculated for C₁₆H₃₂O₃Na = 295.2244 [M+Na]⁺; Found = 295.2251

(7*S*)-7-Hydroxyundecyl-2,2-dimethylpropanoate S-247



To a suspension of copper(I) cyanide (511 mg, 5.70 mmol) in Et₂O (50 ml), cooled to -78 °C under argon, was added *n*-propyl lithium (2.66 ml, 6.84 mmol). The reaction mixture was allowed to warm to 0 °C for 15 mins, ensuring that all the solid had dissolved. This was cooled back to -78 °C before 6-(2*S*)-oxiranhexyl-2,2-dimethylpropanoate (651 mg, 2.85 mmol) in Et₂O (20 ml) was added followed by boron trifluoride diethyletherate (0.38 ml, 3.14 mmol). The resulting solution was stirred for 30 mins until TLC showed no starting material. The reaction

was quenched by addition of NH_4Cl , poured into water and extracted with EtOAc. The combined organics were washed with 2M HCl, dried (MgSO_4) and concentrated under vacuum. The crude product was purified on silica gel (15% EtOAc in pet ether) to give (7S)-7-hydroxyundecyl-2,2-dimethylpropanoate (387 mg, 50% yield) as a colourless oil.

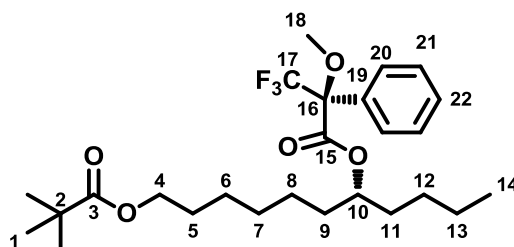
$^1\text{H-NMR}$ (CDCl_3 , 400 MHz) δ : 3.98 (t, 2H, H-4, $J=6.5\text{Hz}$), 3.52 (m, 1H, H-10), 1.54 (m, 2H, H-5), 1.40 – 1.19 (m, 14H, H-6 to 9, 11 to 13), 1.13 (s, 9H, H-1), 0.84 (t, 3H, H-14, $J=6.9\text{Hz}$)

$^{13}\text{C-NMR}$ (CDCl_3 , 100 MHz) δ : 178.52 (C-3), 71.96 (C-10), 64.41 (C-4), 37.37, 37.25, 29.32, 28.58, 27.87, 27.24 (C-1), 25.93, 25.57, 22.79, 14.13 (C-14). 1 signal missing.

IR (cm^{-1}): 3410 (H-O stretch), 1730 (C=O stretch)

HRMS: m/z calculated for $\text{C}_{16}\text{H}_{32}\text{O}_3\text{Na}$ = 295.2244 $[\text{M}+\text{Na}]^+$; Found = 295.2249

((7R)-7-((2S)-3,3,3-Trifluoro-2-methoxy-2-phenyl-propanoyl)undecyloxy)-2,2-dimethylpropanoate (R, S)-255



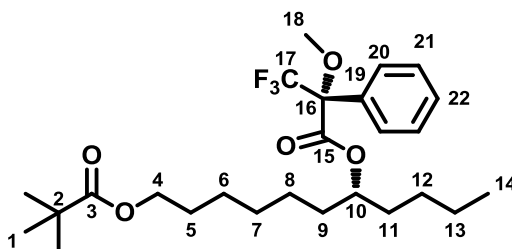
To a solution of (S)- α -methoxy- α -trifluorophenylacetic acid (25 mg, 0.11 mmol) and dicyclohexylcarbodiimide (23 mg, 0.11 mmol) in chloroform (0.8 ml), under argon, was added dimethylaminopyridine (13 mg, 0.11 mmol) and stirred for 15 mins. (7R)-7-Hydroxyundecyl-2,2-dimethylpropanoate (10 mg, 0.037 mmol) in chloroform (0.2 ml) was added and heated to 50 °C for 16 hours. The reaction mixture was filtered through a plug of cotton wool and concentrated under vacuum. The crude product was purified on silica gel (5% EtOAc in pet ether) to give ((7R)-7-((2S)-3,3,3-trifluoro-2-methoxy-2-phenyl-propanoyl)undecyloxy)-2,2-dimethylpropanoate (8 mg, 44% yield) as a colourless oil.

$^1\text{H-NMR}$ (CDCl_3 , 700 MHz) δ : 7.55, 7.39 (m, 5H, H-20 to 22), 5.08 (m, 1H, H-10), 4.02 (t, 2H, H-4, $J=6.4\text{Hz}$), 3.56 (s, 3H, H-18), 1.66 (m, 1H, H-11a), 1.60 – 1.52 (m, 5H, H-5, 9 and 11b), 1.32 – 1.14 (m, 19H, H-1, 6 to 8, 12 and 13), 0.88 (t, 3H, H-14, $J=6.9\text{Hz}$)

$^{13}\text{C-NMR}$ (CDCl_3 , 175 MHz) δ : 178.78 (C-3), 166.47 (C-15), 132.65 (C-19), 129.64, 128.44, 127.47, 123.57 (C-17, qu, $J=289.5\text{Hz}$), 84.61 (C-16, qu, $J=28.3\text{Hz}$), 77.59 (C-10), 64.44 (C-4), 55.57 (C-18), 38.87 (C-2), 33.58, 33.53, 29.08, 28.59 (C-5), 27.51 (C-12), 27.35 (C-1), 25.85, 24.87, 22.63 (C-13), 14.06 (C-14)

HRMS: m/z calculated for $\text{C}_{26}\text{H}_{39}\text{O}_5\text{F}_3\text{Na} = 511.2642$ $[\text{M}+\text{Na}]^+$; Found = 511.2661

((7R)-7-((2R)-3,3,3-Trifluoro-2-methoxy-2-phenyl-propanoyl)undecyloxy)-2,2-dimethylpropanoate (R, R)-255



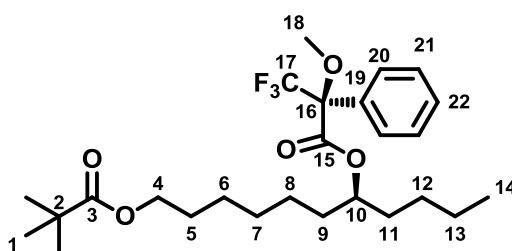
To a solution of (*R*)- α -methoxy- α -trifluorophenylacetic acid (25 mg, 0.11 mmol) and dicyclohexylcarbodiimide (23 mg, 0.11 mmol) in chloroform (0.8 ml), under argon, was added dimethylaminopyridine (13 mg, 0.11 mmol) and stirred for 15 mins. (*7R*)-7-Hydroxyundecyl-2,2-dimethylpropanoate (10 mg, 0.037 mmol) in chloroform (0.2 ml) was added and heated to 50 °C for 16 hours. The reaction mixture was filtered through a plug of cotton wool and concentrated under vacuum. The crude product was purified on silica gel (5% EtOAc in pet ether) to give ((*7R*)-7-((*2R*)-3,3,3-trifluoro-2-methoxy-2-phenyl-propanoyl)undecyloxy)-2,2-dimethylpropanoate (9 mg, 50% yield) as a colourless oil.

$^1\text{H-NMR}$ (CDCl_3 , 700 MHz) δ : 7.54, 7.39 (m, 5H, H-20 to 22), 5.08 (m, 1H, H-10), 4.04 (t, 2H, H-4, $J=6.6\text{Hz}$), 3.55 (s, 3H, H-18), 1.65 (m, 1H, H-9a), 1.61 – 1.52 (m, 5H, H-5, 9b and 11), 1.33 (m, 6H, H-6 to 8), 1.23 – 1.14 (m, 13H, H-1, 12 and 13), 0.82 (t, 3H, H-14, $J=7.1\text{Hz}$)

¹³C-NMR (CDCl₃, 175 MHz) δ: 178.78 (C-3), 166.46 (C-15), 132.61 (C-19), 129.65, 128.45, 127.49, 123.06 (C-17, qu, J=288.7Hz), 84.64 (C-16, qu, J=28.1Hz), 77.57 (C-10), 64.41 (C-4), 55.58 (C-18), 38.88 (C-2), 33.81 (C-9), 33.31 (C-11), 29.17, 28.64 (C-5), 27.34 (C-1), 27.13 (C-12), 25.91, 25.27 (C-8), 22.54 (C-13), 14.01 (C-14)

HRMS: *m/z* calculated for C₂₆H₃₉O₅F₃Na = 511.2642 [M+Na]⁺; Found = 511.2651

((7S)-7-((2S)-3,3,3-Trifluoro-2-methoxy-2-phenyl-propanoyl)undecyloxy)-2,2-dimethylpropanoate (S, S)-255



To a solution of (S)-α-methoxy-α-trifluorophenylacetic acid (25 mg, 0.11 mmol) and dicyclohexylcarbodiimide (23 mg, 0.11 mmol) in chloroform (0.8 ml), under argon, was added 4-dimethylaminopyridine (13 mg, 0.11 mmol) and stirred for 15 mins. (7S)-7-Hydroxyundecyl-2,2-dimethylpropanoate (10 mg, 0.037 mmol) in chloroform (0.2 ml) was added and heated to 50 °C for 16 hours. The reaction mixture was filtered through a plug of cotton wool and concentrated under vacuum. The crude product was purified on silica gel (5% EtOAc in pet ether) to give ((7S)-7-((2S)-3,3,3-trifluoro-2-methoxy-2-phenyl-propanoyl)undecyloxy)-2,2-dimethylpropanoate (10 mg, 56% yield) as a colourless oil.

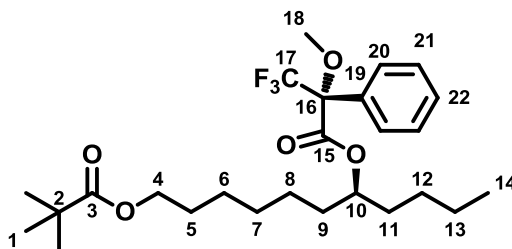
¹H-NMR (CDCl₃, 700 MHz) δ: 7.54, 7.34 (m, 5H, H-20 to 22), 5.09 (m, 1H, H-10), 4.04 (t, 2H, H-4, J=6.5Hz), 3.55 (s, 3H, H-18), 1.65 (m, 1H, H-9a), 1.60 – 1.53 (m, 5H, H-5, 9b and 11), 1.33 (m, 6H, H-6 to 8), 1.25 – 1.14 (m, 13H, H-1, 12 and 13), 0.82 (t, 3H, H-14, J=7.3Hz)

¹³C-NMR (CDCl₃, 175 MHz) δ: 178.64 (C-3), 166.32 (C-15), 132.47 (C-19), 129.51, 128.31, 127.35, 123.41 (qu, C-17, J=288.7Hz), 84.50 (qu, C-16, J=28.3Hz), 77.43 (C-10), 64.27 (C-4),

55.41 (C-18), 38.74 (C-2), 33.67 (C-9), 33.17 (C-11), 29.03, 28.50 (C-5), 27.21 (C-1), 26.99 (C-12), 25.77, 25.13; 22.40 (C-13), 13.87 (C-13)

HRMS: m/z calculated for $C_{26}H_{39}F_3O_5 = 511.2642 [M+Na]^+$; Found 511.2649

((7S)-7-((2R)-3,3,3-Trifluoro-2-methoxy-2-phenyl-propanoyl)undecyloxy)-2,2-dimethylpropanoate (S, R)-255



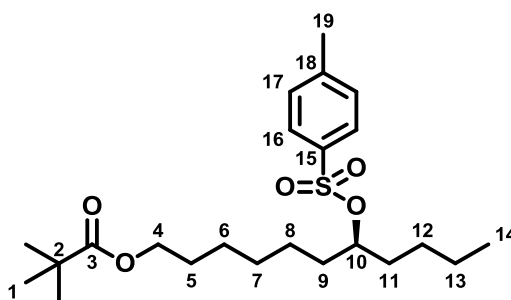
To a solution of (*R*)- α -methoxy- α -trifluorophenylacetic acid (25 mg, 0.11 mmol) and dicyclohexylcarbodiimide (23 mg, 0.11 mmol) in chloroform (0.8 ml), under argon, was added 4-dimethylaminopyridine (13 mg, 0.11 mmol) and stirred for 15 mins. (7*R*)-7-Hydroxyundecyl-2,2-dimethylpropanoate (10 mg, 0.037 mmol) in chloroform (0.2 ml) was added and heated to 50 °C for 16 hours. The reaction mixture was filtered through a plug of cotton wool and concentrated under vacuum. The crude product was purified on silica gel (5% EtOAc in pet ether) to give ((7*S*)-7-((2*R*)-3,3,3-trifluoro-2-methoxy-2-phenyl-propanoyl)undecyloxy)-2,2-dimethylpropanoate (9 mg, 50% yield) as a colourless oil.

1H -NMR (CDCl₃, 700 MHz) δ : 7.54, 7.39 (m, 5H, H-20 to 22), 5.08 (m, 1H, H-10), 4.02 (t, 2H, H-4, $J=6.5$ Hz), 3.56 (s, 3H, H-18), 1.65 (m, 1H, H-11a), 1.59 – 1.54 (m, 5H, H-5, 9 and 11b), 1.31 – 1.16 (m, 19H, H-1, 6 to 8, 12 and 13), 0.88 (t, 3H, H-14, $J=7.0$ Hz)

^{13}C -NMR (CDCl₃, 175 MHz) δ : 178.83 (C-3), 166.51 (C-15), 132.69 (C-19), 129.69, 128.49, 127.51, 123.51 (qu, C-17, $J=288.9$ Hz), 84.66 (qu, C-16, $J=28.4$ Hz), 77.63, (C-10), 64.48 (C-4), 55.62 (C-18), 33.62, 33.57, 29.13, 28.94 (C-2), 28.63 (C-5), 27.39 (C-1), 27.55 (C-12), 25.90, 24.92 (C-6 to 8), 22.68 (C-13), 14.11 (C-14)

HRMS: m/z calculated for $C_{26}H_{39}F_3O_5 = 511.2642 [M+Na]^+$; Found 511.2641

[(7S)-7-(*p*-Tolylsulfonyloxy)undecyl]-2,2-dimethylpropanoate S-248



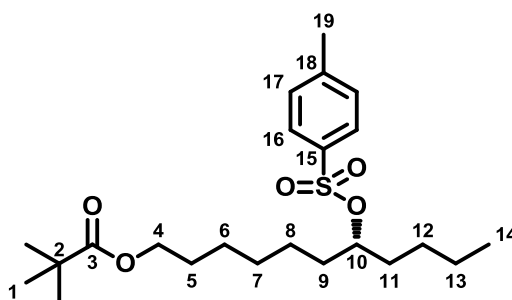
To a solution of (7S)-7-hydroxyundecyl-2,2-dimethylpropanoate (350 mg, 1.28 mmol) in chloroform (20 ml), under argon, was added 4-dimethylaminopyridine (46 mg, 0.38 mmol), triethylamine (0.45 ml, 3.20 mmol) followed by *p*-toluenesulphonyl chloride (316 mg, 1.66 mmol) and heated to 70 °C for 16 hours. The reaction was diluted with CH₂Cl₂ and poured into water. The organic layer was separated, washed with 2M HCl, sat NaHCO₃, dried (MgSO₄) and concentrated under vacuum. The crude product was purified on silica gel (10% EtOAc in pet ether) to give [(7S)-7-(*p*-tolylsulfonyloxy)undecyl]-2,2-dimethylpropanoate (129 mg, 24% yield) as a colourless oil.

¹H-NMR (CDCl₃, 400 MHz) δ: 7.72 (d, 2H, H-16, J=8.2Hz), 7.26 (d, 2H, H-17, J=8.3Hz), 4.47 (m, 1H, H-10), 3.94 (t, 2H, H-4, J=6.6Hz), 2.37 (s, 3H, H-19), 1.49 (m, 6H, H-5, 9 and 11), 1.21 – 1.14 (m, 8H, H-6 to 8, 12), 1.13 (s, 9H, H-1), 0.74 (t, 3H, H-14, J=6.5Hz)

¹³C-NMR (CDCl₃, 100 MHz) δ: 178.57 (C-3), 144.37 (C-18), 134.74 (C-15), 129.65 (C-17), 127.73 (C-16), 84.43 (C-10), 64.31 (C-4), 38.61 (C-2), 34.06, 33.84, 28.94, 28.47, 26.84, 25.73, 24.60, 22.39, 21.63 (C-19), 13.87 (C-14). 1 signal missing.

HRMS: *m/z* calculated for C₂₃H₃₈O₅S = 449.2332 [M+Na]⁺; Found 449.2328

[(7R)-7-(*p*-Tolylsulfonyloxy)undecyl]-2,2-dimethylpropanoate R-248



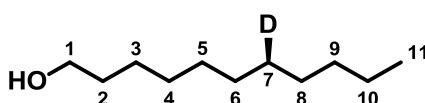
To a solution of (7R)-7-hydroxyundecyl-2,2-dimethylpropanoate (533 mg, 1.96 mmol) in chloroform (30 ml), under argon, was added 4-dimethylaminopyridine (72 mg, 0.59 mmol), triethylamine (0.45 ml, 4.90 mmol) followed by *p*-toluenesulphonyl chloride (486 mg, 2.55 mmol) and heated to 70 °C for 16 hours. The reaction was diluted with CH₂Cl₂ and poured into water. The organic layer was separated, washed with 2M HCl, sat NaHCO₃, dried (MgSO₄) and concentrated under vacuum. The crude product was purified on silica gel (8% EtOAc in pet ether) to give [(7R)-7-(*p*-tolylsulfonyloxy)undecyl]-2,2-dimethylpropanoate (205 mg, 25% yield) as a colourless oil.

¹H-NMR (CDCl₃, 400 MHz) δ: 7.73 (d, 2H, H-16, J=8.2Hz), 7.25 (d, 2H, H-17, J=8.3Hz), 4.48 (m, 1H, H-10), 3.95 (t, 2H, H-4, J=6.4Hz), 2.37 (s, 3H, H-19), 1.49 (m, 6H, H-5, 9 and 11), 1.18 – 1.12 (m, 17H, H-1, 6 to 8, 12 and 13), 0.74 (t, 3H, H-3, J=6.7Hz)

¹³C-NMR (CDCl₃, 100 MHz) δ: 178.54 (C-3), 144.37 (C-18), 134.74 (C-15) 129.64 (C-17), 127.73 (C-16), 84.42 (C-10), 64.32 (C-4), 38.61 (C-2), 34.07, 33.85, 28.93, 27.23 (C-1), 25.73, 24.60, 21.42 (C-19), 13.85 (C-14)

HRMS: *m/z* calculated for C₂₃H₃₈O₅S = 449.2332 [M+Na]⁺; Found 449.2332

(7S)-7-Deuterioundecan-1-ol S-249

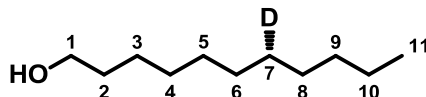


To a suspension of lithium aluminium deuteride (90 mg, 2.15 mmol) in THF (4 ml), cooled to 0 °C under argon, was added [(7*R*)-7-(*p*-tolylsulfonyloxy)undecyl]-2,2-dimethylpropanoate (185 mg, 0.43 mmol) and allowed to warm to RT over 16 hours. The reaction mixture was cooled back to 0 °C and quenched with water before being poured into 1M HCl and extracted with EtOAc. The combined organics were dried (MgSO₄) and concentrated under vacuum. The crude product was purified on silica gel (20% EtOAc in pet ether) to give (7*S*)-7-deuterioundecan-1-ol (18 mg, 24% yield) as a colourless oil.

¹H-NMR (CDCl₃, 400 MHz) δ: 3.57 (m, 2H, H-1), 1.50 (m, 2H, H-2), 1.29 – 1.12 (m, 15H, H-3 to 10), 0.81 (t, 3H, H-11, J=6.6Hz)

¹³C-NMR (CDCl₃, 100 MHz) δ: 63.14 (C-1), 32.84 (C-2), 31.90, 29.71, 29.60, 29.51, 29.45, 29.25, 25.75, 22.70, 14.13 (C-11)

(7*R*)-7-Deuterioundecan-1-ol R-249

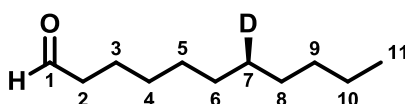


To a suspension of lithium aluminium deuteride (88 mg, 2.10 mmol) in THF (4 ml), cooled to 0 °C under argon, was added [(7*S*)-7-(*p*-tolylsulfonyloxy)undecyl]-2,2-dimethylpropanoate (179 mg, 0.42 mmol) and allowed to warm to RT over 16 hours. The reaction mixture was cooled back to 0 °C and quenched with water before being poured into 1M HCl and extracted with EtOAc. The combined organics were dried (MgSO₄) and concentrated under vacuum. The crude product was purified on silica gel (20% EtOAc in pet ether) to give (7*S*)-7-deuterioundecan-1-ol (41 mg, 56% yield) as a colourless oil.

¹H-NMR (CDCl₃, 400 MHz) δ: 3.57 (m, 2H, H-1), 1.50 (m, 2H, H-2), 1.29 – 1.13 (m, 15H, H-3 to 10), 0.81 (t, 3H, H-11, J=6.6Hz)

¹³C-NMR (CDCl₃, 100 MHz) δ: 63.14 (C-1), 32.89 (C-2), 31.90, 29.71, 29.60, 29.51, 29.46, 29.25, 25.75, 22.70, 14.13 (C-11)

(7S)-7-Deuterioundecanal

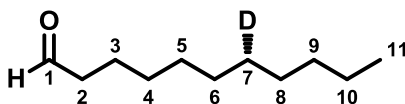


Following the general Swern procedure, the crude product was purified on silica gel (8% EtOAc in pet ether) to give (7S)-deuterioundecanal (10 mg, 59% yield) as a colourless oil.

$^1\text{H-NMR}$ (CDCl_3 , 400 MHz) δ : 9.74 (t, 1H, H-1, $J=1.8\text{Hz}$), 2.40 (td, 2H, H-2, $J_1=7.4\text{Hz}$, $J_2=1.8\text{Hz}$), 1.61 (m, 2H, H-3), 1.27 – 1.23 (m, 13H, H-4 to 10), 0.86 (t, 3H, H-11, $J=6.4\text{Hz}$)

$^{13}\text{C-NMR}$ (CDCl_3 , 100 MHz) δ : 203.04 (C-1), 43.94 (C-2), 31.86, 29.34, 29.20, 22.61, 22.08 (C-3), 14.14 (C-11). 3 signals missing.

(7R)-7-Deuterioundecanal

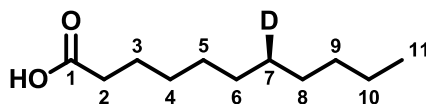


Following the general Swern procedure, the crude product was purified on silica gel (8% EtOAc in pet ether) to give (7R)-deuterioundecanal (26 mg, 67% yield) as a colourless oil.

$^1\text{H-NMR}$ (CDCl_3 , 400 MHz) δ : 9.70 (t, 1H, H-1, $J=1.4\text{Hz}$), 2.35 (td, 2H, H-2, $J_1=7.4\text{Hz}$, $J_2=1.4\text{Hz}$), 1.56 (m, 2H, H-3), 1.27 – 1.22 (m, 13H, H-10), 0.81 (t, 3H, H-11, $J=6.6\text{Hz}$)

$^{13}\text{C-NMR}$ (CDCl_3 , 100 MHz) δ : 203.02 (C-1), 43.94 (C-2), 31.87, 29.34, 29.19, 22.64, 22.11 (C-3), 14.12 (C-11). 3 signals missing.

(7S)-7-Deuterioundecanoic acid S-250



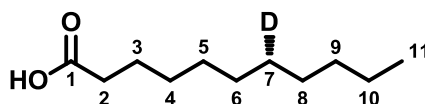
Following the general Oxone procedure gave (7S)-7-deuterioundecanoic acid (8 mg, 74% yield) as a whit solid.

$^1\text{H-NMR}$ (CDCl_3 , 400 MHz) δ : 2.28 (t, 2H, H-2, $J=7.5\text{Hz}$), 1.57 (m, 2H, H-3), 1.26 – 1.19 (m, 13H, H-4 to 10), 0.81 (t, 3H, H-11, $J=6.5\text{Hz}$)

$^{13}\text{C-NMR}$ (CDCl_3 , 100 MHz) δ : 177.74 (C-1), 33.68 (C-2), 31.87, 29.35, 29.21, 29.08, 24.73 (C-3), 14.12 (C-11). 3 signals missing.

HRMS: m/z calculated for $\text{C}_{11}\text{H}_{21}\text{DO}_2 = 186.1610$ [M-H] $^-$; Found 186.1608

(7R)-7-Deuterioundecanoic acid R-250



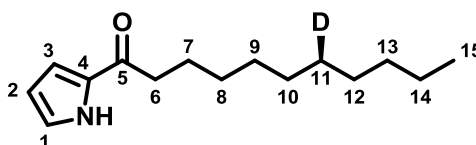
Following the general Oxone procedure gave (7S)-7-deuterioundecanoic acid (21 mg, 75% yield) as a white solid.

$^1\text{H-NMR}$ (CDCl_3 , 400 MHz) δ : 2.28 (t, 2H, H-2, $J=7.5\text{Hz}$), 1.57 (m, 2H, H-3), 1.26 – 1.19 (m, 13H, H-4 to 10), 0.81 (t, 3H, H-11, $J=6.5\text{Hz}$)

$^{13}\text{C-NMR}$ (CDCl_3 , 100 MHz) δ : 177.97 (C-1), 33.71 (C-2), 31.87, 29.34, 29.22, 29.08, 24.72 (C-3), 14.12 (C-11). 3 signals missing.

HRMS: m/z calculated for $\text{C}_{11}\text{H}_{21}\text{DO}_2 = 186.1610$ [M-H] $^-$; Found 186.1610

(7S)-7-Deuterio-1-(1H-pyrrol-2-yl)undecan-1-one



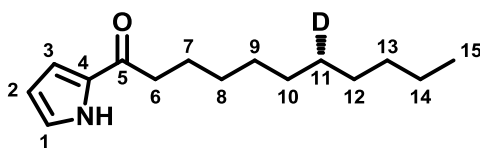
Following the general carboxylic acid coupling procedure, the crude product was purified on silica gel (10% EtOAc in pet ether) to give (7S)-7-deuterio-1-(1H-pyrrol-2-yl)undecan-1-one (8 mg, 87% yield) as a white solid.

$^1\text{H-NMR}$ (CDCl_3 , 400 MHz) δ : 9.20 (bs, 1H, H-N), 6.90 (m, 1H, H-1), 6.85 (m, 1H, H-3), 6.23 (m, 1H, H-2), 2.68 (t, 2H, H-6, $J=7.4\text{Hz}$), 1.64 (m, 2H, H-7), 1.26 – 1.13 (m, 13H, H-8 to 14), 0.81 (t, 3H, H-15)

$^{13}\text{C-NMR}$ (CDCl_3 , 100 MHz) δ : 188.00 (C-5), 131.80 (C-4), 124.31 (C-1), 116.69 (C-3), 110.69 (C-2), 36.71 (C-6), 31.91, 22.69, 14.10 (C-15). 6 signals missing.

HRMS: m/z calculated for $C_{15}H_{24}DNO = 237.2072 [M+H]^+$; Found 237.2070

(7R)-7-Deuterio-1-(1H-pyrrol-2-yl)undecan-1-one



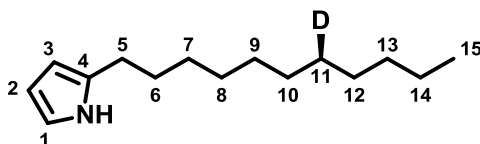
Following the general carboxylic acid coupling procedure, the crude product was purified on silica gel (10% EtOAc in pet ether) to give (7R)-7-deuterio-1-(1H-pyrrol-2-yl)undecan-1-one (16 mg, 63% yield) as a white solid.

1H -NMR ($CDCl_3$, 400 MHz) δ : 9.21 (bs, 1H, H-N), 6.92 (m, 1H, H-1), 6.83 (m, 1H, H-3), 6.21 (m, 1H, H-2), 2.68 (t, 2H, H-6, $J=7.5$ Hz), 1.65 (m, 2H, H-7), 1.28 – 1.15 (m, 13H, H-8 to 14), 0.80 (t, 3H, H-15)

^{13}C -NMR ($CDCl_3$, 100 MHz) δ : 188.01 (C-5), 131.83 (C-4), 124.31 (C-1), 116.69 (C-3), 110.67 (C-2), 36.75 (C-6), 31.91, 22.69, 14.10 (C-15). 6 signals missing.

HRMS: m/z calculated for $C_{15}H_{24}DNO = 237.2072 [M+H]^+$; Found 237.2067

2-((7S)-7-Deuterioundecyl)-pyrrole S-232



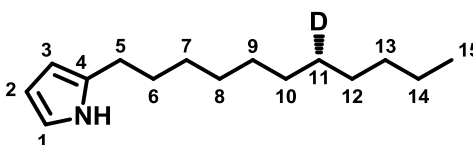
Following the general acyl ketone procedure, the crude product was purified on silica gel (10% EtOAc in pet ether) to give 2-((7S)-7-deuterioundecyl)-pyrrole (8 mg, 54% yield) as a white solid.

1H -NMR ($CDCl_3$, 700 MHz) δ : 7.83 (bs, 1H, H-N), 6.59 (m, 1H, H-1), 6.06 (m, 1H, H-2), 5.84 (m, 1H, H-3), 2.52 (t, 2H, H-5, $J=7.6$ Hz), 1.55 (m, 2H, H-6), 1.26 (m, 2H, H-7), 1.22 – 1.19 (m, 13H, H-8 to 14), 0.81 (t, 3H, H-15, $J=6.7$ Hz)

$^{13}\text{C-NMR}$ (CDCl_3 , 150 MHz) δ : 131.88 (C-4), 114.91 (C-1), 107.21 (C-2), 103.82 (C-3), 30.86, 28.68, 28.65, 28.53, 28.44, 28.27, 28.34, 28.18 (t, C-11, $J=19.3\text{Hz}$), 26.71 (C-5), 13.10 (C-15)

HRMS : m/z calculated for $\text{C}_{15}\text{H}_{26}\text{DN}$ = 223.2279 $[\text{M}+\text{H}]^+$; Found 223.2288

2-((7R))-7-Deuterioundecyl)-pyrrole R-232



Following the general acyl ketone procedure, the crude product was purified on silica gel (10% EtOAc in pet ether) to give 2-((7R))-7-deuterioundecyl)-pyrrole (7 mg, 100% yield) as a white solid.

$^1\text{H-NMR}$ (CDCl_3 , 700 MHz) δ : 7.85 (bs, 1H, H-N), 6.59 (m, 1H, H-1), 6.05 (m, 1H, H-2), 5.84 (m, 1H, H-3), 2.52 (t, 2H, H-5, $J=7.7\text{Hz}$), 1.55 (m, 2H, H-6), 1.28 (m, 2H, H-7), 1.23 – 1.18 (m, 13H, H-8 to 14), 0.81 (t, 3H, H-15, $J=7.0\text{Hz}$)

$^{13}\text{C-NMR}$ (CDCl_3 , 150 MHz) δ : 131.88 (C-4), 114.92 (C-1), 107.20 (C-2), 103.81 (C-3), 30.87, 28.68, 28.66, 28.54, 28.44, 28.27, 28.34, 28.18, (t, C-11, $J=19.4\text{Hz}$), 21.67, 26.71 (C-5), 13.09 (C-15)

HRMS : m/z calculated for $\text{C}_{15}\text{H}_{26}\text{DN}$ = 223.2279 $[\text{M}+\text{H}]^+$; Found 223.2276

6.2 Biology Experimental

Electroporation was carried out using a BioRad GenePulser alongside a BioRad Pulse Controller Plus. Centrifugation was conducted on Eppendorf models 5810R and 5424.

Overlay membranes were purchased from Focus Packaging and Design Ltd and sterilised by autoclaving prior to use.

Additional components of medium was sterilised by autoclaving prior to addition. Trace elements solution was sterilised by filtration through a 0.2µm filter immediately prior to use.

6.2.1 Media and antibiotics

6.2.1.1 R5 medium

Sucrose (103 g), potassium sulphate (0.25 g), magnesium chloride hexahydrate (10 g), glucose (10 g), Casamino acids (0.1 g), Bacto yeast extract (5 g), TES buffer (5 g) and Bacto agar (20 g) was dissolved in distilled water (1 l) and the resulting solution was sterilised by autoclaving. At the time of use, 0.5% potassium dihydrogen phosphate (10 ml; 5 g / l), 5M calcium chloride (4 ml; 732 g / l), 20% L-proline (15 ml; 200 g / l), 1M sodium hydroxide (7 ml; 40 g / l) and trace elements (2 ml; 40 mg zinc(II) chloride, 200 mg iron(III) chloride, 10 mg copper(II) chloride, 10 mg manganese(II) chloride, 10 mg sodium tetraborate, 10 mg ammonium molybdate) was added.

6.2.1.2 GYM medium¹¹⁸

Starch (20 g), malt extract (10 g), glucose (4 g), Bacto yeast extract (4 g), calcium carbonate (2 g) and Bacto agar (15 g) were dissolved in distilled water (1 l) and the resulting solution was sterilised by autoclaving.

6.2.1.3 MP5 medium¹¹⁸

MOPS (20.9 g), Bacto yeast extract (7 g), sodium chloride (5 g), sodium nitrate (1 g) and Bacto agar (15 g) were dissolved in distilled water (1 l) and the pH was adjusted to 7.2 using 2.35M NaOH. The resulting solution was sterilised by autoclaving.

6.2.1.4 Ossamycin production medium

Dry distillate soluble (12.5 g), glucose (10 g), calcium carbonate (10 g) and Bacto agar (15 g) were suspended in distilled water (1 l) and the resulting suspension was sterilised by autoclaving.

6.2.1.5 SMMS medium

Casamino acids (2 g), TES buffer (5.67 g) and Bacto agar (15 g) were dissolved in distilled water (1 l) and the resulting solution was sterilised by autoclaving. At time of use, 50 mM dipotassiumhydrogen phosphate and sodium dihydrogen phosphate (10 ml), 1M magnesium sulphate (5 ml), 50% w/v glucose (18 ml) and trace elements (2 ml; 40 mg zinc(II) chloride, 200 mg iron(III) chloride, 10 mg copper(II) chloride, 10 mg manganese(II) chloride, 10 mg sodium tetraborate, 10 mg ammonium molybdate) were added.

6.2.1.6 SFM medium

Soy flour (20 g), D-mannitol (20 g) and Bacto agar (20 g) were suspended in tap water (1 l) and the resulting suspension was sterilised by autoclaving.

6.2.1.7 LB medium

Tryptone (10 g), Bacto yeast extract (5 g) and sodium chloride (10 g) were dissolved in distilled water (1 l) and the resulting solution was sterilised by autoclaving. For LB plates, Bacto agar (15 g) was added prior to autoclaving.

6.2.1.8 Antibiotics

Antibiotics stock solutions were made as described in Table 6.1 and filtered through a 0.2 µm filter.

Antibiotic	Stock Solution	Working Solutions
Ampicillin	100 mg / 1 ml water	100 µg / 1 ml
Kanamycin	50 mg / 1 ml water	25 µg / 1ml
Chloramphenicol	25 mg / 1 ml water	25 µg / 1 ml
Hygromycin	50 mg / 1 ml water	25 µg / 1 ml
Nalidixic acid	25 mg / 1 ml 0.3M NaOH	25 µg / 1 ml

Table 6.1: Antibiotic stock solutions

6.2.2 Microbial Strains and Plasmids

Bacterial strains used in this work:

- *E. coli* ET12567/pUZ8002 – lab stock from Daniel Zabala
- *Streptomyces coelicolor* A(3)2 ‘wild type’ M511 – lab stock from Paulina Sydor
- *Streptomyces coelicolor* A(3)2 *redL::oriT-apr + redHG* W116 – lab stock from Paulina Sydor
- *Streptomyces coelicolor* A(3)2 M511 Δ *redG::scar* – lab stock from Paulina Sydor
- *Streptomyces albus* ‘wild type’ – lab stock from Paulina Sydor
- *Streptomyces albus* + *redH* – this work
- *Streptomyces albus* + *redHG* – this work

Plasmids used in this work:

- pOSV556 + *redH* – *E. coli* *Streptomyces* shuttle vector containing *redH* under control of the *ermE** promoter, ampicillin and hygromycin resistance gene, *oriT*, the *attP* *Streptomyces* chromosomal integration site and the corresponding integrase

- pOSV556 + *redHG* – *E. coli* *Streptomyces* shuttle vector containing *redHG* under control of the *ermE** promoter, ampicillin and hygromycin resistance gene, *oriT*, the *attP Streptomyces* chromosomal integration site and the corresponding integrase

6.2.3 Preparation and Transformation of Electrocompetent *E. coli* ET12567/pUZ8002

E. coli ET12567/pUZ8002, provided by Daniel Zabala, was inoculated into 10 ml of liquid LB, containing the appropriate antibiotics, and the resulting culture was grown at 37 °C overnight. 100 µl of this preculture was used to inoculate 10 ml of fresh liquid LB and the resulting culture grown to an OD₆₀₀ 5-6 over 3-4 hours. This culture was centrifuged at 3000 rpm and the supernatant was decanted. The cell pellet was resuspended in 10% glycerol and washed twice more with 10 ml of fresh liquid LB. The cell pellet was resuspended in 10% glycerol (100 µl).

A solution of the appropriate plasmid (3 µl) was added to 100 µl of electrocompetent *E. coli* ET12567/pUZ8002 and the resulting suspension was transferred to an ice cold 0.3 cm electroporation cuvette. Electroporation was performed using a BioRad GenePulser II set to 1.8 kV, with a time constant recorded between 4.8 and 5.0 ms. Ice cold liquid LB (1 ml) was added and the resulting mixture was transferred to a sterile 1.5 ml emicrocentrifuge tube, shaken at 180 rpm at 37 °C for 1 hour. The resulting suspension was spread on LB agar containing chloramphenicol, kanamycin and ampicillin.

6.2.4 Conjugation of plasmid with *Streptomyces albus*

A single transformant of *E. coli* ET12567/pUZ8002, as prepared in Section 6.2.3, was used to inoculate 10 ml of liquid LB containing chloramphenicol, kanamycin and hygromycin and the resulting culture was grown at 37 °C overnight. 100 µl of this preculture was used to inoculate 10 ml of fresh liquid LB containing chloramphenicol, kanamycin and hygromycin and the resulting culture was grown to an OD₆₀₀ 5-6 over 3-4 hours. This culture was centrifuged at 3000 rpm and the supernatant was decanted. The resulting cell pellet was resuspended in LB

medium and washed twice more with 10 ml fresh liquid LB. The final cell pellet was resuspended in 0.5 ml of liquid LB.

15 μ l of a *Streptomyces albus* spore stock was added to 0.5 ml of liquid LB and the resulting suspension was heat-shocked at 42 °C for 10 mins, left at 30 °C for 3 hours. The spores were mixed with the *E. coli* cells and the mixture was briefly centrifuged to pellet the cells. The supernatant was decanted and the resulting pellet was serially diluted with sterile water and spread on SFM agar medium containing 10 mM magnesium chloride. After growing for 16 hours, the plates were overlaid with 1 ml of water containing nalidixic acid and hygromycin to select for the desired transconjugants. After a further 5 – 7 days growth at 30 °C, a single colony was picked and spread on SFM agar medium containing nalidixic acid and hygromycin. The resulting culture was grown for a further 7 days at 30 °C.

6.2.5 General procedure for *Streptomyces* spore stock creation

To mannitol-soy flour agar plates was added 20 μ l of a spore stock suspension. The spores were spread across the surface with an inoculation loop and the resulting culture incubated at 30 °C for 7 days. Sterile water (10 ml) was added to the surface of the plate and the spores were suspended in the water by agitation with a sterile inoculation loop. The suspension was filtered through sterile glass wool into 15 ml sterile tubes and centrifuged at 3000 rpm for 10 mins. The liquid was decanted and the pelleted spores were suspended in 0.5 ml 25% glycerol. This spore suspension was stored at -20 °C.

6.2.6 'Suspension' feeding method to *Streptomyces coelicolor*

Plates containing R5 agar medium plated were overlaid with sterile membranes (12 – 14 kDa molecular weight cut off). 7 μ l of the appropriate *Streptomyces* strain spore stock were added to the sterile membrane and spread with an inoculation loop. After 3 days incubation at 30 °C, 3 mg of 2-UP or an analogue in 200 μ l of methanol was diluted with 2 ml of water and the resulting suspension distributed around the plate as small droplets. After a further 2 days

of incubation at 30 °C, the biomass was scrapped off the membrane into a glass vial using a scalpel. 5 ml of 0.1M HCl in methanol was added to the glass vial and the resulting suspension was sonicated for 5 min. 100 µl of this extract was diluted with 0.5 ml of methanol and the resulting suspension was filtered through a 0.2 µm spin filter. Methanol was added to give a total volume of 1 ml and the sample was analysed by LC-MS.

6.2.7 'Precipitation' feeding method to *Streptomyces coelicolor*

Plates containing R5 agar medium plated were overlaid with sterile membranes (12 – 14 kDa molecular weight cut off). 7 µl of the appropriate *Streptomyces* strain spore stock was added to the sterile membrane and spread with an inoculation loop. After 3 days incubation at 30 °C, 2 ml of water was added to the culture followed by 3 mg of 2-UP or an analogue in 200 µl of methanol. After a further 2 days of incubation at 30 °C, the biomass was scrapped off the membrane into a glass vial using a scalpel. 5 ml of 0.1M HCl in methanol was added to the glass vial and the resulting suspension was sonicated for 5 min. 100 µl of this extract was diluted with 0.5 ml of methanol and the resulting suspension was filtered through a 0.2 µm spin filter. Methanol was added to give a total volume of 1 ml and the sample was analysed by LC-MS.

6.2.8 Feeding method to *Streptomyces albus*

Plates containing R5 agar medium plated were overlaid with sterile membranes (12 – 14 kDa molecular weight cut off). 7 µl of the appropriate *Streptomyces* strain spore stock was added to the sterile membrane and spread with an inoculation loop. After 2 days incubation at 30 °C, 3 mg of 2-UP or an analogue in 100 µl of methanol and 3 mg of MBC in 100 µl of DMSO was mixed together and added to the plate as small droplets. After a further 2 days incubation at 30 °C, the biomass was scrapped off into a glass vial using a scalpel. 5 ml of 0.1M HCl in methanol was added to the glass vial and the resulting suspension was sonicated for 5 min. 100 µl of this extract was diluted with 0.5 ml of methanol and the resulting

suspension was filtered through a 0.2 µm spin filter. Methanol was added to give a total volume of 1 ml and the sample was analysed by LC-MS.

6.3 HPLC and LC-MS Experimental

6.3.1 HPLC purification

HPLC purification was performed on an Agilent 1200 HPLC instrument fitted with an Agilent Zorbax XDB-C18 column (21.2 x 150 mm, 5 µm, 25°C) with a flow rate of 20 ml / min. Samples were monitored at 533 nm and collected using an automated fraction collector set to a threshold of 400 mAU.

HPLC grade methanol and water was purchased from either Fisher Scientific or Sigma Aldrich. HPLC grade formic acid was purchased from Sigma Aldrich and used within one month of opening.

HPLC grade formic acid (1 ml / l) was added to HPLC grade methanol and water and filtered through Nylon 0.2 µm membranes purchased from GE Healthcare immediately prior to use.

Time (min)	Water % (0.1% formic acid)	Methanol % (0.1% formic acid)
0.00	60	40
5.00	60	40
20.00	0	100
25.00	0	100
30.00	60	40

Table 6.2: HPLC conditions used for the purification of **76** and **102**

Time (min)	Water %	Methanol %
	(0.1% formic acid)	(0.1% formic acid)
0.00	80	20
5.00	80	20
25.00	0	100
30.00	0	100
35.00	80	20

Table 6.3: HPLC conditions used for the purification of **103** and **256**

6.3.2 LC-MS analysis

Low resolution LC-MS analysis was performed on an Agilent 1100 HPLC instrument fitted with an Agilent Eclipse XDB-C18 column (4.6 x 150 mm, 5 μ m, 25°C) connected to a Bruker HCT ultra mass spectrometer, using either of the elution profile shown in Table 6.4 or 6.5.

Time (min)	Water %	Methanol %
	(0.1% formic acid)	(0.1% formic acid)
0.00	50	50
3.00	50	50
7.00	25	75
24.00	20	80
26.00	50	50

Table 6.4: Elution profile for low resolution LC-MS analysis

Time (min)	Water % (0.1% formic acid)	Methanol % (0.1% formic acid)
0.00	80	20
3.00	80	20
25.00	0	100
27.00	0	100
30.00	80	20

Table 6.5: Alternative elution profile for low resolution LC-MS analysis

High resolution LC-MS analysis was performed using a Dionex 3000 R5 UHPLC instrument fitted with an Agilent Zorbax Eclipse Plus C18 600 Bar (2.1 x 100 mm, 1.8 μ m, 25°C) connected to a Bruker Maxis Impact mass spectrometer, using the elution profile shown in Table 6.6.

Time (min)	Water % (0.1% formic acid)	Methanol % (0.1% formic acid)
0.00	95	5
5.00	95	5
17.00	0	100
23.00	0	100
25.00	95	5

Table 6.6: Elution profile for high resolution LC-MS

6.3.3 Homochiral stationary phase HPLC analysis of Mosher esters (*S, R*)-, (*S, S*)-, (*R, R*)- and (*R, S*)-255

Liquid chromatography on a homochiral stationary phase was used to determine the enantiomeric mixture of the four Mosher diastereomeric esters. Samples were prepared by dissolving 2 mg of Mosher ester in 150 μ l hexane + 0.1% diethylamine. Analysis was performed on an Agilent 1100 HPLC instrument fitted with a Chiral Technologies Europe

ChiralPak IA column (4.6 mm x 250 mm, 25 °C), using the elution profile shown in Table 6.7, with a flow rate of 1 ml/ min. Peaks were collected into individual vials and injected directly into a Bruker Maxis mass spectrometer.

Time (min)	Hexane % (0.1% diethylamine)	Isopropanol % (0.1% diethylamine)
0.00	100	0
5.00	100	0
30.00	50	50
35.00	50	50
40.00	95	5

Table 6.7: Elution profile for HPLC analysis of Mosher esters on a homochiral stationary phase

6.3.3 Homochiral stationary phase HPLC analysis of streptorubin B deuterium analogues

R5 media plated were overlaid with sterile membranes (12 – 14 kDa molecular weight cut off). 7 µl of the *S. albus* + *redHG* spore stock was added to the sterile membrane and spread with an inoculation loop. After 2 days incubation at 30 °C, 3 mg of **S-232** or **R-232** in 100 µl methanol and 3 mg of MBC in 100 µl DMSO was mixed together and added to the plate as small droplets. After a further 2 days incubation at 30 °C, the biomass were scrapped off into plastic tube using a scalpel. 5 ml of 0.1M HCl in methanol was added to the plastic tube and sonicated for 5 mins. The resulting suspension was centrifuged at 3000 rpm for 10 mins before the supernatant was decanted; this process was repeated twice more. The combined organic extracts were concentrated under vacuum before resuspending in 200 µl CH₂Cl₂. This red solution was loaded onto basic alumina and eluted with 5% EtOAc in hexane, collecting the yellow fractions. The solvent was removed under vacuum and resuspended in 1 ml 0.1% HCl methanol. HPLC purification using the elution profile shown in Table 6.8 provided the desired streptorubin B analogues. The solvent from the combined fractions was removed

under vacuum and the resulting aqueous layer adjusted to pH 9 with sat NaHCO₃. The yellow pigment was extract with EtOAc, dried (MgSO₄) and concentrated under vacuum.

These streptorubin B free bases were analysed *via* HPLC using a homochiral stationary phase. Samples were prepared as the free bases and dissolved in 50 µl hexane / isopropanol (95:5) + 0.1% diethylamine. Analysis was performed on an Agilent 1100 HPLC instrument fitted with a Chiral Technologies Europe ChiralPak IA column (4.6 mm x 250 mm, 25 °C), using the elution profile shown in Table 6.9, with a flow rate of 1 ml/ min. Peaks were collected into individual vials and injected directly into a Bruker Maxis mass spectrometer.

Time (min)	Water % (0.1% formic acid)	Methanol % (0.1% formic acid)
0.00	30	70
5.00	30	70
7.50	20	80
10.00	0	100
14.50	0	100
15.00	30	70

Table 6.8: HPLC conditions used for the purification of deuterium labelled streptorubin B analogues

Time (min)	Hexane % (0.1% diethylamine)	Isopropanol % (0.1% diethylamine)
0.00	95	5
20.00	95	5
21.00	90	10
50.00	90	10
51.00	95	5
60.00	95	5

Table 6.9: Elution profile for HPLC analysis of deuterium labelled streptorubin B analogues on a homochiral stationary phase

7. References

References

1. R. P. Williams, C. L. Gott, S. M. Qadri, R. H. Scott, *J. Bacteriol.*, **106**, 1971, 438 – 444
2. F. Wrede, A. Rothhas, *Z. Physiol. Chem.*, **219**, 1933, 267
3. N. N. Gerber, *Tetrahedron Lett.*, **11**, 1970, 809 – 812
4. R. F. Tsuji, M. Yamamoto, A. Nakamura, T. Kotaoka, J. Magae, K. Nagai, M. Yamashita, *J. Antibiot. (Tokyo)*, **43**, 1990, 1293 – 1301
5. R. F. Tsuji, J. Magae, K. Nagai, M. Yamashita, K. Nagai, M. Yamasaki, *J. Antibiot. (Tokyo)*, **45**, 1992, 1295 – 1302
6. A. Mortellaro, S. Songia, P. Gnocchi, M. Terrari, C. Fornasiero, R. D'Alessio, *J. Immunol.*, **162**, 1999, 7102
7. R. D'Alessio, A. Bargiotti, O. Carlini, F. Colotta, M. Ferrari, P. Gnocchi, *et al.*, *J. Med. Chem.*, **43**, 2000, 2557 – 2565
8. B. Montaner, S. Navarro, M. Pique, M. Vilaseca, M. Martinell, E. Giralt, *et al.*, *Br. J. Pharmacol.*, **131**, 2000, 585 – 593
9. S. T. Trudel, Z. H. Li, J. Rauw, R. E. Tiedemann, X. Y. Wen., A. K. Stewart, *Blood*, **109**, 2007, 5430 – 5438
10. L. Chen, S. N. Willis, A. Wei, B. J. Smith, J. I. Fletcher, M. G. Hinds, P. M. Colman, C. L. Day, J. M. Adams, D. C. S. Huang, *Molecular Cell*, **17**, 2005, 393 – 403
11. K. Papireddy, M. Smilkstein, J. X. Kelly, S. Shaimaa, M. Salem, M. Alhamadsheh, S. W. Haynes, G. L. Challis, K. A. Reynolds, *J. Med. Chem.*, **54**, 2011, 5296 – 5306
12. T. Kieser, M. J. Bibb, M. J. Buttner, K. F. Chater, D. A. Hopwood, *Practical Streptomyces Genetics 2nd Edn*
13. S, D, Bently, K. F. Chater, A. M. Cerdeno-Tarranga, G. L. Challis, N. R. Thomson, K. D. James, D. E. Harris, M. A. Quail, H. Kieser, D. Harper, A. Bateman, S. Brown, G. Chandra, C. Chen, M. Collins, A. Cronin, A. Fraser, A. A. Goble, J. Hidalgo, T. Hornsby, S. Howarth, C. H. Huang, T. Kieser, L. Larke, L. Murphy, K. Oliver, S. O'Neil, E. Rabinowitsch, M. A.

- Rajandream, K. Rutherford, S. Rutter, K. S. D. Seegar, R. Squares, K. Taylor, T. Warren, A. Wietzorrek, J. Woodward, B. G. Barrel, J. Parkhill, D. A. Hopwood, *Nature*, **417**, 2002, 141 – 147
14. F. Wrede, A. Rothhaas, *Z. Physiol. Chem.*, **226**, 1934, 95
 15. H. H. Wasserman, J. E. McKeon, U. V. Santer, *Biochem. Biophys. Res. Commun.*, **3**, 1960, 146 – 149
 16. H. H. Wasserman, D. J. Friedland, D. A. Morrison, *Tetrahedron Lett.*, **9**, 1968, 641 – 644
 17. D. A. Morrison, *J. Bacteriol.*, **91**, 1966, 1599 – 1604
 18. H. H. Wasserman, C. K. Shaw, R. J. Sykes, *Tetrahedron Lett.*, **33**, 1974, 2787 – 2790
 19. R. P. Williams, *Appl. Microbiol.*, **25**, 1973, 396 – 402
 20. H. H. Wasserman, R. J. Sykes, P. Peverada, C. K. Shaw, R. J. Cushley, C. R. Lipsky, *J. Am. Chem. Soc.*, **95**, 1973, 6874 – 6875
 21. N. Gerber, A. McInnes, D. Smith, J. Walter, J. Wright, L. Vining, *Can. J. Chem.*, **56**, 1978, 1155 – 1163
 22. N. R. Williamson, H. T. Simonsen, R. A. A. Ahmed, G. Goldet, H. Slater, F. J. Leeper, G. P. C. Salmond, *Mol. Microbiol.*, **56**, 2005, 971 – 989
 23. A. E. Stanley, L. J. Walton, M. Z. Kourdi, C. Corre, G. L. Challis, *Chem. Commun.*, **38**, 2006, 3981 – 3983
 24. S. Mo, P. K. Sydor, C. Corre, M. M. Alhamadsheh, A. E. Stanley, S. W. Haynes, L. Song, K. A. Reynolds, G. L. Challis, *Chem. Biol.*, **15**, 2008, 137 – 148
 25. S. Mo, B. S. Kim, K. A. Reynolds, *Chem. Biol.*, **38**, 2005, 191 – 200
 26. J. White, M. J. Bibb, *J. Bacteriol.*, **179**, 1997, 627 – 633
 27. S. W. Haynes, P. K. Sydor, A. E. Stanley, L. Song, G. L. Challis, *Chem. Commun.*, **38**, 2008, 3981 – 3983
 28. A. M. Cerdeño, M. J. Bibb, G. L. Challis, *Chem. Biol.*, **8**, 2001, 817 – 829
 29. M. G. Thomas, M. D. Burkart, C. T. Walsh, *Chem. Biol.*, **9**, 2002, 171 – 184
 30. Unpublished data from Challis group

31. J. R. Whicher, G. Florova, P. K. Sydor, R. Singh, M. Alhamadsheh, G. L. Challis, K. A. Reynolds, J. L. Smith, *J. Niol. Chem.*, **286**, 2011, 22558 – 22569
32. S. W. Haynes, P. K. Sydor, A. E. Stanley, L. Song, G. L. Challis, *Chem. Commun.*, **16**, 2008, 1865 – 1687
33. P. K. Sydor, S. M. Barry, O. M. Odulate, F. Barona-Gomez, S. W. Haynes, C. Corre, L. Song, G. L. Challis, *Nature Chemistry*, **3**, 2011, 388 – 392
34. L. Lei, M. R. Waterman, A. J. Fulco, S. L. Kelly, D. C. Lamb, *Proc. Natl. Acad. Sci. U.S.A.*, **101**, 2004, 494 – 499
35. T. D. H. Bugg, S. Ramaswamy, *Curr. Opin. Chem. Biol.*, **12**, 2008, 134 – 140
36. A. Bassan, M. R. A. Blomberg, P. E. M. Siegahn, *J. Biol. Inorg. Chem.*, **9**, 2004, 439 – 452
37. L. P. Wackett, *Enzyme Microb. Tech.*, **31**, 2002, 577 – 587
38. V. Rizzo, A. Morelli, V. Pincioli, D. Sciangula, R. D'Alessio, *J. Pharm. Sci.*, **88**, 1999, 73 – 78
39. S. W. Haynes, P. K. Sydor, C. Corre, L. Song, G. L. Challis, *J. Am. Chem. Soc.*, **133**, 2011, 1793 – 1798
40. H. H. Wasserman, G. C. Rodgers, D. D. Keith, *Chem. Comm.*, **22**, 1966, 825 – 826
41. D'Alessio, R.; Rossi, A. *Synlett*, 1996, 513-514
42. H. H. Wasserman, D. D. Kieth, J. Nadelson, *J. Am. Chem. Soc.*, **91**, 1969, 1264 – 1265
43. Furstner, A.; Szillat, H.; Gabor, B.; Mynott, R. *J. Am. Chem. Soc.*, **1998**, *120*, 8305-8314
44. Furstner, A.; Krause, H. *J. Org. Chem.*, **64**, 1999, 8281-8286
45. M. D. Clift, R. J. Thomson, *J. Am. Chem. Soc.*, **131**, 2009, 14579 – 14583
46. Furstner, A.; Szillat, H.; Gabor, B.; Mynott, R. *J. Am. Chem. Soc.* **120**, 1998, 8305-8314
47. D. X. Hu, M. D. Clift, K. E. Lazarski, R. J. Thomson, *J. Am. Chem. Soc.*, **133**, 2011, 1799 – 1804
48. Stuart Haynes PhD Thesis, University of Warwick, 2010
49. G. Attardo, K. Dairi, J. F. Lavallée, E. Rioux, S. Tripathy, PCT International Application, WO 2004/1063282004

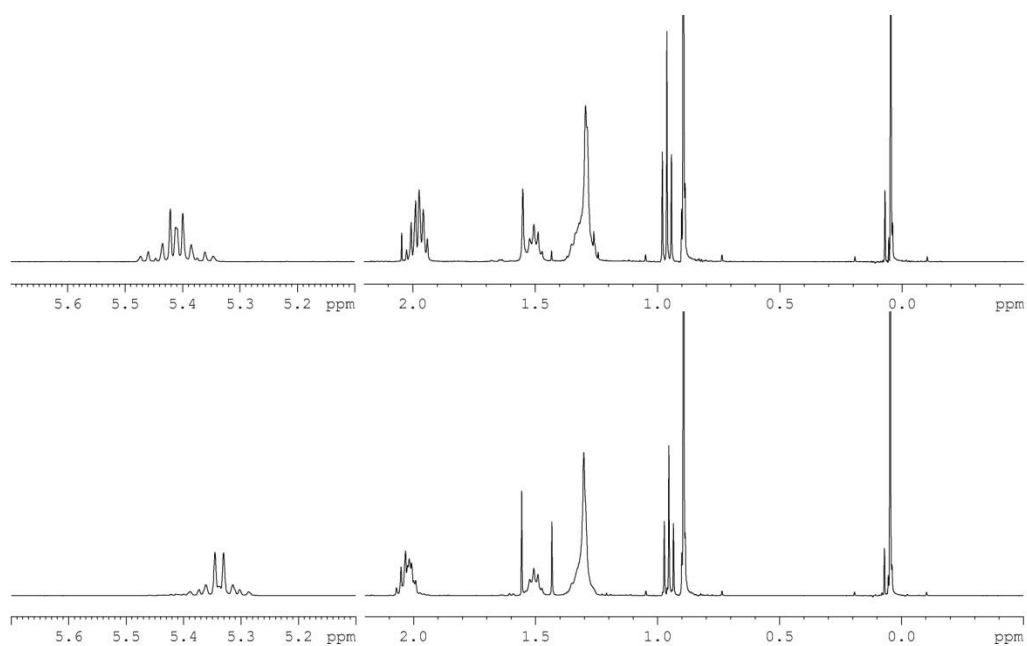
50. K. Dairi, S. Tripathy, G. Attardo, J. F. Lavallée, *Tetrahedron Lett.*, **47**, 2006, 2605 – 2606
51. D. M. Pinkerton, M. G. Banwall, A. C. Willis, *Org. Lett.*, **9**, 2007, 5127 – 5130
52. I. Hasan, E. R. Marinelli, L. C. Lin, F. W. Fowler, A. B. Levy, *J. Org. Chem.*, **46**, 1981, 157 – 164
53. D. W. Slocum, C. A. Jennings, *J. Org. Chem.*, **41**, 1976, 3653 – 3664
54. K. C. Nicolaou, D. A. Claremon, D. P. Papahatjis, *Tetrahedron Lett.*, **22**, 1981, 4647 – 4650
55. M. Araki, S. Sakata, H. Takei, T. Mukaiyama, *B. Chem. Soc. Japan*, **47**, 1974, 1777 – 1780
56. T. Endo, S. Ikenaga, T. Mukaiyama, *B. Chem. Soc. Japan*, **43**, 1970, 2632 – 2633
57. P. G. McDougal, J. G. Rico, Y. Oh, B. D. Condon, *J. Org. Chem.*, **51**, 1986, 3388 – 3390
58. B. R. Travis, M. Sivakumar, G. O. Hollist, B. Borhan, *Org. Lett.*, **5**, 2003, 1031 – 1034
59. M. Renz, B. Meunier, *Eur. J. Org. Chem.*, **4**, 1999, 737 – 750
60. K. Omura, D. Swern, *Tetrahedron*, **34**, 1978, 1651 – 1660
61. J. D. More, N. S. Finney, *Org. Lett.*, **4**, 2002, 3001 – 3003
62. V. Satam, A. Harad, R. Rajule, H. Pati, *Tetrahedron*, **66**, 2010, 7659 – 7706
63. K. Nagajima, M. Kojima, J. Fujita, *Chem. Lett.*, 1986, 1483
64. N. I. Burzlaff, P. J. Rutledge, I. J. Clifton, C. M. H. Hensgens, M. Pickford, R. M. Adlington, P. L. Roach, J. E. Baldwin, *Nature*, **401**, 1999, 721 – 724
65. K. E. Liu, C. C. Johnson, M. Newcomb, S. J. Lippard, *J. Am. Chem. Soc.*, **115**, 1993, 939 – 947
66. M. Dai, I. J. Krauss, S. J. Danishefsky, *J. Org. Chem.*, **73**, 2008, 9576 – 9583
67. R. M. Dixon, B. T. Golding, S. Mwesigye-Kibende, D. N. Ramakrishna, *Phil. Trans. R. Soc. London Ser B 311*, **531**, 1985, 531 – 544
68. S. Chakrabarty, R. N. Austin, D. Deng, J. T. Groves, J. D. Lipscomb, *J. Am. Chem. Soc.*, **129**, 2007, 3514 – 3515
69. H. E. Simmons, R. D. Smith, *J. Am. Chem. Soc.*, **80**, 1958, 5323 – 5324
70. A. B. Charette, A. Beauchemin, *Org. React.*, **58**, 2001

71. C. A. Brown, A. Yamashita, *J. Am. Chem. Soc.*, **97**, 1975, 891 – 892
72. H. Lindlar, *Helv. Chim. Acta.*, **35**, 1952, 446 – 450
73. M. Garcia-Mota, J. Gomez-Diaz, G. Novell-Leruth, C. Vargas-Fuentes, L. Bellarosa, B. Bridier, J. Perez-Ramirez, N. López, *Theor. Chem. Acc.*, **128**, 2011, 663 – 673
74. R. P. Singh, J. M. Shreeve, *Synthesis*, **17**, 2002, 2561 – 2578
75. A. Bouzide, G. Sauvé, *Tetrahedron Letters*, **38**, 1997, 5945 – 5948
76. J. A. Wilkinson, *Chem. Rev.*, **92**, 1992, 505 – 519
77. J. H. Clark, *Chem. Rev.*, **80**, 1980, 429 – 452
78. A. L'Heureux, F. Beaulieu, C. Bennett, D. R. Bill, S. Clayton, F. LaFlamme, M. Mirmehrabi, S. Tadayon, D. Tovell, M. Couturier, *J. Org. Chem.*, **75**, 2010, 3401 – 3411
79. G. A. Olah, J. T. Welch, *Isr. J. Chem.*, **17**, 1978, 148 – 149
80. A. Sattler, G. Haufe, *Liebigs, Ann. Chem.*, 1994, 921 – 925
81. N. A. Petasis, E. I Bzowej, *J. Am. Chem. Soc.*, **112**, 1990, 6392 – 6394
82. J. F. Payack, D. L. Huges, D. Cai, I. F. Cottrell, T. R. Verhoeven, *Organic Synthesis*, **10**, 2004, 355 – 359
83. C. R. Johnson, G. A. Dutra, *J. Am. Chem. Soc.*, **95**, 1973, 7777 – 7782
84. O. Barba, J. C. Bell, T. B. Dupree, P. T. Fry, L. S. Bertram, M. C. T. Fyfe, W. Gattrell, R. P. Jeevaratnam, J. Kelly, T. M. Krulle, R. W. MacDonald, T. Morgan, C. M. Rasamison, K. L. Schofield, A. J. W. Stewart, S. S. A. Swain, D. M. Withall, *PCT Int. Appl.*, 2011, WO 2011147951 A1 2011101
85. O. Barba, S. H. Davis, M. C. T. Fyfe, R. P. Jeevaratnam, K. L. Schofield, T. Staroske, A. J. W. Stewart, S. A. Swain, D. M. Withall, *PCT Int. Appl. (2010) WO2010103335 A1 20100916*
86. D. A. Evans, J. R. Scheerer, *Angew. Chem. Int. Ed.*, **44**, 2005, 6038
87. M. Ramanathan, D. Hou, *Tetrahedron Lett.*, **51**, 2010, 6143 – 6145
88. J. D. Kim, G. Han, O. P. Zee, Y. H. Jung, *Tetrahedron Lett.*, **44**, 2003, 733 – 725
89. H. Liu, J. Yip, *Tetrahedron Lett.*, **38**, 1997, 2253 – 2256
90. C. Paal, *Ber. Dtsch. Chem. Ges.*, **17**, 1884, 2756 – 2767

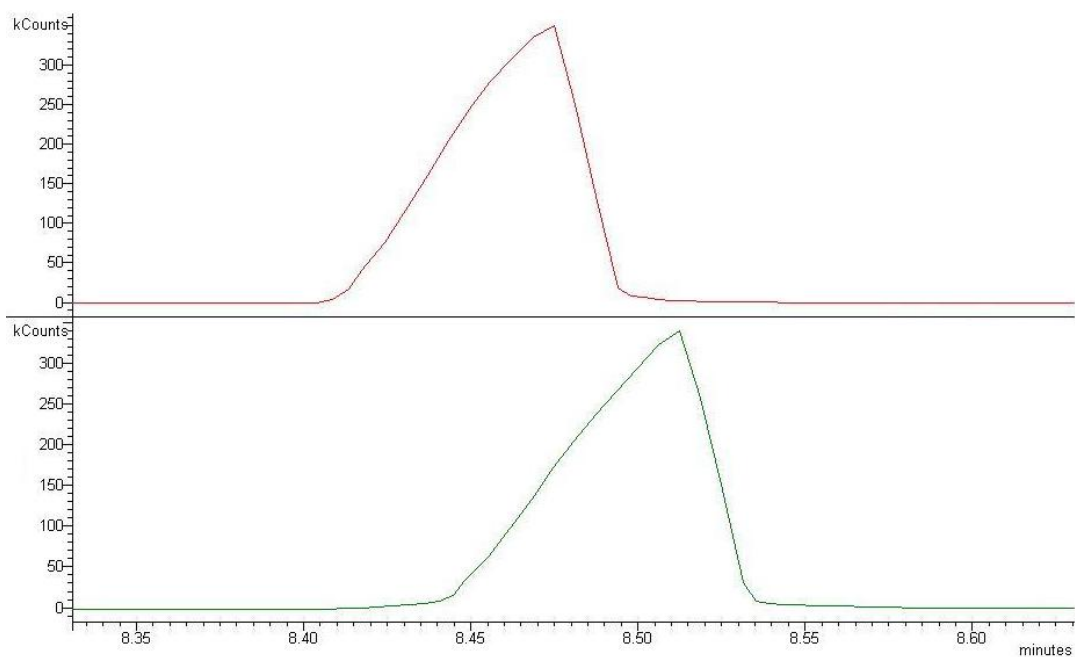
91. L. Knorr, *Ber. Dtsch. Chem. Ges.*, **17**, 1884, 2863 – 2870
92. B. M. Trost, G. A. Doherty, *J. Am. Chem. Soc.*, **122**, 2000, 3801 – 3810
93. M. Yamagishi, K. Nishigain, T. Hata, H. Urabe, *Org. Lett.*, **13**, 2011, 4873 – 4875
94. L. J. Higgins, F. Yan, P. Liu, H. Liu, C. L. Rennan, *Nature*, **437**, 2005, 838 – 844
95. D. Yun, M. Dey, L. J. Higgins, F. Yan, H. Liu, C. L. Drennan, *J. Am. Chem. Soc.*, **133**, 2011, 11262 – 112369
96. J. E. Baldwin, T. S. Wan, *Tetrahedron*, **37**, 1981, 1589 – 1595
97. P. L. Roach, I. J. Clifton, C. M. H. Hensgens, N. Shibata, C. J. Schofield, J. Hajdu, J. E. Baldwin, *Nature*, **137**, 1997, 827 – 830
98. A. Basak, S. P. Salowe, C. A. Townsend, *J. Am. Chem. Soc.*, **112**, 1990, 1654 – 1656
99. K. H. Baggaley, A. G. Brown, C. J. Schofield, *Nat. Prod. Rep.*, **14**, 1997, 309 – 333
100. J. S. Chickos, M. Bausch, R. Alul, *J. Org. Chem.*, **46**, 1981, 3559 – 3562
101. E. C. Ashby, R. N. DePriest, A. B. Goel, B. Wenderoth, T. N. Pham, *J. Org. Chem.*, **49**, 1984, 3545 – 3556
102. J. Abad, G. Villorbina, G. Fabriás, F. Camps, *J. Org. Chem.*, **69**, 2004, 7108 – 7113
103. J. Abad, G. Fabriás, F. Camps, *J. Org. Chem.*, **65**, 2000, 8582 – 8588
104. B. H. Lipshutz, R. S. Wilhelm, J. A. Kozlowski, D. Parker, *J. Org. Chem.*, **49**, 1984, 3928 – 3938
105. B. H. Lipshutz, J. A. Kozlowski, R. S. Wilhelm, *J. Am. Chem. Soc.*, **103**, 1981, 762
106. P. K. Freeman, L. L. Hutchinson, *J. Org. Chem.*, **45**, 1980, 1924 – 1930
107. J. A. Dale, H. S. Mosher, *J. Am. Chem. Soc.*, **95**, 1973, 512 – 519
108. T. R. Hoye, C. S. Jeffrey, F. Shao, *Nat. Protoc.*, **2**, 2007, 2451 – 2458
109. Anna Stanley PhD Thesis, University of Warwick, 2006
110. Paulina Sydor PhD Thesis, University of Warwick, 2010
111. F. Alihosseini, K. S. Ju, J. Lango, B. D. Hammock, G. Sun, *Biotechnol. Prog.*, **3**, 2008, 742 – 747

112. T. Kieser, K. F. Chater, M. J. Bibb, M. J. Buttner, D. A. Hopwood, *Practical Streptomyces Genetics*, 2000
113. P. K. Sydor, G. L. Challis, *Methods in Enzymology*, **516**, 2012, 195 – 218
114. A. Dubas, M. Sami, T. J. N. Brown, C. J. Schofield, J. E. Baldwin, J. M. Frere, *FEBS Lett.*, 2000, **485**, 142 – 146
115. A. Liu, R. Y. N. Ho, L. Que, *J. Am. Chem. Soc.*, 2001, **123**, 5126 – 5127
116. B. Lindgren, T. Nilsson, S. Husebye, Ø. Mikalsen, K. Leander, C. Swahn, *Acta. Chemica Scandinavica*, 1973, **27**, 888 – 890
117. B. S. Bal, W. E. Childers, H. W. Pinnick, *Tetrahedron*, **37**, 1981, 2091 – 2096
118. *Handbook of Microbiological Media 3rd Edition*, R. M. Atlas
119. University of Rochester website, Department of Chemistry, Written by Jeffrey Bode, Date accessed: 21/01/2011,
<http://chem.chem.rochester.edu/~nvd/howtotitrate.html>
120. M. Frigerio, M. Santagostino, S. Sputore, *J. Org. Chem.*, **64**, 1999, 4537 – 4538
121. J. Yin, C. Pidgeon, *Tetrahedron Lett.*, **34**, 1997, 5953 – 5954
122. K. C. Nicolaou, D. A. Claremon, D. P. Papahatjis, *Tetrahedron Lett.*, **46**, 1981, 4647 – 4650
123. K. Omura, D. Swern, *Tetrahedron*, **34**, 1978, 1651 – 1660
124. B. R. Travis, M. Sivakumar, G. O. Hollist, B. Borhan, *Org. Lett.*, **5**, 2003, 1031 – 1034
125. B. M. Trost, D. P. Marecak, *Tetrahedron Asymmetry*, **6**, 1995, 7 – 10
126. N. A. Petasis, S. Lu, *Tetrahedron Lett.*, **36**, 1995, 2393 – 2396
127. J. F. Payack, D. L. Hughes, D. Cai, I. F. Cottrell, T. R. Verhoeven, M. Kerr, L. Hegedus, *Organic Syntheses*, **10**, 2004, 256 – 259

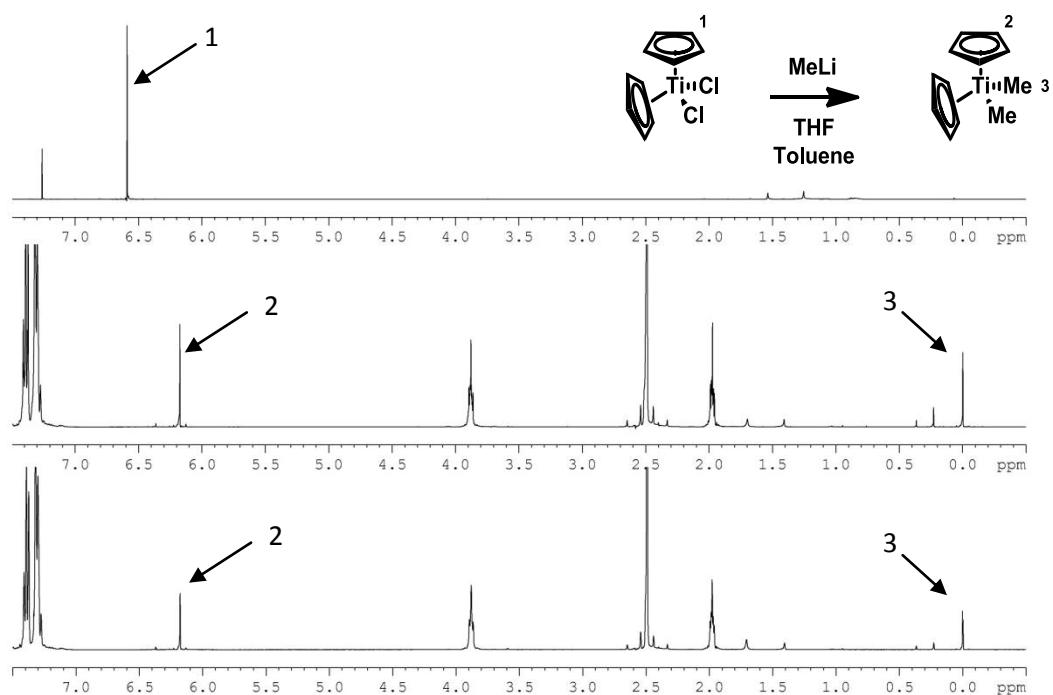
Appendix



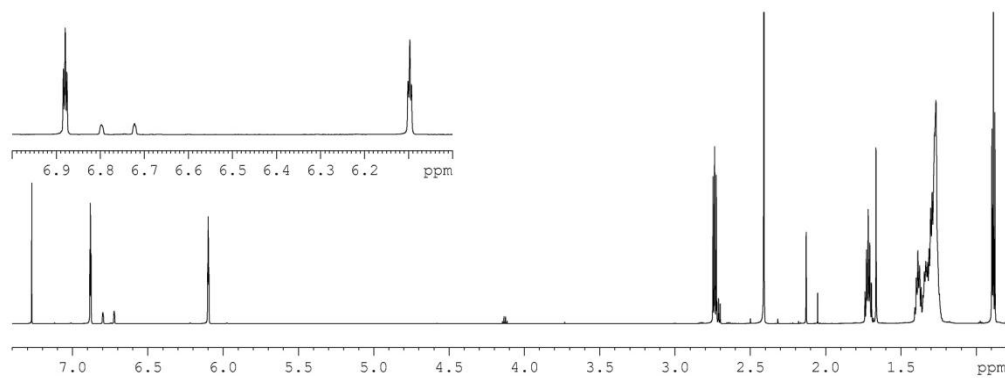
Appendix 1.1: A comparison between 5.70 – 5.10 ppm and 2.20 – -0.50 ppm of the $^1\text{H-NMR}$ spectrum in CDCl_3 at 700 MHz of *E*- (top spectrum) and *Z*-118 (bottom spectrum)



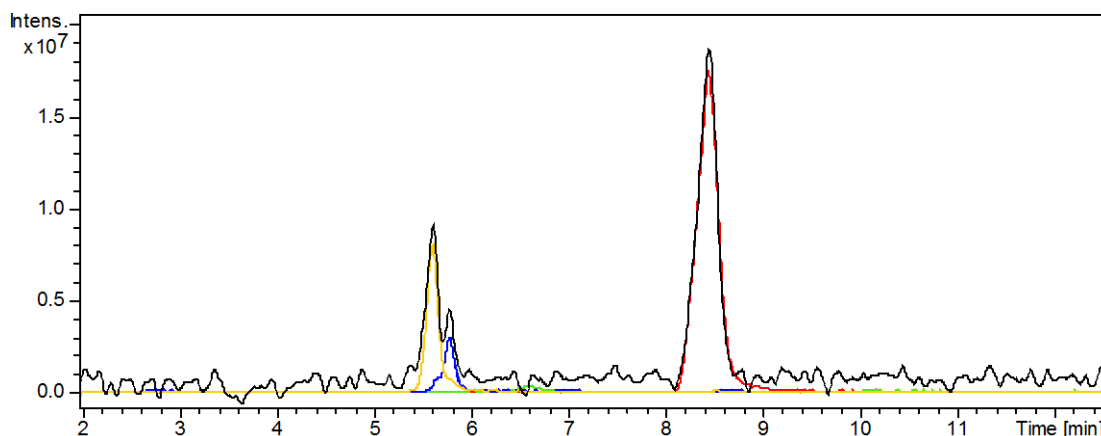
Appendix 1.2: The GC-MS chromatogram for *E*- (top spectra) and *Z*-118 (bottom spectra)



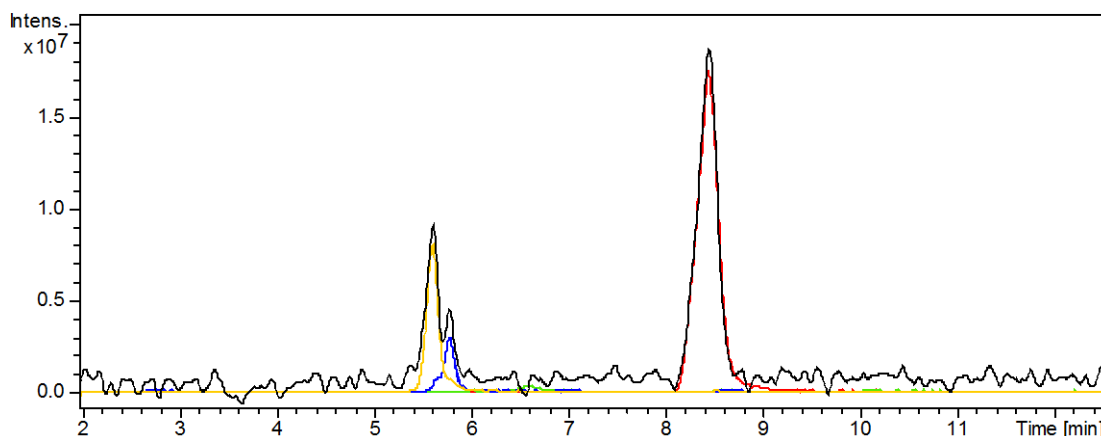
Appendix 1.3: A comparison of the ¹H-NMR spectrum in CDCl₃ at 400 MHz of titanocene dichloride (top spectrum) with the reaction of methyl lithium after 15 mins (middle spectrum) and after 45 mins (bottom spectrum). The additional peaks observed in the spectra are due to the toluene and THF used as a solvent for this reaction



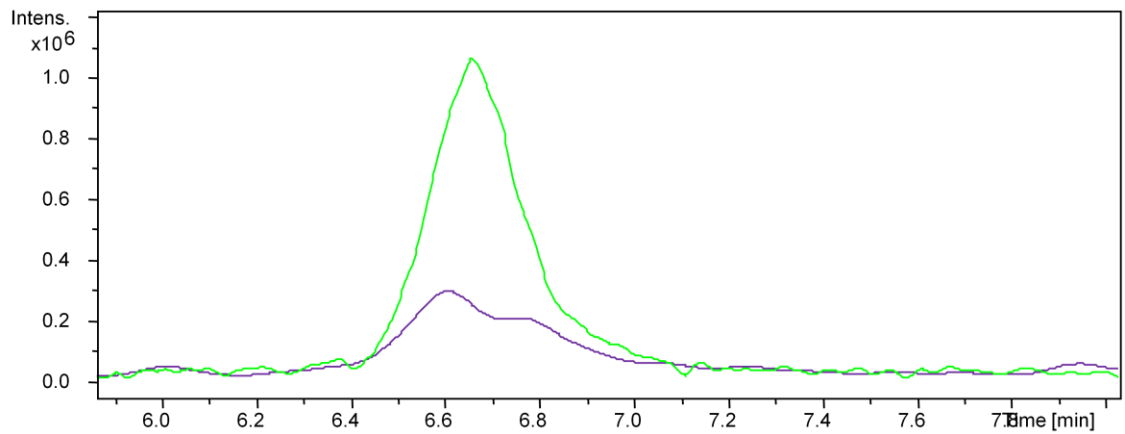
Appendix 1.4: The ¹H-NMR spectrum in CDCl₃ at 700 MHz of **206**



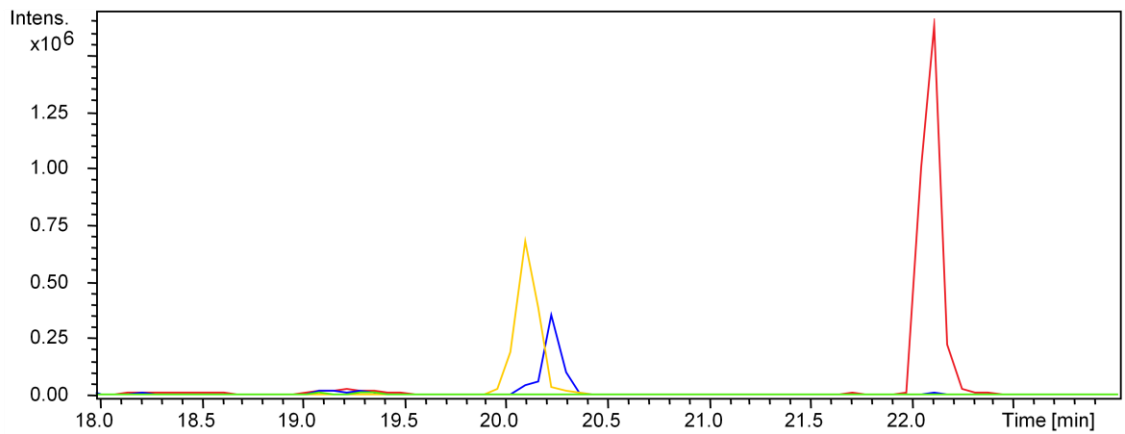
Appendix 1.5: A_{533} chromatogram (black) and extracted ion chromatograms at $m/z = 412$ (red), $m/z = 428$ (blue), $m/z = 444$ (yellow) and $m/z = 410$ (green) from the LC-MS analysis of the mycelial extract of the *redL* mutant fed with 2-UP analogue **269**



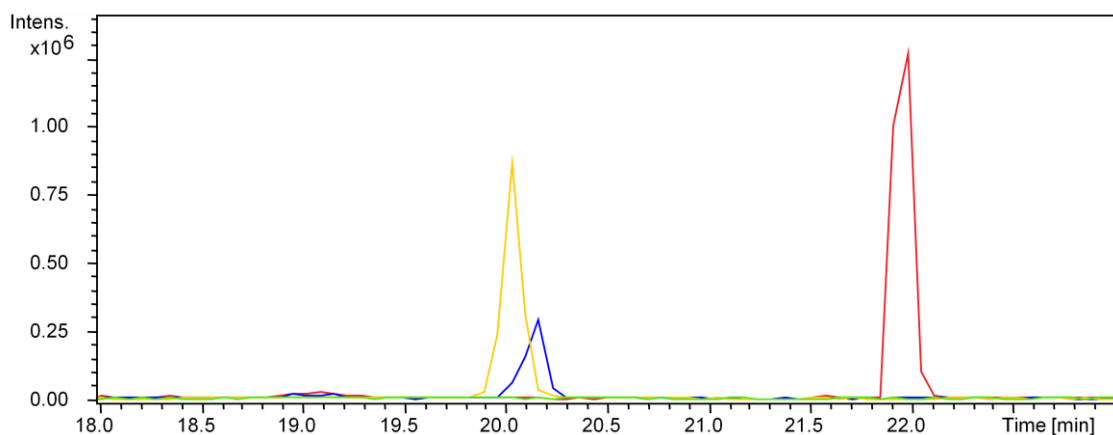
Appendix 1.6: A_{533} chromatogram (black) and extracted ion chromatograms at $m/z = 412$ (red), $m/z = 428$ (blue), $m/z = 444$ (yellow) and $m/z = 410$ (green) from the LC-MS analysis of the mycelial extract of the *redL* mutant fed with 2-UP analogue **270**



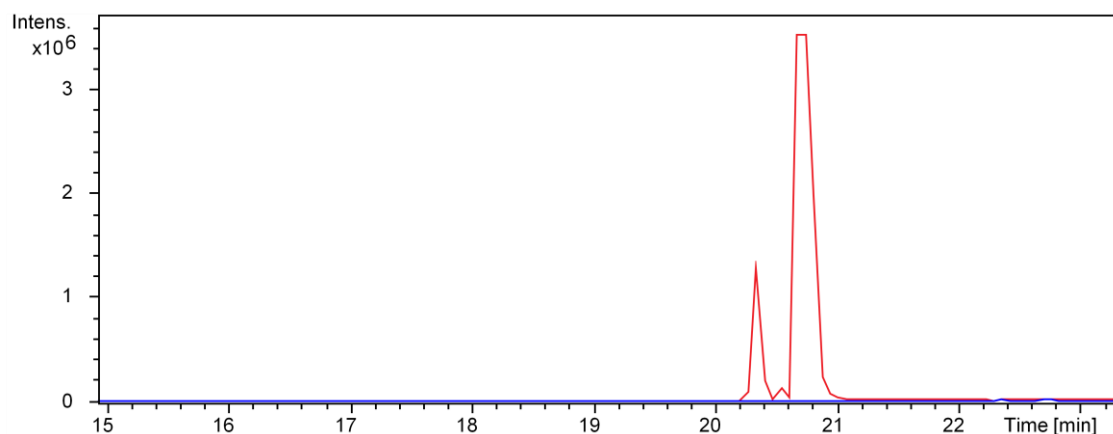
Appendix 1.7: Extracted ion chromatograms at $m/z = 410$ from the LC-MS analysis of the mycelial extract of the *redL* mutant (green) and the *redLG* double mutant (purple) fed with 2-UP analogue **270**



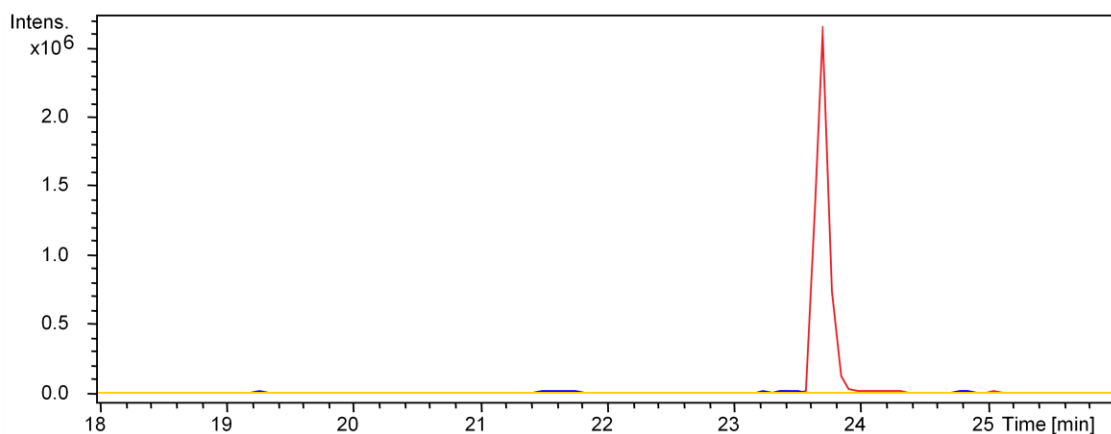
Appendix 1.8: Extracted ion chromatograms at $m/z = 412.24$ (red), $m/z = 428.23$ (blue), $m/z = 444.23$ (yellow) and $m/z = 410.22$ (green) from the LC-MS analysis of the mycelial extract of *S. albus + redHG* fed with 2-UP analogue **268** and MBC **19**



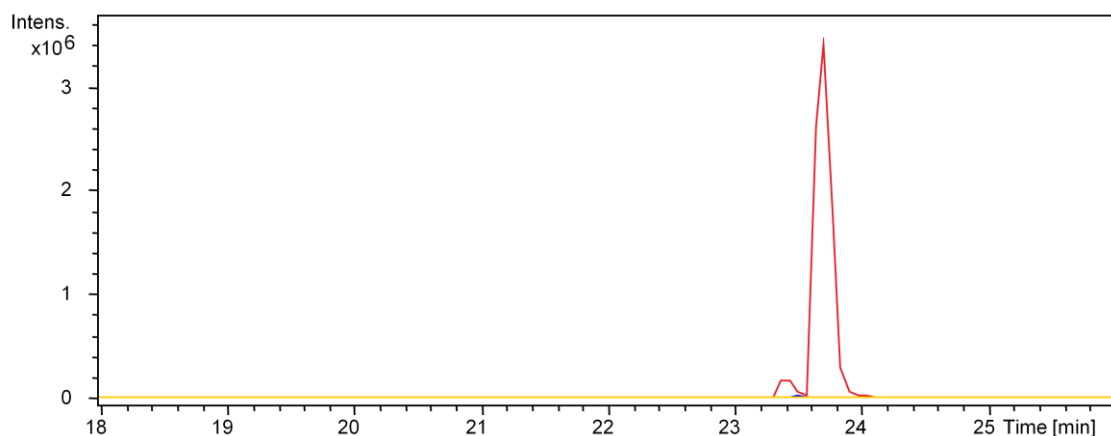
Appendix 1.9: Extracted ion chromatograms at $m/z = 412.24$ (red), $m/z = 428.23$ (blue), $m/z = 444.23$ (yellow) and $m/z = 410.22$ (green) from the LC-MS analysis of the mycelial extract of *S. albus + redHG* fed with 2-UP analogue **267** and MBC **19**



Appendix 1.10: Extracted ion chromatograms at $m/z = 396.26$ (red) and $m/z = 352.20$ (blue) from the LC-MS analysis of the mycelial extract of *S. albus + redHG* fed with 2-UP analogue **86** and MBC **19**



Appendix 1.11: Extracted ion chromatograms at $m/z = 406.28$ (red), $m/z = 404.27$ (blue) and $m/z = 422.28$ (yellow) from the LC-MS analysis of the mycelial extract of *S. albus* + *redHG* fed with 2-UP analogue **Z-118** and **MBC 19**



Appendix 1.12: Extracted ion chromatograms at $m/z = 406.28$ (red), $m/z = 404.27$ (blue) and $m/z = 422.28$ (yellow) from the LC-MS analysis of the mycelial extract of *S. albus* + *redHG* fed with 2-UP analogue **E-118** and **MBC 19**